



Uniwersytet
Gdański



GDAŃSKI
UNIwersYTET
MEDYCZNY

Intercollegiate Faculty of Biotechnology
University of Gdańsk & Medical
University of Gdańsk

DOCTORAL DISSERTATION

M. Sc., Dominika Miroszewska

Characterization of the function and heterogeneity of infiltrating T cells, especially Th17/Treg cells in colorectal cancer and inflammation

Doctoral dissertation presented to the Biotechnology Discipline Council at the University of Gdańsk in application for the doctoral degree in the field of natural sciences in the scientific discipline of biotechnology

Supervisor: Dr. Zhi Chen
Laboratory of Experimental and Translational Immunology
Intercollegiate Faculty of Biotechnology
University of Gdańsk & Medical University of Gdańsk

GDAŃSK 2024

Abstract

Human immune system consists of a variety of molecules, immune cells, and tissues and has one main task – to protect the host. Regardless if it is an effective infection clearance, tissue repair, or cancer cells elimination, immune system is a vital component of this process. In a homeostasis state, components of innate and adaptive immunity work in tandem, however dysregulation of either leads to pathological conditions such as chronic inflammation or cancer. Human gut is highly exposed to potentially harmful, external factors simultaneously hosting commensal microbiota. Therefore, human gut is rich in immune cells ready to carry out the response if needed, simultaneously tolerating human natural microbiota. It is believed that 70% of the immune system is located in gut-associated lymphoid tissue (GALT). As such, intestinal mucosal tissue contains high numbers of T-cells. T-cells play a vital role in the development of inflammatory bowel disease (IBD) and colorectal cancer (CRC). Particularly, T helper 17 cells (Th17) and T regulatory (Treg), in recent years attracted attention in the context of IBD and CRC. Th17 are a pro-inflammatory subset that exerts inflammation leading to IBD, whilst the main Treg role is to regulate immune response. However, high infiltration of Tregs leads to the immunosuppressive environment and promotes tumor growth. Moreover, IBD is considered as one of the risks factors for the CRC development. Therefore, understanding immune response, especially Th17 and Treg mediated immune response, is vital for the development of effective treatment.

Therefore, the first part of this thesis is focused on the identification of how different housing conditions impacts gut microbiota and the subsequent development of colitis in the T cell adoptive transfer colitis mice models. It was revealed that *Helicobacter* strains, and *Klebsiella oxytoca* may correlate with increased numbers of IFN- γ CD4⁺ and IL-17 CD4⁺ T-cells whilst *Akkermansia muciniphila* had negative correlation with the development of colitis. Further, separate Dextran Sulfate Sodium (DSS)-induced model of colitis was used to investigate the role of USP28 in the development of T-cells. Knockout of USP28 led to the more potent suppressive function of Tregs and participated in IL-22/STAT5 signaling. Collectively, these studies revealed additional aspects of Th17 and Tregs control.

Second part of the thesis involved studies performed on formalin-fixed paraffin embedded (FFPE) CRC tissue sections to investigate molecular changes linked to the immune cells infiltration. Spatial transcriptomics analysis of tumor microenvironment (TME) revealed unique upregulation of several genes such as TP53 or CD276 in epithelial tumor clusters, and identified gene expression gradients along the invasive trajectory with identified Tregs interactions with macrophages and epithelial cancer cells in the TME. Furthermore, SIT1, negative regulator of T-cells activation, was identified to be differentially expressed in the tertiary lymphoid structures (TLSs) in the tumor tissue as potential novel indicator of impaired T-cells function. Next, DIA MS-based proteomics of CD4⁺ enriched CRC FFPE revealed a complex expression patterns of proteins linked to the immune evasion, such as NPM3, and simultaneously expression of pro-inflammatory S100A8 or S100A9 proteins in cancer samples. At the same time, inferred Tregs fractions were found to correlate with IDO1 and ARG1 expression, both associated with immunosuppression in the TME. Furthermore, selective expression of MCEMP1 was identified in CRC samples, comparing to normal tissue, whilst in validation proteomics dataset, CD4⁺ T-cells isolated from CRC samples, exhibited higher expression of MCEMP1, what may indicate it's potential regulatory role in T-cells in CRC TME. CRC FFPE studies provided new aspects of ongoing regulation of genes and proteins regulating the immune response landscape in TME.

Last part of the thesis comprises of two proteomics studies which investigated changes of the proteins expression in serum of CRC patients as well as healthy controls. Study performed with proximity extension assay (PEA) showed specific upregulation of proteins such as T-cells chemoattractant CXCL9 and CCL23, and IL-6 together with oncogenic SCRIN1 with simultaneous downregulation of tumor suppressor RET protein expression in the serum samples of CRC patients comparing to healthy controls. At the same time, CSF3, IL12RB1, and CD276 were specifically upregulated in the serum samples of

patients assigned with inflammation, comparing to patients without such status. Lastly, upregulation of IFN- γ , IL-32, IL-17 and ACP6 was found to correlate with early, and late stages of the disease, respectively. The upregulation of CSF3, IFN- γ , IL6, CXCL9, CCL23, and ACP6 expression levels were validated in a separate cohort. This study provided several new biomarkers candidates for CRC diagnosis. Simultaneously, LC-MS/MS study of CRC patients' serum proteins reported, for the first time, elevated LBP and SAA4 levels associated with CRC tumorigenesis. At the same time, proteins involved in complement cascade namely C5, C1QB, C4A, C8A were upregulated in the CRC conditions, with C4A and C8A upregulated levels being linked to the later stages of the disease. Additionally, C5 expression was validated in a separate cohort indicating its potential role as biomarker.

Collectively, this thesis presents a series of studies aiming at deciphering the heterogeneity of immune responses linked to the T-cells functions, especially Th17 and Tregs, and associated changes in protein and gene expression in the tumor settings and inflammation.

Streszczenie

Układ odpornościowy człowieka składa się z różnorodnych cząsteczek, komórek odpornościowych oraz tkanek i ma jeden główny cel – ochrona gospodarza. Niezależnie od tego, czy jest to skuteczne usuwanie infekcji, naprawa tkanek czy eliminacja komórek nowotworowych, układ odpornościowy jest niezbędnym elementem tego procesu. W stanie homeostazy składniki odporności wrodzonej i nabytej działają wspólnie, jednak rozregulowanie któregośkolwiek z nich prowadzi do stanów patologicznych, takich jak przewlekłe zapalenie albo nowotwór. Ludzkie jelita są bardzo narażone na potencjalnie szkodliwe czynniki zewnętrzne, jednocześnie będąc gospodarzem komensalnego mikrobiomu. Dlatego ludzkie jelita są bogate w komórki odpornościowe gotowe do przeprowadzenia reakcji w razie potrzeby, jednocześnie wykazując tolerancję na naturalną mikroflorę. Uważa się, że 70% układu odpornościowego znajduje się w tkance limfatycznej związanej z jelitami (GALT - *ang.* gut-associated lymphoid tissue). W związku z tym tkanka śluzowej jelit zawiera dużą liczbę limfocytów typu T. Limfocyty typu T odgrywają znaczącą rolę w rozwoju choroby zapalnej jelit (IBD - *ang.* inflammatory bowel disease) i raka jelita grubego (CRC - *ang.* colorectal cancer). W szczególności limfocyty T pomocnicze 17 (Th17) i limfocyty T regulatorowe (Treg) w ostatnich latach zwróciły uwagę w kontekście IBD i CRC. Th17 stanowią podgrupę prozapalną, która wywołuje stan zapalny prowadzący do IBD, podczas gdy główną rolą Treg jest regulacja odpowiedzi immunologicznej. Jednakże wzmożony naciek Treg prowadzi do powstania środowiska immunosupresyjnego i sprzyja wzrostowi nowotworów. Co więcej, IBD jest uważana za jeden z czynników ryzyka rozwoju CRC. Dlatego zrozumienie odpowiedzi immunologicznej, a zwłaszcza odpowiedzi immunologicznej za pośrednictwem Th17 i Treg, ma kluczowe znaczenie dla rozwoju efektywnego leczenia.

W związku z tym pierwsza część tej rozprawy skupia się na identyfikacji jaki wpływ mają różne warunki hodowli na mikroflorę jelitową i późniejszy rozwój zapalenia jelita grubego w modelach myszy z adopcyjnym transferem komórek T indukującym zapaleniem jelita grubego. Wykazano, że szczepy *Helicobacter* i *Klebsiella oxytoca* korelują ze zwiększoną liczbą limfocytów T CD4+ IFN- γ i limfocytów T CD4+ IL-17+, podczas gdy *Akkermansia muciniphila* wykazywała ujemną korelację z rozwojem zapalenia jelita grubego. Następnie, osobny myszy model zapalenia jelita grubego wywołany działaniem siarczanu sodu dekstranu (DSS) został użyty w celu zbadania roli proteazy USP28 w rozwoju limfocytów typu T. Knock-out USP28 doprowadził do zwiększonej aktywności supresyjnej Treg i dodatkowo stwierdzono udział USP28 w sygnalizacji IL-22/STAT5. Łącznie badania te ujawniły dodatkowe aspekty kontroli Th17 i Treg.

Druga część rozprawy obejmowała badania wykonane na skrawkach tkanek CRC z blochków parafinowych (FFPE – *ang.* formalin-fixed paraffin embeded) w celu zbadania zmian molekularnych związanych z infiltracją komórek odpornościowych. Analiza transkryptomiki przestrzennej mikrośrodowiska guza (TME - *ang.* tumor microenvironment) ujawniła wyjątkową zwiększoną ekspresję genów, takich jak TP53 lub CD276 w skupiskach komórek nowotworowych, a także ujawniła gradienty ekspresji genów wzdłuż trajektorii inwazyjnej ze zidentyfikowanymi interakcjami Treg z makrofagami i komórkami CRC w TME. Ponadto stwierdzono, że SIT1, negatywny regulator aktywacji limfocytów T, charakteryzuje się zróżnicowaną ekspresją w trzeciorzędowych strukturach limfatycznych (TLS – *ang.* tertiary lymphoid structure) w tkance nowotworowej jako potencjalny nowy wskaźnik upośledzenia funkcji limfocytów typu T w CRC. Następnie, analiza proteomiczna tkanek CRC wzbogaconych w CD4+ oparta o spektrometrię mas ujawniła złożone wzorce ekspresji białek związanych z unikaniem odpowiedzi immunologicznych, takich jak NPM3, i jednoczesną ekspresję prozapalnych białek S100A8 lub S100A9 w tkankach CRC. Jednocześnie stwierdzono, że przewidziane frakcje Treg w tkankach korelują z ekspresją IDO1 i ARG1, białek związanych z immunosupresją w TME. Poza tym zidentyfikowano selektywną ekspresję MCEMP1 w próbkach CRC w porównaniu z normalną tkanką, podczas gdy w zbiorze danych walidacyjnych, komórki T CD4+ wyizolowane z próbek CRC wykazują wyższą ekspresję MCEMP1, co może wskazywać na potencjalną rolę regulacyjną tego białka w limfocytach T w CRC TME. Badania CRC FFPE dostarczyły

nowych aspektów bieżącej regulacji genów i białek regulujących krajobraz odpowiedzi immunologicznej w TME.

Ostatnia część rozprawy obejmuje dwa badania proteomiczne, w których badano zmiany ekspresji białek w surowicy pacjentów z CRC oraz zdrowych osób z grupy kontrolnej. Badanie przeprowadzone za pomocą PEA (PEA - *ang.* proximity extension assay) wykazało specyficzną zwiększoną ekspresję białek, takich jak chemoatraktant limfocytów typu T CXCL9 i CCL23 oraz IL-6 wraz z onkogennym SCRN1 z jednoczesną zmniejszoną ekspresją supresorowego białka RET w próbkach surowicy pacjentów z CRC w porównaniu do zdrowej grupy kontrolnej. Jednocześnie poziomy CSF3, IL12RB1 i CD276 były specyficznie podwyższone w próbkach surowicy pacjentów ze stwierdzonym stanem zapalnym, w porównaniu z pacjentami bez stwierdzonego zapalenia. Dodatkowo stwierdzono, że zwiększenie poziomu IFN- γ , IL-32, IL-17 i ACP6 koreluje odpowiednio z wczesnym i późnym stadium choroby. Zwiększenie poziomu ekspresji CSF3, IFN- γ , IL6, CXCL9, CCL23 i ACP6 potwierdzono w oddzielnej kohorcie. Badanie to dostarczyło kilku nowych potencjalnych biomarkerów diagnostycznych CRC. Jednocześnie badanie LC-MS/MS białek surowicy pacjentów z CRC po raz pierwszy wykazało podwyższone poziomy LBP i SAA4 związane z kancerogenezą CRC. Jednocześnie białka układu dopełniacza, mianowicie C5, C1QB, C4A, C8A, uległy zwiększeniu w warunkach CRC, przy czym zwiększone poziomy C4A i C8A powiązано z późniejszymi stadiami choroby. Dodatkowo potwierdzono ekspresję C5 w oddzielnej kohorcie, co wskazuje na jej potencjalną rolę jako biomarkera.

Podsumowując, niniejsza rozprawa przedstawia serię badań mających na celu rozszyfrowanie heterogeniczności odpowiedzi immunologicznych powiązanych z funkcjami komórek T, zwłaszcza Th17 i Treg, oraz powiązanymi zmianami w ekspresji białek i genów na tle nowotworu i stanu zapalnego.

Acknowledgements

First and foremost, I would like to express my deepest gratitude to my supervisor, Dr. Zhi Chen, for providing me with the opportunity to undertake this PhD project. Your involvement, feedback, and unwavering support over the years have been invaluable. I have learned so much under your guidance, and I am grateful for the development I have experienced as a young researcher. Thank you for this remarkable opportunity.

Next, I would like to thank my fellow PhD student, Víctor Urbiola-Salvador, for sharing countless laughs and genuine camaraderie, especially during stressful moments. Thank you for consistently easing my doubts, for listening to me, for your endless help, and for your friendship.

I extend my gratitude to Dr. Agnieszka Jabłońska for your encouraging words, exceptional organizational skills, and “can-do” attitude. I will fondly remember our playful bets for “a can of Coke”, which made conducting experiments even more thrilling.

I would also like to thank all the members of the Laboratory of Experimental and Translational Immunology for their assistance and engaging conversations.

I am grateful to Dr. hab Mariusz Grinholc for providing me with the opportunity to conduct my didactic hours and for your readiness to help. Additionally, my sincere thanks to Dr. Agata Woźniak-Pawlikowska, Beata Kruszewska-Naczk, and Natalia Burzyńska for making the didactics enjoyable.

Thank you, Agnieszka Sankiewicz for being so helpful and for your willingness to explain all the necessary bureaucratic procedures.

I would like to acknowledge both MD Jacek Kowalski and Dr. Michał Rychłowski for their time and willingness to share their knowledge with me.

My immense appreciation and gratitude go to all the clinicians for their dedicated work, as well as to the patients who generously provided their samples for this research. Their courage in contributing to scientific advancement is a testament to their strength and resilience.

Last but not least, I would like to thank my family, my best friend, and my partner. K & J, I could not have accomplished this without your unwavering support. Thank you for being by my side.

List of abbreviations

2-DE: Two-dimensional electrophoresis	CITE-seq: Cellular indexing of transcriptomes and epitopes by sequencing
A2GL: Leucine-rich alpha-2-glycoprotein	CLEC4A: C-Type Lectin Domain Family 4 Member A
AAHC: antibiotic-associated hemorrhagic colitis	CLEC4G: C-type lectin domain family 4 member G
ABCD: Antibody barcoding with cleavable DNA	CLIP: Class II-associated invariant chain peptide
ACP6: Lysophosphatidic acid phosphatase type 6	CMS: Consensus Molecular Subtypes
ACTA2: Actin Alpha 2, Smooth Muscle	CODEX: CO-Detection by indEXing
ACTG2: Actin Gamma 2, Smooth Muscle	COL18A1: Collagen Type XVIII Alpha 1 Chain
ADAM9: ADAM Metallopeptidase Domain 9	COL3A1: Collagen Type III Alpha 1 Chain
ADRA2: Adrenoceptor Alpha 2A	COL5A1: Collagen Type V Alpha 1 Chain
AGRP: Agouti-related neuropeptidase	COL6A2: Collagen Type V Alpha 2 Chain
AHR: Aryl Hydrocarbon Receptor	CRC: Colorectal cancer
AIRE Autoimmune Regulator	CSF1: Colony Stimulating Factor 3
AJCC: American Joint Committee on Cancer	CSF3: Colony Stimulating Factor 3
AK: AKT Serine/Threonine Kinase 1	CSFR1: Colony Stimulating Factor 1 Receptor
ALDH: Aldehyde Dehydrogenase	CTC: Computed Tomography Colonography
ALN: Axillary lymph node	ctDNA: Circulating tumor DNA
AML: Acute myeloid leukemia	CTLA-4: Cytotoxic T cell antigen-4
AP-1: Activator protein 1	CTLA4: Cytotoxic T-Lymphocyte Associated Protein 4
APBB1IP: Amyloid beta precursor protein binding family B member 1	CXCL: C-X-C Motif Chemokine Ligand
APC: Antigen presenting cell	CXCR: C-X-C Motif Chemokine Receptor
APC: Antigen presenting cell	CyTOF: Cytometry by time of flight
APLP2: Amyloid Beta Precursor Like Protein 2	CyTOF: Cytometry by time-of-flight
APOE: Apolipoprotein E	DAG: Diacylglycerol
ARG1: Arginase1	DAMP: Damage-associated molecular patterns
ARG2: Arginase-2	DC: Dendritic cells
ARHGEF12: Rho guanine nucleotide exchange factor 12	DEG: Differentially expressed gene
B2M: Beta-2-Microglobulin	DEP: Differentially expressed protein
BAFF: B-cell activating factor	DPEP2: Dipeptidase 2
BATF: Basic Leucine Zipper ATF-Like Transcription Factor	DPP4: Dipeptidyl Peptidase 4
BCAP: B-cell adaptor protein	DSS: Dextran Sulfate Sodium
BCL10: B-cell lymphoma/leukemia 10	DUB: Deubiquitinating enzymes
BCL2: B-cell lymphoma 2	ECM: Extracellular matrix
BCL6: BCL6 Transcription Repressor	EGFL7: Epidermal growth factor-like protein 7
BCR: B-cell receptor	EMT: Epithelial-to-mesenchymal transition
BID: BH3 interacting domain death agonist	ENPP5: Ectonucleotide pyrophosphatase/phosphodiesterase family
BLNK: B Cell Linker	ER: Endoplasmic reticulum
BRAF: B-Raf Proto-Oncogene, Serine/Threonine Kinase	ERK: Extracellular signal-regulated kinase
Breg: Regulatory B-cells	ESI: Electrospray ionization
PTM: Post-translational modifications	EV: Extracellular vesicle
CA11: carbonic anhydrase	FAK: Focal adhesion kinase
CAC: Colitis-associated cancer	FAP: Fibroblast Activation Protein Alpha
CAF: Cancer-associated fibroblasts	FAS: Fas Cell Surface Death Receptor
CARD11: Caspase Recruitment Domain Family Member 11	FASLG: FAS ligand
CASP8: caspase-8	FBS: Fetal bovine serum
CCA: Canonical correlation analysis	FC: Flow cytometry
CCL: C-C Motif Chemokine Ligand	FDA: Food and drugs administration
CCR: C-C Motif Chemokine Receptor	FDR: False discovery rate
CD: Cluster of differentiation	FEZF2: FEZ Family Zinc Finger 2
CDC20: Cell Division Cycle 20	FFPE: Formalin-fixed paraffin-embedded
CDCA7: Cell Division Cycle Associated 7	FGF21: Fibroblast growth factor 21
CDH: Cadherin	FIT: Fecal immunochemical test
cDNA: Complementary DNA	FLT4: Fms-related tyrosine kinase 4
CEA: Carcinoembryonic antigen	FN1: Fibronectin 1
CIITA: Class II Major Histocompatibility Complex Transactivator	FOXO: Forkhead Box
CIMP: CpG island methylator phenotype	FoxP3: Forkhead box P3
CIN: Chromosomal instability	FSFC: Full spectrum flow cytometry

FYN: FYN Proto-Oncogene, Src Family Tyrosine Kinase
 GADS: GRB2 related adaptor protein downstream of Shc
 GALT: Gut-associated lymphoid tissue
 GAM: Glioma-associated macrophages
 GATA3: GATA Binding Protein 3
 GBM: Glioblastoma
 GC: Germinal center
 gFOBT: Guaiac fecal occult blood test
 GI: Gastrointestinal
 GPNMB: Glycoprotein Nmb
 GRB2: Growth Factor Receptor Bound Protein 2
 GSK3: Glycogen synthase kinase 3
 GZMB: Granzyme B
 HAGH: Hydroxyacylglutathione hydrolase
 HBA: Hemoglobin
 HIF1 α : Hypoxia Inducible Factor 1 Subunit Alpha
 HLA: Human leukocyte antigen
 HMGB1: High Mobility Group Box 1
 HNPCC: Hereditary nonpolyposis colorectal cancer
 IBD: Inflammatory bowel disease
 ICD-10: International Classification of Diseases version 10
 ICOS: Inducible T-cell costimulator
 ICOSL: Inducible T cell costimulator ligand
 IDO1: Indoleamine 2,3-Dioxygenase 1
 IF: Immunofluorescence
 IFNG: Interferon Gamma
 IFN- α : Interferon Alpha
 IFN- β : Interferon Beta
 IFN- γ : Interferon Gamma
 IFN- γ R1: Interferon Gamma Receptor 1
 IFN- γ R2: Interferon Gamma Receptor 2
 IgA: Immunoglobulin A
 IgE: Immunoglobulin E
 IgG: Immunoglobulin G
 IGHA: Immunoglobulin Heavy Constant Alpha 1
 IGHG1: Immunoglobulin Heavy Constant Gamma 1
 IGHG2: Immunoglobulin Heavy Constant Gamma 2
 IGHM: Immunoglobulin Heavy Constant Mu
 IgM: Immunoglobulin M
 IHC: Immunohistochemistry
 IKK β : Inhibitor Of Nuclear Factor Kappa B Kinase Subunit Beta
 IKK γ : Inhibitor Of Nuclear Factor Kappa B Kinase Regulatory Subunit Gamma
 IKZF1: IKAROS Family Zinc Finger 1
 IL: Interleukin
 IL-12RB1: Interleukin 12 Receptor Subunit Beta 1
 IL-12RB2: Interleukin 12 Receptor Subunit Beta 2
 IL-4RA: Interleukin 4 Receptor Subunit Alpha
 IL-6R: Interleukin 6 Receptor
 IL-6RA: Interleukin 6 Receptor Subunit Alpha
 IL7R: Interleukin 7 Receptor
 IMC: Imaging mass cytometry
 IP3: Inositol trisphosphate
 IPEX: Immune dysregulation, polyendocrinopathy, enteropathy, X-linked Syndrome
 IRF: Interferon Regulatory Factor
 ITAM: Immunoreceptor tyrosine-based activation motif
 ITGA: Integrin subunit alpha
 JAK: Janus kinase
 JAK2: Janus kinase 2
 JCHAIN: Joining Chain Of Multimeric IgA And IgM
 JNK: c-Jun N-terminal kinases
 KEGG: Kyoto Encyclopedia of Genes and Genomes
 KLK: Kallikrein Related Peptidase 4
 KRAS: KRAS Proto-Oncogene, GTPase
 KYNU: Kynureninase
 LAG-3: Lymphocyte activation gene-3
 LAIR1: Leukocyte Associated Immunoglobulin Like Receptor 1
 LAMA4: Laminin Subunit Alpha 4
 LAP: Latent-associated peptide
 LARG: Leukemia-associated Rho guanine-nucleotide exchange factor
 LBP: Lipopolysaccharide-binding protein
 LCM: Laser-capture microdissection
 LC-MS/MS: Tandem mass spectrometry coupled with liquid chromatography
 LEfSe: Linear Discriminant Analysis Effect Size
 LILRB2: Leukocyte Immunoglobulin Like Receptor B2
 LOD: Limit of detection
 LPA: lysophosphatidic acid
 L-R: Ligand-Receptor
 LSM14A: LSM14A MRNA Processing Body Assembly Factor
 LTB: Lymphotoxin Beta
 LTBR: Lymphotoxin Beta Receptor
 LYN: LYN Proto-Oncogene, Src Family Tyrosine Kinase
 mAb: Monoclonal antibody
 MAC: Membrane Attack Complex
 MADCAM1: Mucosal Vascular Addressin Cell Adhesion Molecule 1
 MALDI-TOF: Matrix-assisted laser desorption/ionization time-of-flight
 MALT1: Mucosa-associated lymphoid tissue lymphoma translocation protein 1
 MANSC1: MANSC domain-containing protein 1
 MAPK: Mitogen-activated protein kinase
 MAPKAPK5: MAPK Activated Protein Kinase 5
 MASP: MBL-associated serine proteases
 MMP: Matrix metalloproteinase
 MBL: Mannose-binding lectin
 MC: Mass cytometry
 MCEMP1: Mast Cell Expressed Membrane Protein 1
 MCM7: Minichromosome Maintenance Complex Component 7
 MDK: Midkine
 MDSC: Myeloid-derived suppressor cell
 MEK: Mitogen-activated protein kinase kinase
 MELC: Multi-Epitope Ligand Cartography
 MHC: Major histocompatibility complex
 MIBI: Multiplexed ion beam imaging
 MIST: Multiplexed in situ targeting
 MLN: Mesenteric lymph nodes
 MMP: Matrix Metalloproteinase
 MMR: Mismatch repair
 MNV: Murine norovirus
 mPOP: Minimal ProteOmic sample Preparation

MRD: Molecular residual disease
MS: Mass spectrometry
MSH3: MutS Homolog
MSI: Microsatellite instability
MSI: microsatellite instability
mTORC2: Mechanistic target of rapamycin kinase 2
mt-sDNA: Multitarget stool DNA testing
MUSTN1: Musculoskeletal, Embryonic Nuclear Protein 1
MZB1: Marginal zone B and B1 cell-specific protein
NAFLD: Non-fatty liver disease
nanoPOTS: Nanodroplet processing in one pot for trace samples
NAPPA: Nucleic Acid Programmable Protein Array
NCF2: Neutrophil cytosolic factor 2
NET: Neutrophil extracellular traps
NFAT: Nuclear factor of activated T cells
NF- κ B: Nuclear factor kappa B
NGS: Next-generation sequencing
NK: Natural killer
NOD: Nucleotide-binding oligomerization domain
NOTCH2: Neurogenic locus notch homolog protein 2
NPM3: Nucleophosmin/Nucleoplasmin 3
NPX: Normalized protein expression
NSCLC: Non-small-cell lung cancer
OUT: Operational Taxonomic Unit
PAMP: Pathogen-associated molecular patterns
PBMC: Peripheral blood mononuclear cells
PBS: Phosphate Buffered saline
PC: Principal components
PCA: Principal components analysis
PD-1: Programmed cell death protein 1
PD1: Programmed Death Receptor 1
PDK: Pyruvate Dehydrogenase Kinase 1
PD-L1: Programmed cell death ligand 1
PD-L1: Programmed Death Ligand 1
PEA: Proximity extension assay
PEA: Proximity Extension Assay
PECAM1: Platelet And Endothelial Cell Adhesion Molecule 1
PIGR: Polymeric Immunoglobulin Receptor
PIK3CA Phospholipase C Gamma 2
PIP2: Phosphatidylinositol (4,5)-bisphosphate
PIP3: Phosphatidylinositol (3,4,5)-trisphosphate
PITPNM3: PITPNM Family Member 3
PLAU: Plasminogen Activator, Urokinase
PLAUR: Plasminogen Activator, Urokinase receptor
PLAYR: Proximity Ligation Assay for RNA
PLCy1: Phospholipase C Gamma 1
PLCy2: Phospholipase C Gamma 2
PPY: Pancreatic prohormone
PRDX6: Peroxiredoxin 6
PRF1: Perforin 1
PTM: Posttranslational modification
PTPRC: Protein Tyrosine Phosphatase Receptor Type C
PVR: PVR Cell Adhesion Molecule
qPCR: Quantitative PCR
RA: Retinoic acid
RAG: Recombination Activating Gene
RAS: Rat Sarcoma Virus protein
REAP-seq: RNA expression and protein sequencing
RET: Ret proto-oncogen
RIG: Retinoic acid-inducible gene
ROBO4: Roundabout Guidance Receptor 4
ROR γ t : Retinoic acid-related Orphan Receptor gamma t
ROS: Reactive oxygen species
RPPA: Reverse Phase Protein Arrays
RRM2B: Ribonucleotide reductase regulatory TP53 inducible subunit M2B
rRNA: ribosomal RNA
RSPO3: R-Spondin 3
S100A10: S100 calcium-binding protein A10
S100A12: S100 calcium-binding protein A12
S100A8: S100 Calcium Binding Protein A8
S100A9: S100 Calcium Binding Protein A9
SAA: Serum Amyloid A
SAA4: Serum Amyloid A4, Constitutive
scATAC-seq: Single-cell sequencing assay for transposase-accessible chromatin
SCBC: Single-cell barcode chip
SCGB1A1: Secretoglobin family 1A member 1
SCID: severe combined immunodeficient
SCoPE-MS: Single Cell Proteomics by mass spectrometry
SCRN1: Secernin 1
scRNA: Single-cell RNA
SDF1: Stromal Cell-Derived Factor 1
SELL: Selectin L
SELP: Selectin P
SELPLG: Selectin P ligand
SEMA4D: Semaphorin 4D
SFB: Segmented Filamentous Bacteria
SHC: Src homology/collagen
SIGLEC10: Sialic Acid Binding Ig Like Lectin 10
SIRPa: Signal Regulatory Protein Alpha
SIRT1: Sirtuin 1
SIRT2: Sirtuin 2
SISPROT: Simple and integrated spin tip-based proteomics technology
SIT1: Signaling Threshold Regulating Transmembrane Adaptor 1
SMAD: Mothers against decapentaplegic homolog
SMOC2: SPARC-related modular calcium-binding protein 2, STAT, signal
SN: Sentinel Node
SOS: Son of Sevenless
SPF: Specific-pathogen-free
SPP1: Secreted Phosphoprotein 1
ST: Spatial Transcriptomics
STAT: Signal Transducer And Activator Of Transcription
SUGAR-seq: SUrface-protein Glycan And RNA-seq
TAM: Tumor-associated macrophages
TAP: Transporter associated with antigen processing
TCR: T-cell receptor
TDP2: Tyrosyl-DNA Phosphodiesterase 2
TFF1: Trefoil factor 1
TFF2: Trefoil factor 2
TFF3: Trefoil factor 3
Tfh: T follicular helper cells
TGF- β : Transforming Growth Factor Beta
TGFB: Transforming Growth Factor Beta
TGF-B: Transforming Growth Factor Beta
TGFBI: Transforming Growth Factor Beta Induced
Th: T helper cells
THBS1: Thrombospondin 1

TIGIT: T Cell Immunoreceptor With Ig And ITIM Domains
TIL: Tumor-infiltrating T-cells
Tim-3: T cell immunoglobulin and mucin-domain containing-3
TIM3: T-Cell Immunoglobulin And Mucin Domain-Containing Protein 3
TLR: Toll-like receptor
TLS: Tertiary lymphoid structures
TME: Tumor microenvironment
TMPRSS15: Transmembrane serine protease 15
TNF- α : Tumor Necrosis Factor alpha
TNF: Tumor necrosis factor
TNFAIP: TNF Alpha Induced Protein
TNFRSF11A: TNF Receptor Superfamily Member 11a
TNFRSF21: TNF Receptor Superfamily Member 21
TNFRSF6B: TNF Receptor Superfamily Member 6BTNFSF12: TNF Superfamily Member 12
TNFRSF12A: TNF Receptor Superfamily Member 12A
TNM: Tumor, nodes, metastasis

TP53: Tumor Protein P53
TP53BP1: Tumor Protein P53 Binding Protein 1
TP53I3: Tumor Protein P53 Inducible Protein 3
TP53INP2: Tumor Protein P53 Inducible Nuclear Protein 2
TPM1: Tropomyosin 1
TPM2: Tropomyosin 2
TRADD: TNFRSF1A Associated Via Death Domain
TRAF2: TNF Receptor Associated Factor 2
TRBC2: T Cell Receptor Beta Constant 2
TXNDC15: Thioredoxin domain containing 15
TYK2: Tyrosine kinase 2
UC: Ulcerative colitis
USP: Ubiquitin Specific Peptidase
UV: Ultraviolet
VCAM-1: Vascular Cell Adhesion Molecule 1
VEGFR3: Vascular Endothelial Growth Factor Receptor 3
WFIKKN2: WAP, Follilastin/Kazal, Immunoglobulin, Kunitz And Netrin
FLT: Fms Related Receptor Tyrosine Kinase

List of Communications

The following thesis consists of:

1. Cázares-Olivera, M*, Miroszewska, D*, Hu, L., Kowalski, J., Jaakkola, U. M., Salminen, S., Li, B., Yatkin, E., & Chen, Z. (2022). Animal unit hygienic conditions influence mouse intestinal microbiota and contribute to T-cell-mediated colitis. *Experimental biology and medicine (Maywood, N.J.)*, 247(19), 1752–1763.
* These authors contributed equally to this paper
2. Miroszewska, D., Song, S*, Urbiola-Salvador, V*, Cázares Olivera, M., Jabłońska, A., Duzowska K, Drężek-Chyła K, Zdrenka M, Śrutek E, Szyłberg Ł, Jankowski M, Bała D, Zegarski W, Nowikiewicz T, Makarewicz W, Adamczyk A, Ambicka A, Przewoźnik M, Harazin-Lechowicz A, Ryś J, Filipowicz N, Piotrowski A, Dumanski JP, Bin Li and Chen Z. Spatial mapping of epithelial changes and suppressive immune populations in colorectal cancer tumor microenvironment. *Unpublished manuscript*
3. Urbiola-Salvador, V., Miroszewska, D., Jabłońska, A., Duzowska K, Drężek-Chyła K, Zdrenka M, Śrutek E, Szyłberg Ł, Jankowski M, Bała D, Zegarski W, Nowikiewicz T, Makarewicz W, Adamczyk A, Ambicka A, Przewoźnik M, Harazin-Lechowicz A, Ryś J, Filipowicz N, Piotrowski A, Dumanski JP, Bin Li and Chen Z. Deep proteomics characterization of colorectal cancer tumor microenvironment enriched in CD4+ T cells. *Unpublished manuscript*
4. Urbiola-Salvador, V., Miroszewska, D., Jabłońska, A., Qureshi, T., & Chen, Z. (2022). Proteomics approaches to characterize the immune responses in cancer. *Biochimica et biophysica acta. Molecular cell research*, 1869(8), 119266.
5. Urbiola-Salvador, V*, Jabłońska, A*, Miroszewska, D., Huang, Q., Duzowska, K., Drężek-Chyła, K., Zdrenka, M., Śrutek, E., Szyłberg, Ł., Jankowski, M., Bała, D., Zegarski, W., Nowikiewicz, T., Makarewicz, W., Adamczyk, A., Ambicka, A., Przewoźnik, M., Harazin-Lechowicz, A., Ryś, J., Filipowicz, N., ... Chen, Z. (2023). Plasma protein changes reflect colorectal cancer development and associated inflammation. *Frontiers in oncology*, 13, 1158261.
* These authors contributed equally to this paper
6. Urbiola-Salvador V, Jabłońska A, Miroszewska D, Kamysz W, Duzowska K, Drężek-Chyła K, Baber R, Thieme R, Gockel I, Zdrenka M, Śrutek E, Szyłberg Ł, Jankowski M, Bała D, Zegarski W, Nowikiewicz T, Makarewicz W, Adamczyk A, Ambicka A, Przewoźnik M, Harazin-Lechowska A, Ryś J, Macur K, Czaplewska P, Filipowicz N, Piotrowski A, Dumanski JP, Chen Z. Mass Spectrometry Proteomics Characterization of Plasma Biomarkers for Colorectal Cancer Associated With Inflammation. *Biomark Insights*. 2024 Jun 20;19:11772719241257739.
7. Le Menn, G., Pikkarainen, K., Mennerich, D., Miroszewska, D., Kietzmann, T., & Chen, Z. (2024). USP28 protects development of inflammation in mouse intestine by regulating STAT5 phosphorylation and IL22 production in T lymphocytes. *Frontiers in immunology*, 15, 1401949.

List of figures

- Figure I.1 Schematic representation of CD4+ T-cell and APCs interaction. Created with BioRender.com
- Figure I.2. Interdependencies between Tregs and Th17 in inflammation and colorectal cancer.
- Figure II.1. Graphical abstracts of research papers included in the thesis. A) and B) summarize publications I and II. C) and D) summarize publications III and IV. E) summarizes publications V and VI. Created in Biorender.com
- Table 6-1. Health monitoring results.
- Figure 6-1. Animal housing environment influences pathogenic potential of colitis.
- Figure 6-2. Hygienic conditions in animal housing environment influences Th subsets.
- Figure 6-3. Microbiota composition between SPF and non-SPF groups
- Figure 6-4. LEfSe analysis.
- Figure 6-5. qPCR detection of selected bacteria strains
- Table 7-1. Primer sequences.
- Table 7-2. Luminex – plasma.
- Figure 7-1. USP28 is expressed in differentiated Th17 and Treg cells
- Figure 7-2. USP28 deficiency alters steady-state immune cell composition.
- Figure 7-3. USP28 protects mice against the early development of DSS-induced colitis
- Figure 7-4. USP28 inhibits expression of IL22.
- Figure 7-5. USP28 plays a role in T cell activation and proliferation through CD28/STAT5 signaling
- Figure 7-6. USP28 contributes to Th17 cell differentiation and iTreg cell function.
- Figure 7-7. USP28 regulates STAT5 signaling in T cells.
- Figure 8-1. Spatial profile of cell composition and TME heterogeneity of colorectal cancer.
- Figure 8-2. Genes expression deviation among epithelial clusters
- Figure 8-3. Spatial characterization of CRC myeloid and T-cell infiltration.
- Figure.8-4. Spatial characterization of the CRC invasive trajectory
- Figure 8-5. Pseudotime analysis of IC aggregates within normal and CRC tissue.
- Figure 9-1. Deep proteomics characterization of C4+ T cell enriched CRC tissue and normal matched tissue.
- Figure 9-2. CRC TME enriched in CD4+ T cells and immune infiltration reflects a complex immune network.
- Table 9.1 – Selected proteins involved in metabolic rewiring, stromal infiltration, immunity
- Figure 9-3. Protein changes within CRC TME associated with CRC progression.
- Figure 9-4. Treg fractions and associated protein changes.
- Figure 9-5. Protein changes are associated with specific cell components of CRC TME.
- Table 10-1. Clinical characteristics of patients with CRC.
- Figure 10-1. Colorectal cancer (CRC) development causes cytokine and oncogenic signaling pathway changes in plasma.
- Figure 10-2. Plasma protein changes induced by cancer-associated inflammation in CRC patients.
- Figure 10-3. Plasma protein expression differences between early and late stages of CRC.
- Figure 10-4. Validation of potential candidate biomarkers
- Figure 11-1. LC-MS/MS analysis of plasma proteome from CRC patients and healthy controls.
- Figure 11-2. Functional annotation of the identified plasma proteins
- Figure 11-3. Colorectal cancer (CRC) development causes plasma protein changes involved in complement cascades and cholesterol metabolism.
- Figure 11-4. Plasma protein changes induced by cancer-associated inflammation in CRC patients.
- Figure 11-5. Plasma protein expression differences between early and late stages of CRC.
- Figure 11-6. Complement protein C5 is a potential diagnostic biomarker for CRC
- Figure 12-1. Bottom-up proteomics workflow.

Figure 12-2. Schematic representation of single-cell spatial proteomics approaches

Table 12 - Summary of the presented emerging single-cell proteomics techniques divided by approaches type and with their corresponding advantages and disadvantages.

Table of content

Abstract	II
Streszczenie	IV
Acknowledgements.....	VI
List of abbreviations	VII
List of Communications.....	XI
List of figures	XII
Table of content	XIV
I. Introduction	- 1 -
1. Colorectal cancer	- 1 -
1.1. Epidemiology	- 1 -
1.2. Etiology.....	- 1 -
1.3. Diagnosis	- 2 -
1.4. Tissue examination, TNM, grading	- 2 -
2. Immune system.....	- 5 -
2.1. Innate immunity	- 5 -
2.2. Adaptive immunity.....	- 7 -
3. T cells subsets.....	- 10 -
4. Inflammation in cancer and IBD – role of Th17/Treg	- 14 -
5. Tumor TME	- 15 -
II. Aims of the thesis	- 17 -
III. Publications	- 19 -
6. Publication I: Animal unit hygienic conditions influence mouse intestinal microbiota and contribute to T-cell-mediated colitis	- 19 -
6.1. Abstract	- 19 -
6.2. Introduction	- 19 -
6.3. Materials and methods	- 20 -
6.4. Results	- 22 -
6.5. Discussion	- 28 -
6.6. References.....	- 32 -
7. Publication II: USP28 protects development of inflammation in mouse intestine by regulating STAT5 phosphorylation and IL22 production in T lymphocytes	- 36 -
7.1. Introduction	- 36 -
7.2. Materials and methods	- 37 -
7.3. Result	- 39 -
7.4. Discussion	- 49 -
7.5. References.....	- 50 -
8. Publication III: Spatial mapping of epithelial changes and suppressive immune populations in colorectal cancer tumor microenvironment	- 52 -
8.1. Introduction	- 52 -

8.2.	Materials and methods	- 53 -
8.3.	Results	- 54 -
8.4.	Discussion	- 64 -
8.5.	References.....	- 67 -
9.	Publication IV: Deep proteomics characterization of enriched CD4+ T cells in colorectal cancer tumor microenvironment.....	- 71 -
9.1.	Introduction	- 71 -
9.2.	Materials and methods	- 72 -
9.3.	Results	- 74 -
9.4.	Discussion	- 85 -
9.5.	References.....	- 88 -
10.	Publication V: Plasma protein changes reflect colorectal cancer development and associated inflammation	- 93 -
10.1.	Introduction.....	- 93 -
10.2.	Methods	- 94 -
10.3.	Results	- 96 -
10.4.	Discussion.....	- 102 -
10.5.	References	- 106 -
11.	Publication VI: Mass Spectrometry Proteomics Characterization of Plasma Biomarkers for Colorectal Cancer Associated With Inflammation	- 110 -
11.1.	Introduction.....	- 110 -
11.2.	Materials and Methods	- 111 -
11.3.	Results	- 113 -
11.4.	Discussion.....	- 121 -
11.5.	References	- 124 -
12.	Publication VII: Proteomics approaches to characterize the immune responses in cancer.....	- 126 -
12.1.	Introduction.....	- 126 -
12.2.	A brief overview of proteomics	- 127 -
12.3.	MS-based proteomics approaches applied to study immune responses in cancer	- 129 -
12.4.	Antibody-based technologies to characterize immune responses in cancer	- 132 -
12.5.	Emerging single-cell proteomics applied to characterize the immune TME	- 133 -
12.6.	Conclusions and future perspectives.....	- 139 -
12.7.	References	- 141 -
III.	Conclusions.....	- 150 -
IV.	Literature	- 152 -
V.	Supplemental.....	- 160 -
VI.	Co-authorship statements	- 162 -

I. Introduction

1. Colorectal cancer

1.1. Epidemiology

By 2040 number of diagnosed cases of colorectal cancer (CRC) is estimated to reach 3.2 million and 1.6 deaths, which is twice as many as recorded in 2020¹. Overall recorded number of cases and mortality is significantly higher for highly developed countries, what most likely is linked to longer life expectancy as CRC is associated usually with age over 50, as well as poor dietary habits as high intake of fat, meat or processed food. With such a high burden of CRC being 2nd leading cause of cancer-related death worldwide, and there is an apparent need to investigate the etiology, diagnostic tools, and development cause to prevent the disease globally².

1.2. Etiology

CRC is an umbrella term for all tumors developed both in colon and rectum part of the large bowel. According to International Classification of Diseases version 10 (ICD-10) classification of CRC include C18 - Malignant neoplasm of colon, C19 - Malignant neoplasm of rectosigmoid junction, and C-20 Malignant neoplasm of rectum³. Although the exact underlying cause is not known yet there are several factors contributing to the development of the tumors. There are several risk factors for CRC i.e. diet, sex, age, obesity, and alcohol consumption, which can be changed by the lifestyle of an individual. However, there are several risk factors that are inherently set with the individual's predisposition.

1.2.1. Genetic factors

Genetic alterations contributing to CRC are mutations within oncogenes or loss-of-function mutations in tumor suppressors. Often CRC arise from adenomas - part of epithelium showing signs of dysplastic change and disturbed differentiation of cells⁴. There are several hereditary conditions linked to the increased CRC risk. However, up to only 30% of all CRC cases have their origin in hereditary conditions, whilst the rest of the CRC cases stem from sporadic somatic mutations, and epigenomic alteration⁵.

There are 3 main pathways of development: chromosomal instability (CIN), including sporadic mutations, microsatellite instability (MSI), and epigenetic CpG island methylator phenotype (CIMP)^{4,6}. CIN pathway affects several genes including mutations in genes encoding tumor suppressor *APC* and *TP53* or activating mutations in genes involved in cellular growth and proliferation such as kirsten rat sarcoma viral oncogene homolog (*KRAS*), B-Raf proto-oncogene, serine/threonine kinase (*BRAF*) and Phosphatidylinositol-4,5-bisphosphate 3-kinase catalytic subunit alpha (*PIK3CA*)⁵. MSI pathway involves mutations within DNA mismatch repair genes (MMR). CRC tumors can be divided into MSI-high and MSI-low types depending on the frequency of frameshift⁶. Mutations of the MMR system were also associated with Lynch syndrome, hereditary condition also known as hereditary nonpolyposis colorectal cancer (HNPCC) causing development of CRC⁷. Lastly, CIMP can be described as aberrant methylation of CpG- regions of promoters of suppressive genes⁸. CRC genetic heterogeneity translates to the efficacy of immune checkpoint therapy response as only tumors with MSI-high, which account for up to 15% of all CRC tumors, show significant response to the therapy⁹. Subtyping based on transcriptomics performed by CRC Subtyping Consortium proposed consensus molecular subtype(CMS) CRC division¹⁰. CMS1 tumors are MSI-H with mutation in *BRAF*, characterized by high infiltration of immune cells. CMS2 tumors typically exhibit upregulation of signaling pathways e.g. Wnt signaling. Moreover, they exhibit high CIN and *TP53* mutations. CMS3 CRC mostly metabolic dysregulation with *KRAS* mutations whilst CMS4, called mesenchymal, exhibit upregulation of TGF- β signaling as well as angiogenesis¹⁰. Tumors of different CMS

show different prognosis and response to therapy, similarly as in MSI-high/MSI-low tumors. CMS4 was linked with worse prognosis in CRC tumors, whilst in metastatic tumors the CMS1 has poor prognosis¹¹. At the same time, both CMS2 and CMS3 show improved overall survival after adjuvant treatment¹².

Inflammatory bowel disease (IBD) is one of the major risk factors for colitis-associated cancer (CAC) development¹³. IBD is a state of chronic inflammation which includes ulcerative colitis (UC) and Crohn's disease (CD). UC causes inflammation of mucosa in colon in rectum what leads to colon shortening, bleeding, and possibly ulcers. CD on the other hand can affect any location along gastrointestinal (GI) tract and can cause "narrowing" of the bowel and fistulas¹⁴. Chronic inflammation in IBD contributes to the CRC development by DNA damage induced by oxidative stress what affects the genes expression. Additionally, affected mucosa is more prone to neoplastic transformation¹³. Although, there were multiple studies across global population, fixed rate risk factor for IBD patients to develop CRC is not yet determined. Study from 2010 indicates the risk to be up to 18% within 30 years of the diagnosis¹⁵. Despite the great advancement in latest years improving the understanding of the cause of the disease, the exact mechanism remains elusive. IBD as an inflammatory disease is mostly dependent on the immune system hence deciphering of immune cells interplay in IBD is crucial for understanding of the disease¹⁶.

1.3. Diagnosis

There are several screening tests available in the clinics for the diagnosis of CRC, however each has significant drawbacks. The most accessible, relatively low in cost, and non-invasive tests are fecal occult blood test (FOBT) that include guaiac-based tests (gFOBT) and immunochemical (FIT)¹⁷. The examined material in both is a sample of patient's stool however they differ in the procedural protocol and principal of detection as, in case of gFOBT, stool sample is smeared on the special paper sheet and if the sample contains hemoglobin, the paper will change the color whilst in case of FIT the detection of hemoglobin is antibody-based¹⁷. With the similar principle of detection is applied in Multitarget Stool DNA Testing (mt-sDNA) although here detection covers not only hemoglobin but also several methylated genes¹⁷. However neither has high specificity of detection and in addition even if the test turns positive for hemoglobin presence it does not necessarily mean presence of the CRC tumor as there are other reasons for bleeding from the gastrointestinal tract. More sensitive, imaging diagnostic tests include flexible sigmoidoscopy and colonoscopy. Both of them carry the burden of possible discomfort for the patient due to the nature of the way of imaging itself. Flexible sigmoidoscopy is a test that allows for e.g. removal of a small suspicious mass or biopsy sampling, however only from the left part of the colon. Despite its proven effectiveness, the limitations are still significant. Finally, colonoscopy allows for examination of the whole colon, however due to the discomfort and relative invasiveness, patients are still reluctant to participate in such examination. Although, colonoscopy is the most popular population screening process, including in Poland, for patients between 50 and 69 years old without previous CRC history¹⁸. Lastly, imaging diagnostic tool is Computed Tomography Colonography (CTC), based on CT scans in two- and three- dimensions of the colon, however such test is very expensive and specialized equipment is needed.

1.4. Tissue examination, TNM, grading

Tumor staging is an important diagnostic factor for patient's prognosis which provides information on the development stage of the tumor and affected neighboring tissues¹⁹. Popular classification guidelines was adopted by American Joint Committee on Cancer (AJCC), called TNM Staging System²⁰, which assessed local invasion of the tumor, invasion to lymph nodes and distant metastasis²⁰. TNM classification takes into consideration tumor tissue, lymph nodes, and presence of metastasis. Tumor (T) category is divided into T1-T4, where T1 indicates tumor affected submucosa whilst T4 indicates invasion to serous membrane of the abdominal cavity. Lymph nodes (N) category is assigned either as N0 if lymph nodes are not affected whilst N1-N3 indicates number of regional lymph nodes affected by the tumor. Metastasis (M) is a metric indicating either presence (M1) or lack thereof (M0) of metastasis. Based on the

TNM classification, tumors are assigned stage on a scale from 0 to 4. In the context of CRC stage 0 indicates carcinoma restricted to epithelial tissue²¹. Stage 1 indicates affected submucosa/muscularis propria without affected lymph nodes or metastasis. Both stage 2 and stage 3 indicate advanced tumors with different level of lymph nodes engagement, whilst stage 4 indicates distant metastasis¹⁹. Furthermore, CRC tumor are often assigned a grade of G1 to G4 based on the histological features. Within the regioG1 are assigned with the least disturbed histology, with differentiated cells present. G2 and G3 indicate moderate and poor differentiation of cells, whilst G4 indicates undifferentiated cells indicating the most advanced tumorigenic process²².

1.4.1. Techniques of tissue analysis

There are several methods and objectives in analyzing the tumor tissue post-resection. Several of them are presented in this section.

1.4.1.1 Hematoxylin & Eosine staining

Tissue coming from the resection is either preserved as a fresh-frozen tissue or paraffin fixed (FFPE). The analysis of both is the same by principal – tissue is cut into thin slices 4-5 um, preserved on the glass slide and stained with dyes to visualize tissue architecture. Most commonly applied staining protocol requires hematoxylin and eosin. Hematoxylin(H) binds to nucleic acids and stain them in deep blue/purple colors, whilst pink eosin(E) binds to protein without specificity²³. Based on this simple protocol, features of the tissues can be assessed. Commonly what is assessed is the level of dysplastic changes in the tissue²². Features of dysplasia include: hyperchromatic nuclei with changed shaped comparing to normal tissue, lower content of mucins, or disruption of the tissue architecture²⁴. Evaluation of HE stained tissue also provides valuable information on the morphology of cell populations present at the affected site, what is impossible to obtain with aforementioned TNM staging.

1.4.1.2 Immunohistochemistry/immunofluorescence staining in tissue analysis

Method of molecular profiling of the tissue include i.e. IHC and IF staining. Both techniques require application of the specific antibody, labeled with horseradish peroxidase or a fluorophore respectively, binding to the protein of interest, although the methods of detection is production of colored product upon addition of chromogenic substrate or excitation of the fluorophore with fluorescence light²⁵. Such approach is widely applied to CRC for detection or lack thereof of proteins involved in MMR system²⁶. IHC/IF stained tissues are also analyzed in the context of immune infiltration, as immune component of CRC plays a vital role in disease progression. Immune scoring system is a method that involves analysis of tumor tissue in the context of cellular component of the immune system and their quantification. Immunoscore[®] involves IHC staining for CD3+ and/or CD8+ T-cells infiltrating tumor core and tumor margin with further image analysis using digital pathology software such as QuPath²⁷⁻²⁹.

1.4.1.3 DNA & RNA testing

Standard PCR and DNA sequencing are often used in CRC diagnostics in MSI detection, copy-number variations, or detection of specific mutations as BRAF variant p.V600E associated with poor response to chemotherapy treatment^{30,31}. Nowadays multiple new technologies are being developed to improve CRC diagnosis and treatment, for example, liquid biopsies testing for circulating tumor DNA (ctDNA)³². BESPOKE CRC clinical trial tested plasma samples of patients who underwent adjuvant therapy for molecular residual disease (MRD) (tumor cells undetectable by imaging methods) with ctDNA and established that disease-free survival rate for patients positive for MRD was longer comparing to the control group without treatment³³. Genomic profiling platforms are also being developed such as multiplex DNA-based analysis tools is MSK-IMPACT. MSK-IMPACT is a DNA sequencing method based on capture-based hybridization which allows for analysis of several hundredth genes in DNA extracted from FFPE tissue^{34,35}. Analysis of 1134 CRC samples with MSK-IMPACT revealed potential novel gene mutations linked to the CRC

development, and differences in gene expression between left and right-sided tumors³⁴. In 2017 MSK-IMPACT was approved by Food and Drugs Administration in U.S.A as a tool for tumor profiling³⁶. Furthermore, RNA-based analysis is gaining more attention in the context of tumor profiling. For example, ColoPrint is a RNA-based microarray panel of 18 genes that can determine tumor samples as low or high risk groups for tumor reoccurrence³⁷ whilst ColoSense™ is a newly FDA approved RNA-based stool screening method for CRC detection with 100% detection rate for stage I and 93% detection rate overall in the studied cohort³⁸⁻⁴⁰.

RNA-based technologies nowadays are stirring towards gene expression maintaining spatial context. There are several methods for RNA analysis however they differ in the detection method or used sample type (fresh frozen vs. FFPE)⁴¹. One of the Spatial Transcriptomic (ST) platforms is Visium, developed by 10x Genomics. In this technology FFPE tissue section is mounted, stained, imaged, and de-crosslinked on a barcoded slide. The glass slides contains “spots” composed of poly-T oligonucleotides able to hybridized mRNA released from the tissue⁴². Based on the hybridized mRNA, cDNA library of gene expression is created^{42,43}. Capture areas available with this technology are 6.5 x 6.5 or 11 x 11mm with 500 and 14000 spots respectively, with the spot size of 55 μm^2 . This technology allows for the detection of 18 000 human genes covering significant majority of protein-encoding genome⁴⁴.

Analysis of the protein expression is another approach widely applied in cancer research. One of them is a cytometry by time-of-flight (CyTOF) known as mass cytometry, developed in 2009⁴⁵. This technology requires single cells suspension where cells are stained with heavy metal isotopes-tagged antibodies against specific proteins. Single cells in a droplet form pass through argon plasma where, upon covalent bonds disruption, atoms are released and ionized. Subsequently, after removal of biologically abundant low-mass ions, heavy-metal ions are analyzed by the time-of-flight to acquire their mass-to-charge ratio⁴⁶. In imaging mass cytometry, instead of single cell suspension, either FFPE or fresh frozen tissue section is required. Tissue sections are incubated with isotope-tagged antibodies, and then subjected to laser ablation $1\mu\text{m}^2$ at a time. Laser ablation causes release of the ions, as in MC, that are detected and assigned to the specific spot⁴⁷. Despite its relatively high multiplexing capacity of analyzing up to 40 markers at one, its high costs, long time required for the data acquisition, and destruction of the sample makes it invalid for wider clinical application^{47,48}. In the context of CRC, IMC technology allowed for identification of high content of FOXP3⁺ T-cells in tertiary lymphoid structures in the colon, quantification of p53 abundance, or identification of abnormal EpCAM⁺ PD-L1⁺ CD4⁺T-cells population⁴⁹⁻⁵¹. There is a similar method to IMC called multiplexed ion beam imaging. MIBI, instead of laser ablation, uses a primary ion beam to release isotope-tagged antibodies and create secondary ions that later on are detected. The advantage of using MIBI is that only a small part of tissue up to 50 μm in thickness is erased what allows for re-analysis of the particular region of interest with another set of antibodies⁵².

Nowadays, there are also methods of tissue analysis that allows for simultaneous analysis of transcriptome and protein expression within one sample. One of them is GeoMX Digital Spatial Profiling (DSP). This technology has similar capacity of detection 20000 genes transcripts as Visium spatial transcriptomics, with additional capacity of ~40 protein expression quantification^{41,53}. Here, selected probes specific to selected genes bound to barcodes via linker sensitive to UV light. After hybridization of probes to the mRNA released from the tissue, tissue is stained with antibodies and fluorescence signal is imaged. Based on the imaging, specific region of interest (or several) is selected with subsequent UV light treatment. Released barcodes from probes are collected, followed by library preparation and sequencing⁴¹. In CRC this technology was employed to identify differences in PD-L1 expression in tumor tissue from patients treated with immunotherapy and chemo therapy revealing its higher levels in samples after immunotherapy⁵⁴. In the study by Pelka et. Al. set of interferon-stimulated genes was detected in epithelial tumor cells with the expression of CXCL13 in the neighboring non-epithelial cells indicating axis of communication between tumor cells and T-cells. Simultaneously, inhibitory IDO1 and CD38 expression, linked to interferon stimulated genes hub, showed spatial correlation with CXCL13⁺T-cells activity⁵⁵.

2. Immune system

Immune system has several roles. It protects from the external pathogens as well as plays a vital role in tumor elimination and progression in the process recently described as “cancer immunoediting” comprising of 3 steps^{56,57}. First step, elimination, is often called “immune surveillance” and involves immune cells system in the process of elimination of the affected cell^{56,57}. Next, equilibrium phase occurs. Equilibrium may last for several years, where less malignant cancer cells are not eliminated but rather “kept at bay” by the immune system which prevents further spread of the cancer cells^{56,57}. Lastly, tumor may escape by a series of mechanisms that prevent its recognition by the immune system i.e. downregulation of presented antigens, expression of certain inhibitory factors, such as CTLA4, or editing of local microenvironment to promote differentiation of immune cells with a suppressive profile⁵⁸.

Hence, although there are several molecular mechanisms preventing malignant transformation such as DNA repair mechanisms, cell cycle arrest or apoptosis, some cells will escape and become a threat to further divide and grow tumors. Immune system is a complex and the most important defense system protecting the host from cancer development.

2.1. Innate immunity

2.1.1. Innate immunity recognition

Immunity is distinguished by innate and adaptive immune response. Innate immunity provides rapid/immediate response and protection against harmful factors for example by prevention of entering the hosts body⁵⁹. For example, by forming a physical barrier (e.g. skin), secretion of lysozyme or lactoferrin in saliva to protect from ingested pathogens, or by recognition of pathogen-associated molecular patterns (PAMPs) expressed on the surface of pathogens by innate immunity cells. Simultaneously, immune cells are capable of recognition of molecules released upon damage or cell death called damage-associated molecular patterns (DAMPs)⁵⁹. There are several types of pattern-recognition receptors. Toll-like receptors are membrane-bound and belong to the PAMPs recognition receptors. Toll-like receptors (TLRs) recognize bacterial peptidoglycans or single/double-stranded RNA of viruses. TLR binding to their ligands activate downstream signaling which leads to activation of interferon response factor 3 and 7 (IRF3 and IRF7) or NF- κ B pathway. IRF3 and IRF7 are transcriptional factors that induce expression of inflammatory molecules e.g. monocytes recruiting cytokine CCL2, neutrophil recruiting chemokine CXCL8, IL-1, TNF- α , and interferons type I, IFN- α and IFN- β , vital for innate immune response against viruses⁵⁹. There are also pattern recognition receptors that instead of recognition outside of the cell, recognize internal damage or infection. They include retinoic acid-inducible gene (RIG)-like receptors and NOD-like receptors and, similarly to TLR, they may mediate inflammation via IFN I response⁵⁹.

2.1.2. Cells of innate immunity

Importantly, the main characteristic of innate immunity is induction of rapid response at the site of infection which includes recruitment of immune cells. Cell engaged in innate immunity responses are neutrophils, macrophages, mast cells, monocytes, dendritic cells, and NK cells⁶⁰. Recruitment of particular cell population to the site of infection/injury is mediated by tissue-resident macrophages and DCs that upon pathogen recognition release i.e. IL-15, IL-1 and TNF⁴. Migration of leukocytes from the bloodstream is mediated by P-, and E-selectin expression on the surface of endothelial cells of a blood vessel near the site of injury or infection. Expression of selectins is mediated by TNF and IL-1 expressed by tissue-resident DCs and macrophages or upon recognition of histamine or thrombin⁵⁹. Selectins are crucial in the process of leukocytes rolling as they facilitate initial contact with the endothelial cells. Next, chemokines released by endothelial cells serve as docking ligands for chemokine receptors expressed on the surface of leukocytes whilst simultaneously integrin ligands, such as VCAM-1 or ICAM-1, are being expressed on the endothelial cells what mediates integrins binding. In result, leukocytes escape blood vessels through the process of diapedesis to the affected site⁴. One of the most important functions of

cells involved in innate immunity is effective neutralization of the pathogen that is achieved by phagocytosis by neutrophils and macrophages⁶¹.

2.1.3. Neutrophils

Neutrophils and macrophages are capable of pathogens neutralization, especially opsonized pathogens. Simultaneously IgG, that is involved in the process of opsonization, and IgM activate the complement cascade, mediate phagocytosis⁴. Neutrophils, the most abundant population of leukocytes in the blood stream, accounting for around 50% of the whole leukocytes' population. Their mechanism of effective neutralization of pathogens is largely mediated by granules that are filled with enzymes (collagenase, lysozyme), that upon release digest the pathogens. Their life span upon recruitment lasts around 2 days. Furthermore they can neutralize necrotic cells by-products they form neutrophil extracellular traps that immobilize microbes however may also affect healthy tissue⁶². CXCL8, expressed by tissue-resident macrophages, is a potent neutrophils chemoattractant, similarly to CXCL1.

2.1.4. Macrophages

Macrophages, in contrast to neutrophils, have a longer life-span at the site of infection⁴. Furthermore, as their effector function largely depends on cytokines production, their activation takes longer. Aside of pathogens, they are able to scavenge for apoptotic cells or tissue debris as well as conduct pyroptosis. Pyroptosis is a programmed cell death mediated by the inflammasome⁶³. During pyroptosis caspase-1 is cleaved and activated which leads to the proteolytical cleavage of IL-1B and IL18 precursors to form biologically active form of these pro-inflammatory cytokines what aids the inflammatory response in pathogens clearance⁶³. Simultaneously, macrophages produce i.e. cytokines such as CXCL2, CXCL3, CCL2, and CCL3⁶¹. At the same time, IL-12 induces the differentiation, proliferation and IFN- γ production in both NK cells and Th1, hence regulating both the innate and adaptive immune response⁶⁴. Macrophages population, depending on the local differential factors, may differentiate either into M1 or M2 sub-populations. M1 macrophages are typically described as "proinflammatory" and able to induce Th1 differentiation, whilst anti-inflammatory M2 macrophages are usually associated with the dampening of the immune response⁶⁵. The plasticity of macrophages population is especially important in the context of cancer TME⁶⁵.

2.1.5. Tissue resident cells

Both tissue-resident macrophages and DCs play an important role in linking the innate and adaptive immunity as both are capable of antigen presentation to T-cells⁵⁹. Additionally, DCs are important in induction of naïve T-cells differentiation due to the array of expressed cytokines⁵⁹. Mast cells, similarly to tissue-resident DCs and macrophages reside at sites with higher risk of exposure to foreign antigens i.e. skin or mucosa. In their cytoplasm they contain granules filled with histamine, released upon activation what leads to increased permeability of surrounding blood vessels. They are important mediators of allergy as on their surface IgE receptors are present that upon binding to IgE induce mast cells activation⁶⁶.

2.1.6. NK cells

In case of NK killers cells instead of pathogen recognition, they play a role in elimination of infected host's cells. They are able to secrete IFN- γ and are able to produce perforins that create pores in the target cell's membrane for efficient proteolytic granzymes delivery released from NK cells granules⁵⁹. They are activated upon IL-12 and IL-15 stimulation and, importantly, they complement cytotoxic T-cells actions as some infected or cancerous cells downregulate the expression of MHC molecules to escape T cells recognition whilst NK cells can recognize cells with downregulated MHC expression⁶⁷. NK cells are major producers of interferon- γ (IFN- γ) and are capable of production both pro- and anti-inflammatory cytokines⁶⁷. Furthermore, in the lymph nodes, they are capable of priming naïve T-cells to Th1 phenotype due to IFN- γ production⁶⁸.

2.1.7. Complement cascade

An important component of innate immunity is complement system which consists of over 30 serum and cell-bound proteins⁶. Although it is crucial for innate immunity, it plays a significant role in regulation of the adaptive immunity response. Complement functions as a series of proteolytic cascades that can result in cell lysis caused by membrane attack complex (MAC), inflammation by anaphylatoxins release, and opsonization by C3b of target cell. There are 3 complement pathways: classical, alternative, and lectin. Each complement pathway results in the cleavage of C3 into C3a and C3b by C3 convertase, and similarly, the cleavage of C5 into C5a and C5b by C5 convertase. The classical pathway involves C1 complex, consisting of C1q, and serine proteases (C1r, C1s), binding to IgG1 or IgM on the surface of recognized pathogen. These serine proteases of the complex activate and cleave C4 and C2 into C4a, C4b, and C2a, C2b, respectively⁶⁹. C4b and C2a form a complex of C3 Convertase that cleaves C3 into C3a anaphylatoxin and C3b. C3b attaches to the surface of pathogens and further is recognized by macrophages or neutrophils via C3 receptor. Furthermore, C3b binds to C3 convertase and create C5 convertase⁷⁰. The lectin pathway, instead of recognition of immunoglobulin bound to the cell surface, is based on the member of pattern-recognition receptor mannose-binding lectin (MBL) which binds to PAMP carbohydrate presented on the surface of bacteria or yeast. MBL forms a complex with MBL-associated serine proteases (MASPs) and, similarly to the classical pathway, these serine proteases cleave C4 and C2. Subsequently it leads to C3 convertase formation, C3 cleavage and C3b binding to the cell surface, and similarly to classical pathway, C5 convertase is created upon C3b binding⁶⁹. On the other hand, alternative pathways hydrolyzed C3 binds to Factor B. Once cleaved by Factor D, in a process stabilized by properdin, it creates C3Bb complex which initiates further cleavage of C3 into C3b and C3a. Once C3Bb on the cell surface binds C3b it creates C5 convertase. Eventually, C5 convertase, regardless of the pathway, cleave C5, releases C5b and C5a. In the series of binding events C5b binds to C6-C7-C8 and numerous C9 molecules. C9 molecules form in the cell membrane pore-like structures what collectively is known as a membrane attack complex (MAC)⁶⁹. These pores disrupts cell's integrity, causes osmotic shock, and swelling what leads to the cell lysis^{59,69}.

2.2. Adaptive immunity

In contrast to innate immunity, adaptive immunity is more specialized and “tailored” to respond to the antigen with high specificity⁷¹. Adaptive memory largely rely on T-cells and B-cells. The main role of adaptive immunity is distinguish between “self” and “non-self” antigen, and to develop memory response so at the next encounter of antigen, the antibody-mediated response occurs rapidly⁷¹. Adaptive and innate immunity work in tandem as DCs or macrophages engaged in the innate response are capable of antigen presentation – process crucial in “teaching” the adaptive immunity⁷¹. Initial contact with the antigen leads to activation of T-cells and B-cells, their activation, and their partial differentiation into memory cells capable to recognize the antigen years after the first encounter. Ability of memory development by the adaptive immunity is a basis for successful vaccination program and maintenance of herd-immunity^{72,73}.

2.2.1. B-cells development

Adaptive immunity can be divided into cell- or antibody-mediated. Antibody-mediated immunity relies on the ability of B-cells to produce immunoglobulins (antibodies). B-cells develop in bone marrow from common lymphoid progenitor (CLP). One of the genes essential in B-cells development is EBF1 which regulates expression of CD79a, one of the B-cells markers, and Pax5 found to be essential for B-cells commitment to pro-B cells⁷⁴. In bone marrow pro-B cells develop in three stages according to the V(D)J rearrangement of antibodies, heavy and light chains, process mediated by RAG1 and RAG2, DNA binding and cleaving enzymes. V(D)J rearrangement leads to the production of antibodies able to recognize over 5×10^{13} antigens⁷⁵. It results in pro-B cells expressing pre-B-cell receptor (pre-BCR). Pre-BCR is crucial in

maintaining cell's proliferation, differentiation, and survival⁷⁶. Pre-BCR undergoes further development to form fully mature BCR. Those that have functional B-cell receptor (BCR) and express surface-bound IgM leave the bone marrow and migrate to spleen where they undergo selection for high-affinity to foreign antigens and low-avidity to self-antigens⁷⁷. Later on, they become mature B-cells expressing BCR, IgM, and IgD into either marginal-zone B-cells upon weak BCR signaling and notch homolog protein 2 (NOTCH2) expression or follicular B-cells upon strong BCR signaling. Marginal-zone B-cells reside in spleen are mainly involved in recognition of T-independent antigen, support germinal center (GC), and produce unspecific IgM^{78,79}. On the other hand, follicular B-cells reside both in spleen and lymph nodes are almost exclusively responsible for production of isotope-switched, high-affinity antibodies upon T-cells. Furthermore, they can develop into memory B-cells and plasma cells⁷⁹. BCR receptor consist of membrane bound IgM or IgD and Igα/Igβ (CD79A/CD79B) heterodimer that aids expression of membrane Igs and transmits the signal through immune receptor tyrosine-based activation motif (ITAM) located in the cytoplasmic end⁸⁰.

2.2.2. BCR signaling

Upon BCR receptor binding to its cognate antigen cytoplasmic ITAM domains are phosphorylated by Src kinases, such as LYN and FYN, what recruits and activates Syk⁸¹. Syk phosphorylates BLNK, BCAP, SHC that form a scaffold for other protein that together form a BCR signalosome. BCR signalosome recruits and activates PI3Kδ which converts PIP2 to PIP3 with subsequent BTK activation. Downstream signalling induces PLCγ2 activation and IP3 and DAG generation⁸¹. IP3 activates transcriptional factor NFAT by inducing Ca²⁺ release from the ER whilst DAG signalling leads to CARD11-BCL10-MALT1 complex formation and NF-κB activation. Simultaneously PIP3 recruits AKT kinase, which is activated by PDK1 and mTORC2. Activated AKT phosphorylates GSK3 and FoxO what downregulates the expression of proapoptotic protein what leads to the cell survival affecting cell survival⁸². Furthermore, BCR binding activates MAPK pathway that regulate cells survival and proliferation⁸¹.

2.2.3. T- cells development

All T-cells are developed from thymocytes, originating from common lymphoid progenitor cells, similarly to B-cells, that leave the bone marrow and migrate to thymus, which unique environment provides necessary stimulation for T-cells development⁵⁹. In the thymus they enter the double negative stage that is further divided into 4 stages based on the expression of surface markers c-KIT, CD44, and CD25. At first, thymocytes express only c-KIT and CD44. Upon stimulation within mid-cortex CD25 expression is induced with simultaneous downregulation of CD44 and c-KIT⁸³. In CD44^{low}CD25^{high} thymocytes V(D)J recombination within TCR-β, TCR-δ, and TCR-γ. V(D)J recombination is vital for adaptive immunity as it allows for recognition of variety of different antigens⁸⁴. Importantly, simultaneously as CD44 expression declines, upregulation of RAG occurs. RAG1 and RAG2 are crucial for TCR genes rearrangement. If γδTCR rearrangement was successful these cells become γδ T-cells and escape the thymus^{59,83}. In case of TCR-β rearrangement, once cell start expressing β-chain, it forms pre-T-cell receptor of β-chain and a “surrogate” pre-T cell α-chain that together form a complex with CD3 on the cell surface^{59,83}. It leads to the termination of rearrangement within TCR-β gene, proliferation of the cell, TCR-α chain gene rearrangement and substation of pre-T cell α-chain, and induction of CD4 and CD8 expression with simultaneous downregulation of CD25 (except for Tregs), c-KIT, and CD44^{59,83}. Next, double-positive selection takes place by recognition of MHC-I and MHC-II. Cells that fail the recognition of either undergo apoptosis. Upon binding, these cells loose the expression of one of the MHC class, yielding CD4+ T helper cells able to recognize MHC-II and CD8+ T cytotoxic cells able to recognize MHC-I^{59,83}. Lastly, cell are migrating to medulla region of the thymus where stromal cells, by AIRE and FEZF2 transcriptional factor, promote expression of a great variety of self-proteins, to provide environment where T-cells recognizing self-antigens⁸⁵. It is vital for negative selection of cells that bind to MHC proteins either with too high/low affinity or without presented antigen. This selection process only 2% of T-cell successfully pass and become naïve

T cell which migrate to secondary lymphoid organs where they can interact with DCs^{59,83}. Upon recognition of the specific MHC II-bound antigen, naïve CD4 T-cells become activated, rapidly proliferate and differentiate into specific subset.

2.2.4. TCR signaling and activation

TCR receptors consist of either of the two heterodimers: TCR α /TCR β or TCR γ /TCR δ . Majority of T-cells present $\alpha\beta$ TCR, whilst $\gamma\delta$ T-cells constitute a minority of the population⁸⁶. Either of them bind in a non-covalent hydrophobic interaction with 3 CD3 protein dimers: $\delta\epsilon$ and $\gamma\epsilon$ heterodimers and $\zeta\zeta$. CD4 and CD8 coreceptors are expressed as a form of monomer with 2 V domains and 2 C domains in the extracellular domain in case of CD4 or homo/heterodimers of CD8 isoforms in case of CD8 T cells. CD8 T cells usually express CD8 $\alpha\beta$ heterodimer but intraepithelial lymphocytes express CD8 $\alpha\alpha$ ⁸⁷.

CD3, similarly as CD79A/CD79B in BCR, contains ITAMs motifs. Upon binding of MHC molecule presenting peptide and TCR, phosphorylated at their tyrosine residues by SRC kinases (LCK and FYN). Simultaneously Zap70 kinases bind to ITAM via SH2 domain. Zap70 phosphorylates linker for activation of T cells (LAT) that recruits PLC γ 1, Grb2 and Gads. PLC γ 1 hydrolyzes PIP2 into IP3 and DAG, similarly as in BCR signaling⁸⁷. IP3 triggers Ca²⁺ release from ER and leads to NFAT translocation to the nucleus what activates NF- κ B signalling⁸⁸. DAG leads to the stimulation of RAS, what is further reinforced by SOS-Grb2. Ras activates Ras-MAPK cascade leading to phosphorylation of MEK1/2 and ERK1/2. Activation of Ras-MAPK signalling regulates the T-cells development and differentiation, and simultaneously leads to AP-1 complex formation. AP-1 work in synergy with NFAT and induce the expression of IL-2⁸⁸. Furthermore, upon TCR engagement, mTOR1 and mTOR2 become activated that are critical in further T-cell lineage commitment⁸⁹.

MHC-antigen complex recognition by TCR is not sufficient for activation of T-cells. It requires “second signal” such as binding of CD28 on T-cells with co-stimulatory ligands B7-1 (CD80)/B7-2 (CD86) presented on the surface of APCs. CD28 ligation is crucial for T-cells signalling as it induces expression of IL-2, vital for the survival and further differentiation⁹⁰. CD28 can also be hijacked by co-inhibitory CTLA4 what inhibits T-cells activity⁹⁰. There are several stimulatory interactions such as CD40-CD40L, OX40-OX40L or GITR-GITRL, and inhibitory interactions such as PD1-PDL1, LAG3-MHC, LAIR1-collagen, TIM3-Galectin 9, that regulate the T-cells activity to precisely control the immune response however some of them can be hijacked by e.g. tumors to escape the recognition⁹¹.

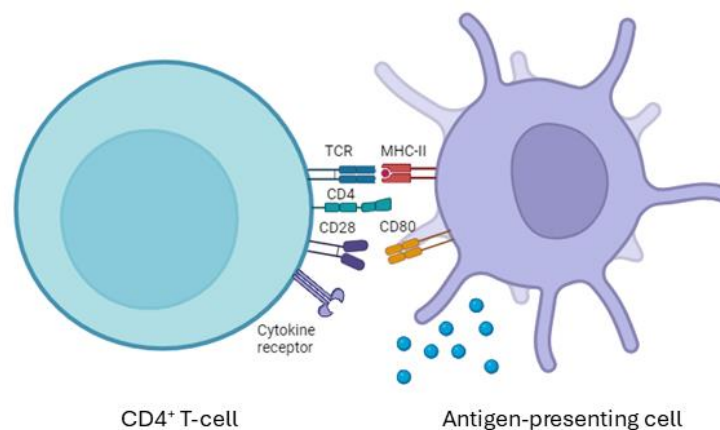


Figure I.1. Schematic representation of CD4⁺ T-cell and APCs interaction. Created with BioRender.com

2.2.5. MHC molecules

Antigen presentation by MHC molecules is another key component of the adaptive immunity. Genes encoding MHC molecules, otherwise known as human leukocyte antigens (HLA) are located in chromosome 6 and are characterized by high polymorphism⁹². There are 2 MHC classes: class I and class

II, recognized by CD8⁺ cytotoxic or CD4⁺ helper T-cells, respectively. MHC class I is further subdivided into classical HLA-A, -B, and -C, and non-classical HLA-E, F, G, H. Classical HLAs are widely presented on different type of cells whilst non-classical HLAs are restricted to the specific tissues or cells⁹³. Moreover, non-classical HLAs, bind peptides of smaller diversity and are often linked to the diseases as e.g. HLAs -E and HLA-G were implicated with immune evasion in cancer and viral infections^{94,95}. MHC II class consists of HLA-DR, HLA-DP, and HLA-DQ expressed exclusively on antigen presenting cells⁹⁶. MHC class I molecules are heterodimers of α -chain and β -chain, also called β 2-microglobulin (B2M) that are bound by a non-covalent bond. MHC I molecule is embedded in the cell membrane by α -chain transmembrane domain (α 3) domains α 1 and α 2 form a binding groove for peptides (antigens) of up to 11 amino acids in length. β -chain stabilizes the heterodimer and has no transmembrane region. MHC II heterodimer on the other hand, is embedded in the cell membrane by transmembrane domains of both α and β chains whilst the antigen-binding groove, formed by α 1 and β 1 domains is able to bind peptides of up to 18 amino acids⁹⁷. The antigen loading onto the MHC molecule differs between the classes. In case of MHC I, ubiquitinated proteins in the cytosol are directed to and digested by the proteasome into shorter peptides⁹⁸. Then, antigen processing and presentation transporter (TAP) loads these peptides into ER where they bind to the MHC class I. Simultaneously, in the ER lumen, chaperon proteins assemble the MHC I complex. MHC class I molecule-chaperons complex associates to the TAP and peptide loading onto MHC I groove takes place. Next, MHC class I-peptide complex, by Golgi apparatus, is transported to the cell membrane⁹³. MHC II class molecules are able to bind to a greater variety of antigens comparing to MHC I. The main function of the MHC II is presentation of foreign antigens. The source of these antigens are e.g. phagocytosed bacteria⁹⁹. Similarly to MHC I, MHC II is synthesized in the ER in the process guided by invariant chain (I chain) or CD74¹⁰⁰. I-chain later on guides MHC II complex to the late endosomal compartment, MIIC¹⁰¹. I-chain is then degraded to class II-associated invariant chain peptide (CLIP) that stays bound to the antigen binding groove¹⁰¹. Subsequently, CLIP is removed by HLA-DM to allow antigen binding, and MHC II complex is transported to the cell membrane¹⁰⁰.

3. T cells subsets

Naïve T-cells are capable of differentiation towards different effector T-cells upon various environmental factors. Each T-cell population poses a different function, however in some cases, expressed cytokines profiles might overlap. Whilst CD8⁺ T-cells main function is to kill damaged/infected cell by FAS-FASL interaction or granzyme production, CD4⁺ T-cells outnumber CD8 T-cells in healthy conditions in human body^{102,103}. Hence, in this section differentiation and function of Th1, Th2, T follicular Th17, and Treg cells is described.

3.1.1. Th1

Th1 phenotype is characterized by the expression of cytokines IL-2, IL-12, TNF α , IFN- γ and is mainly engaged in eradicating pathogens like viruses and bacteria infections by activation of macrophages^{104,105}. Th1 population differentiates from naïve T cells by environmental IL-12 stimulation expressed by i.e. antigen presenting cells^{106,107}. Some studies indicate participation of other cytokine in induction of Th1 phenotype such as IL-18. IL-18, although on its own cannot induce proliferation, it enhances production of IFN- γ what indirectly impacts the Th1 differentiation¹⁰⁸. At the same time, IL-12 can enhance expression of IL-18 receptor, IL-18R α , in a IFN- γ -dependent manner¹⁰⁹. IL-12 receptor consists of IL-12R β 1 and IL-12R β 2 subunits associated with Janus family kinases members TYK2 and JAK2, respectively. Upon IL-12 binding TYK2 and JAK2 phosphorylate STAT4 transcriptional factor¹¹⁰. Next, STAT4 undergoes dimerization, translocation to the nucleus and induces transcription of several genes crucial genes such as IFN- γ and IL12RB2¹¹¹. In a similar manner, IFN- γ binding to its receptor, consisting of IFN- γ R1 and IFN- γ R2 subunits, leads to phosphorylation of STAT1 via Jak1 and Jak2¹¹². Jointly, STAT1 and STAT4 signaling lead to induction of T-bet expression, also called master transcription factor responsible for induction of expression of signatory cytokines in Th1¹¹³.

3.1.2. Th2

Th2 lymphocytes play a role in protection against parasites, and tissue damage repair by their ability to activate eosinophils, mast cells, basophils, and induce M2 polarization in macrophages^{114,115}. At the same time Th2 subset is implicated in allergy and asthma due to their ability to impact B-cells to switch immunoglobulin class to IgE mediated by the expression of IL-4^{116,117}. IgE in turns binds to FcεRI receptor on mast cells and basophiles what upon re-exposure to the allergen, leads to the their activation and release of i. e. histamines, cytokines, and prostaglandins acting inducing inflammation⁵⁹. Signatory cytokines expressed by this subset are IL-3, IL-4, IL-5, IL-13 and similarly as in the case of Th1, one of the signatory cytokines, namely IL-4 controls the differentiation of this subset. IL-4 binds to its receptor consisting of IL-4Rα (CD124) subunit and IL2RG, which is shared among receptors of other cytokines¹¹⁸. Subsequently, STAT6 transcriptional factor becomes phosphorylated, in a process mediated by JAK1 and JAK3 kinases, and induces the expression of major transcriptional factor GATA3 which bind to locus of IL-13, IL-4, and IL-5 genes¹¹⁸. In addition, Th2 might be primed in a IL-4 independent process by IL-2/STAT5 signaling pathway to express *Il4ra*^{119,120}. Although there are studies in mice models implicating Th2 population with enhanced colon tumors growth, in Rag1^{-/-} mice administered with polarized Th2 cells noted reduced colon tumor growth comparing to the controls, due to high secretion of IL-5, increased eosinophiles recruitment and increased expression of cytotoxic factors, *Gzmb* and *Prf1*, which shows that the role of Th2 cells in tumorigenesis can be context-dependent and that under certain conditions, Th2 cells can exert anti-tumorigenic effects despite their involvement in M2 macrophages polarization^{121,122}.

3.1.3. T follicular helper cells

Unlike Th1 or Th2 mainly engaged in the defense against pathogens and parasites, the primary role of T follicular(Tfh) cells is regulation of B-cells within germinal centers of secondary lymphoid organs. This interaction is crucial for the formation of high-affinity antibody-producing plasma cells and long-lived memory B cells¹²³. Tfh as a population was first identified in 2009 when B-cell lymphoma 6 (BCL6) was found to play a vital role as a lineage-specific transcription factor of Tfh, with earlier reports identifying CXCR5⁺T-cells as effective in induction of antibodies production by B-cells¹²⁴⁻¹²⁷.

Priming and differentiation of T follicular cells depends on many factors, unlike e.g. Th1. Initial contact with conventional DCs induce naïve T-cells to express CXCR5, ICOS, and master repressor Bcl6, which suppresses expression of transcription factors specific to other T-cells populations. In addition, expression of Bcl6 highly depends on the IL-6 controlled signaling via engagement of STAT1 and STAT3, and ICOS¹²⁸⁻¹³¹. Bcl6 inhibits expression of CCR7 and indirectly upregulates expression of CXCR5 crucial for Tfh cells migration to B-cells follicles border, where they interact with B-cells via ICOS-ICOSL and CD40-CD40L signaling to induce B-cells activation, differentiation, and proliferation what in turns leads to creation of germinal centers(GC). In GCs Tfh mature to GC Tfh expressing CXCL13, IL-21, and IL-4, cytokines crucial for the maintenance of B-cells differentiation¹³¹⁻¹³⁴. As a population participating in shaping enduring humoral immunity via B-cells stimulation, Tfh were found to correlate with better survival in CRC patients¹³⁵.

3.1.4. Th17

In 1995, researchers discovered expression of IL-17 in T cells, marking a significant milestone in immunology¹³⁶. A decade later, in 2005, the distinct Th17 cell population was proposed, highlighting it as a newly recognized subset within the T-helper cell family^{137,138}. This identification underscored the unique role of Th17 cells in immune responses and inflammation¹³⁷. Th17 is a pro-inflammatory T cells subset, expressing signatory cytokines IL-17A, IL-17F, IL-21, and IL-22, widely engaged in inflammation in response to pathogens but also involved in autoimmune diseases including IBD¹³⁹. First reports identified IL-23 cytokine, which shares subunit p40 with Th1-specific IL-12, as potent inducer of IL-17 expressing T-cells¹⁴⁰⁻

¹⁴². This discovery arose from observations in knockout mice lacking interferon signaling components IFN- γ and IL-12R β 2, which remained susceptible to autoimmune diseases^{143,144}. This challenged the initial assumption that Th1 cells were solely responsible for pathological Inflammation^{143,144}. In mice models, determining differential factors for Th17 are TGF- β and IL-6 whilst IL-23 plays a role in the expansion and survival¹⁴⁵. On the other hand, studies on human naïve CD4 T-cells revealed that stimulation with IL-1 β in combination with IL-6 or IL-23 is sufficient to induce expression of signatory IL-17 and, whilst co-stimulation with IL-23, is sufficient to induce expression of master transcriptional factor ROR γ ^{146,147}. Despite differences in the signaling needed for the differentiation in mice and human T-cells, agreed consensus highlight importance of IL-6 and TGF- β in the development of Th17 population.

IL-6 binds to its membrane receptor IL-6R consisting of IL-6Ra chain and the gp130 subunit. Upon binding, activation of gp130 subunits leads to activation of JAK1 and JAK2 and phosphorylation of STAT3 transcriptional factor¹⁴⁸. STAT3 directly binds to *Rorc* and *Il21* promoter sites inducing their expression^{149,150}. ROR γ t (product of *Rorc*) induce expression of signatory Th17 cytokines, whilst IL-21 (product of *Il21*) induce expression of IL-17 and further expression of ROR γ t^{149,150}. Simultaneously, TGF- β signaling leads to the activation of SMAD pathway which precise mechanism of action is not well understood. TGF- β signaling leads to SMAD2 and SMAD3 receptors phosphorylation which interact with SMAD4 mediator to form a complex^{151,152}. There are reports indicating SMAD2 role in modulation of IL-6R expression in T-cells and impaired ability for Th17 differentiation in the absence of SMAD2^{151,152}. On the other hand, Smad3 knock-out in mice led to increased Th17 cell differentiation as SMAD3 decreases the activity of ROR γ t¹⁵³. Nonetheless, there is evidence that TGF- β and IL-21 induce differentiation of human naïve T-cells to Th17 and induce expression of RORC2 (homolog of ROR γ t in humans)¹⁵⁴. In addition, TGF- β inhibits activation of SOCS3, negative regulator of STAT3 signaling, induced by IL-6 what further supports Th17 signalling¹⁵⁵. Hence, despite extensive research on the exact mechanism of action and significance of TGF- β it is not well characterized how this cytokine contribute to the development of Th17 population. Furthermore, murine models showed that the differentiation of the Th17 population induced with IL-23, without TGF- β , leads to the expression of T-bet, a master transcription factor for Th1¹⁵⁶. This results in Th17 lymphocytes that can produce Th1-signatory cytokines such as IFN- γ ¹⁵⁶. Pathogenic IFN- γ -expressing Th17 cells may participate in conditions such as multiple sclerosis¹⁵⁷. Th17 have also gained attention in the context of gut microbiota. In mice model in the intestinal environment, Th17 is induced by i.e. segmented filamentous bacteria (SFB) adherence to the epithelial cells what triggers expression of serum amyloid A (SAA) and reactive oxygen species (ROS) that indirectly induce Th17 whereas in germ-free models, Th17 are not detectable in the gut environment what indicates a strong link between microbiota and local Th17 development^{158,159}. Additionally, for Th17 induction, presentation of specific bacteria antigens by DCs in the intestine is required¹⁶⁰. Furthermore, SFB metabolites may also participate in Th17 induction. SFB produce aldehyde dehydrogenase (ALDH), enzyme that converts vitamin A into retinoic acid (RA) which, at physiological conditions induce Th17 whilst in high concentrations repress Th17¹⁶¹. At the same time, T-cells deficient in Retinoic acid receptor alpha (RAR α) are unable to differentiate into Th17 what highlights the vital role of vitamin A in the development of this population¹⁶¹. As Th17 is an abundant population in the intestine, its regulation by gut-microbiota is one of the mechanisms to maintain homeostasis to avoid excessive inflammatory response¹⁶². Moreover, Th17 excessive activation has been linked to several autoimmune diseases¹³⁹.

3.1.5. Tregs

Tregs is T-cells population mostly involved in self-tolerance and homeostasis by regulating other immune cells such as regulating differentiation of Th1 and Th2 or production of Ig by B-cells^{163,164}. The discovery of Tregs overlapped with the discovery of Th17 as in 1995 studies on CD4⁺ CD25⁺ T-cells were published in which this population was linked to maintaining self-tolerance whilst in 2003 studies discovered Foxp3 as a master transcription factor for this population^{165,166}. In fact, FOXP3 is crucial for proper immune homeostasis as mutation in *FOXP3* gene lead to Immune Dysregulation,

Polyendocrinopathy, Enteropathy, X-linked Syndrome (IPEX)¹⁶⁷. Tregs are heterogenic population that can be divided into Tregs developed in thymus (tTreg) and developed in the peripheral tissues after antigen encounter (pTreg) with high TCR affinity towards self-antigens and foreign-antigens, respectively^{168,169}. In mice models, despite different genes expression, tTregs and pTregs were shown to work synergistically in colitis treatment¹⁷⁰. Although functionally linked, tTregs and pTregs have separate development pathways. In thymus, tTreg development can be divided into 2 steps: TCR dependent and independent phase. In TCR-dependent phase upon strong TCR signaling and recognition of self-antigens with high affinity, population of CD25^{hi}FOXP3-CD4+CD8- thymocytes arises. Then, in the TCR-independent stage, interleukins IL-2 and IL-15 induce FOXP3 expression in the absence of antigen presenting cells¹⁷¹. Upon IL-2 binding, dimerization of IL-2RB and IL-2RG occurs, what leads to JAK1 and JAK3 activation, and phosphorylation of transcriptional factor STAT5. Phosphorylated STAT5 dimerizes, translocates to the nucleus where it binds to its target genes promoters and induce expression of i.e. FOXP3¹⁷². On the other hand, pTregs differentiation requires additional signaling of TGF-B, retinoic acid or short chain fatty acids. pTregs can develop from naive CD4+ T cells when stimulated with TGF-B. TGF-B binding to TGF-BR leads to phosphorylation of transcription factors SMAD2 and SMAD3. Either one can bind to Smad4 or TIF1y and, as a complex, be translocated to the nucleus to induce expression of FOXP3¹⁷³. SMAD2 and SMAD3 are important for Tregs development as knock-out of SMAD2 and SMAD3 in mice models was lethal already at embryonic stage of development leads to inflammatory conditions^{174,175}. However, for stable FOXP3 expression, IL-2 is required showing synergistic effect of TGF-B/IL-2 in maintenance of pTregs¹⁷⁶. Furthermore, Smad3 was found to collaborates with NFAT to induce histone acetylation within FOXP3-enhancer region¹⁷⁷. Retinoic acid (RA) may facilitate TGF-B-induced FOXP3 expression by enhancing SMAD3 binding to the enhancer region. Simultaneously, this process may be inhibited by IL-27¹⁷⁸. This population is characterized by the expression of its signatory, immunosuppressive cytokines: IL-10, IL-32, and TGF-B. Generally, Tregs account for up to 10% of all CD4+ T cells, however particularly high levels of Tregs are observed in human intestines¹⁷⁹. Higher proportions of Tregs in the intestine is linked to the local immune cells compositions, especially DCs¹⁸⁰. CD103+ DCs of gut-associated lymphoid tissue (GALT) are able to produce RA, from vitamin A, which induces Tregs to express gut-homing molecules CCR9 and a4b7¹⁸⁰. Furthermore, via $\alpha\text{v}\beta\text{8}$, these DCs are capable of latent TGF-B activation to induce Tregs differentiation locally¹⁸¹. In addition, commensal bacteria of gut microbiota can produce short-chain fatty acid butyrate can further induce Tregs activation and proliferation⁵⁹.

Tregs are potent immunosuppressive population capable of inhibiting other effector T-cells as well as B-cells, NK-cells, and DCs among others¹⁸². One of the main inhibitory molecules expressed by Tregs is CTLA4, also expressed on activated T-cells. Structurally, CTLA4 is similar to CD28, and both of these can bind to CD80/CD86 expressed on APCs, but CTLA4 has much higher affinity of binding^{59,182}. Upon binding, in the process of trans endocytosis, CTLA4 bound to its ligand, is internalized and effectively availability of CD80/CD86 on APCs decreases what prevents other T-cells activation^{59,182}. Despite the fact that CTLA4-mediated immunosuppression participates in pathological states such as cancer, in humans CTLA4 haploinsufficiency causes abnormal lymphocyte infiltration of organs whilst CTLA4 mutation leads to the dysregulation of T-cells and B-cells^{183,184}. In mice, CTLA4 deletion is fatal at 3-4 weeks of age therefore CTLA4 expression is crucial for maintenance of immune homeostasis¹⁸⁵. CTLA4 interaction with CD80/CD86 expressed by APCs, induces expression of enzyme indoleamine 2,3-dioxygenase (IDO), which regulates tryptophane metabolism by converting tryptophane into other metabolites, effectively leading to tryptophane starvation in T-cells and apoptosis of i.e. Th1 cells^{186,187}. One of the tryptophane metabolites is kynurenine which plays a vital role in regulating immune response. Kynurenine participates in induction of naïve T-cells differentiation towards Tregs phenotype whilst simultaneously inhibits ROR γ t¹⁸⁸. Furthermore, IDO1 activity and kynurenine, in tumor microenvironment, induce CD8+ T cell exhaustion¹⁸⁹. Lymphocyte-activation gene 3 (LAG3) is an inhibitory receptor, CD4 homolog, with which it shares the ability to bind to MHC II what limits the availability of MHCII for T-cells activation¹⁹⁰. It is highly expressed on activated T-cells and constitutively expressed on Tregs, hence it is proposed to play a role in Tregs-

mediated immunosuppression¹⁹¹. Furthermore, by high expression of CD25 receptor, Tregs scavenge IL-2 what leads to IL-2 deprivation, induction of apoptosis of CD4+ T-cells, and inhibition of CD8+ T-cells^{192,193}. Except for expression of specific molecules on the surface, Tregs modulate immunosuppression by expression of cytokines, granzymes, and perforins. Expression of IL-10 and TGF-B contributes to suppression of CD8+ response against cancer, whilst IL-10 on its own was found to induce expression of B7-H4 on DCs which negatively affects T-cells response^{194,195}. Simultaneously, expression of perforins and granzyme A leads to cell death in monocytes, DCs, and T-cells¹⁹⁶. Furthermore, TIGIT+ Tregs modulate dendritic cells cytokines production by TIGIT-PVR binding, what leads to elevated production of IL-10 with parallel downregulation of IL-12 production, and subsequently inhibition of T effector cells functions¹⁹⁷. TIGIT+ Tregs-derived IL-10 together with fibrinogen-like protein 2 (Fgl2) suppress production of pro-inflammatory interleukins, IL-12 and IL-23, by DCs what leads to the inhibition of Th1 and Th17 cells¹⁹⁸.

3.1.6. T cells plasticity

The "Th1/Th2 paradigm" was discovered in 1986. It stated that T cells can be categorized into distinct populations based on their cytokine profiles¹⁹⁹. However, since then T-cells plasticity, so "switch" in the expression between different cytokines, has been widely discussed, particularly in the context of Th17 and Tregs. These two populations are linked at their development by TGF-B stimulation. There is evidence confirming that depending on the concentration TGF-B, together with other stimuli, may prompt the differentiation towards either one of the populations. High concentrations of TGF-B, together with stimulation by IL-6 and IL-21 promote the expression of IL-23 receptor what favors Th17 differentiation. On contrary, low concentrations of TGF-B, the expression of IL23r is downregulated what leads to the differentiation towards Tregs²⁰⁰. In addition, FOXP3 was found to physically bind to ROR γ t preventing the differentiation towards Th17 phenotype²⁰¹. Differentiation of these populations is also jointly controlled by retinoic acid. In hypoxic conditions, HIF1 α can hydroxylase FOXP3 and direct it for degradation whilst simultaneously promote expression of ROR γ t²⁰². In mice models, Tregs via IL-6/STAT3 activation can produce IL17, Th17 signatory cytokine, hence IL-6 was proposed as one of the main regulators of balance between Treg and Th17^{203,204}. There are also several reports investigating suppressor functions of ROR γ t+ Th17-like Tregs and inflammatory properties of IL-17+ Th17-like Tregs and their role in various inflammation-related diseases what shows the significance of Treg/Th17 in immune²⁰⁵⁻²⁰⁷.

4. Inflammation in cancer and IBD – role of Th17/Treg

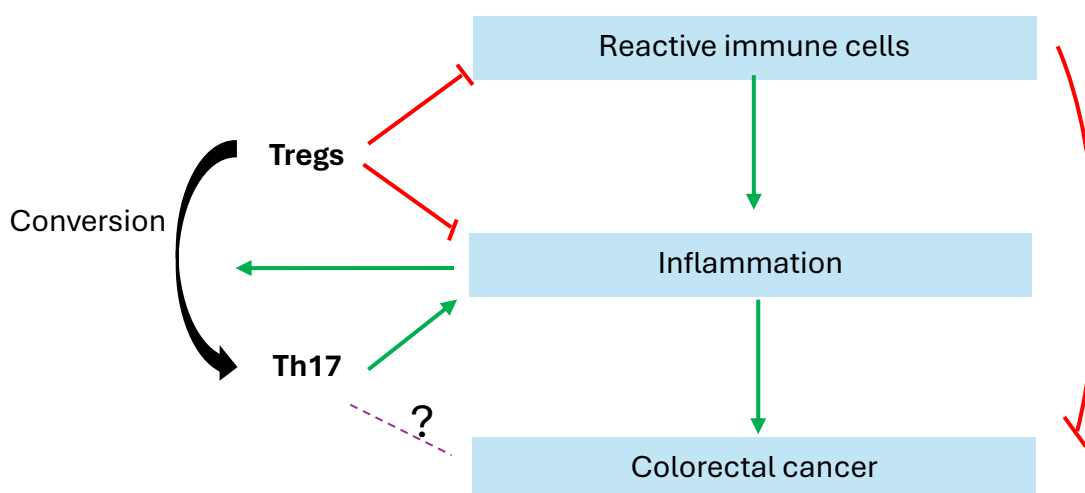


Figure I. 2. Interdependencies between Tregs and Th17 in inflammation and colorectal cancer.

Both Th17 and Tregs populations are abundant in the intestine and are regulated by the local gut microbiota²⁰⁸. However, dysregulation of their function has been linked to multiple diseases including inflammatory bowel disease (IBD)²⁰⁸. In the physiological conditions Th17 induce the expression of polymeric immunoglobulin receptor (pIgR), via IL-17 expression, what facilitates transport of IgA from lamina propria to the intestine lumen, whilst Treg can control Th17^{209,210}. In addition, IgA can induce the expression of peptides with antimicrobial properties, and may influence the expression of proteins involved in tight junction formation what effectively translates to the protection from infections, whilst the differentiation of Th17 population highly relies on the gut microbiota^{159,161,211}. Disruption in gut microbiota composition and growth of e.g. SFB that indirectly contribute to the excessive Th17 differentiation²¹². Furthermore, IL-23 derived from i.e. activated DCs promotes Th17 to produce pro-inflammatory IL-17 and IFN- γ what promotes the disease progression²¹³. Furthermore, Th17-derived IL-8 leads to the accumulation of neutrophils which prolong the inflammation by release of NETs^{214,215}. Simultaneously, there are studies indicating ROR γ t⁺ Treg population capable of pro-inflammatory cytokines (IL-17, IFN- γ and TNF) production in mice models what together with reported elevated levels of ROR Treg in serum of CRC patients indicates intertwined significance of Th17/Treg balance in IBD and CRC^{216,217}.

Prolonged inflammation was found to be directly linked to cancerous lesions development in ulcerative colitis (UC)²¹⁸. As stated in 1.2.2 CRC develops due to inflammation – dysplasia – carcinoma sequence in IBD patients. Chronic inflammation within epithelia leads to mutations accumulation, including loss of TP53 and oxidative DNA damage what contributes to carcinoma²¹⁹. Furthermore, in IBD altered NF- κ B signaling and IL-6/STAT3 signaling may contribute to the CRC development as mutant p53 enhances NF- κ B leading to the tissue damage whilst IL-6 expression associates with downregulation of *MSH3*, what leads to MSI instability²¹⁹. The role of Th17 in CRC is dual. In CRC Th17 were found to impact endothelial cells and tumor-associated stromal cells were found to produce IL-6 in a IL-17 mediated way whilst simultaneously Th17 mediated cytotoxic CD8⁺ T-cells to the tumor²²⁰. IL-17, although considered to be a signatory cytokine for Th17 population, was found to be expressed by myeloid-derived suppressor cells (MDSCs) and to attract Tregs in the hepatocarcinoma models²²¹. Tregs suppressive functions are vital in CRC progression, however there are a few studies indicating high Treg infiltration is correlated with better overall survival^{222,223}. In addition in CRC ratio of Th17/Tregs is important for the tumor progression. It was found that higher Tregs to Th17 ratios inhibit MMP-dependent metastasis TGF- β -dependent manner. Conversely, IL-17 might promote MMPs, therefore further establishing Th17 role in cancer progression²²⁴. Understanding the interplay between these two populations and mechanisms by which they influence each other is crucial for understanding the IBD and CRC development²²⁵.

5. Tumor TME

The tumor microenvironment is a complex, dynamic, highly variable ecosystem where immune cells, stromal cells, cancer cells, the extracellular matrix, and soluble molecules intricately interact, shaping the communication between cancer and host cells²²⁶. Cancer cells are able to evade the recognition by the immune system e.g. By downregulation of MHC molecules presentation to avoid recognition by T-cells. Other mechanisms of evasion include reduction of co-stimulatory molecules expression, reduced expression of T-cells chemoattractant, production of immunosuppressive factors such as IL-10, or in cooperation with cancer-associated fibroblasts (CAFs) change the content of extracellular matrix (ECM) to form a physical barrier to prevent infiltration²²⁷. Cellular composition of CRC, especially T-cells infiltration was shown to correlate with the clinical prognosis. For example, high density of tumor infiltrating CD8⁺ T-cells (TILs) and stromal-derived factor-1 (SDF1) indicate favorable prognosis for stage III CRC²²⁸. Study performed on fresh-frozen CRC tissue linked high infiltration of Th1 to the longer disease-free survival with simultaneous high Th17 indicating poor prognosis²²⁹. Local signaling majorly impact T-cells to promote their exhaustion and attract immunosuppressive Tregs population i.e. by cytokines expressed by M2 tumor associated macrophages (TAMs)^{65,223,230}. TAMs exert several other functions within the TME such as enhancing the invasion, metastasis, angiogenesis and cooperate with the local microbiota as e.g.

Fusobacterium nucleatum infected macrophages are expressing higher levels of IDO which leads to the immunosuppression⁶⁵. Similarly, CAFs may participate in the induction of EMT, angiogenesis, proliferation but also can orchestrate the immune response within the TME²³¹. For example, in melanoma, CAFs expressing CXCL5 induce expression of PD-L1, inhibitory ligand for T-cells activation, by activating PI3K/AKT signalling²³². Highly heterogenic TME environment is one of the main obstacles in the development of personalized and effective treatment in CRC²³³.

II. Aims of the thesis

CRC as well as IBD are multifactorial conditions where gene expression, Th17/Treg balance, microbiota as well as environmental factors contribute to the disease progression^{234,235}. Hence, the goal of this thesis is to investigate the function and heterogeneity of infiltrating T cells, especially Th17/Treg cells, influencing the local environment in colorectal cancer and inflammation.

The specific aims of this PhD thesis were:

Aim 1: To investigate the effect of animal care facilities conditions impact the gut composition and in turn the development of colitis mediated by T-cells in mice models

Aim 2: Identify the role of USP28 in T cell activation and function, especially Th17 and Tregs, and its role in intestinal inflammation in dextran sulfate sodium (DSS)-induced colitis

Aim3: Investigate the TME and participating immune-related interactions in spatial context using spatial transcriptomics in FFPE tissue

Aim 4: Identify the protein expression changes linked with the tumor progression and immune response within CD4⁺ enriched CRC tissues sections

Aim 5: Identify plasma protein changes and association with the immune response and tumorigenesis using proteomics strategies.

List of publications in this thesis:

- 1. Animal unit hygienic conditions influence mouse intestinal microbiota and contribute to T-cell-mediated colitis**-co-first author
Publication I aimed to investigate the influence of microbiota on the development and progression of colitis through T-cell-mediated mechanisms in mice with subsequent changes in the epithelium impacted by aberrant immune response
- 2. USP28 protects development of inflammation in mouse intestine by regulating STAT5 phosphorylation and IL22 production in T lymphocytes**
Publication II focused on the role of USP28 on Tregs and Th17 functions in the inflammatory settings in mice models.
- 3. Spatial mapping of epithelial changes and suppressive immune populations in colorectal tumor microenvironment**
Publication III aimed to characterize TME and participating immune-related interactions, especially Tregs, in spatial context using spatial transcriptomics and CRC FFPE tissue with subsequent validation in public single cell RNA-seq dataset
- 4. Deep proteomics characterization of colorectal cancer tumor microenvironment enriched in CD4⁺ T cells**
Publication IV focused on identification of protein expression changes linked with the tumor progression and immune response within CD4⁺ enriched CRC and matching normal tissue sections
- 5. Plasma protein changes reflect colorectal cancer development and associated inflammation**
In publication V, plasma samples obtained from CRC patients and healthy controls, were analyzed using proximity extension assay (PEA) to investigate changes in protein expression associated with tumor development and presence of inflammation
- 6. Mass Spectrometry Proteomics Characterization of Plasma Biomarkers for Colorectal Cancer Associated With Inflammation**

Publication VI described CRC plasma protein changes identified using a different proteomics strategy, LC-MS/MS proteomics

7. Proteomics approaches to characterize the immune responses in cancer

Publication VII is a review article describing antibody-based and MS-based proteomics approaches applied in research on TME and cancer immune responses with the emphasis on CD4⁺T-cells

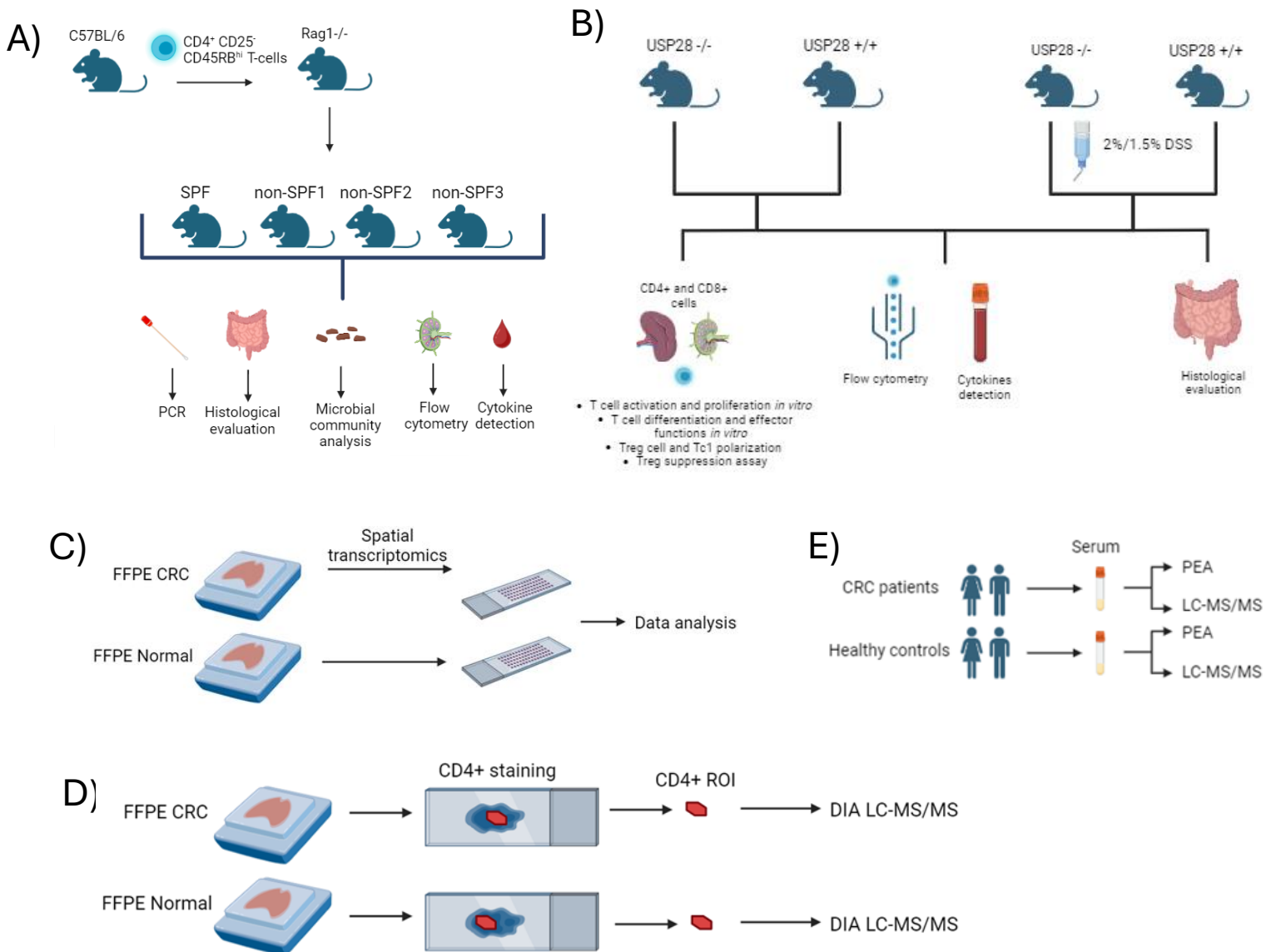


Figure II. Graphical abstracts of research papers included in the thesis. A) and B) summarize publications I and II. C) and D) summarize publications III and IV. E) summarizes publications V and VI. Created in Biorender.com

III. Publications

6. Publication I: Animal unit hygienic conditions influence mouse intestinal microbiota and contribute to T-cell-mediated colitis

Published: *Experimental Biology and Medicine* 2022;247(19):1752-1763.
doi:10.1177/15353702221113826

Mariana Cázares-Olivera^{1*}, Dominika Miroszewska^{2*}, Lili Hu¹, Jacek Kowalski³, Ulla-Marjut Jaakkola⁴, Seppo Salminen⁵, Bin Li⁶, Emrah Yatkin⁴ and Zhi Chen^{1,2}

*These authors contributed equally to this paper.

6.1. Abstract

Inflammatory bowel disease (IBD) is a group of chronic inflammatory disorders of the gastrointestinal tract with worldwide increasing incidence. Recent studies indicate that certain species of intestinal bacteria are strongly associated with IBD. Helper T lymphocytes are not only the key players in mediating host defense against a wide variety of pathogens but also contribute to pathogenesis of many immune-related diseases. Here, using the T cell transfer model of colitis, we observed that the mice maintained in a specific-pathogen free (SPF) unit after receiving naïve CD4⁺ T cells developed mild disease. The same mice developed different degrees of disease when they were maintained in a conventional animal facility (non-SPF), where some pathogens were detected during routine health monitoring. Consistently, increased circulating inflammatory cytokines as well as Th1 and Th17 cells were detected in mice housed in non-SPF units. 16S rRNA sequencing of feces samples enabled us to identify changes in the microbiota composition of mice kept in different facilities. Our data indicate that environmental factors influence gut microbiota composition of mice, leading to development of colitis in a T-cell-dependent manner. In conclusion, changes in environmental conditions and microbial status of experimental animals appear to contribute to progression of colitis

6.2. Introduction

Inflammatory bowel disease, comprising Crohn's disease (CD) and ulcerative colitis (UC), is characterized by chronic intestinal inflammation. Although the pathogenesis of these diseases has not been fully elucidated, both genetic and environmental factors contribute to the development of IBD. An increased incidence of chronic inflammatory diseases, such as IBD, has been linked to lifestyle, dietary changes, and the resulting impact on gut microbiota composition.¹ Loss of microbiota diversity and the prevalence of distinct bacterial species in IBD patients, compared to healthy controls, further suggest that the microbiome plays an important role in IBD development, relapse, and response to treatment.^{2,3} Murine models have been demonstrated as a powerful tool to explore host-microbiota interactions in mucosa.^{4,5} Animal studies have demonstrated that the gut microbiota is indispensable for pathogenesis in most animal models of colitis.⁶ Mice have a similar microbiota composition to humans, with 90% of the bacterial population composed of Firmicutes and Bacteroidetes.⁷ This similarity makes these models relevant to the understanding of IBD, although it is also important to consider how microbiota variations in laboratory mice affect disease phenotype, reproducibility, and relevance to an understanding of the human disease. Several factors affect laboratory mouse gut microbiota including less exposure to pathogens, different diets, housing conditions, and genetics. Different microbiota compositions are observed in laboratory mice depending on the supplier.⁸ In general, laboratory mice have relatively simplified microbiomes compared to wild mice, and the variation in the prevalence of specific bacterial

populations can affect experimental results. Differences in susceptibility to infection have been observed between specific-pathogen-free (SPF) mice and germ-free mice.⁷ Furthermore, the presence of commensal bacteria can protect from colonization of pathobionts.

The T cell transfer colitis is one of the animal models of human IBD. In this model, naïve CD4⁺ T cells isolated from immunocompetent mice are transferred to immunodeficient Rag^{-/-} or severe combined immunodeficient (SCID) mice, and consequently cause colitis.⁹ In an early study, upon transfer of naïve cells, a high proportion of IFN- γ -producing cells was detected in the lamina propria of diseased SCID mice.⁹ Therefore, it was generally believed that IFN- γ -producing Th1 cells are the key players in IBD pathogenesis. However, later studies demonstrated the requirement of additional mechanisms for colitis development, including the IL23 signaling pathway and Th17 cells. The significance of targeting these mechanisms has been shown in several animal models of IBD, including the T cell transfer colitis model,¹⁰⁻¹² and in clinical trials of CD.¹³ The essential role of Th17 cells in IBD has been well documented. The IL23/IL-17 axis plays pivotal roles as the immediate effectors of IBD, whereas defects in Treg cells play distinct causative roles in IBD.¹⁴⁻¹⁶ Genomewide association studies^{17,18} further support the importance of IL-23/IL-17 signaling in the pathogenesis of IBD.¹⁹

As previously mentioned, different environmental factors such as housing of mice in different caging systems may influence the microbiota composition and activity. It has been reported that gut microbial communities are protected from environmental contamination in mice housed in an individually ventilated caging system.²⁰ However, it remains unclear how environmental factors in different facilities change the gut microbiota composition and contribute to the development of colitis.

In this study, we investigated how animal housing conditions in an SPF or non-SPF animal unit influenced gut microbiota of mice and consequently the development of colitis in a T-cell-dependent manner.

6.3. Materials and methods

6.3.1. Animal husbandry and diet

This study included the use of mice and was carried out in strict accordance with the European (the Directive 2010/63/ EU of the European Parliament and of the Council on the protection of animals used for scientific purposes) and Finnish legislation (Act 497/2013 and Government Decree 564/2013 on the Protection of Animals Used for Scientific or Educational Purposes). The study protocols and procedures were reviewed and approved by the National Project Authorization Board of Finland (license number ESAVI/ 2502/04.10.07/2015). Rag1^{-/-} (NOD.129 S7(B6)-Rag1^{tm1Mom/J}) and C57BL/6J mice were supplied by Jackson laboratories (USA). Animals were housed (2–5 animals per cage) in individually ventilated cages (IVC) in the SPF animal facility and in open top cages in the non-SPF animal facility with Aspen bedding and nesting material (Tapvei Oy, Estonia) and polycarbonate tunnels as enrichment. The temperature in the experimental animal room was 21 \pm 3°C, with relative humidity of 55 \pm 15% and following a 12-h light and 12-h dark light cycle. The mice were fed *ad libitum* with RM3 soy-free diet (Special Diet Services, Witham, Essex, England), and tap water was provided *ad libitum*. Mice were housed in the respective experimental conditions, in SPF group, *n* = 7; in non-SPF1, *n* = 6; in non-SPF2, *n* = 5; and in non-SPF3, *n* = 6. The mice were monitored for signs of colitis and euthanized at the indicated time point of 13 weeks for SPF mice, 10 weeks for non-SPF1 and non-SPF2 mice, and 8 weeks for non-SPF3 mice. Fecal samples for DNA extraction and blood samples for serum cytokine detection were collected at the time of euthanasia.

6.3.2. T cell transfer model of colitis

A well-characterized mouse model of IBD was used to study T-cell-dependent colitis in mice. Colitis was induced in immunodeficient Rag1^{-/-} mice that lack mature B and T lymphocytes, by adoptive transfer of naïve CD4⁺ CD45RB^{hi}CD25⁻ T cells, which were isolated from immunocompetent, wild type C57BL/6J mice. Spleens were isolated from 6- to 7-week-old male C57BL/6J mice and were disaggregated by pressing through a 70- μ m filter, red blood cells were lysed with ACK lysing buffer (Invitrogen). CD4⁺ T cells

were enriched using magnetic separation with a CD4⁺ T cell isolation kit (Miltenyi Biotec, Bergisch Gladbach, Germany). Naïve CD4⁺ CD45RB^{hi}CD25⁻ T cells were further purified by FACS sorting using antibodies recognizing CD4, CD45RB, CD62L, and CD25 (eBiosciences). 400,000 FACS-sorted naïve T cells in a total volume of 200 µL PBS were injected into male Rag1^{-/-} mice. Mice were weighed prior to the injection and weekly thereafter.

6.3.3. Flow cytometry

For colitis experiments, spleen and mesenteric lymph nodes (MLN) were harvested from mice and quantified prior to re-stimulation for 4 h in the presence of PMA and ionomycin plus Golgi inhibitor. For analysis of surface markers, cells were stained in PBS containing either 5% or 0.1% (wt/vol) fetal bovine serum (FBS) with anti-CD4 and anti-CD3 purchased from eBiosciences. Stimulated cells were fixed and permeabilized with Transcription Factor Staining Buffer Set (eBiosciences, San Diego, CA, USA) stained with anti-IFN-γ and anti-IL-17A (both from eBiosciences) according to the manufacturer's instructions, and cells were acquired using an LSRII flow cytometer (Becton Dickinson, San Jose, CA, USA). Events were collected and analyzed using FlowJo software (Tree Star, Ashland, OR, USA).

6.3.4. Histopathology

Colonic sections from mice were collected, weighted, measured, and then fixed in 10% neutral-buffered formalin for 24 h at room temperature. Complete cross-sections of formalin-fixed intestinal sections were placed in cassettes, embedded in paraffin, sectioned at 4 µm thickness, mounted on glass slides, and stained with hematoxylin and eosin (H&E). Histological sections were evaluated and scored according to the following criteria: (A) Distribution of the inflammation: 0 = None, 1 = Focal, 2 = Multifocal, 3 = Diffuse, 4 = total/ whole/maximal distribution; (B) Degree of inflammation: 0 = None, 1 = Low level of inflammation with scattered infiltrating mononuclear cells (1–2 foci), 2 = Moderate inflammation with multiple foci, 3 = High level of inflammation with increased vascular density and marked wall thickening, 4 = Maximal severity of inflammation with transmural leukocyte infiltration and loss of goblet cells. The cumulative score represents the sum of these two independent criteria.

6.3.5. Cytokine detection

Serum samples were collected from colitis experiment mice at the time of euthanasia. Serum cytokines were quantified using a Millipore (Billerica, MA, USA) MILLIPLEX[®] MAP Kit.

6.3.6. Health monitoring of animal units

Health monitoring was carried out according to FELASA recommendations.²¹ Samples were collected from sentinel mice kept in the animal rooms by direct sampling of Rag^{-/-} mice. Sentinel mice are weekly exposed to soiled beddings of other animals maintained in the animal facility. A few blood drops were collected to Opti-Spot strips (IDEXX BioResearch, Stuttgart, Germany) for serologic analysis. Oral and fur swabs and feces were collected for PCR analyses. Up to five samples were pooled separately for oral, fur, and feces and sent to IDEXX BioResearch. In addition, SPF was tested by PCR from pooled feces samples.

6.3.7. Microbial community analysis

Fecal samples were collected from mice in colitis experiments at the time of euthanasia. Total DNA was extracted using QIAamp Fast DNA Stool Mini Kit (QIAGEN, Hilden, Germany) according to the manufacturer's instructions. All the qualified DNAs were used to construct libraries of 16S rRNA gene (V3 V4 region) followed by sequencing by 300 bp paired-end run on an Illumina HiSeq 2500 instrument at the BGI Genomics (New Territories). Data analysis was performed by BGI Genomics (New Territories). Clean reads were obtained after filtering and cleaning, then paired-end reads with overlap were merged to tags, which were clustered to Operational Taxonomic Unit (OTU) at 97% sequence similarity. Taxonomic ranks

were assigned to OTU representative sequence using Ribosomal Database Project (RDP) Naive Bayesian Classifier v2.2. Finally, alpha diversity, beta diversity and the different species screening were analyzed based on OTU and taxonomic ranks. Linear Discriminant Analysis Effect Size (LEfSe) was used to identify microbial biomarkers enriched/depleted in each group.²²

PCR primers targeted to total bacteria (forward: 5'-AGCA CGTGAAGGTGGGGAC-3', reverse: 5'-CCTTGCGGTTGGC TTCAGAT-3'), Enterobacteriaceae family (forward: 5'-CATT GACGTTACCCGAGAAAGC-3', reverse: 5'-CTCTACG AGACTCAAGCTTGC-3'), *Akkermansia muciniphila* (forward: 5'-CAGCACGTGAAGGTGGGGAC-3', reverse: 5'-CCTTG CCGTTGGCTTCAGAT-3') and segmented filamentous bacteria (SFB, forward: 5'-AGGAGGAGTCTGCGGCACATTAGC-3', reverse: 5'-TCCCCACTGCTGCCTCCCGTAG-3') were used to perform specific Quantitative real-time PCR (qPCR) in a LightCycler[®] 480 Real-Time PCR System (Roche[®]) by use of SYBR[®] Green PCR Master Mix (Roche[®]). A melting curve analysis was conducted at the end of the PCR, and bacterial concentration was calculated by comparing the Ct values from standard curves.

6.3.8. Statistical analysis

p-values were calculated using Student's *t*-test and one-way ANOVA + Tukey's multiple comparisons test. Error bars represent means ± SEM.

6.4. Results

6.4.1. Hygienic condition in the animal unit contributes to T-cell-dependent colitis development

To perform the T cell transfer model of colitis in our animal facility, flow cytometry sorted naïve (CD4⁺ CD25⁻CD45RB^{hi}) T cells from C57BL/6 mice were transferred to Rag1^{-/-} recipients housed in individually ventilated cages in the specific-pathogen-free (SPF) unit. The mice were weighed weekly to monitor colitis development. We observed that the Rag1^{-/-} recipient mice kept gaining weight until the time of sacrifice (13 weeks) after naïve CD4⁺ T cell reconstitution (Figure 6-1(A)). Histology evaluation confirmed that colons of these mice appeared essentially normal or with mild observable pathology (Figure 6-1(B)). Health monitoring reports indicated that many of the pathogenic microbes were not detected in the SPF unit (Table 6.1).

To investigate whether the microbiota in the housing environment influence colitis development, we transferred Rag1^{-/-} mice to non-SPF units, where mice were kept in open top cages. Later, the same experiment was performed and we observed that post transfer of naïve CD4⁺ T cells, Rag1^{-/-} mice stopped gaining weight and even started losing weight by week 7 (Figure 6-1(A), non-SPF2). These mice had diarrhea and at the time of sacrifice we observed increased colonic weight/length ratio, a marker of tissue edema (Figure 6-1(D)), indicating that these mice developed more colitis compared to previous experiments performed in the SPF unit. Histopathologic quantitation of colitis development demonstrated that distribution, degree of inflammation, and cumulative score was significantly higher in animals kept in the non-SPF2 unit. Mice that were transferred to the non-SPF2 unit developed significant colonic inflammation after 4 months of transfer (Figure 6-1(A) to (C), non-SPF2). Interestingly, Rag1^{-/-} mice maintained all the time in a separate non-SPF unit also just developed mild colitis as shown by body weight loss and histology evaluation (Figure 6-1(A) to (C), non-SPF1 group).

Importantly, several pathogenic bacteria species, including *H. hepaticus* and *H. typhlonius* as well as *Klebsiella oxytoca*, *Pasteurella pneumotropica* biotype Heyl (*Rodentibacter Heylii*) performed at the same period, which was 8 months following were detected from our Rag1^{-/-} mice housed in the non- the transfer to the non-SPF unit, Rag1^{-/-} mice were found to SPF3 unit (Table 6-1).

Table 6-1. Health monitoring results.

	SPF	Non-SPF1	Non-SPF2	Non-SPF3
Mouse norovirus (MNV)	-		-	-
Helicobacter spp.	-	-	-	+
H. bilis	-	-	-	-
H. ganmani	-	-	-	-
H. hepaticus	-	-	-	+
H. mastomyrinus	-	-	-	-
H. rodentium	-	-	-	-
H. typhlonius	-	-	-	+
SFB	+		+	+
Klebsiella	-		-	+
Pasterurella pneumotropica biotype Heyl		-	-	+

SPF: specific-pathogen free; MNV: murine norovirus; SFB: segmented filamentous bacteria.

In the T cell transfer colitis experiment stop gaining weight 4 weeks after receiving naïve CD4⁺ T cells, started to lose weight from the fifth week post injection, and kept losing weight until the eighth week when they were sacrificed (Figure 6-1(A), non-SPF3). Meanwhile, we observed that some of these mice had severe diarrhea and blood in the stool. Not surprisingly, these mice showed very high colonic weight/length ratio (Figure 6-1(D)) and significant histologic changes (Figure 6-1(B) and (C)) indicating that Rag^{-/-} mice which received naïve CD4⁺ T cells developed severe colitis.

Murine norovirus (MNV),²³ a prevalent pathogen in animal facilities, is routinely detected by serology in sentinel mice in our non-SPF2 and non-SPF3 facility, but not in SPF and non-SPF1 units. However, MNV was not detected in Rag^{-/-} mice even 8 months post transfer from the SPF facility to a non-SPF2 and non-SPF3 facility. In order to ensure that immunodeficient Rag^{-/-} mice are indeed negative for MNV, we also analyzed the feces samples from Rag^{-/-} mice by PCR for MNV. Again, no MNV was detected in these samples (Table 6.1).

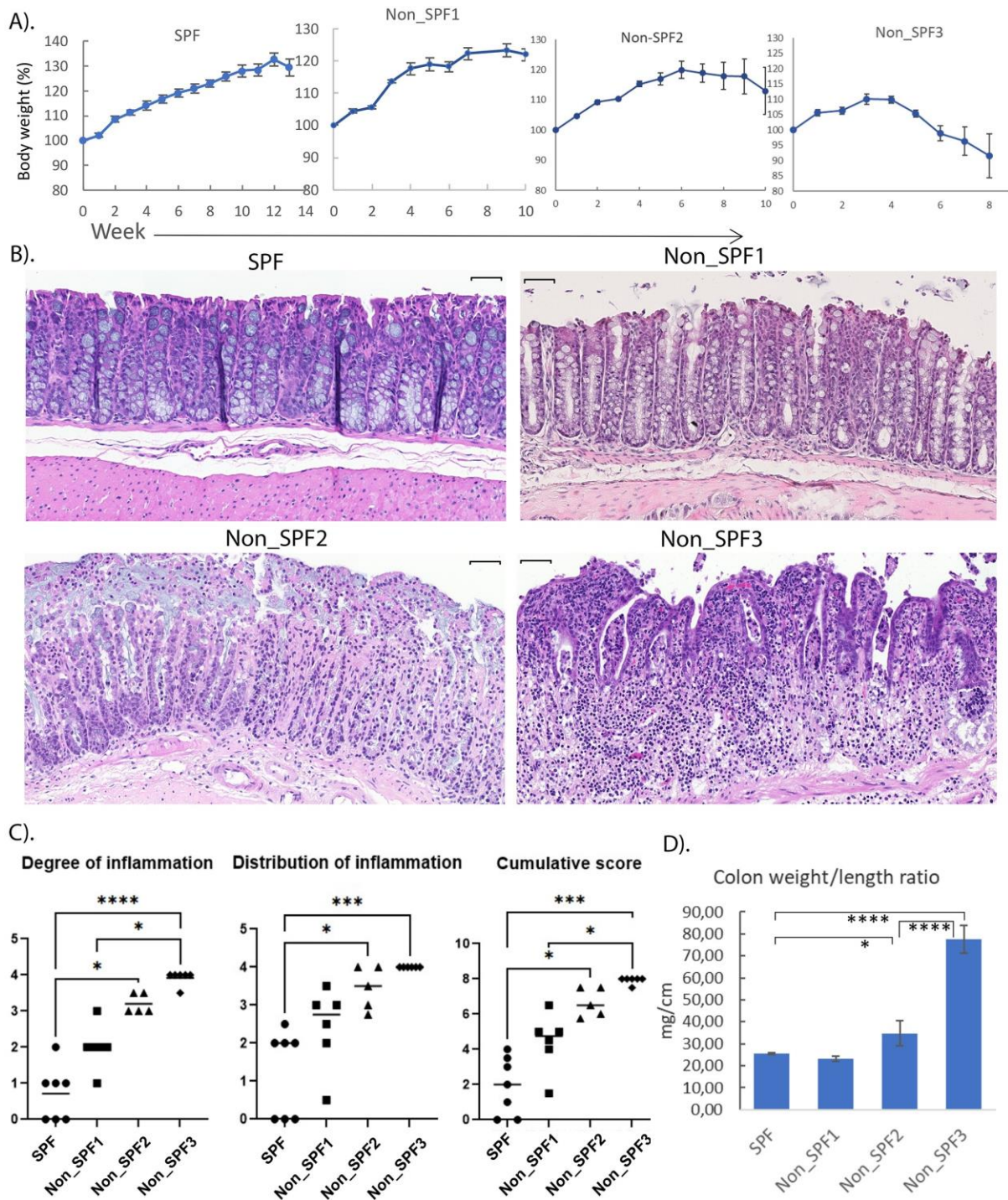


Figure 6.1. Animal housing environment influences pathogenic potential of colitis. (A) Rag1^{-/-} mice housed in SPF or non-SPF units received 400,000 sorted naïve CD4⁺ CD45RB^{hi}CD25⁻ T cells isolated from C57BL/6 mice, and mice were weighed weekly to monitor the onset of colitis. In SPF, n = 7; in non-SPF1, n = 6; in non-SPF2, n = 5; and in non-SPF3, n = 6. (B) Colon sections were used for H&E staining. Representative histological images (H&E) are shown. Scale bar, 50 μ m. (C) Histological scoring. Development of colitis was assessed by monitoring the (a) degree of inflammation, (b) distribution of inflammation, and (c) cumulative score. Data were analyzed by Kruskal–Wallis test ($p < 0.05$) followed by Dunn’s multiple comparisons test (* $p < 0.05$; *** $p < 0.0005$; **** $p < 0.0001$). (D) Colonic weight and length were measured at the time of sacrifice. * $p < 0.1$, ** $p < 0.05$, *** $p < 0.01$, **** $p < 0.001$; two-tailed Student’s t-test was used. (A color version of this figure is available in the online journal.)

6.4.2. Animal housing environment alters Th subsets that contribute to colitis development

To further evaluate the severity of inflammation developed from Rag^{-/-} recipient mice housed in both SPF and nonSPF environments, we measured inflammatory cytokines in peripheral blood samples taken from these mice at the time of sacrifice. Compared to mice housed in SPF units, which were without clear signs of colitis (experiment SPF), a significantly higher level of circulating cytokines, including IFN- γ , IL-17, and TNF α , were detected from mice which received naïve T cells and were housed in non-SPF2 units (Figure 6.2(A)). Consistent with observations from body weight changes and histology, significantly higher concentrations of inflammatory cytokines IL-1 β , IL-6, IFN- γ , and IL-17 were detected in the peripheral blood of mice which had lost more weight from the non-SPF3 experiment compared to those mice that experienced less weight loss from the non-SPF2 experiment (Figure 6.2(A)).

Since we detected increased circulating IFN- γ and IL-17, we next examined whether recipient Rag1^{-/-} mice had enhanced Th1 or Th17 cell differentiation. We performed intracellular cytokine staining to detect the proportion of IFN- γ and IL-17A-producing CD4⁺ T cells in spleens and mesenteric lymph nodes (MLN) from recipient Rag1^{-/-} mice.

Mice housed in non-SPF2 units had a significantly increased number of IFN- γ + as well as more IL-17+ cells both in the spleen and MLN (Figure 6.2(B)). Notably, in the non-SPF3 group, in addition to the detected increased serum IL-17, we also observed a higher proportion of IL-17 producing CD4⁺ T cells in the spleen and MLN (Figure 6.2(B)). Interestingly, even though IFN- γ producing Th1 cells were detected in all non-SPF experiments, only in the spleen of non-SPF3 mice did we find both IL-17+ and IFN γ + IL-17+ CD4⁺ T cells. The IL-23 and Th17 signaling pathways are supposed to be principal to colitis pathogenesis. Since several bacterial species were detected by PCR in feces samples, including *Helicobacter bacteria*, *K. oxytoca*, and *Pasteurella pneumotropica biotype Heyl*, and this might also contribute to the enhanced IFN- γ and IL-17 production. As a conclusion, conventional housing conditions influence the induction of Th1 and Th17 responses that lead to the development of more severe colitis.

6.4.3. Altered gut microbiota correlates with development of T-cell-dependent colitis

To explore how the hygiene conditions in the animal housing environment influences gut microbiota of mice and the development of colitis, we collected fecal samples from Rag^{-/-} mice housed in one SPF and three non-SPF units. DNA was extracted from these fecal samples and processed with 16S rRNA sequencing (V3-V4 region) on an Illumina HiSeq 2500-platform to further extensively compare the difference of the composition of bacteria of Rag^{-/-} mice maintained in different hygiene environments. First, to examine the differences of Operational Taxonomic Unit (OTU) composition in different samples, principal component analysis (PCA) was used to construct a 2D graph to summarize factors mainly responsible for this difference. PCA analysis showed that the SPF and non-SPF groups could be distinguished based on their relative abundance of each OTU in each sample. Out of all three of the non-SPF groups, the non-SPF1 group displayed a very different OTU abundance profile, while samples from the non-SPF2 and non-SPF3 groups were closely located, indicating that the similarity between these two groups is high (Figure 6.3(A)). This correlated well with the degree of inflammation, as mice in these two groups developed more severe colitis compared to the non-SPF1 and SPF groups (Figure 6.1).

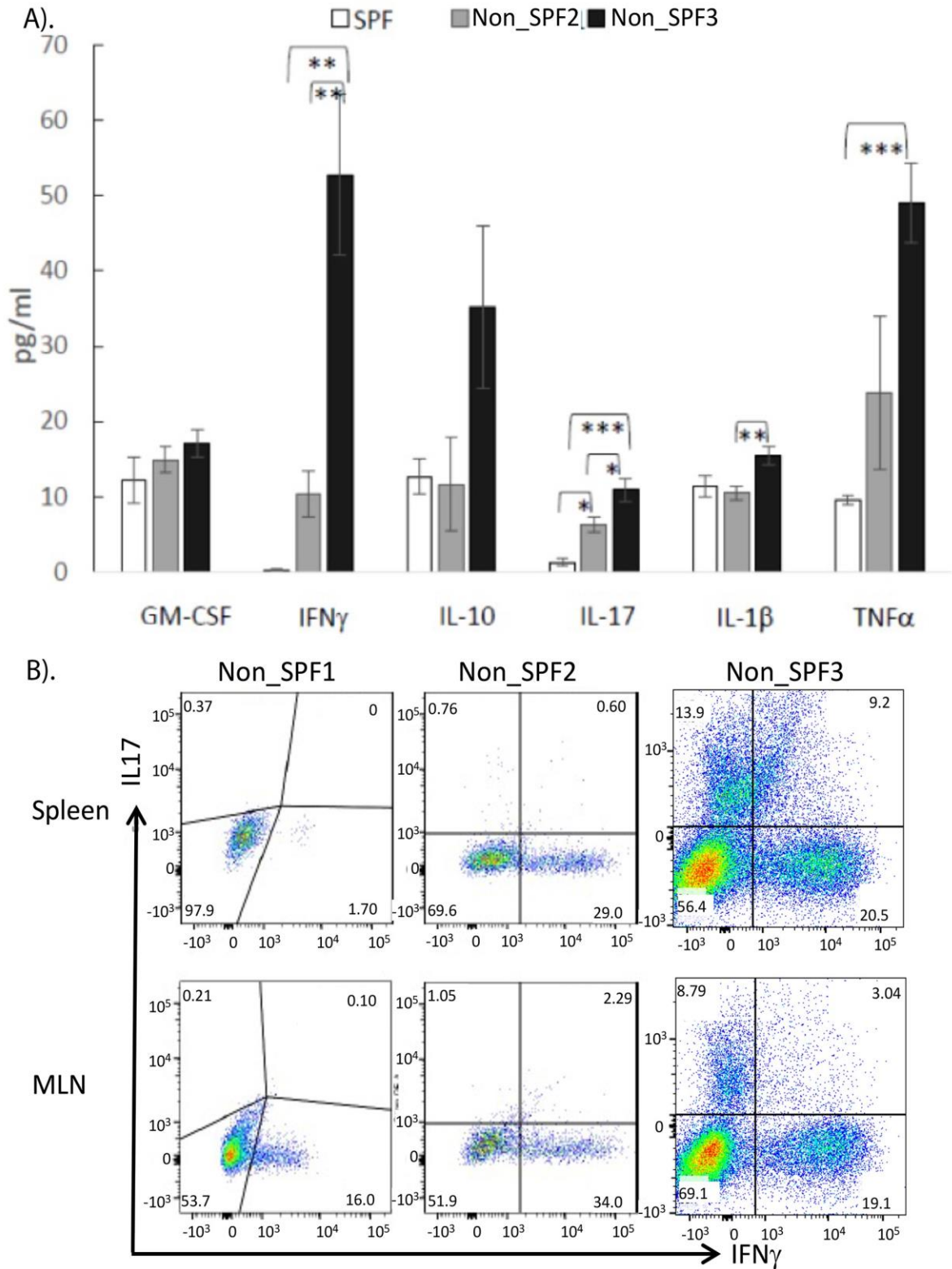


Figure 6.2. Hygienic conditions in animal housing environment influences Th subsets. (A) Pro-inflammatory cytokines correlate with colitis development. Serum samples were collected at the time of sacrifice. GM-CSF, IFN- γ , IL-10, IL-17, IL-1 β , and TNF α were measured using a Luminex MILLIPLEX MAP Mouse Cytokine/Chemokine Magnetic Bead Panel. * $p < 0.1$, ** $p < 0.05$; *** $p < 0.01$, two-tailed Student's t-test. (B). Representative intracellular cytokine staining for IFN- γ and IL-17 within gated CD4 $^+$ T cells isolated from spleens and MLN of colitic mice is shown. Spleens and MLNs were harvested, cells were stimulated with PMA and ionomycin for 4 h. Cells were stained with anti-CD4 followed by intracellular cytokine staining

performed using Transcription Factor Staining Buffer Set (eBiosciences, San Diego, CA, USA) with antibodies against IFN- γ and IL-17A (both from eBiosciences) according to the manufacturer's instructions. (A color version of this figure is available in the online journal.)

Alpha diversity was then applied to analyze complexity of species diversity. The lowest Chao value, which reflects the species richness of community, was observed in the SPF group (Figure 6.3(B)). Non-SPF2 and non-SPF3 groups showed no difference of Chao value. The highest species richness was seen in the non-SPF1 group, which developed much milder intestine inflammation compared to non-SPF2 and non-SPF3 groups. The diversity of microbiota also may lead to initiating the development of inflammatory disease. The Shannon value, reflecting the species diversity of the community, was also higher in the non-SPF1 group compared to the non-SPF2 and non-SPF3 groups (Figure 6-3(B)). Again, the lowest species diversity was observed in the SPF group, in which mice were maintained in a facility with the best hygiene conditions among the four study groups. These results indicate that bacterial richness and diversity may contribute to development of intestine inflammation

Next, we further studied species composition and abundance differences among the four groups. We found that compared to the non-SPF2 and non-SPF3 group, in the non-SPF1 group, *Tenericutes* phylum was enriched, whereas *Proteobacteria* phylum was lower (Figure 6.3(C)). At the family and genus level, the non-SPF3 and non-SPF2 groups showed higher relative abundance of *Enterococcaceae* (such as enterococcus) and *Escherichia coli* (Figure 6.3(D)). Consistent with the routine health monitoring results, non-SPF2 and non-SPF3 groups showed increased relative abundance of *Helicobacteraceae* (Figure 6-3(D)), indicating it to be an important pathogenic agent in intestinal inflammation in the mouse model. Increased relative abundance of *Bacteroidaceae* (such as *bacteroides* species) was detected in the non-SPF2 and non-SPF3 groups, in which more severe colitis had developed compared to the non-SPF1 group. However, although the SPF group developed very mild inflammation, no significant changes of *Bacteroides* level were observed between SPF and non-SPF2 or non-SPF3 (Figure 6.3(D), Table 1).

We also performed linear discriminant analysis effect size (LEfSe) to compare the alteration of gut microbiota in the four groups.²² As shown in Figure 4, a significant enrichment of *Helicobacteraceae* and *Enterobacteriaceae* in the *Proteobacteria* phylum is observed in the non-SPF3 group. Notably, significant shifts in the microbiota composition at the phylum level were observed in our LEfSe analysis. In contrast to the enriched *Proteobacteria* phylum detected in the highly inflammatory non-SPF3 group, as seen in Figure 6.3(C), an increased *Tenericutes* phylum in the non-SPF1 group and increased *Verrucomicrobia* phylum in the SPF group were observed (Figure 6.4).

Taken together, the 16S rRNA sequencing data show that a clear variation of intestine microbiota was detected from mice housed in different hygiene conditions. Bacteria species richness and diversity, composition of commensal and pathogenic bacteria may contribute to the development of T-cell-dependent colitis.

We further detected the level of SFB in fecal samples collected from different units using qPCR. We used a universal primer pair for the 16S ribosomal RNA coding sequence as endogenous control. qPCR results showed that SFB indeed was present in all facilities. Interestingly, the highest relative abundance was seen in mice feces from the non-SPF1 group with mild colitis, compared with the nonSPF2 and non-SPF3 group with more severe inflammation (Figure 6.5(A)).

In the *Verrucomicrobia* phylum, *A. muciniphila* is a Gramnegative mucin-degrading bacterium. Here, we observed that the *Akkermansiaceae* family (*A. muciniphila* species) in the *Verrucomicrobiales* phylum was enriched in the SPF group (Figures 7.3(D) and 4). Because changes of *A. muciniphila* abundance was associated with colitis and IBD, we also performed qPCR analysis to detect *A. muciniphila* in mouse fecal samples from these four groups. The most relatively abundant level of *A. muciniphila* was detected in the SPF group, while the lowest was present in the non-SPF3 group. Notably, the relative level of *A. muciniphila* was inversely correlated with the degree of inflammation (Figures 7.1 and 7.5(B)).

6.5. Discussion

In this study, we investigated how animal housing conditions influenced the composition shifts of gut microbiota of mice, and consequently the changes of Th subsets for development of colitis.

We have observed that upon transfer from SPF to non-SPF housing conditions, after naïve CD4⁺ T cell reconstitution, Rag1^{-/-} mice developed more colitis compared to previous experiments performed in the SPF unit. Several pathogenic bacteria species were detected from our Rag1^{-/-} mice housed in the non-SPF3 unit during routine health monitoring. These findings suggest that the pathogenic species detected by health monitoring may contribute to the severe intestinal inflammation observed in the T cell transfer colitis experiment.

Elevated levels of inflammatory cytokines IFN- γ and IL-17 in peripheral blood of mice from non-SPF3 experiments are consistent with the reports stating that elevated Th17 and Th1 responses are observed in animal models of colitis as well as in patients with IBD.^{4,9} Studies have indicated that *Helicobacter*, through stimulation of IL-23 production, expands Th17 cells.^{24,25} In the non-SPF3 experiment, we also observed a higher proportion of IL-17 producing CD4⁺ T cells both in the spleen and MLN. Consistently, *Helicobacter* bacteria strains were also detected from mice in this experiment. In addition, several other bacterial species were also detected by PCR in feces samples, including *K. oxytoca* and *Pasteurella pneumotropica* biotype *Heyl*, and this might also contribute to the enhanced IFN- γ and IL-17 production. Moreover, only in the spleen of non-SPF3 mice did we find both IL-17⁺ and IFN- γ + IL-17⁺ CD4⁺ T cells. Taken together, these findings suggest that conventional housing conditions influence the induction of Th1 and Th17 responses that lead to the development of more severe colitis.

Using 16S rRNA sequencing, we found several bacteria species that may be associated with the development and progress of colitis. The non-SPF1 group, which has developed the milder intestine inflammation compared to the other two groups, was characterized by highest species richness and species diversity of the community what may suggest that reduced bacterial richness correlates with development of T-cell-dependent colitis.

K. oxytoca is able to colonize in human skin or the human intestine²⁶ and is described as an opportunistic pathogen rather than a part of healthy human microbiota.²⁷ *K. oxytoca* has been linked to antibiotic-associated hemorrhagic colitis (AAHC).²⁸ In addition, there has been at least one case study suggesting the association of *K. oxytoca* with refractory colitis independent of antibiotic treatment.²⁹ The source of *K. oxytoca* infection often comes from the hospital environment³⁰ and as such may pose a danger to patients undergoing treatment, such as with *K. oxytoca* contamination upon intravenous injection causing septic arthritis.³¹ Despite the emerging importance of *K. oxytoca* as a human pathogen, to the best of our knowledge, no studies on the interaction between this bacteria and T cells in colitis are available. In this study, we observed that Rag1^{-/-} mice with detectable *K. oxytoca* developed more severe colitis after receiving naïve CD4⁺ T cells, supporting the correlation between *K. oxytoca* infection and T-cell-dependent colitis development.

Helicobacteraceae have been reported to be important pathogenic agents in intestinal inflammation in both mouse models and humans.^{32,33} Some commensal bacteria, such as *Bacteroides fragilis* protect mice from *Helicobacter hepaticus*-induced colitis by suppressing IL-17 expression and by promoting suppressive Treg differentiation in the intestine.³⁴ Unlike previous reports,³⁵⁻³⁷ here we detected increased relative abundance of *Bacteroidaceae* (such as *bacteroides* species) in the non-SPF2 and non-SPF3 groups, in which more severe colitis was developed compared to the non-SPF1 group. However, no significant changes of *Bacteroides* level were observed between SPF and non-SPF2 or non-SPF3, suggesting the role of *Bacteroides* species in regulation of intestine inflammation may need to be further characterized.

Proteobacteria has been previously reported to be associated with CD.^{32,33,38-48} In this study, a lower level of *Proteobacteria* was detected in a mild disease non-SPF1 group. However, in an LEfSe analysis, we found a significant enrichment of *Helicobacteraceae*, *Enterobacteriaceae*, *E. coli*, *Sutterella*,

and *Parabactreioides* in the group that developed severe colitis. The increased prevalence of *Helicobacteraceae*, *E. coli*, *Sutterella*, *Enterobacteriaceae*, and *Parabacteroides* are commonly observed in intestinal inflammation and IBD.^{38-41,49} The genus *Sutterella* and the genus *Parabacteroides*, although present in healthy individuals, may have a role in IBD.⁴² Although *Sutterella* has a low proinflammatory potential, it may affect the host's intestinal barrier function, but whether it contributes to inflammation in IBD is still unclear.⁴² Results from clinical trials of fecal microbiota transplanted to UC and CD patients suggest that the role of the species *Sutterella wadsworthensis* may be disease specific. In mouse models, the immunomodulatory role of *Sutterella* is associated with a low IgA phenotype, which can be transmitted through fecal microbiota transplant. Mice with this phenotype also presented more severe ulceration in a DSS model of colitis.⁴³ The strain *Parabacteroides distasonis* has been isolated from lesions in CD patients⁴⁴ and it is enriched in their microbiota.^{45,46} Interestingly, some *in vitro* studies and IBD mouse models show a potential strain-dependent anti-inflammatory effect.^{47,48} Our results are in line with these studies, indicating the presence of certain pathogenic bacteria is critical for colitis development.

A. muciniphila, first isolated from human fecal samples in 2004,⁴⁹ accounts for 1–5% of the gut microbial community in healthy adults.⁵⁰ Studies have confirmed the obvious relationship between *A. muciniphila*, chronic inflammatory metabolic diseases, and cardiometabolic risk factors associated with a low-grade inflammatory tone such as type 2 diabetes, obesity, and IBD.⁵¹⁻⁵³ As a marker of a healthy microbiome, *A. muciniphila* has been shown to increase the integrity of the intestinal barrier both in humans and mice.^{54,55} Furthermore, a purified membrane protein from *A. muciniphila* or the pasteurized bacterium has been reported to ameliorate colitis.⁵⁶

Some results of this study correlate with the observations previously reported on the human microbiota and IBD patients. For instance, in our study, we observed the increased relative abundance of microbiota of *Actinobacteria* and *Proteobacteria* phyla and the decrease of some families of phyla *Firmicutes*, specifically *Lachnospiraceae*, in groups with more severe inflammation. Nevertheless, we also detected some bacterial strain changes that are different than previously reported in human IBD patients. Since Th17 cells are known to play an essential role in colitis development and SFB was reported to be a potent inducer of Th17 cell differentiation,⁵⁷⁻⁶¹ we observed that SFB was detected in fecal samples from all our animal facilities and was not correlated with colitis severity, suggesting that the presence of commensal together with pathogenic bacterial species determines disease severity.

Finally, the increase of *A. muciniphila* negatively correlates with the development of colitis in mice kept in different facilities. Further studies are warranted to characterize whether and how *A. muciniphila* affects the dynamic changes of Th cell subsets in the intestine, to reveal the potential of *A. muciniphila* in modulating intestine immune response, and the effect on development of colitis. Overall, our data help understand how microbiota variation in mice can affect IBD development in a T-cell-dependent manner. The species identified here that are important for disease development in mice could be further studied to understand how similar changes may impact human gut health and whether they are relevant in disease progression.

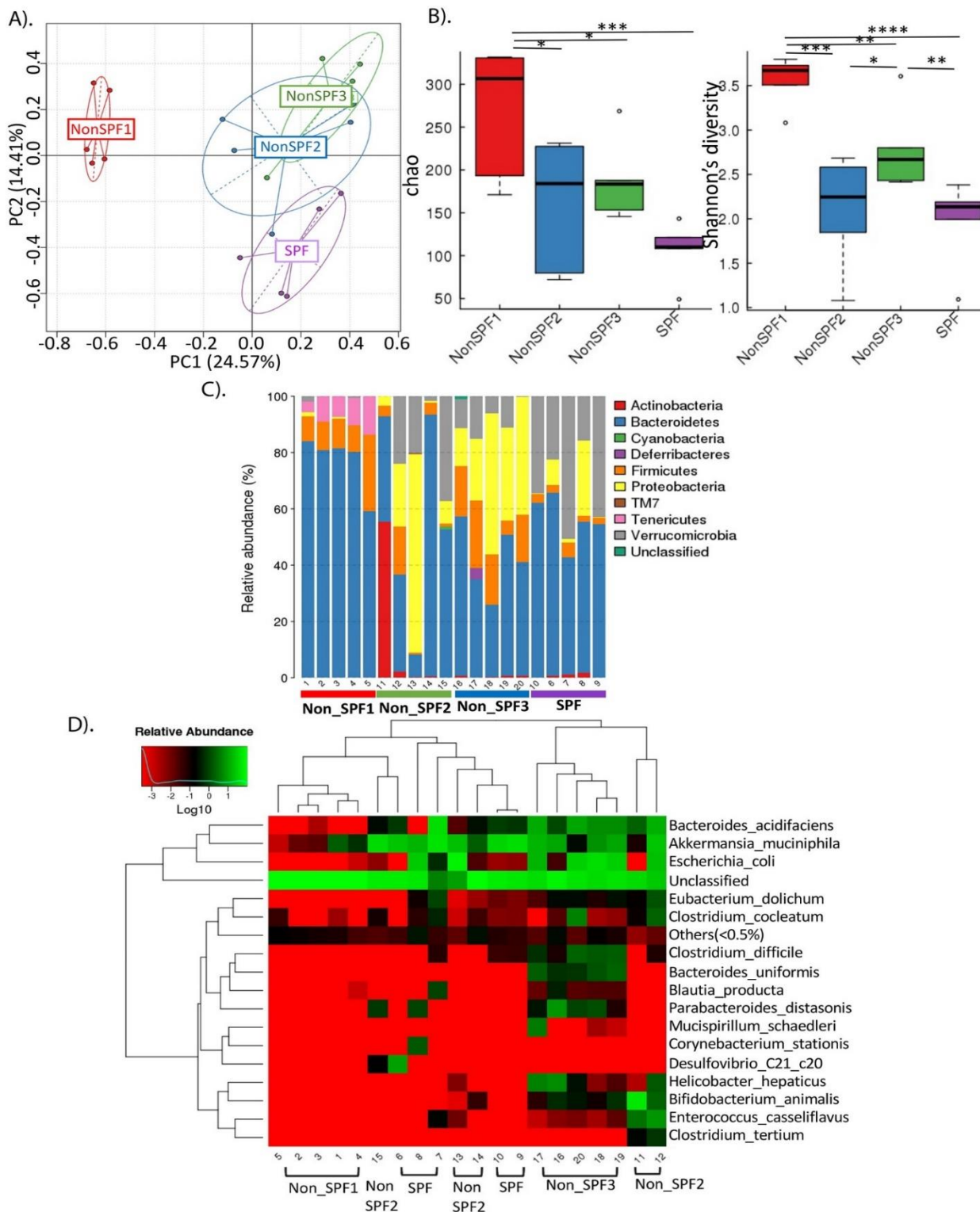


Figure 6.3. Microbiota composition between SPF and non-SPF groups. (A) PCA based on OTU abundance. X-axis represents the first principal component and Y-axis, second principal component. Number in brackets represents contributions of principal components to differences among samples. A dot represents each sample, and different colors represent different groups. (B) Boxplot displays the differences of the alpha diversity among groups. * $p < 0.1$, ** $p < 0.05$; *** $p < 0.01$, **** $p < 0.001$ two tailed Student's t-test. (C) The taxonomic composition distribution in samples of phylum-level and (D) log-scaled percentage heat map of species-level. Presented data were obtained by 16S rRNA sequencing. (A color version of this figure is available in the online journal.)

Cladogram

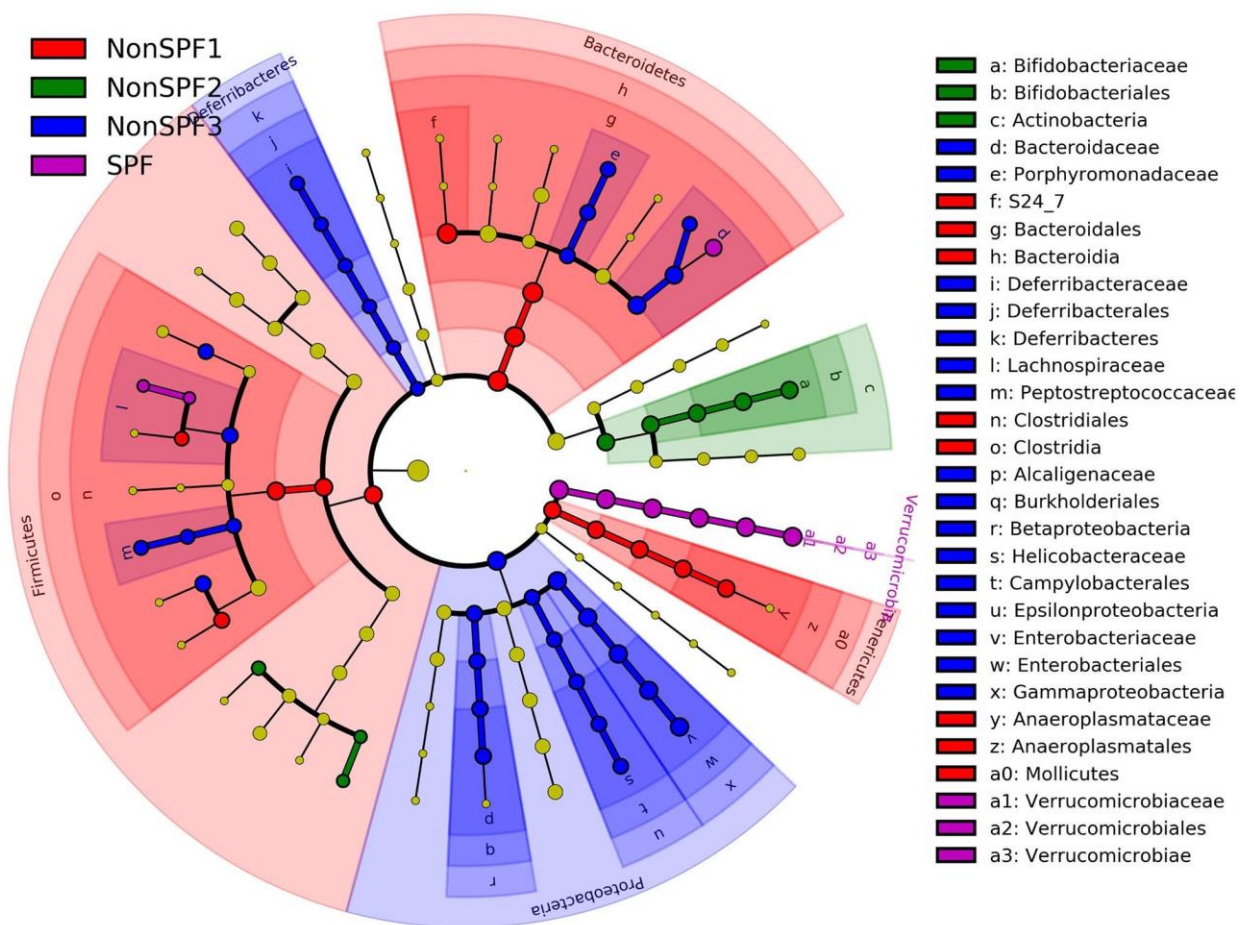


Figure 6.4. LEfSe analysis. In the LEfSe tree, different colors indicate different groups. Note colored in a group color shows an important microbe biomarker in the group and their names are listed on the right. The yellow notes represent the biomarker which does not show any importance in groups. (A color version of this figure is available in the online journal.)

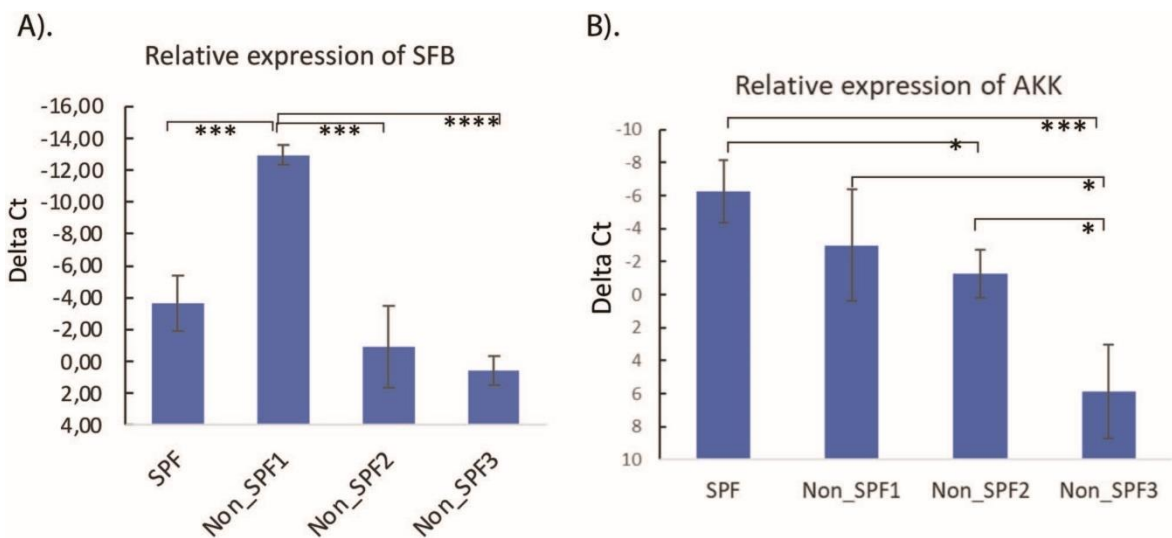


Figure 6.5. qPCR detection of selected bacteria strains. qPCR detection of *Segmented filamentous bacterium* (SFB, A) and *Akkermansia mucin* (B), showing the relative abundance of *Akkermansia mucin*

and SFB with universal bacteria. For each group, n = 5. *p < 0.1, **p < 0.05, ***p < 0.01, ****p < 0.001; two-tailed Student's t-test was used. (A color version of this figure is available in the online journal.)

6.6. References

1. Castro F, de Souza HSP. Dietary composition and effects in inflammatory bowel disease. *Nutrients* 2019;11:1398
2. Clooney AG, Eckenberger J, Laserna-Mendieta E, Sexton KA, Bernstein MT, Vagianos K, Sargent M, Ryan FJ, Moran C, Sheehan D, Sleator RD, Targownik LE, Bernstein CN, Shanahan F, Claesson MJ. Ranking microbiome variance in inflammatory bowel disease: a large longitudinal intercontinental study. *Gut* 2021;70:499–510
3. Kansal S, Catto-Smith A, Boniface K, Thomas S, Cameron D, Oliver M, Alex G, Kirkwood C, Wagner J. The microbiome in paediatric Crohn's disease—a longitudinal, prospective, single-centre study. *J Crohns Colitis* 2019;13:1044–54
4. Kobayashi T, Okamoto S, Hisamatsu T, Kamada N, Chinen H, Saito R, Kitazume MT, Nakazawa A, Sugita A, Koganei K, Isobe K, Hibi T. IL23 differentially regulates the Th1/Th17 balance in ulcerative colitis and Crohn's disease. *Gut* 2008;57:1682–9
5. Höring E, Göpfert D, Schröter G, von Gaisberg U. Frequency and spectrum of microorganisms isolated from biopsy specimens in chronic colitis. *Endoscopy* 1991;23:325–7
6. Ni J, Wu G, Albenberg L, Tomov V. Gut microbiota and IBD: causation or correlation? *Nat Rev Gastroenterol Hepatol* 2017;14:573–84
7. Zhang C, Franklin CL, Ericsson AC. Consideration of gut microbiome in murine models of diseases. *Microorganisms* 2021;9:1062
8. Ericsson AC, Franklin CL. The gut microbiome of laboratory mice: considerations and best practices for translational research. *Mamm Genome* 2021;32:239–50
9. Powrie F, Leach MW, Mauze S, Menon S, Caddle LB, Coffman RL. Inhibition of Th1 responses prevents inflammatory bowel disease in scid mice reconstituted with CD45RBhi CD4+ T cells. *Immunity* 1994; 1:553–62
10. Becker C, Dornhoff H, Neufert C, Fantini M, Wirtz S, Huebner S, Nikolaev A, Lehr H, Murphy A, Valenzuela D, Yancopoulos G, Galle P, Karow M, Neurath MF. Cutting edge: IL-23 cross-regulates IL-12 production in T cell-dependent experimental colitis. *J Immunol* 2006;177:2760–4
11. Fuss IJ, Becker C, Yang Z, Groden C, Hornung RL, Heller F, Neurath MF, Strober W, Mannon PJ. Both IL-12p70 and IL-23 are synthesized during active Crohn's disease and are down-regulated by treatment with anti-IL-12 p40 monoclonal antibody. *Inflamm Bowel Dis* 2006;12:9–15
12. Yen D, Cheung J, Scheerens H, Poulet F, McClanahan T, McKenzie B, Kleinschek MA, Owyang A, Mattson J, Blumenschein W, Murphy E, Sathe M, Cua DJ, Kastelein RA, Rennick D. IL-23 is essential for T cell-mediated colitis and promotes inflammation via IL-17 and IL-6. *J Clin Invest* 2006;116:1310–6
13. Simon EG, Samuel S, Ghosh S, Moran GW. Ustekinumab: a novel therapeutic option in Crohn's disease. *Expert Opin Biol Ther* 2016;16:1065–74
14. Mucida D, Park Y, Cheroutre H. From the diet to the nucleus: vitamin A and TGF- β join efforts at the mucosal interface of the intestine. *Semin Immunol* 2009;21:14–21
15. Rudensky AY. Regulatory T cells and Foxp3. *Immunol Rev* 2011;241: 260–8
16. Ahern PP, Izcue A, Maloy KJ, Powrie F. The interleukin-23 axis in intestinal inflammation. *Immunol Rev* 2008;226:147–59
17. Duerr RH, Taylor KD, Brant SR, Rioux JD, Silverberg MS, Daly MJ, Steinhart AH, Abraham C, Regueiro M, Griffiths A, Dassopoulos T, Bitton A, Yang H, Targan S, Datta LW, Kistner EO, Schumm LP, Lee AT, Gregersen PK, Barnada MM, Rotter JI, Nicolae DL, Cho JH. A genome-wide association study identifies IL23R as an inflammatory bowel disease gene. *Science* 2006;314:1461–3
18. Jostins L, Ripke S, Weersma RK, Duerr RH, McGovern DP, Hui KY, Lee JC, Philip Schumm L, Sharma Y, Anderson CA, Essers J, Mitrovic M, Ning K, Cleynen I, Theatre E, Spain SL, Raychaudhuri S, Goyette P, Wei Z, Abraham C, Achkar JP, Ahmad T, Amininejad L, Ananthakrishnan AN, Andersen V, Andrews JM, Baidoo L, Balschun T, Bampton PA, Bitton A, Boucher G, Brand S, Büning C, Cohain A, Cichon S, D'Amato M, De Jong D, Devaney KL, Dubinsky M, Edwards C, Ellinghaus D, Ferguson LR, Franchimont D, Fransen K, Geary R, Georges M, Gieger C, Glas J, Haritunians T, Hart A, Hawkey C, Hedl M, Hu X, Karlsten TH, Kupcinskis L, Kugathasan S, Latiano A, Laukens D, Lawrance IC, Lees CW, Louis E, Mahy G, Mansfield J, Morgan AR, Mowat C, Newman W, Palmieri O, Ponsioen CY, Potocnik U, Prescott NJ, Regueiro M, Rotter JI, Russell RK, Sanderson JD, Sans M, Satsangi J, Schreiber S, Simms LA, Sventoraityte J, Targan SR, Taylor KD, Tremelling M, Verspaget HW, De Vos M, Wijmenga C, Wilson DC, Winkelmann J, Xavier RJ, Zeissig S, Zhang B, Zhang CK, Zhao H, Silverberg MS, Annesse V, Hakonarson H, Brant SR,

- Radford-Smith G, Mathew CG, Rioux JD, Schadt EE, Daly MJ, Franke A, Parkes M, Vermeire S, Barrett JC, Cho JH. Host-microbe interactions have shaped the genetic architecture of inflammatory bowel disease. *Nature* 2012;491:119–24
19. Rivas MA, Beaudoin M, Gardet A, Stevens C, Sharma Y, Zhang CK, Boucher G, Ripke S, Ellinghaus D, Burt N, Fennell T, Kirby A, Latiano A, Goyette P, Green T, Halfvarson J, Haritunians T, Korn JM, Kuruvilla F, Lagacé C, Neale B, Lo KS, Schumm P, Törkvist L, Dubinsky MC, Brant SR, Silverberg MS, Duerr RH, Altshuler D, Gabriel S, Lettre G, Franke A, D'Amato M, McGovern DPB, Cho JH, Rioux JD, Xavier RJ, Daly MJ. Deep resequencing of GWAS loci identifies independent rare variants associated with inflammatory bowel disease. *Nat Genet* 2011;43:1066–73
 20. Lundberg R, Bahl MI, Licht TR, Toft MF, Hansen AK. Microbiota composition of simultaneously colonized mice housed under either a gnotobiotic isolator or individually ventilated cage regime. *Sci Rep* 2017;7:42245
 21. Mähler M, Berar M, Feinstein R, Gallagher A, Illgen-Wilcke B, Pritchett-Corning K, Raspa M. FELASA recommendations for the health monitoring of mouse, rat, hamster, guinea pig and rabbit colonies in breeding and experimental units. *Lab Anim* 2014;48:178–92
 22. Segata N, Izard J, Waldron L, Gevers D, Miropolsky L, Garrett WS, Huttenhower C. Metagenomic biomarker discovery and explanation. *Genome Biol* 2011;12:R60
 23. Seamons A, Treuting PM, Meeker S, Hsu C, Paik J, Brabb T, Escobar SS, Alexander JS, Ericsson AC, Smith JG, Maggio-Price L. Obstructive lymphangitis precedes colitis in murine norovirus-infected Stat1-deficient mice. *Am J Pathol* 2018;188:1536–54
 24. Hue S, Ahern P, Buonocore S, Kullberg MC, Cua DJ, McKenzie BS, Powrie F, Maloy KJ. Interleukin-23 drives innate and T cell-mediated intestinal inflammation. *J Exp Med* 2006;203:2473–83
 25. Kullberg MC, Jankovic D, Feng CG, Hue S, Gorelick PL, McKenzie BS, Cua DJ, Powrie F, Cheever AW, Maloy KJ, Sher A. IL-23 plays a key role in *Helicobacter hepaticus*-induced T cell-dependent colitis. *J Exp Med* 2006;203:2485–94
 26. Darby A, Lertpiriyapong K, Sarkar U, Seneviratne U, Park DS, Gamazon ER, Batchelder C, Cheung C, Buckley EM, Taylor NS, Shen Z, Tannenbaum SR, Wishnok JS, Fox JG. Cytotoxic and pathogenic properties of *Klebsiella oxytoca* isolated from laboratory animals. *PLoS ONE* 2014;9:e100542
 27. Joainig MM, Gorkiewicz G, Leitner E, Weberhofer P, Zollner-Schwetz I, Lippe I, Feierl G, Krause R, Hinterleitner T, Zechner EL, Högenauer C. Cytotoxic effects of *Klebsiella oxytoca* strains isolated from patients with antibiotic-associated hemorrhagic colitis or other diseases caused by infections and from healthy subjects. *J Clin Microbiol* 2010;48:817–24
 28. Högenauer C, Langner C, Beubler E, Lippe IT, Schicho R, Gorkiewicz G, Krause R, Gerstgrasser N, Krejs GJ, Hinterleitner TA. *Klebsiella oxytoca* as a causative organism of antibiotic-associated hemorrhagic colitis. *N Engl J Med* 2006;355:2418–26
 29. Micic D, Hirsch A, Setia N, Rubin DT. Enteric infections complicating ulcerative colitis. *Intest Res* 2018;16:489–93
 30. Leitner E, Zarfel G, Luxner J, Herzog K, Pekard-Amenitsch S, Hoenigl M, Valentin T, Feierl G, Grisold AJ, Högenauer C, Sill H, Krause R, Zollner-Schwetz I. Contaminated handwashing sinks as the source of a clonal outbreak of KPC-2-producing *Klebsiella oxytoca* on a hematology ward. *Antimicrob Agents Chemother* 2015;59:714–6
- Experimental Biology and Medicine
31. Hertting O, Gremak O, Källman O, Guler L, Bergström J. An infant with *Klebsiella oxytoca* septic arthritis. *J Microbiol Immunol Infect* 2018; 51:153–4
 32. Hansen R, Thomson JM, Fox JG, El-Omar EM, Hold GL. Could *Helicobacter* organisms cause inflammatory bowel disease? *FEMS Immunol Med Microbiol* 2011;61:1–14
 33. Yu Y, Zhu S, Li P, Min L, Zhang S. *Helicobacter pylori* infection and inflammatory bowel disease: a crosstalk between upper and lower digestive tract. *Cell Death Dis* 2018;9:961
 34. Round JL, Mazmanian SK. Inducible Foxp3+ regulatory T-cell development by a commensal bacterium of the intestinal microbiota. *Proc Natl Acad Sci USA* 2010;107:12204–9
 35. Zhou Y, Zhi F. Lower level of bacteroides in the gut microbiota is associated with inflammatory bowel disease: a meta-Analysis. *Biomed Res Int* 2016;2016:5828959
 36. Osaka T, Moriyama E, Arai S, Date Y, Yagi J, Kikuchi J, Tsuneda S. Meta-analysis of fecal microbiota and metabolites in experimental colitic mice during the inflammatory and healing phases. *Nutrients* 2017;9:1–13
 37. Frank DN, St. Amand AL, Feldman RA, Boedeker EC, Harpaz N, Pace NR. Molecular-phylogenetic characterization of microbial community imbalances in human inflammatory bowel diseases. *Proc Natl Acad Sci USA* 2007;104:13780–5
 38. Mirsepasi-Lauridsen HC, Vallance BA, Krogfelt KA, Petersen AM. *Escherichia coli* pathobionts associated with inflammatory bowel disease. *Clin Microbiol Rev* 2019;32:e00060-18

39. Lee JG, Han DS, Jo SV, Lee AR, Park CH, Eun CS, Lee Y. Characteristics and pathogenic role of adherent-invasive *Escherichia coli* in inflammatory bowel disease: potential impact on clinical outcomes. *PLoS ONE* 2019;14:e0216165
40. Costa RFA, Ferrari MLA, Bringer MA, Darfeuille-Michaud A, Martins FS, Barnich N. Characterization of mucosa-associated *Escherichia coli* strains isolated from Crohn's disease patients in Brazil. *BMC Microbiol* 2020;20:178
41. Yang H, Mirsepasi-Lauridsen HC, Struve C, Allaire JM, Sivignon A, Vogl W, Bosman ES, Ma C, Fotovati A, Reid GS, Li X, Petersen AM, Gouin SG, Barnich N, Jacobson K, Yu HB, Krogfelt KA, Vallance BA. Ulcerative Colitis-associated *E. coli* pathobionts potentiate colitis in susceptible hosts. *Gut Microbes* 2020;12:1847976
42. Hiippala K, Kainulainen V, Kalliomäki M, Arkkila P, Satokari R. Mucosal prevalence and interactions with the epithelium indicate commensalism of *Sutterella* spp. *Front Microbiol* 2016;7:1706
43. Kaakoush NO. *Sutterella* species, IgA-degrading bacteria in ulcerative colitis. *Trends Microbiol* 2020;28:519–22
44. Yang F, Kumar A, Davenport KW, Kelliher JM, Ezeji JC, Good CE, Jacobs MR, Conger M, West G, Fiocchi C, Cominelli F, Earl A, Dichosa K, Rodriguez-Palacios A. Complete genome sequence of a parabacteroides distasonis strain (CavFT hAR46) isolated from a gut wall- cavitating microlesion in a patient with severe Crohn's disease. *Microbiol Resour Annou* 2019;8:e00585-19
45. Imhann F, Vich Vila A, Bonder MJ, Fu J, Gevers D, Visschedijk MC, Spekhorst LM, Alberts R, Franke L, van Dullemen HM, Ter Steege RWF, Huttenhower C, Dijkstra G, Xavier RJ, Festen EAM, Wijmenga C, Zhernakova A, Weersma RK. Interplay of host genetics and gut microbiota underlying the onset and clinical presentation of inflammatory bowel disease. *Gut* 2018;67:108–19
46. Lopetuso LR, Petito V, Graziani C, Schiavoni E, Paroni Sterbini F, Poscia A, Gaetani E, Franceschi F, Cammarota G, Sanguinetti M, Masucci L, Scaldaferrri F, Gasbarrini A. Gut microbiota in health, diverticular disease, irritable bowel syndrome, and inflammatory bowel diseases: time for microbial marker of gastrointestinal disorders. *Dig Dis* 2017;36:56–65
47. Cuffaro B, Assouhoun ALW, Boutillier D, Súkeníková L, Desramaut J, Boudebouze S, Salomé-Desnoullez S, Hrdý J, Waligora-Dupriet AJ, Maguin E, Grangette C. In vitro characterization of gut microbiota-derived commensal strains: selection of parabacteroides distasonis strains alleviating TNBS-induced colitis in mice. *Cells* 2020;9:2104
48. Kverka M, Zakostelska Z, Klimesova K, Sokol D, Hudcovic T, Hrcir T, Rossmann P, Mrazek J, Kopecny J, Verdu EF, Tlaskalova-Hogenova H. Oral administration of Parabacteroides distasonis antigens attenuates experimental murine colitis through modulation of immunity and microbiota composition. *Clin Exp Immunol* 2011;163:250–9
49. Baldelli V, Scaldaferrri F, Putignani L, Del Chierico F. The role of enterobacteriaceae in gut microbiota dysbiosis in inflammatory bowel diseases. *Microorganisms* 2021;9:697
50. Derrien M, Van Baarlen P, Hooiveld G, Norin E, Müller M, de Vos WM. Modulation of mucosal immune response, tolerance, and proliferation in mice colonized by the mucin-degrader *Akkermansia muciniphila*. *Front Microbiol* 2011;2:166–14
51. Seregin SS, Golovchenko N, Schaf B, Chen J, Pudlo NA, Mitchell J, Baxter NT, Zhao L, Schloss PD, Martens EC, Eaton KA, Chen GY. Erratum: NLRP6 protects *Il10*^{-/-} mice from colitis by limiting colonization of *Akkermansia muciniphila*. *Cell Rep* 2017;19:733–45
52. Plovier H, Everard A, Druart C, Depommier C, Van Hul M, Geurts L, Chilloux J, Ottman N, Duparc T, Lichtenstein L, Myridakis A, Delzenne NM, Klievink J, Bhattacharjee A, Van Der Ark KCH, Aalvink S, Martinez LO, Dumas ME, Maiter D, Loumaye A, Hermans MP, Thissen JP, Belzer C, De Vos WM, Cani PD. A purified membrane protein from *Akkermansia muciniphila* or the pasteurized bacterium improves metabolism in obese and diabetic mice. *Nat Med* 2017;23:107–13
53. Zhang T, Li Q, Cheng L, Buch H, Zhang F. *Akkermansia muciniphila* is a promising probiotic. *Microb Biotechnol* 2019;12:1109–25
54. Everard A, Belzer C, Geurts L, Ouwerkerk JP, Druart C, Bindels LB, Guiot Y, Derrien M, Muccioli GG, Delzenne NM, De Vos WM, Cani PD. Cross-talk between *Akkermansia muciniphila* and intestinal epithelium controls diet-induced obesity. *Proc Natl Acad Sci USA* 2013;110:9066–71
55. Reunanen J, Kainulainen V, Huuskonen L, Ottman N, Belzer C, Huhtinen H, de Vos WM, Satokari R. *Akkermansia muciniphila* adheres to enterocytes and strengthens the integrity of the epithelial cell layer. *Appl Environ Microbiol* 2015;81:3655–62
56. Wang L, Tang L, Feng Y, Zhao S, Han M, Zhang C, Yuan G, Zhu J, Cao S, Wu Q, Li L, Zhang Z. A purified membrane protein from *Akkermansia muciniphila* or the pasteurised bacterium blunts colitis associated tumorigenesis by modulation of CD8 + T cells in mice. *Gut* 2020;69:1988–97
57. Ivanov II, Atarashi K, Manel N, Brodie EL, Shima T, Karaoz U, Wei D, Goldfarb KC, Santee CA, Lynch SV, Tanoue T, Imaoka A, Itoh K, Takeda K, Umesaki Y, Honda K, Littman DR. Induction of intestinal Th17 cells by segmented filamentous bacteria. *Cell* 2009;139:485–98

58. Yang Y, Torchinsky MB, Gobert M, Xiong H, Xu M, Linehan JL, Alonzo F, Ng C, Chen A, Lin X, Sczesnak A, Liao JJ, Torres VJ, Jenkins MK, Lafaille JJ, Littman DR. Focused specificity of intestinal TH17 cells towards commensal bacterial antigens. *Nature* 2014;510:152–6
59. Wu HJ, Ivanov II, Darce J, Hattori K, Shima T, Umesaki Y, Littman DR, Benoist C, Mathis D. Gut-residing segmented filamentous bacteria drive autoimmune arthritis via T helper 17 cells. *Immunity* 2010;32:815–27
60. Hooper LV, Littman DR, Macpherson AJ. Interactions between the microbiota and the immune system. *Science* 2012;336:1268–73
61. Gaboriau-Routhiau V, Rakotobe S, Lécuyer E, Mulder I, Lan A, Bridonneau C, Rochet V, Pisi A, De Paepe M, Brandi G, Eberl G, Snel J, Kelly D, Cerf-Bensussan N. The key role of segmented filamentous bacteria in the coordinated maturation of gut helper T cell responses. *Immunity* 2009;31:677–89

7. Publication II: USP28 protects development of inflammation in mouse intestine by regulating STAT5 phosphorylation and IL22 production in T lymphocytes

Published: 2024 *Frontiers in immunology* Jul 15;15:1401949. doi: 10.3389/fimmu.2024.1401949

Authors: Le Menn, G., Pikkarainen, Keela., Mennerich, D., Miroszewska, D., Kietzmann, T., Chen, Z.,

7.1. Introduction

The balance between T helper cell 17 (Th17) and T regulatory (Treg) cells is crucial in the development of multiple inflammatory diseases such as auto-immune disease, obesity, and some cancers (1–3). A better understanding of the different molecular mechanisms involved in T cell development, differentiation and/ or function is essential to control this balance and develop novel strategies for the treatment of these inflammatory diseases.

Post-translational modifications (PTMs) play a crucial role in regulating the balance between Th17 and Treg cells (4–6). Among these PTMs, ubiquitination has been demonstrated to directly target FOXP3 and ROR γ t, which are key transcription factors involved in Treg and Th17 cell differentiation. In Treg cells, polyubiquitination of the transcription factor FOXP3, leads to its degradation through the proteasome as well as impairs Treg suppressive function (7, 8). In Th17 cells, ubiquitination of ROR γ t can have opposite effects depending on the E3 ubiquitin ligase utilized. ROR γ t ubiquitination through the E3 ubiquitin ligase TRAF5 stabilizes ROR γ t protein and enhances IL17 expression (9) while the E3 ligase Itch leads to ROR γ t proteasomal degradation and a reduction in Th17 differentiation (10).

Ubiquitination is reversible through the action of deubiquitinating enzymes (DUBs). The largest subfamily of DUBs are the ubiquitin-specific proteases (USPs), which have recently been discovered as drug targets for cancer treatment. Interestingly, FOXP3 and ROR γ t are not only targeted by different E3 ligases but also by multiple USPs. For example, USP44 and USP7 appeared to promote FOXP3 function in regulating Th17- and Treg-cell differentiation (11, 12). By contrast, USP4 and USP15 were found to promote Th17 immune cell differentiation through deubiquitination of ROR γ t (13, 14).

Apart from FOXP3 and ROR γ t, several other transcription factors such as STAT3, IRF4, BATF, HIF-1a, MYC, and NFAT play a role in Th17 cell differentiation (15–19), but their connections to the ubiquitin-proteasome system and the USPs involved are not well characterized. Notably, evidence from diverse cancer models supports the notion that MYC, HIF-1a, and STAT3 can be regulated by USP28 (20–22). Known for its impact on apoptosis, DNA damage, and cell proliferation, USP28 is extensively studied in cancer where it accelerates the progression and correlates with poor prognosis in various cancers, such as glioma, colorectal, and breast cancers (23). Apart from its role in cancer, the functions of USP28 beyond this context remain largely unexplored. Given that MYC is essential for the global metabolic reorganization that occurs early in activated T cells, that HIF-1a promotes Th17 differentiation under hypoxic conditions, and that STAT3 has a crucial role in Th17 cell differentiation through its association with ROR γ t expression, we hypothesize that USP28 may play a role in T cell development and function.

To investigate this hypothesis, we utilized previously generated USP28 knockout (USP28^{-/-}) and littermate control (USP28^{+/+}) mice. Our study extends to explore the impact of USP28 on intestinal inflammation using acute and chronic DSS-induced colitis in vivo models.

7.2. Materials and methods

7.2.1. 2.1 DSS colitis models

Control (USP28^{+/+}) and USP28 knockout (USP28^{-/-}) mice were obtained as described previously (24). All animals were maintained at the Laboratory Animal Center of the University of Oulu. All experimental procedures were performed in accordance with the license number ESAVI/7374/2019, approved by the National Project Authorization Board of Finland. DSS was added in the drinking water of 10-12 weeks old USP28^{+/+} and USP28^{-/-} male mice to induce colitis. For the acute DSS colitis model, mice were treated with 2% DSS-water for seven days. DSS-water was replaced by autoclaved water for the following 3 days. Mice were sacrificed on Day 10. For the chronic DSS colitis model, mice received 3 cycles alternating 7 days of 1.5% DSS-water and 14 days of autoclaved water. Blood, spleen, mesenteric lymph nodes (mLN) and colon were collected on the day of the sacrifice for cytokines detection, flow cytometry, and histological staining, respectively.

7.2.2. T cell preparation and isolation

CD4⁺ and CD8⁺ cells were isolated from mouse spleen and lymph nodes respectively using L3T4 microbeads and CD8a (Ly-2) microbeads (Miltenyi). Naïve CD4⁺ T cells were obtained by CD4⁺ enrichment (CD4⁺ T cell isolation kit, Miltenyi) followed by positive isolation of naïve cells (CD62L microbeads, Miltenyi). All T cell isolations were performed according to the manufacturer's instructions.

7.2.3. In vitro mouse cell culture

Complete RPMI1640 medium containing 10% fetal bovine serum (FBS), 2 mM glutamine, penicillin (100 IU/ml), streptomycin (0.1 mg/ml; Sigma-Aldrich), and 2.5 µM β-mercaptoethanol was used in in vitro cultures except when mentioned otherwise. Naïve CD4⁺ T cells were used for activation, proliferation, and polarization assays.

7.2.4. T cell activation assay

T cells were activated with different concentrations: 0, 0.5, 1, 2, and 5 µg/ml, of plate-bound anti-CD3 (16-0031-86) and anti-CD28 (16-0281-85, both from eBioscience) each for 24 and 48 h, respectively. The cells were then stained with antibodies against CD69 (11-0691-85) and CD25 (12-0251-83, both from eBioscience) and were analyzed by flow cytometry.

7.2.5. T cell proliferation assay

T cells were labeled with 2.5 µM CellTrace Violet dye (Invitrogen) according to the manufacturer's instructions, then activated and cultured in the presence of anti-CD3 (1 µg/ml) and anti-CD28 (1 µg/ml) for 3, 4 or 5 days. T-cell proliferation was analyzed by flow cytometry.

7.2.6. Treg cell polarization

T cells were cultured with anti-CD3 and anti-CD28 (1 µg/ml) in the presence of recombinant IL2 (10 ng/ml; R&D Systems) and TGFβ1 (10 ng/ml; PeproTech).

Th17 cell polarization: T cells were cultured with anti-CD3 and anti-CD28 (1 µg/ml) in the presence of recombinant mouse IL6 (60 ng/ml), human TGFβ1 (5 ng/ml), human IL23 (30 ng/ml) and anti-mouse anti-IFNγ (500-P119, 1 µg/ml, all from PeproTech) in complete IMDM culture medium.

7.2.7. Treg suppression assay

Celltrace violet labeled wild-type CD4⁺ cells (Tresp; 0.05x10⁶ cells per well) were co-cultured with polarized Treg cells in 96-well plates (1 µg/ml anti-CD3/CD28). Cells were mixed at a Treg/Tresp cell ratio of 2:1 to 1:4 (serial dilution of Treg cells, factor 2). Dye dilution was analyzed by flow cytometry on day 5.

7.2.8. Tc1 cell polarization

CD8+ T cells were cultured with anti-CD3 (1 µg/ml) and anti-CD28 (1 µg/ml) in the presence of recombinant mouse IL12 (20 ng/ml), and mouse anti-IL4 (500-P54, 1 µg/ml, both from PeproTech).

7.2.9. Flow cytometry

For surface staining, cells were stained in PBS + 0.5% BSA with the following antibodies: CD3 (560590), CD4 (550954), CD8 (553035), CD44 (561860), CD62L (561919), CD11b (553311), Gr1 (553129), B220 (553089), NK1.1 (553164, all from BD Biosciences, Franklin Lakes, NJ), CD69, CD25, and CD11c (11-0114-82, eBioscience, San Diego, CA) for 40 min at 4°C.

For intracellular staining of cytokines, cells were stimulated in the presence of phorbol 12-myristate 13-acetate (PMA) and ionomycin plus Golgi inhibitor for 4 hours before permeabilization and fixation steps. Foxp3 staining kit (eBioscience) and the following antibodies were used: anti-IL17A (17-7177-81), anti-IFN γ (53-7311-82), anti-Foxp3 (12-4774-42, all from eBioscience) and anti-T-bet (sc-21749, Santa Cruz Biotechnology). Stained cells were analyzed on an LSR Fortessa flow cytometer (BD Biosciences). Data were analyzed using FlowJo software (version 10, Tree Star, Ashland, OR).

7.2.10. RNA extraction and real-time quantitative PCR

RNA was extracted using the RNeasy kit (Qiagen) according to the manufacturer's instructions. Total RNA was reverse transcribed using the SuperScript VILO cDNA Synthesis Kit (Invitrogen). Quantitative PCR was performed using either Luna universal qPCR Master Mix (Biolabs) for the SYBER Master Mix or PROBE FAST ABI Prism 2X qPCR Master Mix (Kapa Biosystems) for the TaqMan Master Mix. The corresponding primer sequences are listed below in Table 8-1. Data were analyzed using the Hprt gene (Applied Biosystems) as an endogenous control.

Table 7.1 Primer sequences.

Gene name	Forward primer sequence 5' -3'	Reverse primer sequence 5' -3'
<i>Hprt</i>	GTAATGATCAGTCAA CGGGGGAC	CCAGCAAGCTTGCAA CCTTAACCA
<i>Ifng</i>	GCCATCAGCAACAA CATAAGC	TGGGACAATCTCTTC CCCAC
<i>Ttx21</i>	GCCAGGGAACCGCT TATATG	GACGATCATCTGGGT CACATTGT
<i>Granzyme B</i>	CCATCGTCCCTAGA GCTGAG	TTGTGGAGAGGGCA AACTTC
<i>Perforin</i>	GCCTGGTACAAAA CCTCCA	AGGGCTGTAAGGAC CGAGAT
<i>IL22</i>	GCCCTCACCGTGAC GTTTTA	CCACCATAGGAGGCC ACAAG
<i>IL2</i>	CTGCGCATGTTCT GGATTT	TGTGTTGTCAGAGCC CTTTAG
<i>Tgf-β</i>	CGTGGAAATCAAC GCTCCAC	AGAAGTTGGCATGGT AGCCC

Primer sequences used for real-time quantitative PCR.

7.2.11. Western blot detection

Primary antibodies against mTOR (2983s), Akt (9272), MAPKAPK5 (7419s), Stat3 (9132), p-Stat3 (9145), Stat5 (9363s), p-Stat5 (9359s), Jak1 (3332), p-Jak1 (3331s), Jak2 (3229), and p-Jak2 (3771l) were purchased

from Cell Signaling Technology; USP28 (HPA006778), and β -actin (A5441) were from Sigma Aldrich. Results were normalized according to β -actin expression that served as loading control.

7.2.12. Cytokine detection

Luminex technology [ProcartaPlex Mouse 11-Plex Mix and Match Panel (PPX-11-MXH6CNK); ThermoFisher Scientific] was used to measure IFN γ , IL1 β , IL10, IL12/IL23p40, IL17A, IL2, IL22, IL4, IL6, MIP-1 α and TNF α in mice plasma samples. All quantifications were done according to the protocols provided by the manufacturer.

7.2.13. Histopathology

For colitis experiments, colons were excised, washed with PBS, sectioned and divided into four equal parts: proximal (prox), middle 1 (mid1), middle 2 (mid2) and distal segments. Colon segments were then fixed in 10% neutral buffer formalin for 24h at room temperature before paraffin embedding. Tissues cross sections of 5 μ m were stained with hematoxylin and eosin and histologic evaluation of colitis severity was performed. Each colon section was analyzed and scored separately. The degree of inflammation was scored according to the Wirtz protocol. Sections were scored according to the following criteria: 0 = no evidence of inflammation, 1 = low level of inflammation, 2 = moderate level of inflammation, 3 = high level of inflammation, and 4 = maximum inflammation. The overall inflammation score was determined as the sum of the scores for the proximal, middle1, middle2, and distal segments.

7.2.14. Statistics

Statistical analyses were performed using the Prism 9.0 software (GraphPad Software, La Jolla, CA, USA). P values between groups were calculated using the student t-test. Differences were considered statistically significant at $p < 0.05$.

7.3. Result

7.3.1. USP28 deficiency alters steady state immune cell composition

Very little is known about the function of the deubiquitinating enzyme USP28 in T cell biology so far. First, we determined whether USP28 is expressed in different Th cell subsets and CD8 $^+$ cells. Analysis of RNA-seq data from our group (25) showed that USP28 was expressed in CD4 $^+$ cells and was preferentially expressed in in vitro differentiated Th17 compared to Th0 (control) and Treg cells (Figure 7.1A). In Treg cells, USP28 expression appeared to be increased at both the mRNA and protein levels compared to Th0 (Figures 7.1A, B). In CD8 $^+$ T cells activated under control conditions (Tc0) or differentiated under Tc1 conditions to induce IFN γ production, no difference in USP28 mRNA level was observed when comparing the two conditions (Appendix I Supplementary Figure 1A). However, a trend towards increased USP28 protein expression was detected in CD3/CD28 activated helper T cells at 72h compared to resting naïve T cells (Figure 7.1C), suggesting that USP28 protein levels are induced by T cell activation.

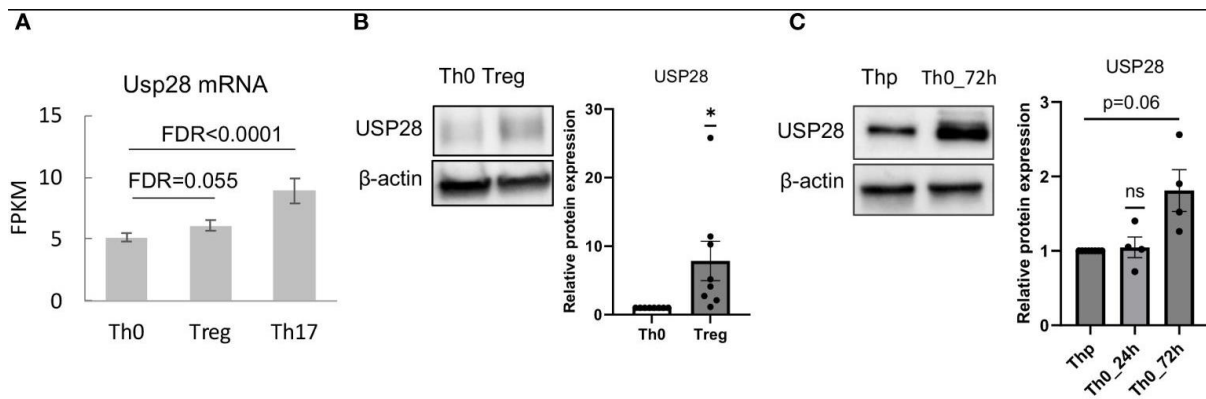


Figure 7-1 USP28 is expressed in differentiated Th17 and Treg cells. (A) USP28 mRNA expression level in CD4+ naïve T cells differentiated into Th0, Th17 and Treg cells analyzed by RNA sequencing (n=3). (B) USP28 protein expression. Representative Western blot images of one experiment (left) and USP28 protein expression relative to beta-actin (right) in in vitro differentiated Th0 and Treg cells (n=8). Data are expressed as mean \pm SEM. One-sample t-test * p < 0.05 between control cells (Th0) and effector T cells (Treg or Th17), ns, not significant between genotypes. (C) Representative Western blot image of USP28 protein expression in resting naïve CD4+ cells (Thp) and activated CD4+ T cells (n=4).

To better understand the role of USP28 in T cells, USP28 knockout (USP28^{-/-}) and their littermate control mice (USP28^{+/+}) were generated as previously described (24). First, the knockout of USP28 in T cells was confirmed by Western blot analysis (Figure 7.2A). Characterization of immune cell populations was then performed by flow cytometry analysis in the thymus, spleen, and blood of these mice. Overall, in the thymus, although USP28^{-/-} mice exhibited a decreased proportion of DN1 cells (CD44⁺CD25⁻), no further defect of thymic T-cell development could be observed, as similar proportions of single positive CD4⁺ and CD8⁺ cells were quantified in both genotypes (Appendix I Supplementary Figure S1B). In the spleen, the proportions of T cells (CD4⁺, CD8⁺ and, CD4⁺ naïve cells), NK cells and, myeloid cells are similar between USP28^{-/-} and USP28^{+/+} mice (Appendix I Supplementary Figure S1C). Next, the lymphoid cell proportions of B and T cells appear to be altered in the blood of USP28^{-/-} mice, with a decrease in B cells and an increase in T cells compared to USP28^{+/+} mice (Figure 7.2B).

Looking at the T cells population (CD3⁺ cells), CD8⁺ cells were significantly increased while CD4⁺ cells (naïve and helper cell subsets such as Th1, Th17 and Treg cells) remained unchanged in the blood of USP28^{-/-} mice (Figure 7.2B and Appendix I Supplementary Figure S1C). Similarly, the proportions of other cell types such as NK cells (NK1.1⁺), dendritic cells (CD11b⁺CD11c⁺), granulocytes (Gr1⁺), myeloid cells (CD11b⁺) and myeloid-derived suppressor cells (CD11b⁺Gr1⁺) were similar between USP28^{-/-} and USP28^{+/+} mice (Appendix I Supplementary Figure S1C). Overall, we observed a preferential expression of USP28 in Th17 and Treg cells, and an altered T cell distribution in USP28 knockout mice. These results led us to hypothesize that USP28 may play a role in T cell homeostasis or function.

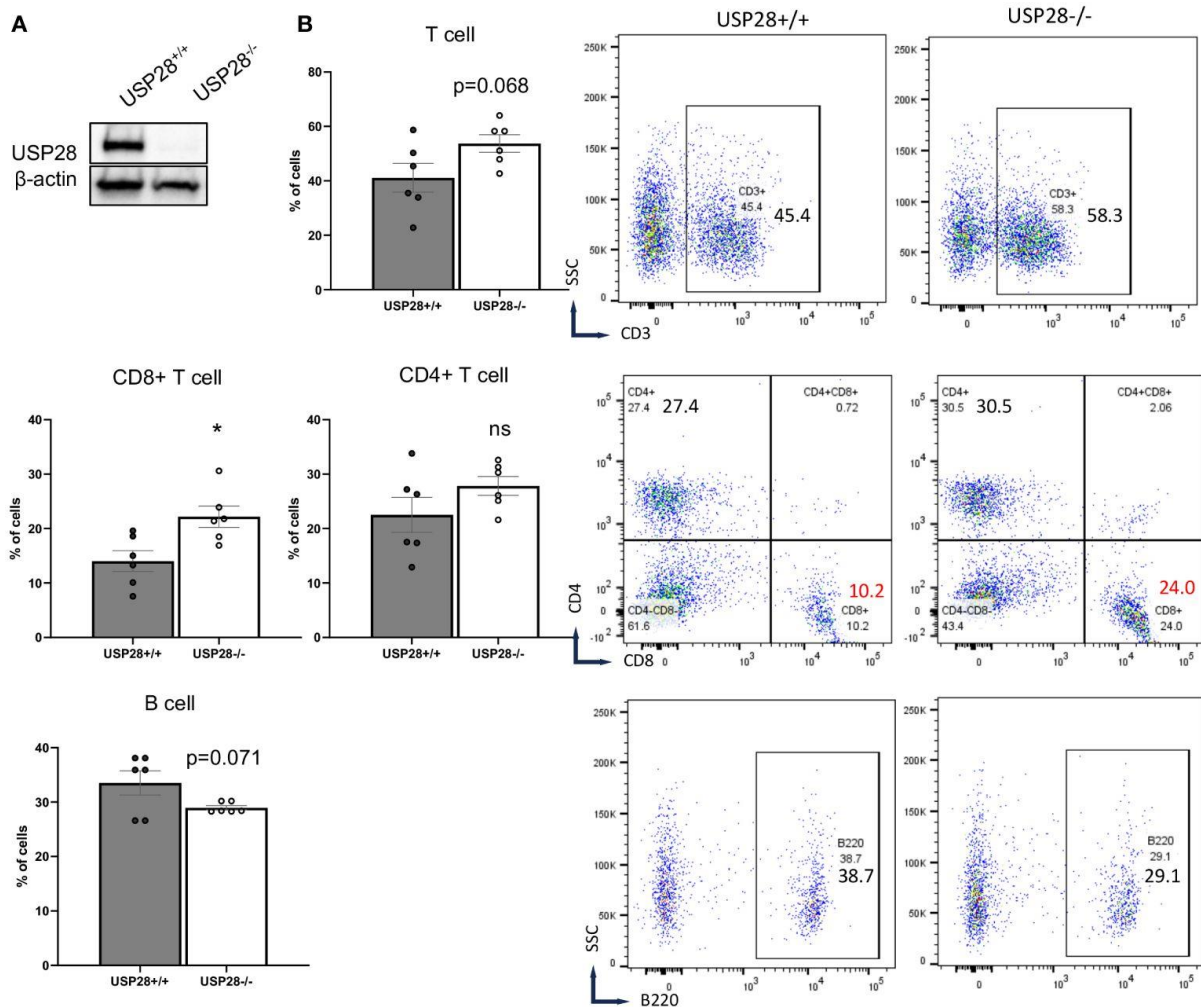


Figure 7.2 USP28 deficiency alters steady-state immune cell composition. (A) USP28 detection in control and USP28^{-/-} CD4⁺ naive cells. Representative Western blot image from three experiments. (B) Flow cytometry analysis of T cells (CD3⁺, CD8⁺ and CD4⁺ cells) and B cells in the blood of USP28^{-/-} and USP28^{+/+} mice. Data are expressed as mean ± SEM (n=5-6). Student T-test *p < 0.05 between genotypes, ns, not significant between genotypes.

7.3.2. USP28 protects mice against the early development of DSS-induced colitis

Since T cells play an essential role in the development of inflammation, to investigate the role of USP28 on T cell effector function, a DSS-induced colitis model was applied to USP28^{-/-} and littermate control mice. Chronic DSS-induced colitis was induced by three cycles of DSS treatment. Compared to control mice, USP28^{-/-} mice tended to lose more weight after the first two cycles of DSS feeding. However, at the end of the experiment, no differences in weight loss, spleen weight and colon weight/length ratio were observed between USP28^{-/-} and USP28^{+/+} mice (Figures 7.3A, B and Appendix Supplementary Figure S2A). Histological analysis was performed on the colon samples. The overall score was slightly increased in USP28^{-/-} mice compared to control mice (Figure 7.3C), and an increase in immune cell infiltration was particularly observed in the mid2 segment (Figure 7.3D). Furthermore, a disruption of mucosal structure in the mid2 segment can be observed in USP28^{-/-} DSS-challenged mice compared to USP28^{+/+} DSS-challenged mice (Figure 7.3E). Characterization of immune cells in spleen and mLN did not show any difference between the two groups (Appendix I Supplementary Figure S2B).

Because greater weight loss was observed in USP28^{-/-} mice after the first cycle of DSS treatment, we decided to evaluate the effect of USP28 in an acute DSS-induced colitis model. Throughout the acute DSS treatment, USP28^{-/-} mice lost significantly more weight compared to USP28^{+/+} control mice (Figure 7.3F). Reduced colon length and a trend towards increased inflammatory scoring of whole colon samples were consistently observed between the two groups (Figures 7.3G, H). Flow cytometric analyses of immune cells in the mLN showed changes in the CD8⁺ cell subset in both spleen and mLN. USP28 deficiency resulted in a reduced proportion of CD8⁺ cells compared to control mice, along with a shift in the proportion of central memory, effector and naïve CD8⁺ cells. This shift was characterized by a decrease in memory and naïve CD8⁺ cells in favor of effector CD8⁺ cells (Figures 7.3I, J and Appendix I Supplementary Figures S3A, B). Notably, a trend toward increased frequency of IFN γ ⁺ cells was observed in CD4⁻ cells, possibly from CD8⁺ cells. No differences were observed between the two groups for B cells, NK cells, myeloid cells, T cells or CD4⁺ T cell subsets (Appendix I Supplementary Figures S3C, D). Together, USP28 protects mice against early DSS-induced colitis development and long-term intestinal structural integrity.

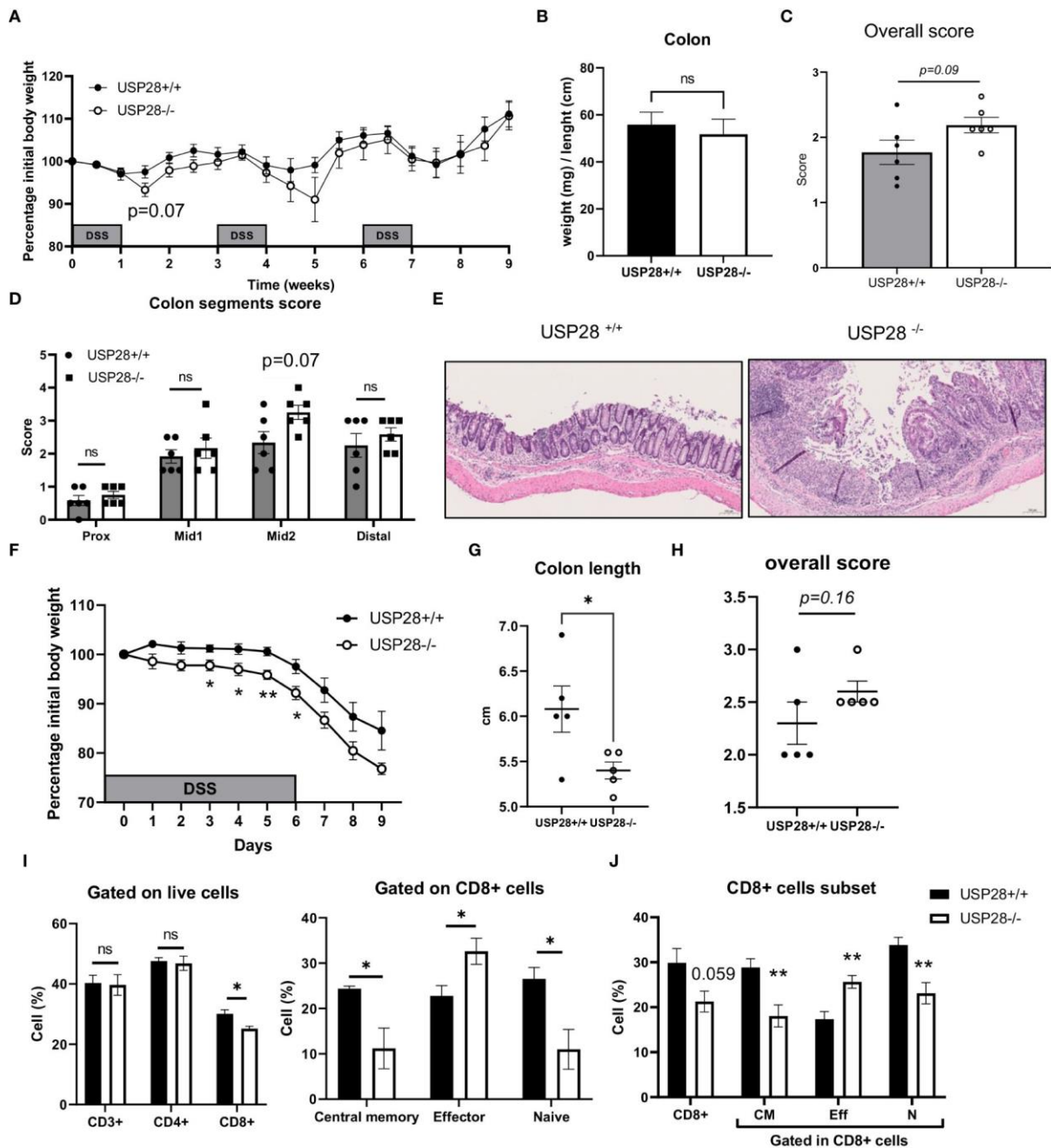


Figure 7.3 USP28 protects mice against the early development of DSS-induced colitis. USP28^{-/-} and USP28^{+/+} mice were challenged with chronic (A–E) or acute (F–J) DSS-induced colitis (n=6–7 and n=5 mice, respectively) prior to sacrifice and analysis of colitis severity and immune response. (A, F) Percentage of weight loss compared to the initial weight of the mice. (B) Colon weight/length ratio on the day of sacrifice. (C, H) Histology score for total colon segments and (D) details of histology score for each colon segment for chronic DSS-induced colitis samples. (E) H/E staining of mid2 colon segment. 20x (G). Colon length on the day of sacrifice from acute DSS colitis. (I) Flow cytometric analysis of T cell subset in draining mLN and spleen (J) samples from acute DSS-induced colitis. Data are expressed as mean \pm SEM. Unpaired T-test was used to compare between USP28^{-/-} and littermate control USP28^{+/+} mice. * $p < 0.05$, ** $p < 0.01$, ns, not significant between genotypes.

7.3.3. USP28 inhibits expression of IL22

We then characterized the cytokine profile in the peripheral blood of USP28 deficient and littermate control mice from the colitis experiments. In non-challenged mice, IL22 levels stood out. They were significantly higher in USP28 deficient mice compared to control mice, whereas no significant differences in other cytokine levels were observed between the two groups. In both acute and chronic DSS-induced colitis settings, cytokine levels were comparable between USP28^{-/-} and USP28^{+/+} mice and the level of IL22 was still increased in USP28^{-/-} mice compared to control mice (Table 7-2 and Figure 7-4A). To further elucidate the alterations in IL22, we conducted mRNA quantification of IL22 along with IFN γ and IL2, known to be necessary for optimal IL22 production (26) in mesenteric lymph node (mLN) samples from the acute DSS-challenged mice. The results revealed a significant upregulation in the mRNA expressions of both IL22 and IFN γ in USP28^{-/-} mice (Figure 7.4B). Together, this suggests a potential regulatory role of USP28 in modulating IL22 and IFN γ expression during acute DSS-induced colitis, with implications for the involvement of the IL2 pathway in this context.

Table 7.2 Luminex – plasma.

pg/ml	Baseline		Acute DSS		Chronic DSS	
	USP28 ^{+/+}	USP28 ^{-/-}	USP28 ^{+/+}	USP28 ^{-/-}	USP28 ^{+/+}	USP28 ^{-/-}
IFN γ	0,0843 \pm 0,08	1,46 \pm 0,91	0,45 \pm 0,45	2,94 \pm 1,67	ND	ND
IL1b	1,46 \pm 0,48	4,22 \pm 3,29	2,79 \pm 0,97	4,46 \pm 2,93	2,31 \pm 0,92	2,99 \pm 2,31
IL10	ND	ND	1,62 \pm 1,28	2,07 \pm 1,35	2,22 \pm 2,21	0
IL12	92,67 \pm 14,35	103,48 \pm 8,89	22,70 \pm 9,34	17,99 \pm 9,39	54,78 \pm 12,98	77,83 \pm 11,14
IL17a	8,31 \pm 3,29	4,86 \pm 3,30	ND	ND	ND	ND
IL22	16,49 \pm 4,37	48,52 \pm 11,37*	9,38 \pm 8,72	33,74 \pm 13,85	9,04 \pm 5,72	13,1 \pm 7,34
IL6	7,31 \pm 6,47	3,88 \pm 3,88	143,29 \pm 48,75	138,19 \pm 51,6	30,57 \pm 17,85	19,23 \pm 9,48
TNF α	0,87 \pm 0,87	1,11 \pm 1,11	5,71 \pm 4,23	8,12 \pm 4,96	ND	ND

Quantification of plasmatic cytokines in USP28^{-/-} and littermate control USP28^{+/+} mice under non-challenge (n=6), acute DSS colitis (n=5) or chronic DSS colitis (n=6) experimental conditions. Quantification was performed using multiplex technology and data are presented as mean \pm SEM, with ND indicating not determined. *p < 0.05 unpaired t-test comparing USP28^{+/+} and USP28^{-/-} mice from the same experimental condition.

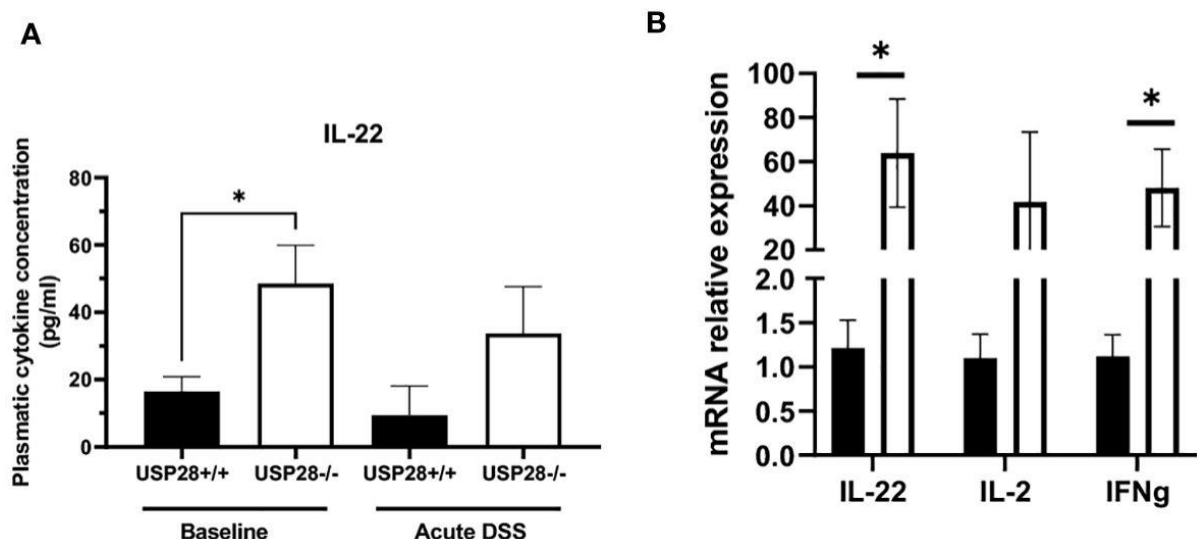


Figure 7.4 USP28 inhibits expression of IL22. (A) Graph showing IL22 cytokine quantification in plasma of USP28^{+/+} and USP28^{-/-} mice under baseline or acute DSS colitis condition (n=5-6). (B) Relative mRNA expression level of indicated genes in mLN of USP28^{+/+} and ^{-/-} mice under acute DSS colitis condition (vs. Hprt) (n=5). Data are expressed as mean \pm SEM. Unpaired t-test was used to compare USP28^{-/-} and littermate control USP28^{+/+} mice *p < 0.05.

7.3.4. USP28 is required for early T cell activation

IL2 is known to activate the JAK/STAT and MAPK pathways (27). IL2 and its downstream signaling play an important role in T cell activation and proliferation. Therefore, we decided to investigate the role of USP28 on T cell activation and proliferation in vitro by using USP28^{-/-} mice compared to control mice. For the T cell activation assay, naïve CD4⁺ cells were activated with elevated concentrations of anti-CD3 and anti-CD28 for 24h and 48h. T cell activation markers, CD69 for early activation and CD25 for mid-late activation, were then analyzed by flow cytometry (Figure 7-5A). At 24h post activation, cells only activated with anti-CD3 showed no differences in the proportion of CD69⁺ cells between USP28^{-/-} and USP28^{+/+} T cells. However, when the cells were activated with different concentrations of both anti-CD3 and anti-CD28, a significantly reduced frequency of CD69 expression was observed in USP28^{-/-} T cells compared to control T cells (Figure 7.5A). This effect was lost after 48h of activation (Appendix Supplementary Figure S4A). In response to activation, the cytokine IL2 is produced by T cells before binding to its own receptor (IL2R) on the surface of the T cells, inducing a positive feedback loop that promotes the IL2 signaling pathway (28). Therefore, the expression of CD25, the alpha subunit of the IL2R, was analyzed by flow cytometry. CD25 expression was observed in T cells at 24h, 48h and 72h after activation. Our data show that CD25 expression is significantly lower in USP28^{-/-} T cells at 24h post activation compared to USP28^{+/+} cells. The reduced CD25 and CD69 expression in USP28^{-/-} T cells were observed at an even earlier time point (Appendix I Supplementary Figure S4B). However, with prolonged activation, CD25 expression became similar in both USP28^{-/-} and USP28^{+/+} cells (Figure 7.5B).

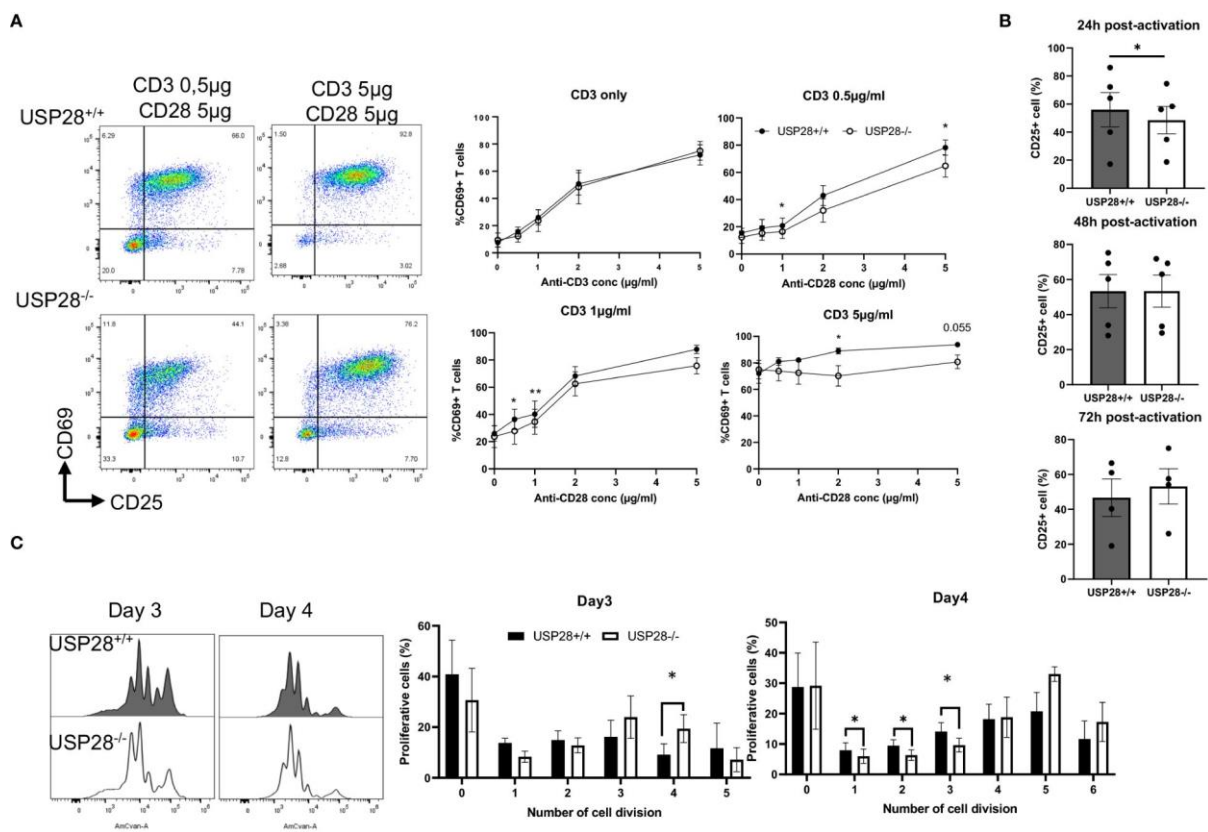


Figure 7.5 USP28 plays a role in T cell activation and proliferation through CD28/STAT5 signaling. (A) Flow cytometry analysis of in vitro naïve CD4⁺ T cell activation assay 24 hours after activation with increased concentrations of anti-CD3 and anti-CD28. Dot plot of one experiment and quantification of percentage of CD69⁺ cells (n=4). (B) Flow cytometric quantification of CD25 expression in T cells at 24h, 48h or 72h post activation (n=4-5). (C) Flow cytometry analysis of in vitro naïve CD4⁺ T cell proliferation assay after

activation for 3 and 4 days. A representative histogram image of T cells labeled with Celltrace Violet (AmCyan channel) and quantification of the percentage of proliferative cells for each cell division (n=5). Data are expressed as mean \pm SEM. Paired t-test was used to compare USP28^{-/-} and littermate control USP28^{+/+} T cells. *p \leq 0.05, **p<0.01.

Next, we examined in vitro T cell proliferation in USP28^{+/+} and USP28^{-/-} helper T cells after 3 and 4 days of activation. The distribution of proliferative T cells for each cell division is altered in USP28^{-/-} T cells (Figure 7.5C). Our results show a decrease in the percentage of proliferative cells in the undivided and early stage of division whereas there is an increase in the percentage of proliferative cells in the late stage of division in USP28^{-/-} T cells (Figure 7.5C).

Collectively, our results suggest that USP28^{-/-} T cells have an early defect in activation that may be mediated by IL2R/CD28 signaling. However, at a later stage an increase in their proliferation rate was observed upon TCR activation compared to USP28^{+/+} control T cells. Overall, USP28 appears to alter the early phase of T cell activation and proliferation.

7.3.5. USP28 contributes to Th17 cell differentiation and iTreg cell function

We then investigated the effect of USP28 on in vitro T cell differentiation and effector functions. First, CD8⁺ cells were isolated and cultured in vitro under anti-CD3/CD28 activation conditions (Tc0) or Th1 like inflammatory conditions (Tc1). Flow cytometric analysis of IFN γ ⁺ and T-bet⁺ cells as well as mRNA levels of these genes in USP28^{+/+} and USP28^{-/-} cells under either Tc0 or Tc1 condition did not show any differences between these two groups (Appendix I Supplementary Figures S5A, B). However, the mRNA levels of granzyme B and perforin in Tc1 condition seemed to be increased in USP28^{-/-} CD8 cells compared to their littermate controls (Appendix I Supplementary Figure S5B).

Next, we investigated the role of USP28 in the differentiation of CD4⁺ cells into Th17 or Treg cells and analyzed the Treg suppressive function. USP28^{-/-} and USP28^{+/+} naïve CD4⁺ T cells were isolated and cultured in different differentiation media for 3 days before flow cytometric analysis of Foxp3 and IL17 expression in these cells. No significant differences were observed in the proportion of Foxp3⁺ cells in Treg differentiation between USP28^{-/-} and USP28^{+/+} cells (Figure 7.6A). Since other members of the USP family, USP7 and USP44 have been shown to be involved in Treg suppressive function (11,12), we then performed an in vitro Treg suppression assay using Treg from USP28^{+/+} and USP28^{-/-} mice. The ability of Treg cells to inhibit the proliferation of responder T cells was assessed by Celltrace labelling and flow cytometry analysis. A decrease in the proliferation of responder T cells was observed when the cells were co-cultured with USP28^{-/-} Treg cells compared to control Treg cells (Figure 7.6B). On the Th17 side, we observed a consistently and significantly reduced proportion of IL17⁺ cells in USP28^{-/-} vs USP28^{+/+} cells under Th17 polarizing conditions at both protein and mRNA level (Figures 7.6C, D). Surprisingly, we also detected a significantly increased expression of IL22 at the mRNA level (Figure 7.6D).

Taken together, our results indicate that USP28 is not required for CD4⁺ Treg differentiation and Tc1 differentiation. However, USP28 is involved in Th17 cell differentiation, and more importantly, it contributes to Treg cell suppressive function.

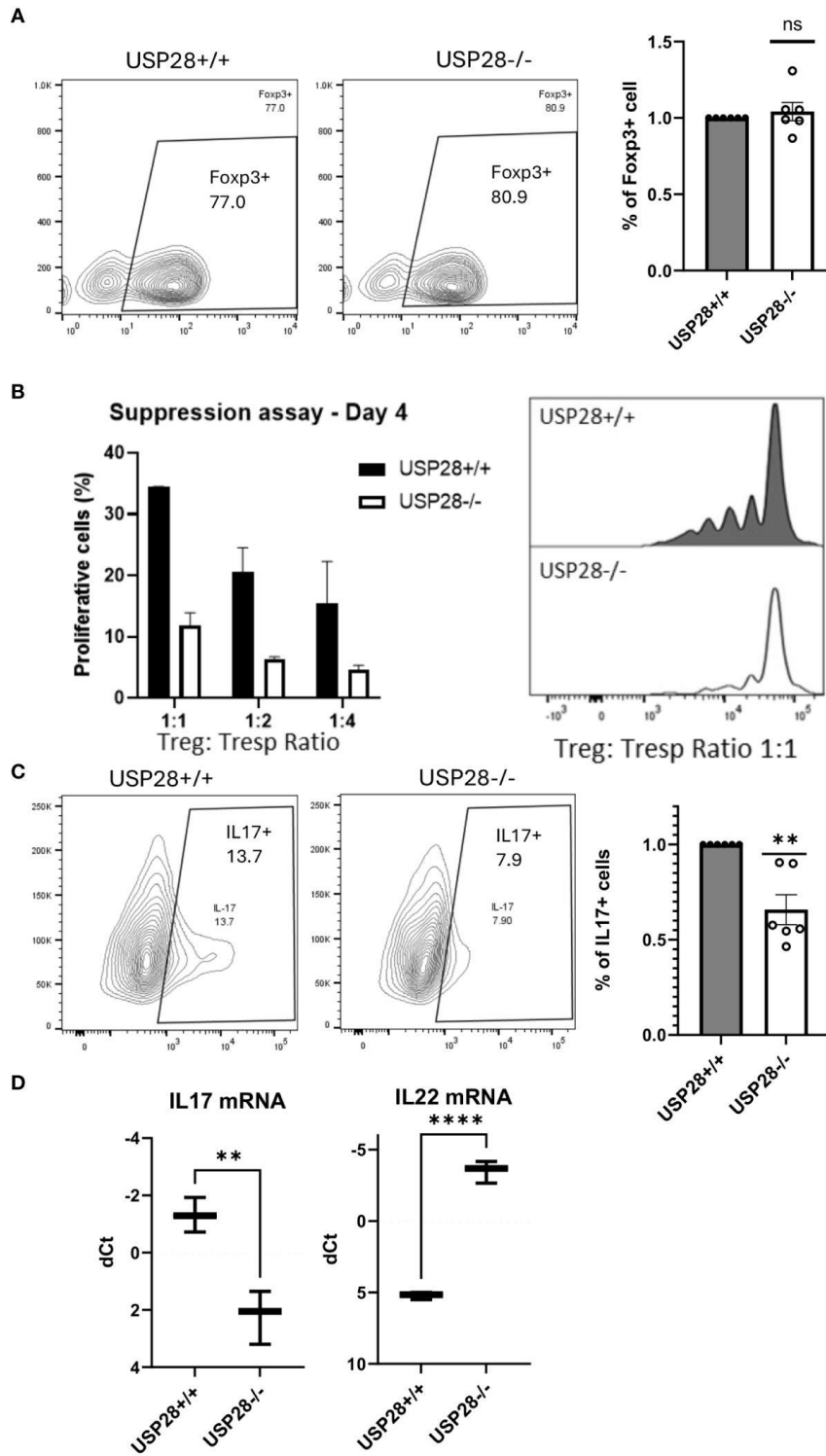


Figure 7.6 USP28 contributes to Th17 cell differentiation and iTreg cell function. In vitro differentiation of CD4⁺ naïve cells isolated from a pool of spleen and lymph node cells from USP28^{-/-} and USP28^{+/+} mice. (A) Flow cytometry image of a representative experiment and quantification of Fopx3⁺ cells in Treg (n=6) differentiated cells. (B) Treg suppression assay (n=2). Flow cytometric analysis of the percentage of proliferative T effector cells co-cultured with different ratios of Treg polarized cells and an image of a representative example (right panel). (C). Flow cytometry image of a representative experiment and quantification of IL17⁺ cells in Th17 (n=6) differentiated cells. (D). Relative mRNA expression level of indicated genes in Th17 polarized CD4⁺ cells (vs. Hprt) (n=3). Data are expressed as mean ± SEM (A–C). T-test was performed to compare USP28^{-/-} samples with littermate control. **p<0.01, ****p<0.0001 between genotypes.

7.3.6. USP28 regulates STAT5 signaling in T cells

Given our observations of decreased CD25 expression at early stages of T cell activation, but increased T cell proliferative capacity at later stages of activation, and increased IL22 expression in polarized Th17 cells, our aim was to investigate the underlying mechanisms. Given the established links between the CD28 costimulatory, IL2-activated JAK/STAT, and PI3K/AKT/mTOR pathways (28–33), we analyzed the expression of proteins related to these pathways in activated naive CD4+ T cells (Figure 7-7A and Appendix I Supplementary Figure S7-6A). The relative protein expressions of mTOR, AKT, MAPKAPK5, STAT3, p-STAT3, STAT5, JAK1, JAK2 and p-JAK2 were similar between USP28^{-/-} and control T cells, whereas we observed an increase of p-JAK1 and p-STAT5 expression in USP28^{-/-} T cells compared to control T cells (Figure 7.7B). Our results indicate that USP28 deficiency in T cells leads to an increase in the activation of JAK1/STAT5 signaling pathways. Next, we analyzed the kinetic activity of the STAT5 pathway in response to IL2 stimulation using Western blot analysis (Figure 7.7C). In response to IL2 stimulation, USP28^{-/-} T cells showed an increase in STAT5 phosphorylation after 30min and 6h, but not after 24h of stimulation compared to control T cells (Figure 7.7D). Furthermore, the increased STAT5 phosphorylation was also observed in

USP28^{-/-} T cell-depleted splenocytes in response to IL7 (Appendix I Supplementary Figure S7.6B). Together, these results suggest that USP28 regulates the activity of the STAT5 pathway by affecting STAT5 phosphorylation.

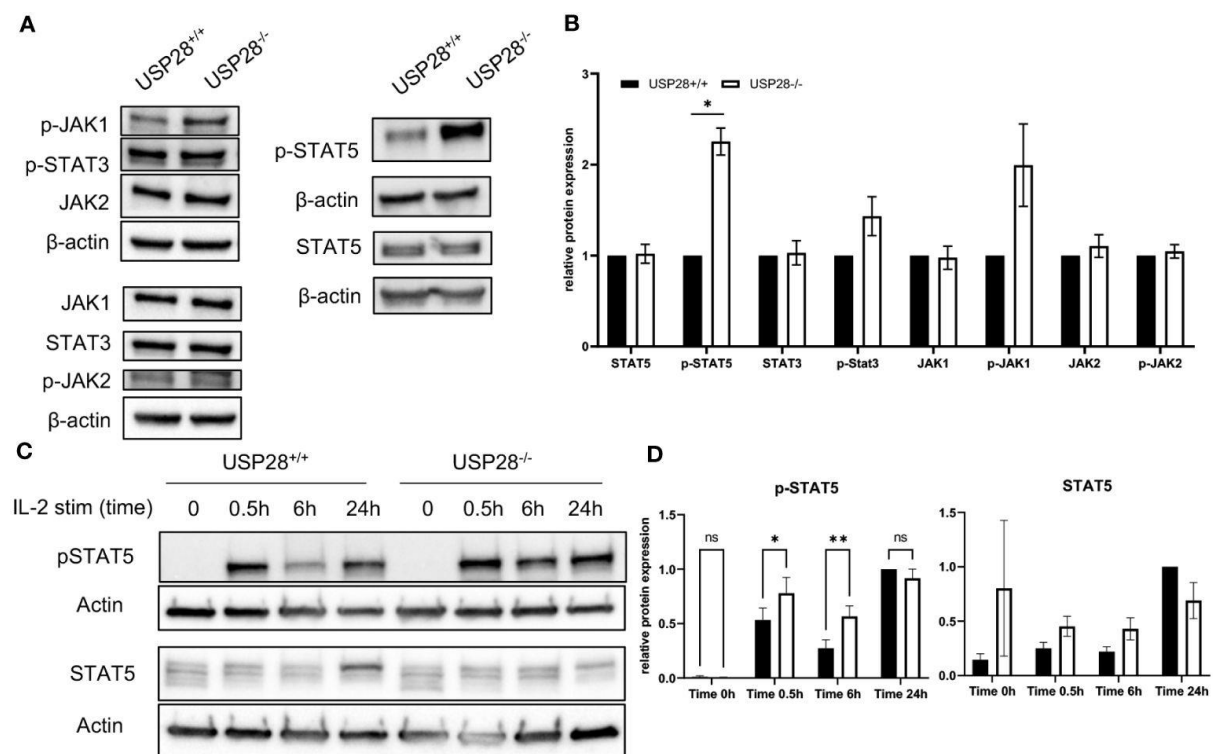


Figure 7.7 USP28 regulates STAT5 signaling in T cells. (A, B) Western blot analysis of the indicated proteins in USP28^{-/-} and USP28^{+/+} naive CD4+ T cells activated in vitro for 3 days (n=3). (A) Representative Western blot images. (B) Relative protein quantification to β-actin. (C, D) Kinetics of STAT5 signaling in response to IL2 stimulation and TCR activation in USP28^{-/-} or USP28^{+/+} CD4+ cells (n=2-3). (C) Representative Western blot images. (D) Quantification of p-STAT5 and STAT5 protein relative to β-actin and calculated ratio of p-STAT5/STAT5. Data are expressed as mean ± SEM or SD. One-sample t-test in (A, B) and 2-way ANOVA (D) were used to compare between genotypes. *p < 0.05, **p < 0.01, ns, not significant.

7.4. Discussion

In this study we have shown that USP28 plays a protective role in inflammation associated with DSS-induced colitis. We further characterized that USP28 contributes to T cell activation, subsets differentiation and/or function, possibly by mediating through the STAT5 pathway. As a member of the IL10 cytokine family, IL22 is secreted by various immune cell subsets such as Th17/Th1, CD8⁺ Tc22 subset cells, $\gamma\delta$ T cells or innate lymphoid cells (ILCs) (34-37). Previous studies have shown that IL22 positively regulates epithelial homeostasis while also activating pro-inflammatory immune responses, leading to a dual role in inflammatory diseases (38,39). Among the various immune cells analyzed, only CD8⁺ T cells seem to be affected by the deletion of USP28. The increase in CD8⁺ T cells in the blood and the increase in effector CD8⁺ T cells in the mLN in non-challenged mice and in mice with acute DSS colitis, respectively, were associated with elevated level of IL22 in the same organs. There is a possibility that USP28 deletion would favor CD8⁺ T cells producing IL22. In this case, the increased expression of granzyme B and perforin in CD8⁺ cells would result in a highly cytotoxic profile of these cells in USP28^{-/-} mice, which would be consistent with the exacerbated symptoms seen in acute DSS colitis. However, we cannot rule out the possibility that other immune cells are responsible for the increased IL22 production as we used constitutive USP28 knock-out mice and did not examine other immune cells.

Prior to cytokine production or T cell differentiation, T cell activation is required and is achieved through the recognition of at least two distinct signals, the TCR and the co-stimulatory CD28 molecule. During this process, inhibitory, degradative or activating ubiquitination and deubiquitination action can occur (40,41). Some members of the USP family, such as USP18, USP12 and USP9X, are known to directly affect the CD28 signaling pathway. Depletion of USP18 leads to hyperactivation and overproduction of IL2 in T cells, whereas deficiency of USP12 and USP9X causes a decrease in NF- κ B activation, which subsequently reduces proliferation and cytokine production upon TCR activation(42-44). Compared to other USPs, nothing is known about the role of USP28 in T cell activation or the potential target protein associated with this pathway. However, in our study, we observed a transient defect of the CD28/IL2R signaling pathway in USP28^{-/-} T cells upon early activation. Since STAT5 regulates the expression of CD25 (IL2RA), the increased expression of CD25 and increased T cell proliferation at a later time point may be due to increased STAT5 phosphorylation (45).

While examining proteins involved in T cell activation/proliferation signaling pathways, we observed an over-activation of the STAT5 pathway associated with an increase in STAT5 phosphorylation levels as well as a decrease in total STAT5 protein in USP28^{-/-} T cells. In non-small-cell lung cancer, USP28 appears to mediate STAT3 signaling through deubiquitination and stabilization (21). Although that study did not report changes in STAT5 levels, a similar interaction between USP28 and STAT5 would be consistent with our results in which ubiquitination of STAT5 in the absence of USP28 would lead to its proteasomal degradation (46). Our results seem to show a different role of USP28 on the STAT5 pathway.

Upon binding to its receptor, IL22 activates several signaling pathways, including phosphorylation of JAK1, TYK2 and STAT1, STAT3 and STAT5 (27,47). STAT5 has been reported to regulate IL22 expression (26). In this study, we observed both increased STAT5 phosphorylation and enhanced IL22, suggesting that USP28 is involved in the IL22/STAT5 positive regulatory feedback loop.

Finally, STAT5 and IL2 are also known to play a central role in Treg development and function (48). Treatment with neutralizing antibodies against IL2, transgenic mice lacking IL2, IL2R or STAT5 show a deficit in Treg cells and develop autoimmune disease(49,50). Treg suppressive function can be restored by expressing a gain-of-function form of STAT5 (51). The increased activation of the STAT5 pathway in USP28^{-/-} T cells may therefore be linked to the higher suppressive function found in the Treg cells. Importantly, STAT5 has been shown to suppress Th17 differentiation (52), here we observed the reduced IL17 expression in USP28^{-/-} T cells most likely due to increased STAT5 phosphorylation.

In conclusion, using USP28^{-/-} mice, we have uncovered the essential role of USP28 in multiple aspects of T cell functionality. Our data demonstrate that USP28 contributes to the protective effect for the early development of intestinal inflammation by regulating STAT5 signaling and IL22 production.

7.5. References

1. Knochelmann HM, Dwyer CJ, Bailey SR, Amaya SM, Elston DM, Mazza-McCrann JM, et al. When worlds collide: Th17 and Treg cells in cancer and autoimmunity. *Cell Mol Immunol.* (2018) 15:458–69. doi: 10.1038/s41423-018-0004-4
2. Lee G. The balance of th17 versus treg cells in autoimmunity. *IJMS.* (2018) 19:730. doi: 10.3390/ijms19030730
3. Zhang S, Gang X, Yang S, Cui M, Sun L, Li Z, et al. The alterations in and the role of the th17/treg balance in metabolic diseases. *Front Immunol.* (2021) 12:678355. doi: 10.3389/fimmu.2021.678355
4. Kim HK, Jeong MG, Hwang ES. Post-translational modifications in transcription factors that determine T helper cell differentiation. *MolCells.* (2021) 44:318–27. doi: 10.14348/molcells.2021.0057
5. Le Menn G, Jabłońska A, Chen Z. The effects of post-translational modifications on Th17/Treg cell differentiation. *Biochim Biophys Acta (BBA) - Mol Cell Res.* (2022) 1869:119223. doi: 10.1016/j.bbamcr.2022.119223
6. Zhang W, Liu X, Zhu Y, Liu X, Gu Y, Dai X, et al. Transcriptional and posttranslational regulation of Th17/Treg balance in health and disease. *Eur J Immunol.* (2021) 51:2137–50. doi: 10.1002/eji.202048794
7. Chen Z, Barbi J, Bu S, Yang HY, Li Z, Gao Y, et al. The ubiquitin ligase stub1 negatively modulates regulatory T cell suppressive activity by promoting degradation of the transcription factor foxp3. *Immunity.* (2013) 39:272–85. doi: 10.1016/j.immuni.2013.08.006
8. Shi LZ, Wang R, Huang G, Vogel P, Neale G, Green DR, et al. HIF1 α -dependent glycolytic pathway orchestrates a metabolic checkpoint for the differentiation of TH17 and Treg cells. *J Exp Med.* (2011) 208:1367–76. doi: 10.1084/jem.20110278
9. Wang X, Yang J, Han L, Zhao K, Wu Q, Bao L, et al. TRAF5-mediated lys-63-linked polyubiquitination plays an essential role in positive regulation of ROR γ t in promoting IL-17A expression. *J Biol Chem.* (2015) 290:29086–94. doi: 10.1074/jbc.M115.664573
10. Kathania M, Khare P, Zeng M, Cantarel B, Zhang H, Ueno H, et al. Itch inhibits IL-17-mediated colon inflammation and tumorigenesis by ROR- γ t ubiquitination. *Nat Immunol.* (2016) 17:997–1004. doi: 10.1038/ni.3488
11. van Loosdregt J, Fleskens V, Fu J, Brenkman AB, Bekker CPJ, Pals CEGM, et al. Stabilization of the transcription factor foxp3 by the deubiquitinase USP7 increases treg-cell-suppressive capacity. *Immunity.* (2013) 39:259–71. doi: 10.1016/j.immuni.2013.05.018
12. Yang J, Wei P, Barbi J, Huang Q, Yang E, Bai Y, et al. The deubiquitinase USP44 promotes Treg function during inflammation by preventing FOXP3 degradation. *EMBO Rep.* (2020) 21:e50308. doi: 10.15252/embr.202050308
13. He Z, Wang F, Ma J, Sen S, Zhang J, Gwack Y, et al. Ubiquitination of ROR γ t at lysine 446 limits th17 differentiation by controlling coactivator recruitment. *J Immunol.* (2016) 197:1148–58. doi: 10.4049/jimmunol.1600548
14. Yang J, Xu P, Han L, Guo Z, Wang X, Chen Z, et al. Cutting edge: Ubiquitin-specific protease 4 promotes th17 cell function under inflammation by deubiquitinating and stabilizing ROR γ t. *J Immunol.* (2015) 194:4094–7. doi: 10.4049/jimmunol.1401451
15. Brüstle A, Heink S, Huber M, Rosenplänter C, Stadelmann C, Yu P, et al. The development of inflammatory TH-17 cells requires interferon-regulatory factor 4. *Nat Immunol.* (2007) 8:958–66. doi: 10.1038/ni1500
16. Durant L, Watford WT, Ramos HL, Laurence A, Vahedi G, Wei L, et al. Diverse targets of the transcription factor STAT3 contribute to T cell pathogenicity and homeostasis. *Immunity.* (2010) 32:605–15. doi: 10.1016/j.immuni.2010.05.003
17. Gomez-Rodriguez J, Sahu N, Handon R, Davidson TS, Anderson SM, Kirby MR, et al. Differential expression of interleukin-17A and -17F is coupled to T cell receptor signaling via inducible T cell kinase. *Immunity.* (2009) 31:587–97. doi: 10.1016/j.immuni.2009.07.009
18. Schraml BU, Hildner K, Ise W, Lee WL, Smith WAE, Solomon B, et al. The AP-1 transcription factor Batf controls TH17 differentiation. *Nature.* (2009) 460:405–9. doi: 10.1038/nature08114
19. Shen H, Shi LZ. Metabolic regulation of TH17 cells. *Mol Immunol.* (2019) 109:81–7. doi: 10.1016/j.molimm.2019.03.005
20. Flügel D, Görlach A, Kietzmann T. GSK-3 β regulates cell growth, migration, and angiogenesis via Fbw7 and USP28-dependent degradation of HIF-1 α . *Blood.* (2012) 119:1292–301. doi: 10.1182/blood-2011-08-375014
21. Li P, Huang Z, Wang J, Chen W, Huang J. Ubiquitin-specific peptidase 28 enhances STAT3 signaling and promotes cell growth in non-small-cell lung cancer. *OTT.* (2019) 12:1603–11. doi: 10.2147/OTT
22. Popov N, Wanzel M, Madiredjo M, Zhang D, Beijersbergen R, Bernards R, et al. The ubiquitin-specific protease USP28 is required for MYC stability. *Nat Cell Biol.* (2007) 9:765–74. doi: 10.1038/ncb1601
23. Ren X, Jiang M, Ding P, Zhang X, Zhou X, Shen J, et al. Ubiquitin-specific protease 28: the decipherment of its dual roles in cancer development. *Exp Hematol Oncol.* (2023) 12:27. doi: 10.1186/s40164-023-00389-z
24. Richter K, Paakkola T, Mennerich D, Kubaichuk K, Konzack A, Ali-Kippari H, et al. USP28 deficiency promotes breast and liver carcinogenesis as well as tumor angiogenesis in a HIF-independent manner. *Mol Cancer Res.* (2018) 16:1000–12. doi: 10.1158/1541-7786.MCR-17-0452
25. Mohammad I, Nousiainen K, Bhosale SD, Starskaia I, Moulder R, Rokka A, et al. Quantitative proteomic characterization and comparison of T helper 17 and induced regulatory T cells. *PLoS Biol.* (2018) 16:e2004194. doi: 10.1371/journal.pbio.2004194
26. Bauché D, Joyce-Shaikh B, Fong J, Villarino AV, Ku KS, Jain R, et al. IL-23 and IL-2 activation of STAT5 is required for optimal IL-22 production in ILC3s during colitis. *Sci Immunol.* (2020) 5:eaav1080. doi: 10.1126/sciimmunol.aav1080
27. Lejeune D, Dumoutier L, Constantinescu S, Kruijer W, Schuringa JJ, Renauld JC. Interleukin-22 (IL-22) activates the JAK/STAT, ERK, JNK, and p38 MAP kinase pathways in a rat hepatoma cell line. *J Biol Chem.* (2002) 277:33676–82. doi: 10.1074/jbc.M204204200

28. Ross SH, Cantrell DA. Signaling and function of interleukin-2 in T lymphocytes. *Annu Rev Immunol.* (2018) 36:411–33. doi: 10.1146/annurev-immunol-042617-053352
29. Appelman LJ, van Puijenbroek AAFL, Shu KM, Nadler LM, Boussiotis VA. CD28 costimulation mediates down-regulation of p27kip1 and cell cycle progression by activation of the PI3K/PKB signaling pathway in primary human T cells. *J Immunol.* (2002) 168:2729–36. doi: 10.4049/jimmunol.168.6.2729
30. Appelman LJ, Berezovskaya A, Grass I, Boussiotis VA. CD28 costimulation mediates T cell expansion via IL-2-independent and IL-2-dependent regulation of cell cycle progression. *J Immunol.* (2000) 164:144–51. doi: 10.4049/jimmunol.164.1.144
31. Kane LP, Andres PG, Howland KC, Abbas AK, Weiss A. Akt provides the CD28 costimulatory signal for up-regulation of IL-2 and IFN- γ but not TH2 cytokines. *Nat Immunol.* (2001) 2:37–44. doi: 10.1038/83144
32. Kelly E, Won A, Refaeli Y, Van Parijs L. IL-2 and related cytokines can promote T cell survival by activating AKT. *J Immunol.* (2002) 168:597–603. doi: 10.4049/jimmunol.168.2.597
33. Ray JP, Staron MM, Shyer JA, Ho PC, Marshall HD, Gray SM, et al. The interleukin-2-mTORc1 kinase axis defines the signaling, differentiation, and metabolism of T helper 1 and follicular B helper T cells. *Immunity.* (2015) 43:690–702. doi: 10.1016/j.immuni.2015.08.017
34. Lindahl H, Olsson T. Interleukin-22 influences the th1/th17 axis. *Front Immunol.* (2021) 12:618110. doi: 10.3389/fimmu.2021.618110
35. Pappotto PH, Reinhardt A, Prinz I, Silva-Santos B. Innately versatile: $\gamma\delta$ 17 T cells in inflammatory and autoimmune diseases. *J Autoimmunity.* (2018) 87:26–37. doi: 10.1016/j.jaut.2017.11.006
36. St. Paul M, Saibil SD, Lien SC, Han S, Sayad A, Mulder DT, et al. IL6 induces an IL22+ CD8+ T-cell subset with potent antitumor function. *Cancer Immunol Res.* (2020) 8:321–33. doi: 10.1158/2326-6066.CIR-19-0521
37. Yan J, Yu J, Liu K, Liu Y, Mao C, Gao W. The pathogenic roles of IL-22 in colitis: its transcription regulation by muscudin in T helper subsets and innate lymphoid cells. *Front Immunol.* (2021) 12:758730. doi: 10.3389/fimmu.2021.758730
38. Keir ME, Yi T, Lu TT, Ghilardi N. The role of IL-22 in intestinal health and disease. *J Exp Med.* (2020) 217:e20192195. doi: 10.1084/jem.20192195
39. Shohan M, Dehghani R, Khodadadi A, Dehnavi S, Ahmadi R, Joudaki N, et al. Interleukin-22 and intestinal homeostasis: Protective or destructive? *IUBMB Life.* (2020) 72:1585–602. doi: 10.1002/iub.2295
40. Gavali S, Liu J, Li X, Paolino M. Ubiquitination in T-cell activation and checkpoint inhibition: new avenues for targeted cancer immunotherapy. *IJMS.* (2021) 22:10800. doi: 10.3390/ijms221910800
41. Wang A, Zhu F, Liang R, Li D, Li B. Regulation of T cell differentiation and function by ubiquitin-specific proteases. *Cell Immunol.* (2019) 340:103922. doi: 10.1016/j.cellimm.2019.103922
42. Fu Y, Wang P, Zhao J, Tan Y, Sheng J, He S, et al. USP12 promotes CD4+ T cell responses through deubiquitinating and stabilizing BCL10. *Cell Death Differ.* (2021) 28:2857–70. doi: 10.1038/s41418-021-00787-y
43. Liu X, Li H, Zhong B, Blonska M, Gorjestani S, Yan M, et al. USP18 inhibits NF- κ B and NFAT activation during Th17 differentiation by deubiquitinating the TAK1-TAB1 complex. *J Exp Med.* (2013) 210:1575–90. doi: 10.1084/jem.20122327
44. Park Y, Liu YC. Regulation of T cell function by the ubiquitin-specific protease USP9X via modulating the Carma1-Bcl10-Malt1 complex. *Proc Natl Acad Sci USA.* (2013) 110:9433–8. doi: 10.1073/pnas.1221925110
45. Li J, Wang J, Pan T, Zhou X, Yang H, Wang L, et al. USP25 deficiency promotes T cell dysfunction and transplant acceptance via mitochondrial dynamics. *Int Immunopharmacology.* (2023) 117:109917. doi: 10.1016/j.intimp.2023.109917
46. Shibata N, Ohoka N, Tsuji G, Demizu Y, Miyawaza K, Ui-Tei K, et al. Deubiquitylase USP25 prevents degradation of BCR-ABL protein and ensures proliferation of Ph-positive leukemia cells. *Oncogene.* (2020) 39:3867–78. doi: 10.1038/s41388-020-1253-0
47. Pickert G, Neufert C, Leppkes M, Zheng Y, Wittkopf N, Warntjen M, et al. STAT3 links IL-22 signaling in intestinal epithelial cells to mucosal wound healing. *J Exp Med.* (2009) 206:1465–72. doi: 10.1084/jem.20082683
48. Colamatteo A, Carbone F, Bruzzaniti S, Galgani M, Fusco C, Maniscalco GT, et al. Molecular mechanisms controlling foxp3 expression in health and autoimmunity: from epigenetic to post-translational regulation. *Front Immunol.* (2020) 10:3136. doi: 10.3389/fimmu.2019.03136
49. Malek TR, Yu A, Vincek V, Scibelli P, Kong L. CD4 regulatory T cells prevent lethal autoimmunity in IL-2R β -deficient mice. *Immunity.* (2002) 17:167–78. doi: 10.1016/S1074-7613(02)00367-9
50. Setoguchi R, Hori S, Takahashi T, Sakaguchi S. Homeostatic maintenance of natural Foxp3+ CD25+ CD4+ regulatory T cells by interleukin (IL)-2 and induction of autoimmune disease by IL-2 neutralization. *J Exp Med.* (2005) 201:723–35. doi: 10.1084/jem.20041982
51. Chinen T, Kannan AK, Levine AG, Fan X, Klein U, Zheng Y, et al. An essential role for the IL-2 receptor in Treg cell function. *Nat Immunol.* (2016) 17:1322–33. doi: 10.1038/ni.3540
52. Laurence A, Tato CM, Davidson TS, Kanno Y, Chen Z, Yao Z, et al. Interleukin-2 signaling via STAT5 constrains T helper 17 cell generation. *Immunity.* (2007) 26:371–81. doi: 10.1016/j.immuni.2007.02.009

8. Publication III: Spatial mapping of epithelial changes and suppressive immune populations in colorectal cancer tumor microenvironment

Unpublished manuscript

Authors: Miroszewska, D., Song, S*, Urbiola-Salvador, V*, Cazares Olivera, M., Jabłońska, A., Duzowska, K., Drężek-Chyła, K., Zdrenka, M., Śrutek, E., Szyłberg, Ł., Jankowski, M., Bała, D., Zegarski, W., Nowikiewicz, T., Makarewicz, W., Adamczyk, A., Ambicka, A., Przewoźnik, M., Harazin-Lechowicz, A., Ryś, J., Filipowicz, N., Piotrowski, A., Dumanski, JP., Li, B., Chen, Z.

8.1. Introduction

As of 2020, colorectal cancer (CRC) was diagnosed in almost 2 million patients and accounted for almost 1 million deaths worldwide. These numbers are predicted to increase to 3.2 million and 1.6 million respectively by 2040¹.

Tumor microenvironment (TME) composition is highly complex and heterogenous including cells such as T-cells, macrophages, dendritic cells, and cancer-associated fibroblast that are usually attracted by the tumor signaling². In the TME there is a constant interaction between cancer cells and host cells, which leads to infiltration of immunosuppressive cells, angiogenesis, and creation of tumor-favorable environment³. In case of tumor immunosurveillance is ineffective, tumor cells escape the detection by the host's immune system⁴. For example, SIRT1 expressed by the CRC cells enhances the migration of tumor associated macrophages (TAMs) via CXCL12/CXCR4 axis and TAMs downregulate the activity of cytotoxic CD8+ T-cells that are main killers of foreign cells via MHC I presentation^{5,6}. TAMs are characterized by a high plasticity and upon stimulation of external factors may differentiate into either M1 or M2 populations playing opposite roles in the tumor progression. Typically M1 macrophages exhibit anti-tumor functions by secreting pro-inflammatory cytokines, whilst M2 macrophages play pro-tumorigenic roles by secretion of growth factors, matrix metalloproteinases, or secretion of anti-inflammatory cytokines such as IL4 or IL10⁷. Mainly M2 TAMs facilitate epithelial-to-mesenchymal transition (EMT) and angiogenesis. However, M1 macrophages were found to promote tumor progression via NF-κB/FAK signaling⁸. Similarly, the exact role and the significance of tumor infiltrating lymphocytes (TILs) in predicting CRC patient's prognosis is not well established. In CRC, CD8+ cytotoxic TILs are linked to better prognosis while regulatory T-cells (Tregs) exhibit immunosuppressive functions and were associated with poor prognosis⁹⁻¹³.

Moreover, there is existing evidence of M2 macrophages inducing Tregs in CRC to facilitate cancer development by enforcing immunosuppressive environment¹⁴. This points toward the importance of investigation of TME composition and the interactions that may take place between cells populations. The wide range of cells interactions and their modalities presents an expansive frontier, largely unexplored even with existing research. Thus, further investigation is essential to uncovering this complex landscape. In exploring the dynamic gene expression changes, single-cell RNA sequencing (scRNA-seq) has gained much deserved attention in the recent years. ScRNA-seq allows for almost unlimited, in terms of number of cells, detailed, investigation of heterogeneity of RNA expression at a single-cell level¹⁵. However, this type of analysis requires the dissociation of the cells, therefore the spatial location is irreversibly forsaken. Spatial transcriptomics (ST) analyses RNA expression within the tissue, maintaining the spatial patterns of expression so crucial in the understanding of the TME. Application of this technology led to identification of interaction between SPP1⁺ macrophages and FAP⁺ fibroblasts as potential therapeutic target in CRC¹⁶. Similarly, a combination of scRNA-seq and ST was applied to analyze CRC samples, yielding PLAU-PLAUR interaction associated with myofibroblasts and macrophages as potentially participating in tumor progression¹⁷.

The aim of the study was to investigate spatial epithelial and immune cells gene expression changes. In this study, we applied ST technology to investigate the cell populations and changes of gene expression patterns in the CRC tumor and adjacent normal tissue, with a focus on immune cells present within the TME. We identified spatially dependent changes, reflected in the clustering, of cell populations directly linked to the tumor invasion and secondary lymphoid structures. Moreover, high infiltration of Tregs and M2-macrophages within the tumor core was characterized by CCL18-CCR8 and CCL22-CCR4 chemokine signaling. At the same time, we identified TNF signaling and interferon-related genes involved in CRC invasive trajectory as well as a potentially novel regulator of T-cells activation within the tertiary lymphoid structures (TLS) SIT1.

8.2. Materials and methods

8.2.1. Spatial transcriptomics: tissue handling and processing

Samples of CRC tumor and corresponding normal tissue of 63 years old female patient diagnosed with G2 tumor were collected from the 3P-Medicine Laboratory¹⁸, Medical University of Gdansk with the following clinical parameters listed in the table1.

FFPE tissue sections of 5 µm were placed on Visium Spatial Gene Expression Slides with a 6.5 mm x 6.5 mm capture area and processed according to the Visium spatial gene expression reagent kit manual (10xGenomics). Prior to tissue processing, sections were H&E stained with hematoxylin and eosin. The slides were imaged (Zeiss Axio Imager.M2m, Zeiss AxioCam 506 color) at 20X magnification. Probe hybridization and ligation, RNA digestion, probe extension and elution, and cDNA library preparation were performed according to manufacturer's instructions. Post library construction quality control was performed with an Agilent 2100 Bioanalyzer with a High Sensitivity DNA kit (Agilent). Next generation sequencing was performed by Macrogen Europe. Sequencing readouts were demultiplexed using SpaceRanger (v 1.3.1) and mapped to human genome GRCh38.ST public data was obtained from repositories of 10XGenomics and public repositories (zenodo ID: 7760264¹⁷, GEO: GSE158328¹⁹, GEO: GSE226997²⁰, GEO: GSE225857²¹).

8.2.2. Data integration, dimension reduction, and clustering

SpaceRanger output ST files were analyzed using Seurat (v4.4.0). Tumor and normal samples were analyzed via canonical correlation analysis (CCA) subspace alignment²² with default parameters using 3000 integration features. Next, dimensional reduction was performed with Principal Component Analysis (PCA) and Uniform Manifold Approximation and Projection (UMAP) with 30 principal components (PCs) followed by unsupervised clustering with resolution set to 1. Cluster annotation was performed based on manual annotation and positive markers per cluster using *FindAllMarkers* with default parameters.

8.2.3. Differential gene expression analysis

Tumor and normal ST datasets were merged and UMI counts were normalized with *NormalizeData* function with default parameters. DEG analysis between tumor and normal spots for each annotated cluster was performed with *FindMarkers* function with default parameters. Differential expression was considered with an absolute logarithmic Fold Change (FC) > 0.1 and adjusted p-value < 0.05. Obtained DEGs were used as input for pathway enrichment analysis via active subnetworks based on GO-BP, KEGG, and Reactome with pathfindR (v. 2.3.0).

8.2.4. Cell-type hierarchical deconvolution

Spots deconvolution was performed using SpaCET package (v. 1.0.0) using a public reference scRNA-seq dataset (accession GSE132465) of 23 patients who underwent CRC tumor resection^{23,615}. The reference dataset was filtered according to the canonical markers expression and T-cells specific markers to re-annotate T-cells in CD8+ T, gamma delta T, Th1, Th2, Th17, Treg, T follicular, T naive¹⁵. Constrained linear regression estimated hierarchical cell identity fractions within the spots²³ for main cell types (Epithelial,

Stromal, B-cells, T-cells, Myeloid, Mast cells, and NK cells) was applied followed by subsequent estimation of cell subtypes.

8.2.5. Ligand-receptor interaction analysis

To determine Ligand-receptor (L-R) interactions, Fantom5 and Omnipath L-R databases^{24,25} were combined. L-R estimated scores within proximal spots were calculated with NICHES (v. 1.0.0)²⁶ *RunNICHES* function with CelltoCellSpatial mode and k = 1. Following NICHES manual, *FindAllMarkers* Seurat function determined the significant L-R interactions for each proximal spot combination indicated as Sender – Receiver such as Epithelial_1 – Epithelial_2. All circo plots were made using CPlotR package (v1.0.0).

8.2.6. Invasive spatial trajectory analysis

STdeconvolve (v. 1.6.0) reference-free deconvolution was performed with default parameters, except *fitLDA* function with k = 15, to analyze spatial gene topics within CRC tissue. SPATA2 (v. 2.0.4) was used to analyze spatial gradients of gene expression and L-R changes along the defined tumor invasive trajectory. Dynamic feature changes were analyzed with *spatialTrajectoryScreening* function with default parameters for 17 models of expression. Pathway enrichment analysis was performed with significantly changed genes with pathfindR to investigate enriched pathways in specific patterns of expression.

8.2.7. Pseudotime trajectory analysis

To investigate the developmental relationship between immune cell aggregates cluster in normal and tumor tissue, pseudotime analysis was applied with Monocle3 (v. 1.3.4) with default parameters. Pseudotime trajectory orders ST spots according to changes in gene expression along lineages. The inferred pseudotime trajectory was transferred to TradeSeq (v. 1.14.0) to identify lineage-specific gene expression and L-R changes with *fitGAM* and *diffEndTest* functions with default parameters²⁷.

8.3. Results

8.3.1. Spatial characterization of cell composition and TME heterogeneity of colorectal cancer

To comprehensively investigate cell-cell interaction, cell subpopulation changes and key molecules in CRC development at the spatial composition of CRC tissue (T) architecture, we performed spatial transcriptomics analysis (10x Genomics) on CRC tumor and the corresponding normal tissue samples collected from one patient in parallel to minimize technical variation and to determine spatial gene expression changes originating from the tumor progression. Prior to the ST analysis, tissues were stained with H&E and evaluated based on the cells' morphology, yielding annotation of tumor, stroma, endothelial cells, muscle, and immune cells (IC) aggregates (Fig 8.1A,B). To explore the composition differences between CRC and normal-matched tissue, canonical correlation analysis (CCA) subspace alignment (implemented in Seurat) followed by clustering was applied resulting in 19 clusters with different distribution in CRC and normal tissue. Differential gene expression analysis among clusters determined their molecular identity and clusters were annotated according to canonical marker expression and tissue location (Fig 8.1C, Appendix II Fig.S1A).

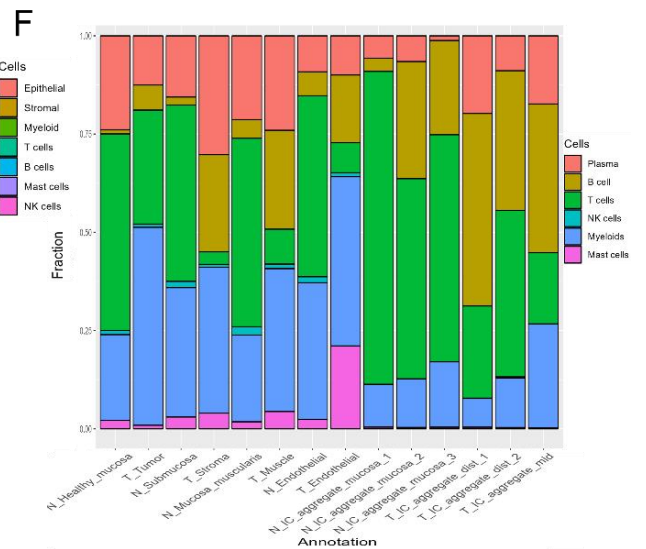
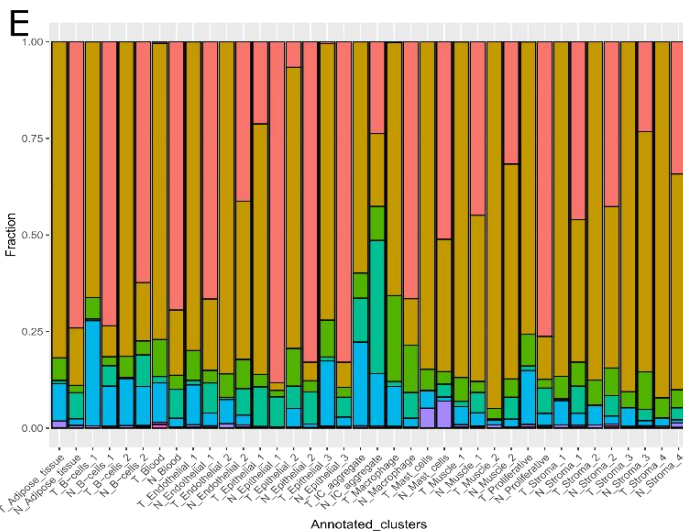
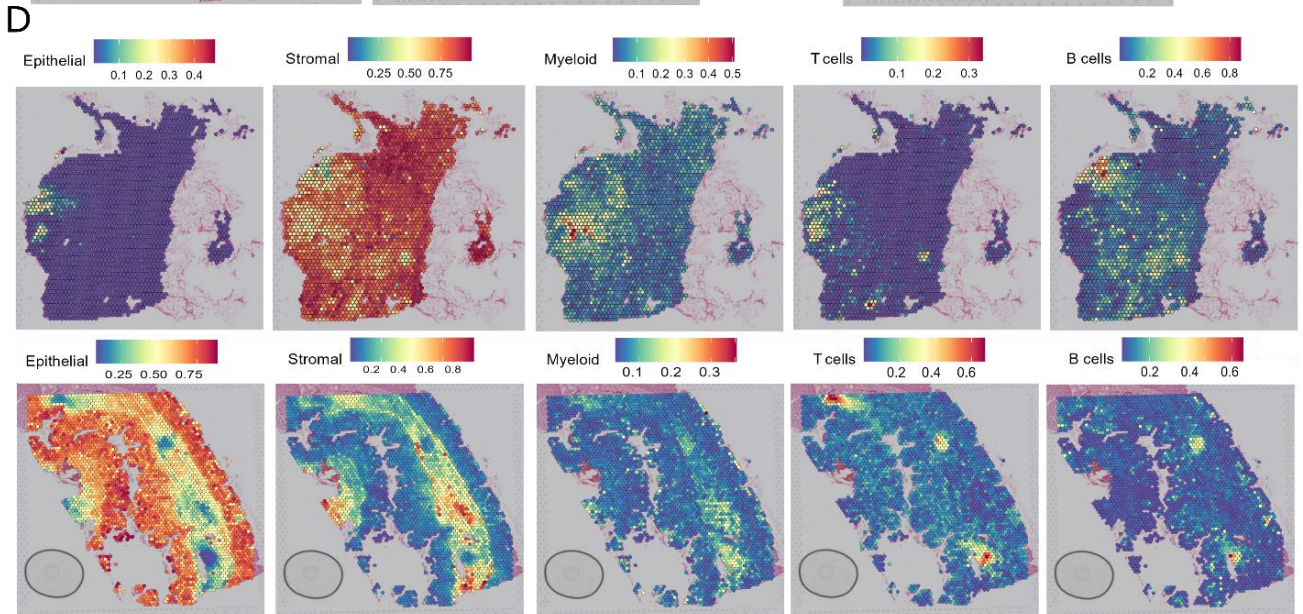
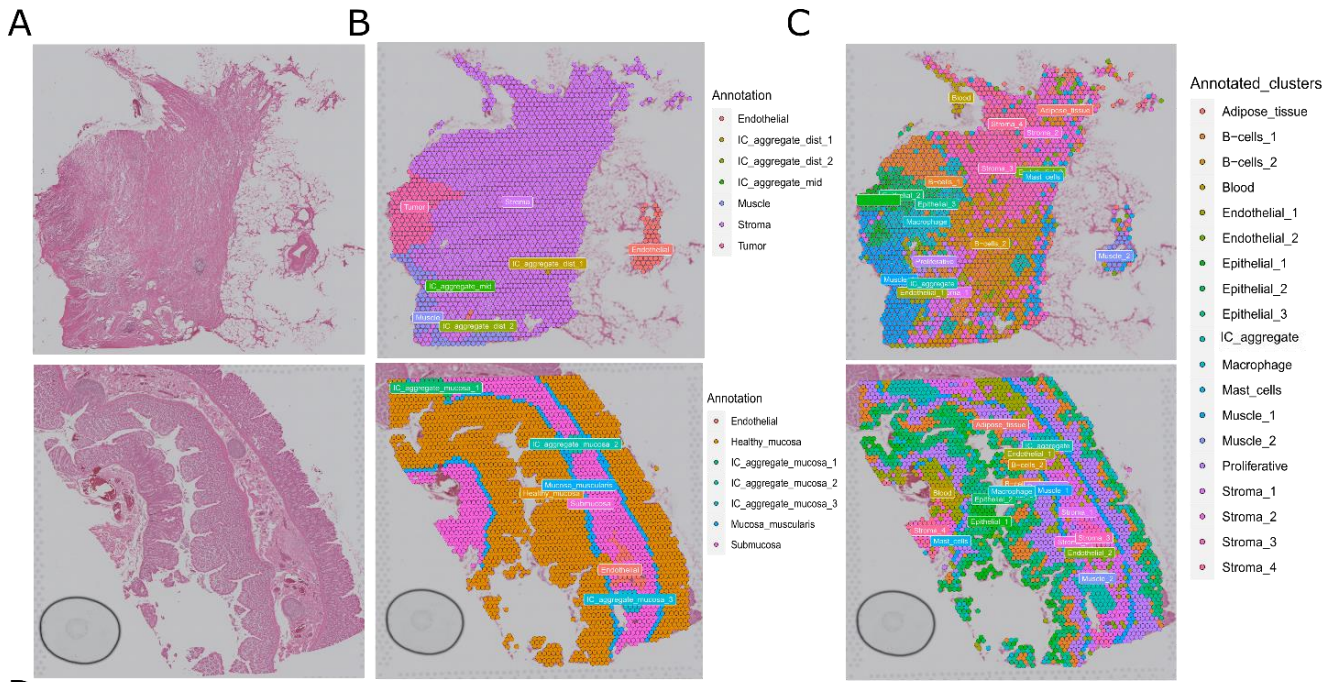


Figure 8.1. Spatial profile of cell composition and TME heterogeneity of colorectal cancer. (A) H&E staining of CRC tumor and normal samples (up and down, respectively), (B) the manual annotation, and (C) annotated clusters according to gene expression and location. (D) Spatial plots with predicted cell fractions from spot deconvolution results for five main cell types in tumor and normal tissue samples. (E) Barplot of the mean predicted fractions for each main cell type in each annotated cluster and (F) of immune cell fractions in manually annotated regions separated by their origin (tumor (T) and normal (N)).

Among clusters, the proliferative cells were marked with high expression levels of CDCA7, CDC20, MCM7, genes linked with cell division. B-cell clusters showed upregulated immunoglobulin genes, including JCHAIN, IGHA1, IGHA1, IGHM, IGHG1, IGHG2, epithelial clusters were with increased levels of BEST4, CDHR5, MUC4, macrophages showed high expression of APOE, CD68, CXCL14, stromal clusters expressed higher levels of COL6A2, COL5A1, COL3A1, MMP2, whereas signature genes ACTG2, ACTA2, TPM1, TPM2, MUSTN1 were detected in muscle, CD34, CDH5, CD93, ROBO4 in endothelial, TPSB2, CPA3, KIT in mast cells, PLIN1, PLIN4, ADIPOQ in adipose tissue, and HBA1, HBA2 in blood. Lastly, upregulation of genes highly expressed in immune cells (PTPRC, IKZF1, LTB, IL7R) with CD3D and T-cell receptor beta constants (TRBC1, TRBC2) showed presence of T-cells in the IC aggregate cluster (Appendix II Fig.S1B, Table S1). In addition, Epithelial_1 cluster showed the highest transcriptional activity and the most diverse gene expression in tumor tissue, comparing to the rest of the clusters (Fig. S8.1C, D). As hyper-transcription is one of the hallmarks of cancer, cluster Epithelial_1 was assigned as a tumor core²⁸.

To further identify the cellular composition of the samples, hierarchical deconvolution was employed. Five main types of cell and tissue types were identified (Fig 8.1D), whilst NK cells and mast cells were barely present within the tumor region (Fig. S8.1E). The deconvolution revealed that epithelial predicted fractions were localized within the H&E annotated tumor region and mainly in clusters Epithelial_1 and Epithelial_2 (Fig 8.1 B, C,D), Stromal fractions were higher in tumor than normal tissue, whilst in normal tissue stromal fraction was predominantly limited to submucosa (Fig 8.1A, B, D). Consistently, the mean distribution of deconvoluted cell populations within each cluster and manual annotation showed high epithelial fractions in normal tissue and stromal fractions in CRC, in which the predicted epithelial cell fraction is decreased from the tumor core to invasive Epithelial_2 and Epithelial_3 clusters (Fig. 8.1E, Appendix II Table S2, S9.3). In CRC, high stromal content has been linked to worse disease-free survival as stromal cells support tumor growth by extracellular matrix (ECM) modulation, hence elevated stromal signature may indicate stromal cells shaping the TME^{29,30}.

Among immune cell types, T-cells deconvoluted fractions were mainly present in IC aggregates with lower fractions in tumor than normal tissue, whilst T-cells were confined into the epithelial clusters with high infiltration in the tumor core (Epithelial_1 cluster) suggesting active communication between T-cells and cancer cells (Fig. 8.1D, E, F).

Meanwhile, deconvoluted B-cells fractions, consistent with the annotated B-cell clusters, were present in IC aggregates in both normal and tumor tissue (Fig. 8.1D, E, F). Myeloid signatures were scattered throughout the tumor with higher fractions in epithelial clusters than normal counterparts and with the highest myeloid fractions appearing to encircle these epithelial clusters consistent with the annotated macrophage cluster in tumor tissue (Fig. 8.1C,D,E). In contrast, the myeloid signature in normal tissue was mostly present in the submucosa in the vicinity of IC aggregates and in specific spots along the apical epithelia (Fig. 8.1A,D). As such, clustering and spot deconvolution revealed the TME heterogeneity with substantial disruption of intestinal architecture in CRC tissue together with immune cell infiltration, namely T-cells and myeloid cells, adjacent to CRC cells, that indicated immune recruitment in response to the ongoing tumorigenic process.

Transcriptomics changes of CRC tumor clusters reflected EMT and immunosuppressive TME To determine transcriptomics changes occurring in CRC development, differential gene expression analysis was

performed between the tumor epithelial clusters and their normal counterparts (Appendix II Table S4-S6). Next, pathway enrichment analysis of significant differentially expressed genes (DEGs) revealed that integrin-mediated signalling was highly enriched along the three epithelial clusters (Fig. 8.2A-B, Appendix II Table S7-S9). Integrins play a variety of roles, including cell adhesion, angiogenesis, invasion and participate in epithelial-to-mesenchymal transition (EMT)³¹ in CRC. Moreover, all epithelial tumor clusters showed enrichment of terms related to cell adhesion, cell migration, positive regulation of EMT, and negative regulation of canonical Wnt signaling pathway whose dysregulation is extensively associated with CRC progression and metastasis (Fig. 8.2A, Appendix II Table S7-S9)³². Several genes were uniformly upregulated in the tumor/epithelial clusters such as cancer-stem cells marker CD44³³, gene linked to proliferation KLK10³⁴, linked to EMT TFF1³⁵, and to development CD81³⁶ or interferon induced IFI6 (Fig. 8.2C). Furthermore, CD44 was involved in “cell adhesion” term in all epithelial clusters (Fig 8.2A, Appendix II Table S7-9). Interestingly, Epithelial_1 cluster showed unique overexpression of CD47 and TP53, whilst all epithelial clusters showed different expression patterns of other p53-induced genes (Fig. 8.2C). At the same time, increased well-established immunosuppressor Transforming growth factor-beta1 (TGFβ)³⁷ and its induced gene TGFBI together with inhibitory immune checkpoint CD276³⁸ suggested an immunosuppressive TME within tumor clusters. Epithelial clusters were also characterized by high expression of TNF-related genes (TNFRSF6B, TNFRSF12A, TNFAIP) and downregulation of TNFRSF11A, and TNFRSF21 (Fig. 8.2C).

Additionally, elevated AHR in all and KYNU in Epithelial_2 together with high tryptophan deprivation signature in tumor regions surrounding the tumor core may indicate immunosuppression through tryptophan deprivation (Fig. 8.2C, E)³⁹. Moreover, KYNU was highly expressed in epithelial and myeloid cells of CRC compared to normal tissue in the validation scRNA-seq dataset (Fig. 8.2F).

To determine potential cell-cell communications within tumor clusters and adjacent spots, differential ligand-receptor (L-R) interaction analysis was conducted. Several chemokines and their receptors interactions were significantly increased between Epithelial_1 and Epithelial_2 (Fig. 8.2G, Appendix II Table S16). Interestingly, a signaling of CD24-SIGLEC10, recognized as “don’t eat me” signal⁴⁰ in various tumors was observed between Epithelial1 and Epithelial2 clusters. (Fig. 8.2G, Appendix II Table S16). Meanwhile, Epithelial_3 and the adjacent enriched B-cell cluster showed chemotactic interaction of CCL28-CCR10 where CCR10 plays a vital role in regulation of IgA response^{41,42}. At the same time, DPP4 peptidase responsible for chemokines signaling regulation⁴³, was found to interact with several chemokines such as CXCL9 (Fig. 8.2G). In addition, interaction of CCL18-PITPNM3 between Epithelial 3 and Epithelial 2 clusters was found (Fig. 8.2G). Further validation in 8 FFPE and 14 fresh frozen public ST CRC samples confirmed increased expression of CD44, CD47, TDO2-KYNU-AHR, PITPNM3, TNFRSF6B, SIGLEC10 in tumor tissue compared to normal and stromal tissue (Fig. S8.2B-C). Taken together, CRC epithelial transcriptomic changes reflected ongoing EMT, oncogenic alterations in TP53-related genes and Wnt signaling, and immunosuppressive TME with Tregs and macrophages infiltration.

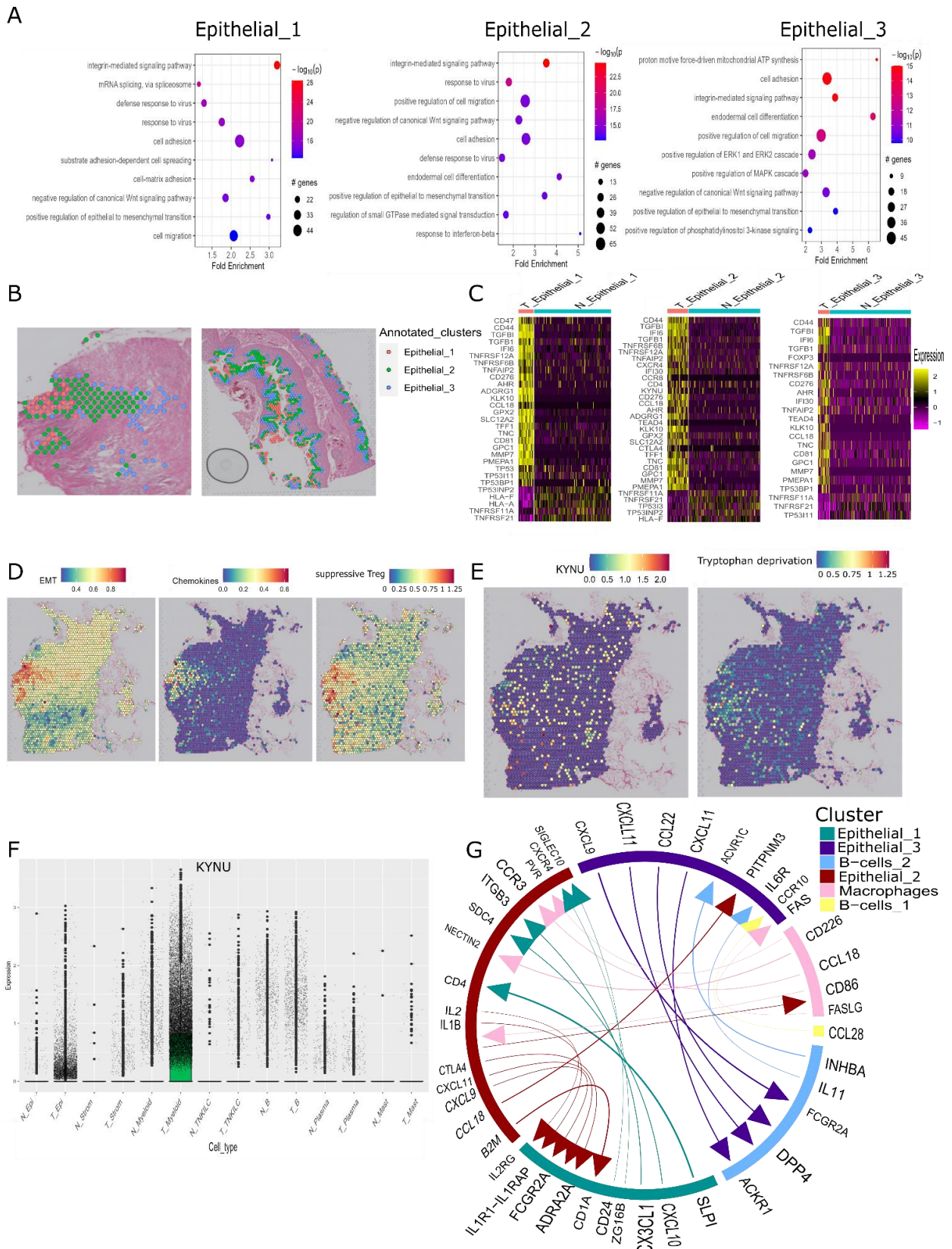


Figure 8.2. Genes expression deviation among epithelial clusters (A) Location of epithelial clusters annotation in tumor (left) and normal (right) tissue, (B) Heatmaps of selected DEGs of epithelial clusters (C) Enrichment charts of selected enriched terms in Epithelial_1 (left), Epithelial_2 (middle), and Epithelial_3 (right) clusters. (D) Gene signature scores in tumor samples, (E) Spatial plot of KYNU gene expression (left) and tryptophane metabolism signature(right), (F) Box

plot of KYNU expression in tumor(T) and normal (N) cell types in validation scRNA-seq dataset, (G) Circo plot of ligand-receptor interaction of epithelial clusters.

8.3.2. In-depth exploration of infiltrating T-cells and myeloid cell sub-populations in CRC TME

Considering the predicted high immune cells infiltration within tumor tissue, in-depth exploration of immune cells was undertaken. Hierarchical deconvolution showed clear spatial separation of identified myeloid cell subtypes included in the scRNA-seq reference dataset. Inflammatory macrophages were concentrated within tumor epithelial clusters followed by SPP1+ macrophages, encircling the tumor tissue, and conventional DCs (cDCs) residing in the tumor border below (Fig. 3A-B). Furthermore, the annotated tumoral Macrophage cluster contained higher SPP1+ macrophage fractions than the normal counterpart and other clusters (Fig. 8.3C). Meanwhile, tumoral monocytes and TAMs exhibited higher SPP1 expression comparing to other myeloid populations in the validation scRNA-seq dataset (Appendix II Fig. S3A-B). SPP1+ macrophages, reported to participate in CRC metastasis and ECM remodeling, typically present an immunosuppressive M2-like phenotype^{44,45}.

Among increased DEGs in the Macrophage cluster compared to its normal counterpart, there were several M2-like macrophages-related genes such as SPP1, MHC class II genes (HLA-DRA, HLA-DMB, HLA-DMA, HLA, DPB1), apolipoproteins APOE and APOD, CCL18 and CD4, and similarly to epithelial clusters, CD276, (Fig. 8.3D, Table S8.17). Moreover, increased MMP2 and other metalloproteinases (MMP11 and MMP14) together with enriched cell-cell and cell-matrix adhesion suggested an active ECM remodeling by macrophages (Appendix II Table S18). Furthermore, significant L-R interactions within this cluster included HLA-F interaction with B2M and CD3D, HLA-A-APLP2, and HLA-A-LILRB2 (Fig. 8.3E). Apart from CCL18-CCR8 Tregs attracting interaction, Epithelial_2 and Macrophage clusters showed increased T-cells apoptosis inducer LGALS1-PTPRC with inhibitory T-cells signaling CD86-CTLA4 and CCL18-CCR3, that can impair anti-tumor eosinophiles⁴⁶⁻⁴⁸ (Fig. 8.2G). In contrast, elevated CD226-PVR interaction between Epithelial_2 and Macrophage clusters might indicate activation of cytotoxic T-cells⁴⁹ (Fig. 8.2G). Similarly, apoptotic FAS-FASLG interaction was found between Epithelial_3 and Macrophage (Fig. 8.2G). These results highlight the complexity of ongoing interactions between tumor cells and immune cells within CRC TME. Collectively, this immunosuppressive macrophages population may “guard” the tumor core, suggesting an essential role in the immune regulation of CRC invasive fronts (Fig. 8.1C)⁵⁰.

One of the key immune players of the TME are T-cells populations that might either serve as tumor suppressors or tumor facilitators⁵¹. Distinct location patterns of T-cells subtypes were predicted between normal and tumor tissue. Within annotated IC_aggregate cluster, normal tissue contained higher predicted fractions of T cell subtypes (T naïve, and Tregs) and minor content of other T-cell subtypes (Fig. 8.3B-C, Appendix II Fig.S3C). Immune cells aggregates cluster was also enriched in myeloid fractions (Fig. 8.1E). Meanwhile, Tregs were higher in the tumor region, especially in the tumor core (Epithelial_1) with increased Treg chemoattractant CCL22⁵² (Appendix II Table S4). Moreover, other upregulated immune-related genes included pro-apoptotic serine protease GZMB, CXCL12, CD276, and IgG immunoglobulins (Fig. 8.3D, Appendix II Table S19)

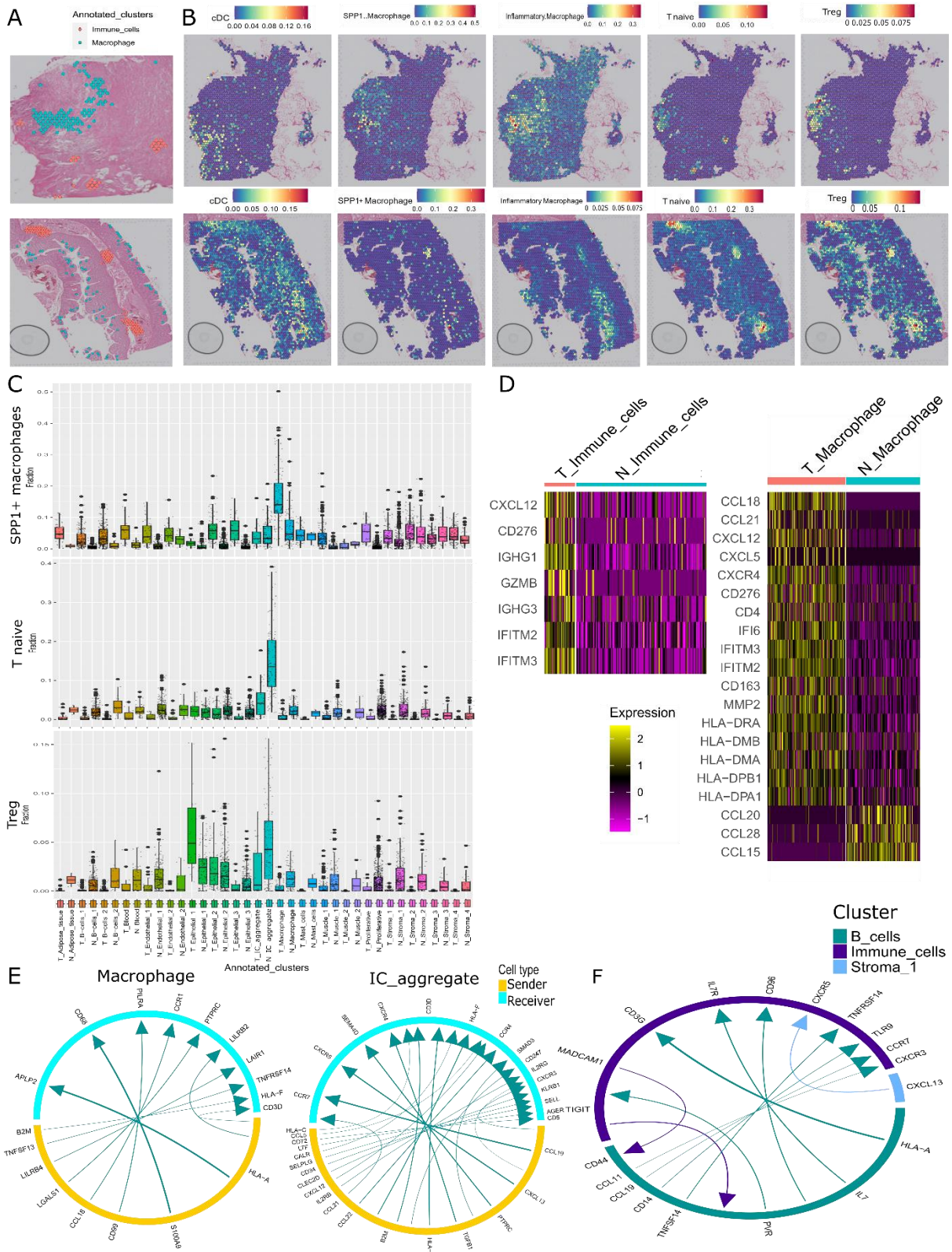


Figure 8.3. Spatial characterization of CRC myeloid and T-cell infiltration. (A) Spatial plot of annotated of macrophage and IC_ aggregate clusters. (B) Spatial plots of deconvoluted fractions of myeloid subtypes, T naive, and Tregs. (C) Boxplots of deconvoluted fractions of SPP1+ macrophages, T naive, and Treg along annotated clusters. (D) Heatmaps of selected DEGs between tumor and normal spots for both clusters. (E) Circo plots of L-R interactions within each corresponding cluster. (F) Circo plot of L-R interactions of IC_aggregate cluster with surrounding clusters.

L-R interaction within tumor IC aggregate cluster confirmed T-cells homing and Tertiary Lymphoid Structure (TLS) formation such as CXCL13-CXCR5⁵³, CCL19-CCR7, and CCL21-CCR7⁵⁴ together with leukocyte rolling SELPLG-SELL⁵⁵. Moreover, this cluster exhibited TCR signaling mediated by B2M-CD247⁵⁶, T-cells activation with PTPRC-SEMA4D⁵⁷, antigen presentation B2M-CD3D, HLA-A-CD3D, HLA-CD3D as well as interaction of non-classical MHCI HLA-F with B2M (Fig. 8.3E). Interestingly, another increased interaction was CD72-CD5, which plays a crucial role in maintaining homeostasis between Bregs and Tregs⁵⁸. Moreover, interaction of CCL5-CCR4 and CXCL12-CCR4 was observed whilst CCR4 is highly expressed on Tregs⁵⁹. Meanwhile, significantly increased interactions between tumor IC_aggregate cluster and adjacent B_cells-2 cluster supported active T-cells migration, homing, and activation (CCL19-CCR7, CCL11-CXCR3, IL7-IL7R), proinflammatory cytokines production (CD14-TLR9), and antigen presentation (HLA-A-CD3G) (Fig. 8.3F). Moreover, MADCAM-CD44 and TNFSF14-TNFSFR14 supported TLS formation and surrounding vascularization (Fig. 8.1A, 8.3F)⁶⁰. Although TLS formation is usually linked to the favorable prognosis and more potent immune response to cancer, increased PVR-TIGIT and PVR-CD96 with the adjacent B_cell cluster may promote local immunosuppressive signaling (Fig. 8.3E)⁶¹. Furthermore, a tendency to higher expression of CCL18, CCR8, CCL22, CCR4, and LAIR1 in tumor tissue as well as in tumoral IC aggregates compared to normal counterparts was validated by using public ST data. (Appendix II Fig.S4A-D).

8.3.3. CRC invasive trajectory involved TNF and interferon induced gradients

Further investigation of spatially variable genes with STdeconvolve reference-free deconvolution showed an epithelial topic (S100A6, S100A4, MMPs, EPCAM, IL32, CDH1, CD44) that determined the invasive margin of CRC within the stroma (Fig. S8.4E). To investigate differential gene expression and L-R interaction changes from the tumor core to further beyond the invasive margin, we performed invasive spatial trajectory analysis (Fig. 9.4A). Significant descending genes from the tumor core to the end of the invasive front included genes involved in CRC progression (S100A10, CD151), tryptophane metabolism (SLC7A5), and immune-related genes (CXCL5, HLA-F, IL-32) (Fig.8.4B, Table S8.20). Importantly, observed descending gene patterns from S100A10 or CXCL5 supported their upregulation in tumoral epithelial clusters (Fig. 8.2C, Appendix II Table S4-6). L-R interactions with descending pattern along the invasive trajectory included stromal signaling (ADAM9-ITGA3, COL18A1-ITGA3, FN1-ITGA3, LAMA4-ITGA3), TNF signaling (TNF-TRAF2), interactions related to immunosuppression (THBS1-ITGA3, CD151-ITGA3, HLA-A-APLP2, CD55-ADRA2), and migration (TFF3-CXCR4) (Fig. 8.4C, Appendix II Table S21). For instance, THBS1 produced by infiltrating monocytes-like cells was found to significantly contribute to immunosuppressive environment in a CRC mice model, supporting the impact of infiltrated macrophages located in the Macrophage cluster⁶².

Similar to descending genes, genes following early peak expression gradients supported increased expression in the tumor epithelial clusters such as CXCL9, CXCL3, MMP9, and S100A2 (Fig. 8.4D, Appendix Table S4-6). Furthermore, early L-R peaks included TNF interactions (TNF-TRADD, TNF-TNFRSF1A, TNFSF14-TNFRSF6B, and TNFSF14-LTBR) that highlighted the relevant role of TNF signaling along the invasive trajectory (Fig.8.4E). Interestingly, interferon-induced genes followed different expression patterns with linear descending trajectories of IFI27 and IFITM1, early peak of IFI44L and late peak of IFI16, suggesting an active role of interferon-related genes shaping the TME along the invasive trajectory (Fig. 8.4F).

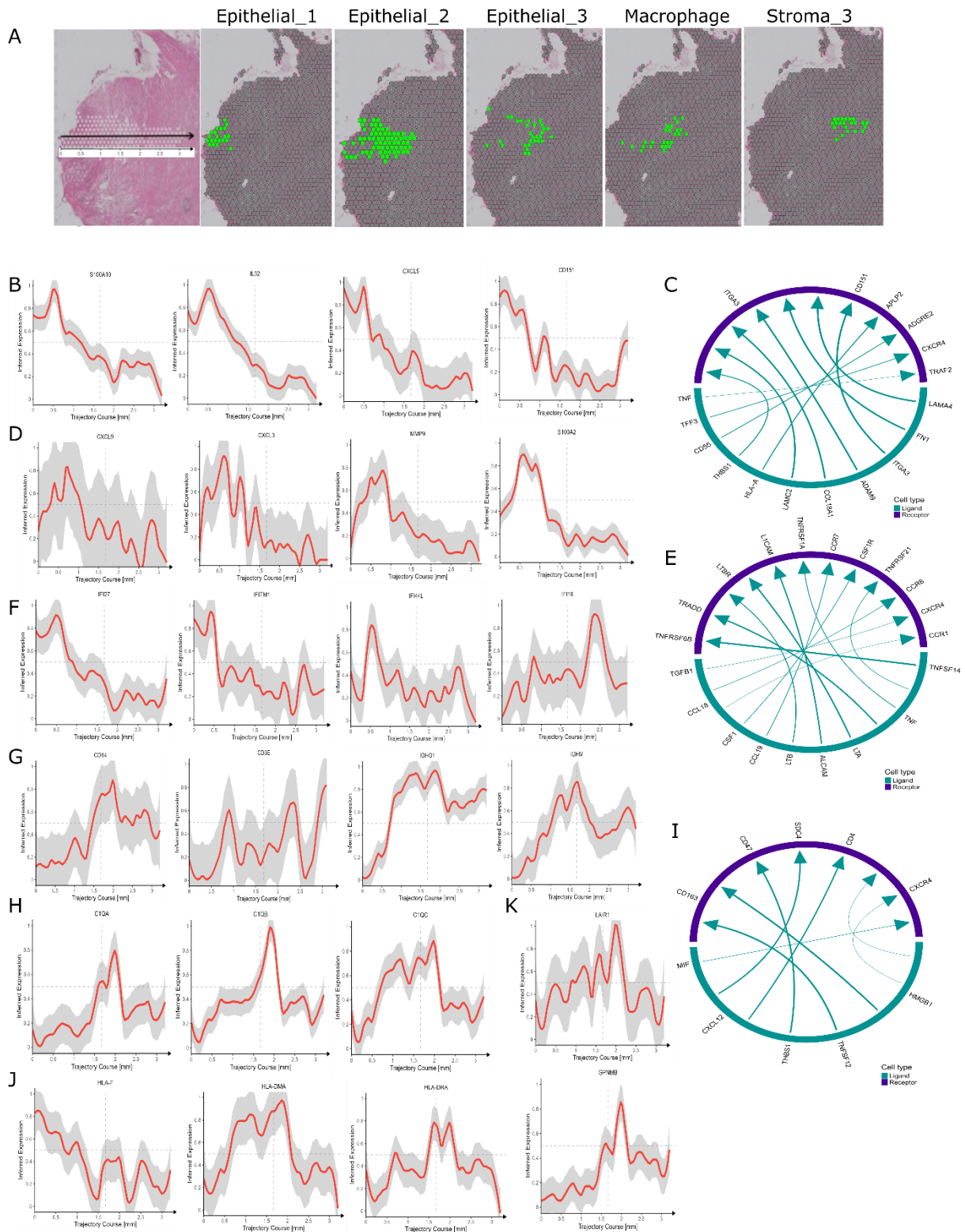


Figure 8.4. Spatial characterization of the CRC invasive trajectory. (A) Spatial plots representing the spatial trajectory from the tumor core to the invasive margin within stromal tissue. (B) Line plots of selected differentially ascending genes within the spatial trajectory. (C) Circo plot of L-R interactions with a descending trajectory. (D) Line plots for selected early peak trajectory genes and (E) circo plot of corresponding L-R interactions. (F) Line plots for selected interferon-induced genes, (G) for key immune cell markers (H) for complement genes. (I) Circo plot of L-R interactions with ascending expression pattern. (J) Line plots for selected MHC genes and (K) for LAIR1 and GPNMB.

Lastly, ascending expression patterns indicated macrophage activation at the tumor invasive margin, including CD14 and complement genes (C1QA, C1QB, C1QC) (Fig. 9.4G-H). Infiltrated macrophages were increased along with HMGB1-CD163 and TNFSF12-CD163 interactions between Epithelial_3 cluster and stromal neighboring tissue (Fig. 8.4A,I). CD3E expression pattern confirmed T-cell infiltration along Epithelial_2 cluster and between Epithelial_3 and Stromal tissue while immunoglobins (IGHG1, IGHM) reflected B-cell infiltration along the invasive margin (Fig. 8.4A,G). Different antigen presentation gene patterns were observed with ascending trajectories for MHC class II genes (HLA-DMA, HLA-DRA) in contrast to HLA-F descending pattern (Fig. 8.4J).

Interestingly, LAIR1 expression peak was observed at the Epithelial_3 cluster - Stromal tissue interface that may promote T-cell inhibition in the tumor margin (Fig. 8.4K). LAIR1 is an inhibitory receptor that blocks the activation of T-cells and macrophages whilst its blockage leads to increased numbers of anti-tumor T-cells and stimulates their activation⁶³. GPNMB showed a similar expression pattern (Fig. 8.4K) that was previously reported in macrophages within invasive margins of CRC liver metastasis⁶⁴. Moreover, active T-cells – myeloid communication in the invasive margin was further supported by the L-R interactions of CCL18-CCR8, CCL18-CCR1, and CSF1-CSFR1 (Fig. 8.4E). In fact, CSFR1 is not only crucial for M2 macrophages differentiation, but also CSFR1+ macrophages were found to aid pancreatic cancer cells growth by suppressing T-cells^{65,66}. Collectively, this CRC invasive trajectory was characterized by active immune cell-cell communication that may support CRC invasion and immune evasion.

8.3.4. Pseudotime analysis revealed altered T-cell signaling and Treg signatures in CRC immune cell aggregates

To investigate transcriptomics changes stemming from immune cell aggregates development from physiological conditions to CRC TME, we performed pseudotime trajectory analysis along IC_aggregate cluster from normal to tumor tissue. As a result, two developmental trajectory lineages were revealed, Lineage 1 from normal lymph nodes to tumoral IC aggregates and Lineage 2 from normal lymph nodes to their periphery (Fig. 8.5A-C). DEG analysis between lineages showed that Lineage 1 to tumor IC_aggregates (further named “tumor lineage”) contained higher expression of anti-bacterial (LTF), inflammation-related genes such as S100A9, complement cascade (C1R, C1S, C3), innate immunity (LSM14A), and anti-tumoral against CRC (GZMB, CLEC4A) (Fig. 8.5D, Appendix I Table S22)⁶⁷⁻⁶⁹. Meanwhile, altered NF-KB signaling exhibited as upregulation of NFKBIA and downregulation of IKBKB and IKBKG in tumor lineage. Higher antigen presentation in tumoral IC_aggregates was presented with upregulation of MHC I genes (B2M, HLA-A, HLA-E), MHC II genes (HLA-DPB1, HLA-DRA, HLA-DPA1, HLA-DQA1), CD74⁷⁰, CIITA⁹⁶, TAP2⁹⁷ and high CD99-CD81 interaction involved in immunological synapse and T-cells proliferation⁷¹ (Fig. 8.5D). Simultaneously, impaired T-cell signaling in tumor IC_aggregate spots was reflected in the increased negative TCR regulator SIT1⁷² and SIRT2 as well as downregulation of co-stimulatory CD28 in tumor lineage (Fig. 8.5D). Interestingly, SIT1 was also increased in public ST data with a tendency to higher levels in proximal IC aggregates to CRC tissue (Figure 8.4A-D). Furthermore, L-R interactions along the pseudotime trajectory indicated increased vascularization (MMP2-PECAM1, TIMP3-CD44) in tumor lineage that are involved in angiogenesis (Fig. 8.5E, Appendix I Table S23) as well as several interactions of CXCL12 (CXCL12-CXCR4, CXCL12-CD4, CXCL12-ITGB1) (Fig. 8.5E). Taken together, the pseudotime trajectory reflected the immune cell aggregates development in CRC with altered T-cells activation and enhanced Tregs signatures.

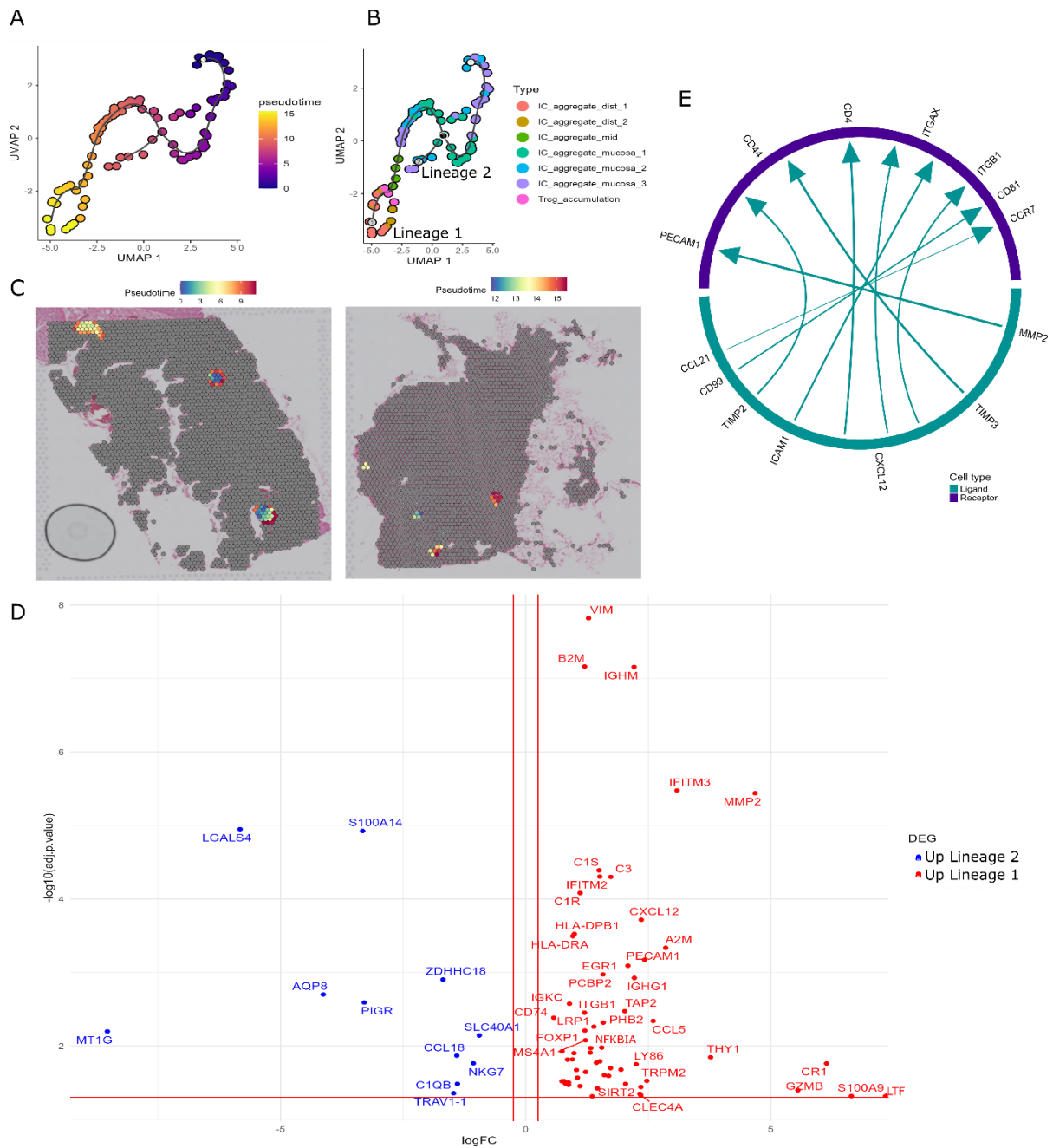


Figure 8.5. Pseudotime analysis of IC aggregates within normal and CRC tissue. (A) UMAP plot with calculated pseudotime along IC_aggregate spots. (B) UMAP plot of IC_aggregate spots with annotation according to their location and marked two developmental lineages. (C) Spatial plots with pseudotime in CRC and normal tissue. (D) Volcano plot with immune-related DEGs between the end of lineages.

8.4. Discussion

Application of spatial transcriptomics in CRC research provides an innovative approach to understand spatial coordination of gene expression within TME. For instance, ST and scRNA-seq analyses in CRC liver metastasis unveiled that CAFs participate in generating a tumor-specific CXCL13+ CD8+ T-cells via NOTCH signaling and CXCL13+ T-cells role in TLS formation²¹. In this study, in-depth ST analysis of CRC and normal matched tissue highlighted the intricate spatial complexity within CRC TME. Three epithelial clusters were identified spatially confined into the tumor region with unique expression profiles.

Several oncogenic pathways were identified such as Wnt signaling and altered expression of tumor suppressor TP53 and related genes among CRC epithelial clusters. Increased tumor suppressor TP53 and its inducer TP53BP1 within tumor core may promote apoptosis⁷³. Meanwhile down-regulation of TP53BP1 and TP53INP2 in Epithelia_2 cluster may counteract TP53-mediated apoptosis⁷⁴ by activating β -catenin that promotes CRC progression in mice models⁷⁵. Moreover, high TGF- β ⁵, TGFBI⁶, and tumor-promoter GPC-1 showed that TGF- β signaling may create a favorable TME and potentially participate in angiogenesis⁷⁸. While the CRC stem cell marker CD44 was expressed in all epithelial tumor clusters⁷⁹, specific up-regulation of CD47 in the tumor core may inhibit tumor apoptosis and promote immune evasion via interaction with SIRP α , expressed by macrophages⁸⁰. Moreover, high expression of both CD47 and CD44 is linked to EMT and hindered response to PD1/PD-L1 inhibitors⁸¹. Another “don’t eat me” signal of CD24-SIGLEC10 interaction, identified in tumor epithelial clusters, was found to promote tumor immune evasion in ovarian cancer⁸².

Ozato et al previously reported the accumulation of SPP1⁺ macrophages in the invasive front contributing to EMT, tumor growth and immunosuppression⁸³. In our study, predicted Tregs infiltration and myeloid cells with SPP1⁺ macrophages surrounding tumor clusters promoted an immunosuppressive TME. Importantly, high tumoral CCL18 expression, mainly from macrophages, but also CRC cells, induced CCR8⁺ Tregs trafficking to tumor site and was reported to impact tumor progression⁸⁴. CCL18-CCR8 presented a peak gradient along the invasive trajectory within the Macrophage cluster resulting in CCR8⁺ Treg infiltration in tumor clusters. Within the epithelial tumor clusters, CCL18-PITPNM3 interaction may mediate invasion, migration, and EMT as in breast cancer and hepatocellular cancer^{85,86} whilst CCL18 binding to CCR1 and CCR3 causes inhibition of chemotactic responses^{46,87}. Another Treg chemoattractant CCL22, mainly secreted by mreg DC, was detected within CRC TME supporting tumor-favorable environment^{88,89}. Moreover, tryptophan metabolism with TDO2-KYNU-AHR signaling increases macrophage-derived CXCL5 in CRC tissue what may promote angiogenesis¹¹⁵ as well as M2 macrophages attraction based on the previous studies³⁹. Observed impaired immune response within CRC TME was also reflected in high T-cells co-inhibitory CD276 and CTLA4 and CD86-CTLA4 interaction between macrophages and epithelial clusters⁹⁰.

TLSs are temporary accumulations of immune cells that develop in non-lymphoid tissue which resemble lymph nodes⁹¹. Although, their presence usually is linked with the better prognosis²³⁷, here we demonstrated these immune cell aggregates were associated with impaired T-cell activation and Tregs chemoattraction. Within tumoral immune cell aggregates, increased MHC genes and T-cell activation genes suggested ongoing active antigen presentation. However, impaired T-cell activation was observed with upregulation of inhibitory SIT1 and SIRT2, which were reported in mice models⁹² and in NSCLC⁹³ to inhibit TCR signaling and T-cells effector functions, respectively. Previously, SIT1 was found to be differentially expressed in CRC patients with high PD-L1 expression⁹⁴. However, to the best of our knowledge, SIT1 has not been studied in the context of tumor CRC progression. In breast cancer, SIT1 was proposed as an independent prognostic marker⁹⁵ whilst in cutaneous melanoma, SIT1 was proposed to play a role in regulating the immune microenvironment⁹⁶. Considering its inhibitory properties on T-cells activation⁷² and its differential expression in the TLSs we speculate it plays an important role in impairing the functional properties of the T-cells located in the tumor vicinity. Moreover, we observed interaction of CCL5, CXCL12, and CCL22 with CCR4, that is highly expressed on Tregs⁵⁹. CCR4⁺ Tregs in colon adenocarcinoma were found to be selectively recruited via CCL22⁹⁷. Furthermore, CCL22 is highly expressed in lymph nodes by various cell populations, including DCs what is crucial for Tregs immunosuppression⁹⁸. Our findings suggested that CCL22 recruited Tregs, not only to tumoral TLSs, but also to CRC tissue, favoring an immunosuppressive TME.

The tumoral invasive trajectory to the neighboring stroma was characterized by activation of IFN and TNF signaling playing a fundamental role in CRC invasion. For instance, TNF binding to its receptor TNFRSF1A (TNFR1) leads to the activation of NF- κ B pathway responsible for cell survival and proliferation⁹⁹. Furthermore, TNFSF14-TNFRSF6B¹⁰⁰ blocks several pathways including immune responses whilst

TNFRSF6B was found to inhibit T-cells chemotaxis and induce apoptosis of DCs via PKC- δ and JNK, effectively contributing to the immunosuppressive TME^{101,102}. The role of IFN-related genes in CRC is not well established yet. Among identified Interferon-related genes, the early peak of IFI44L may stem from CD8+ pre-exhausted T cells within the tumor core as previously it was identified to be differentially expressed in pre-exhausted CD8+ T cells in CRC¹⁰³. Moreover, other high IFN induced genes in tumor promoted CRC invasion such as IFITM1, involved in CRC metastasis via CAV-1, whilst IFITM3 was proposed as TGF- β pathway intermediate¹⁰⁴ and was previously found to play a crucial role in maintenance of Tregs suppressive properties¹⁰⁵. Further investigation of tumor spots with Treg infiltration determined increased apoptosis suppressor IFI6 that may induce CRC proliferation^{106,107}. In esophageal carcinoma, IFI6 was also associated with mesenchymal and immunosuppressive microenvironment¹⁰⁸, supporting that IFI6 modulates the immune composition of CRC TME.

The limitation of this study lies in the single-paired sample cohort but ST public data could validate single-sample findings. Although the used spatial transcriptomics technology does not reach single-cell resolution, the number of cells within the spot varies between up to a few cells. To mitigate this limitation, cell-type deconvolution was applied and public scRNA seq datasets were implemented in the analysis. However, validation at the protein level of identified DEGs such as SIT1 would help to assess its function in CRC.

In conclusion, CRC TME is enriched in different immunosuppressive signaling pathways, impaired T-cells signaling, and Tregs infiltration in the tumor core surrounded by SPP1+ macrophages. In CRC invasion, CCL18 played a dual tumorigenic role inducing EMT and recruit Tregs via CCR8 together with CCL22-CCR4. At the same time upregulation of SIT1 in TLSs in CRC is reported for the first time.

8.5. References

1. Morgan E, Arnold M, Gini A, et al. Global burden of colorectal cancer in 2020 and 2040: Incidence and mortality estimates from GLOBOCAN. *Gut*. 2023;72(2):338-344.
2. Li J, Chen D, Shen M. Tumor Microenvironment Shapes Colorectal Cancer Progression, Metastasis, and Treatment Responses. *Front Med*. 2022;9:869010.
3. Sun S, Zhang Y, Li Y, Wei L. Crosstalk between colorectal cancer cells and cancer-associated fibroblasts in the tumor microenvironment mediated by exosomal noncoding RNAs. 2023;(May):1-13.
4. Kim SK, Cho SW. The Evasion Mechanisms of Cancer Immunity and Drug Intervention in the Tumor Microenvironment. *Front Pharmacol*. 2022;13(May):1-16.
5. Fang H, Huang Y, Luo Y, et al. SIRT1 induces the accumulation of TAMs at colorectal cancer tumor sites via the CXCR4/CXCL12 axis. *Cell Immunol*. 2022;371.
6. Dhatchinamoorthy K, Colbert JD, Rock KL. Cancer Immune Evasion Through Loss of MHC Class I Antigen Presentation. *Front Immunol*. 2021;12(March).
7. Hou S, Zhao Y, Chen J, Lin Y, Qi X. Tumor-associated macrophages in colorectal cancer metastasis: molecular insights and translational perspectives. *J Transl Med*. 2024;22(1):1-14.
8. Wang H, Wang X, Li X, et al. CD68+HLA-DR+ M1-like macrophages promote motility of HCC cells via NF- κ B/FAK pathway. *Cancer Lett*. 2014;345(1):91-99.
9. Jin HY, Yoo SY, Lee JA, et al. Combinatory statuses of tumor stromal percentage and tumor infiltrating lymphocytes as prognostic factors in stage III colorectal cancers. *J Gastroenterol Hepatol*. 2022;37(3):551-557.
10. Lazarus J, Maj T, Smith JJ, et al. Spatial and phenotypic immune profiling of metastatic colon cancer. *JCI insight*. 2018;3(22).
11. Toor SM, Murshed K, Al-Dhaheri M, Khawar M, Abu Nada M, Elkord E. Immune Checkpoints in Circulating and Tumor-Infiltrating CD4+ T Cell Subsets in Colorectal Cancer Patients. *Front Immunol*. 2019;0:2936.
12. Liu Z, Huang Q, Liu G, et al. Presence of FOXP3 + Treg cells is correlated with colorectal cancer progression. *Int J Clin Exp Med*. 2014;7(7):1781-1785.
13. Ma Q, Liu J, Wu G, et al. Co-expression of LAG3 and TIM3 identifies a potent Treg population that suppresses macrophage functions in colorectal cancer patients. *Clin Exp Pharmacol Physiol*. 2018;45(10):1002-1009.
14. Ma X, Gao Y, Chen Y, et al. M2-type macrophages induce tregs generation by activating the $\text{tgf-}\beta$ /smad signalling pathway to promote colorectal cancer development. *Onco Targets Ther*. 2021;14:5391-5402.
15. Lee HO, Hong Y, Etliglu HE, et al. Lineage-dependent gene expression programs influence the immune landscape of colorectal cancer. *Nat Genet*. 2020;52(6):594-603.
16. Qi J, Sun H, Zhang Y, et al. Single-cell and spatial analysis reveal interaction of FAP+ fibroblasts and SPP1+ macrophages in colorectal cancer. *Nat Commun* 2022 131. 2022;13(1):1-20.
17. Valdeolivas A, Amberg B, Giroud N, et al. Profiling the heterogeneity of colorectal cancer consensus molecular subtypes using spatial transcriptomics. *npj Precis Oncol* 2024 81. 2024;8(1):1-16.
18. Filipowicz N, Dręzek K, Horbacz M, et al. Comprehensive cancer-oriented biobanking resource of human samples for studies of post-zygotic genetic variation involved in cancer predisposition. *PLoS One*. 2022;17(4):e0266111.
19. Fawkner-Corbett D, Antanaviciute A, Parikh K, et al. Spatiotemporal analysis of human intestinal development at single-cell resolution. *Cell*. 2021;184(3):810-826.e23.
20. Park SS, Lee YK, Choi YW, et al. Cellular senescence is associated with the spatial evolution toward a higher metastatic phenotype in colorectal cancer. *Cell Rep*. 2024;43(3).
21. Wang F, Long J, Li L, et al. Single-cell and spatial transcriptome analysis reveals the cellular heterogeneity of liver metastatic colorectal cancer. *Sci Adv*. 2023;9(24).
22. Zhang F, Wu Y, Tian W. A novel approach to remove the batch effect of single-cell data. *Cell Discov* 2019 51. 2019;5(1):1-4.
23. Ru B, Huang J, Zhang Y, Aldape K, Jiang P. Estimation of cell lineages in tumors from spatial transcriptomics data. *Nat Commun* 2023 141. 2023;14(1):1-13.
24. Ramilowski JA, Goldberg T, Harshbarger J, et al. A draft network of ligand-receptor-mediated multicellular signalling in human. *Nat Commun*. 2015;6.
25. Türei D, Valdeolivas A, Gul L, et al. Integrated intra- and intercellular signaling knowledge for multicellular omics analysis. *Mol Syst Biol*. 2021;17(3).
26. Raredon MSB, Yang J, Kothapalli N, et al. Comprehensive visualization of cell-cell interactions in single-cell and spatial transcriptomics with NICHES. *Bioinformatics*. 2023;39(1).
27. Van den Berge K, Roux de Bézieux H, Street K, et al. Trajectory-based differential expression analysis for single-cell sequencing data. *Nat Commun* 2020 111. 2020;11(1):1-13.
28. Zatzman M, Fuligni F, Ripsman R, et al. Widespread hypertranscription in aggressive human cancers. *Sci Adv*. 2022;8(47).
29. Smit MA, van Pelt GW, Terpstra V, et al. Tumour-stroma ratio outperforms tumour budding as biomarker in colon cancer: a cohort study. *Int J Colorectal Dis*. 2021;36(12):2729-2737.
30. Conti J, Thomas G. The Role of Tumour Stroma in Colorectal Cancer Invasion and Metastasis. *Cancers (Basel)*. 2011;3(2):2160.
31. Hou S, Wang J, Li W, Hao X, Hang Q. Roles of Integrins in Gastrointestinal Cancer Metastasis. *Front Mol Biosci*. 2021;8.
32. Chen Y, Chen M, Deng K. Blocking the Wnt/ β -catenin signaling pathway to treat colorectal cancer: Strategies to improve current therapies (Review). *Int J Oncol*. 2023;62(2).

33. Walcher L, Kistenmacher AK, Suo H, et al. Cancer Stem Cells—Origins and Biomarkers: Perspectives for Targeted Personalized Therapies. *Front Immunol.* 2020;11:539291.
34. Luo Y, Chao L, Lv Y, Lin H, Xu R, Shi X, Xia J, Jiang T. Kallikrein-related peptidase 10 predicts prognosis and mediates tumor immunomodulation in colorectal cancer. *Biochem Biophys Res Commun.* 2023;689:149217.
35. Yusufu A, Shayimu P, Tuerdi R, Fang C, Wang F, Wang H. TFF3 and TFF1 expression levels are elevated in colorectal cancer and promote the malignant behavior of colon cancer by activating the EMT process. *Int J Oncol.* 2019;55(4):789.
36. Bailly C, Thuru X. Targeting of Tetraspanin CD81 with Monoclonal Antibodies and Small Molecules to Combat Cancers and Viral Diseases. *Cancers* 2023, Vol 15, Page 2186. 2023;15(7):2186.
37. Villar VH, Subotički T, Đikić D, Mitrović-Ajtić O, Simon F, Santibanez JF. Transforming Growth Factor- β 1 in Cancer Immunology: Opportunities for Immunotherapy. *Adv Exp Med Biol.* 2023;1408:309-328.
38. Leitner J, Klausner C, Pickl WF, et al. B7-H3 is a potent inhibitor of human T cell activation: No evidence for B7-H3 and TREM2 interaction. *Eur J Immunol.* 2009;39(7):1754.
39. Lee R, Li J, Li J, et al. Synthetic Essentiality of Tryptophan 2,3-Dioxygenase 2 in APC-Mutated Colorectal Cancer. *Cancer Discov.* 2022;12(7):1702-1717.
40. Li X, Tian W, Jiang Z, Song Y, Leng X, Yu J. Targeting CD24/Siglec-10 signal pathway for cancer immunotherapy: recent advances and future directions. *Cancer Immunol Immunother.* 2024;73(2):31.
41. Hu S, Yang K, Yang J, Li M, Xiong N. Critical roles of chemokine receptor CCR10 in regulating memory IgA responses in intestines.
42. Yu SY, Luan Y, Tang S, et al. Uncovering Tumor-Promoting Roles of Activin A in Pancreatic Ductal Adenocarcinoma. *Adv Sci.* 2023;10(16):2207010.
43. Mortier A, Gouwy M, Damme J, Van, Proost P, Struyf S. CD26/dipeptidylpeptidase IV—chemokine interactions: double-edged regulation of inflammation and tumor biology. *J Leukoc Biol.* 2016;99(6):955.
44. Sathe A, Mason K, Grimes SM, et al. Colorectal Cancer Metastases in the Liver Establish Immunosuppressive Spatial Networking between Tumor-Associated SPP1+ Macrophages and Fibroblasts. *Clin Cancer Res.* 2023;29(1):244.
45. Liu X, Qin J, Nie J, et al. ANGPTL2+cancer-associated fibroblasts and SPP1+macrophages are metastasis accelerators of colorectal cancer. *Front Immunol.* 2023;14.
46. Nibbs RJB, Salcedo TW, Campbell JDM, et al. C-C Chemokine Receptor 3 Antagonism by the β -Chemokine Macrophage Inflammatory Protein 4, a Property Strongly Enhanced by an Amino-Terminal Alanine-Methionine Swap. *J Immunol.* 2000;164(3):1488-1497.
47. Lopez-Perez D, Prados-Lopez B, Galvez J, Leon J, Carazo A. Eosinophils in Colorectal Cancer: Emerging Insights into Anti-Tumoral Mechanisms and Clinical Implications. *Int J Mol Sci* 2024, Vol 25, Page 6098. 2024;25(11):6098.
48. Derakhshani A, Hashemzadeh S, Asadzadeh Z, et al. Cytotoxic T-Lymphocyte Antigen-4 in Colorectal Cancer: Another Therapeutic Side of Capecitabine. *Cancers (Basel).* 2021;13(10).
49. Gilfillan S, Chan CJ, Cella M, et al. DNAM-1 promotes activation of cytotoxic lymphocytes by nonprofessional antigen-presenting cells and tumors. *J Exp Med.* 2008;205(13):2965-2973.
50. Zlobec I, Lugli A. Invasive front of colorectal cancer: Dynamic interface of pro-/anti-tumor factors. *World J Gastroenterol.* 2009;15(47):5898.
51. Zheng Z, Wieder T, Mauere B, Schäfer L, Kesselring R, Braumüller H. T Cells in Colorectal Cancer: Unravelling the Function of Different T Cell Subsets in the Tumor Microenvironment. *Int J Mol Sci.* 2023;24(14):11673.
52. Mizukami Y, Kono K, Kawaguchi Y, et al. CCL17 and CCL22 chemokines within tumor microenvironment are related to accumulation of Foxp3+ regulatory T cells in gastric cancer. *Int J cancer.* 2008;122(10):2286-2293.
53. Hsieh CH, Jian CZ, Lin LI, et al. Potential Role of CXCL13/CXCR5 Signaling in Immune Checkpoint Inhibitor Treatment in Cancer. *Cancers (Basel).* 2022;14(2):294.
54. Luther SA, Bidgol A, Hargreaves DC, et al. Differing activities of homeostatic chemokines CCL19, CCL21, and CXCL12 in lymphocyte and dendritic cell recruitment and lymphoid neogenesis. *J Immunol.* 2002;169(1):424-433.
55. Harakawa N, Shigeta A, Wato M, et al. P-selectin glycoprotein ligand-1 mediates L-selectin-independent leukocyte rolling in high endothelial venules of peripheral lymph nodes. *Int Immunol.* 2007;19(3):321-329.
56. Dexiu C, Xianying L, Yingchun H, Jiafu L. Advances in CD247. *Scand J Immunol.* 2022;96(1):e13170.
57. Elhabazi A, Marie-Cardine A, Chabbert-de Ponnat I, Bensussan A, Boumsell L. Structure and function of the immune semaphorin CD100/SEMA4D. *Crit Rev Immunol.* 2003;23(1-2):65-81.
58. Zheng M, Xing C, Xiao H, et al. Interaction of CD5 and CD72 is involved in regulatory T and B cell homeostasis. *Immunol Invest.* 2014;43(7):705-716.
59. Suzuki S, Ishida T, Yoshikawa K, Ueda R. Current status of immunotherapy. *Jpn J Clin Oncol.* 2016;46(3):191-203.
60. Skeate JG, Otsmaa ME, Prins R, Fernandez DJ, Da Silva DM, Kast WM. TNFSF14: LIGHTing the Way for Effective Cancer Immunotherapy. *Front Immunol.* 2020;11:922.
61. Gorvel L, Olive D. Targeting the “PVR–TIGIT axis” with immune checkpoint therapies. *F1000Research.* 2020;9.
62. Omatsu M, Nakanishi Y, Iwane K, et al. THBS1-producing tumor-infiltrating monocyte-like cells contribute to immunosuppression and metastasis in colorectal cancer. *Nat Commun* 2023 141. 2023;14(1):1-19.
63. Xie J, Gui X, Deng M, et al. Blocking LAIR1 signaling in immune cells inhibits tumor development. *Front Immunol.* 2022;13:996026.
64. Cortese N, Carriero R, Barbagallo M, et al. High-Resolution Analysis of Mononuclear Phagocytes Reveals GPNMB as a Prognostic Marker in Human Colorectal Liver Metastasis. *Cancer Immunol Res.* 2023;11(4):405-420.

65. Zhu M, Bai L, Liu X, et al. Original research: Silence of a dependence receptor CSF1R in colorectal cancer cells activates tumor-associated macrophages. *J Immunother Cancer*. 2022;10(12):5610.
66. Candido JB, Morton JP, Bailey P, et al. CSF1R+ Macrophages Sustain Pancreatic Tumor Growth through T Cell Suppression and Maintenance of Key Gene Programs that Define the Squamous Subtype. *Cell Rep*. 2018;23(5):1448-1460.
67. Actor JK, Hwang SA, Kruzel ML. Lactoferrin as a Natural Immune Modulator. *Curr Pharm Des*. 2009;15(17):1956.
68. Johnstone KF, Wei Y, Bittner-Eddy PD, et al. Calprotectin (S100A8/A9) is an innate immune effector in experimental Periodontitis. *Infect Immun*. 2021;89(10).
69. Trimaglio G, Sneiderger T, Raymond BBA, et al. The C-type lectin DCIR contributes to the immune response and pathogenesis of colorectal cancer. *Sci Reports* 2024 141. 2024;14(1):1-14.
70. Schröder B. The multifaceted roles of the invariant chain CD74 — More than just a chaperone. *Biochim Biophys Acta - Mol Cell Res*. 2016;1863(6):1269-1281.
71. Pata S, Otáhal P, Brdikča T, Laopajon W, Mahasongkram K, Kasinrer K. Association of CD99 short and long forms with MHC class I, MHC class II and tetraspanin CD81 and recruitment into immunological synapses. *BMC Res Notes*. 2011;4.
72. Arndt B, Krieger T, Kalinski T, et al. The transmembrane adaptor protein SIT inhibits TCR-mediated signaling. *PLoS One*. 2011;6(9).
73. Bi J, Huang A, Liu T, Zhang T, Ma H. Expression of DNA damage checkpoint 53BP1 is correlated with prognosis, cell proliferation and apoptosis in colorectal cancer. *Int J Clin Exp Pathol*. 2015;8(6):6070.
74. Jin M, Park SJ, Kim SW, Kim HR, Hyun JW, Lee JH. PIG3 Regulates p53 Stability by Suppressing Its MDM2-Mediated Ubiquitination. *Biomol Ther (Seoul)*. 2017;25(4):396-403.
75. Shi K, Shan Y, Sun X, Chen K, Luo Q, Xu Q. TP53INP2 modulates the malignant progression of colorectal cancer by reducing the inactive form of β -catenin. *Biochem Biophys Res Commun*. 2024;690:149275.
76. Waldner MJ, Neurath MF. TGF β and the Tumor Microenvironment in Colorectal Cancer. *Cells*. 2023;12(8):1-14.
77. Zhu J, Chen X, Liao Z, He C, Hu X. TGFBI protein high expression predicts poor prognosis in colorectal cancer patients. *Int J Clin Exp Pathol*. 2015;8(1):702.
78. Lu F, Chen S, Shi W, Su X, Wu H, Liu M. GPC1 promotes the growth and migration of colorectal cancer cells through regulating the TGF- β 1/SMAD2 signaling pathway. *PLoS One*. 2022;17(6).
79. Ozawa M, Ichikawa Y, Zheng YW, et al. Prognostic significance of CD44 variant 2 upregulation in colorectal cancer. *Br J Cancer*. 2014;111(2):365-374.
80. Sugimura-Nagata A, Koshino A, Inoue S, et al. Expression and Prognostic Significance of CD47–SIRPA Macrophage Checkpoint Molecules in Colorectal Cancer. *Int J Mol Sci* 2021, Vol 22, Page 2690. 2021;22(5):2690.
81. Fujiwara-Tani R, Sasaki T, Ohmori H, et al. Concurrent Expression of CD47 and CD44 in Colorectal Cancer Promotes Malignancy. *Pathobiology*. 2019;86(4):182-189.
82. Barkal AA, Brewer RE, Markovic M, et al. CD24 signalling through macrophage Siglec-10 is a target for cancer immunotherapy. *Nat* 2019 5727769. 2019;572(7769):392-396.
83. Ozato Y, Kojima Y, Kobayashi Y, et al. Spatial and single-cell transcriptomics decipher the cellular environment containing HLA-G+ cancer cells and SPP1+ macrophages in colorectal cancer. *Cell Rep*. 2023;42(1).
84. Sun Z, Du C, Xu P, Miao C. Surgical trauma-induced CCL18 promotes recruitment of regulatory T cells and colon cancer progression. *J Cell Physiol*. 2019;234(4):4608-4616.
85. Chen J, Yao Y, Gong C, et al. CCL18 from Tumor-Associated Macrophages Promotes Breast Cancer Metastasis via PTPN23. *Cancer Cell*. 2011;19(4):541-555.
86. Lin Z, Li W, Zhang H, et al. CCL18/PITPNM3 enhances migration, invasion, and EMT through the NF- κ B signaling pathway in hepatocellular carcinoma. *Tumor Biol*. 2016;37(3):3461-3468.
87. Krohn SC, Bonvin P, Proudfoot AEI. CCL18 Exhibits a Regulatory Role through Inhibition of Receptor and Glycosaminoglycan Binding. *PLoS One*. 2013;8(8):e72321.
88. Wågsäter D, Dienus O, Löfgren S, Hugander A, Dimberg J. Quantification of the chemokines CCL17 and CCL22 in human colorectal adenocarcinomas. *Mol Med Rep*. 2008;1(2):211-217.
89. Li J, Zhou J, Huang H, Jiang J, Zhang T, Ni C. Mature dendritic cells enriched in immunoregulatory molecules (mregDCs): A novel population in the tumour microenvironment and immunotherapy target. *Clin Transl Med*. 2023;13(2).
90. Chikuma S. CTLA-4, an Essential Immune-Checkpoint for T-Cell Activation. *Curr Top Microbiol Immunol*. 2017;410:99-126.
91. Trajkovski G, Ognjenovic L, Karadzov Z, et al. Tertiary Lymphoid Structures in Colorectal Cancers and Their Prognostic Value. *Open Access Maced J Med Sci*. 2018;6(10):1824.
92. Arndt B, Krieger T, Kalinski T, et al. The transmembrane adaptor protein SIT inhibits TCR-mediated signaling. *PLoS One*. 2011;6(9).
93. Hamaidi I, Zhang L, Kim N, et al. Sirt2 Inhibition Enhances Metabolic Fitness and Effector Functions of Tumor-Reactive T Cells. *Cell Metab*. 2020;32(3):420-436.e12.
94. Chung BS, Liao IC, Lin PC, et al. PD-L1 Expression in High-Risk Early-Stage Colorectal Cancer—Its Clinical and Biological Significance in Immune Microenvironment. *Int J Mol Sci*. 2022;23(21):13277.
95. Ye Q, Han X, Wu Z. Bioinformatics analysis to screen key prognostic genes in the breast cancer tumor microenvironment. *Bioengineered*. 2020;11(1):1280-1300.
96. Jia M, Liu C, Liu Y, Bao Z, Jiang Y, Sun X. Discovery and Validation of a SIT1-Related Prognostic Signature Associated with Immune Infiltration in Cutaneous Melanoma. *J Pers Med*. 2023;13(1):13.

97. Svensson H, Olofsson V, Lundin S, et al. Accumulation of CCR4+ CTLA-4hi FOXP3+CD25hi Regulatory T Cells in Colon Adenocarcinomas Correlate to Reduced Activation of Conventional T Cells. *PLoS One*. 2012;7(2).
98. Rapp M, Wintergerst MWM, Kunz WG, et al. CCL22 controls immunity by promoting regulatory T cell communication with dendritic cells in lymph nodes. *J Exp Med*. 2019;216(5):1170-1181.
99. Goodla L, Xue X. The Role of Inflammatory Mediators in Colorectal Cancer Hepatic Metastasis. *Cells*. 2022;11(15).
100. Lin WW, Hsieh SL. Decoy receptor 3: a pleiotropic immunomodulator and biomarker for inflammatory diseases, autoimmune diseases and cancer. *Biochem Pharmacol*. 2011;81(7):838-847.
101. Shi G, Wu Y, Zhang J, Wu J. Death Decoy Receptor TR6/DcR3 Inhibits T Cell Chemotaxis In Vitro and In Vivo. *J Immunol*. 2003;171(7):3407-3414.
102. You RI, Chang YC, Chen PM, et al. Apoptosis of dendritic cells induced by decoy receptor 3 (DcR3). *Blood*. 2008;111(3):1480-1488.
103. Hu J, Han C, Zhong J, et al. Dynamic Network Biomarker of Pre-Exhausted CD8+ T Cells Contributed to T Cell Exhaustion in Colorectal Cancer. *Front Immunol*. 2021;12:691142.
104. Rajapaksa US, Jin C, Dong T. Malignancy and IFITM3: Friend or Foe? *Front Oncol*. 2020;8(10):593245.
105. Liu X, Zhang W, Han Y, et al. FOXP3+ regulatory T cell perturbation mediated by the IFN γ -STAT1-IFITM3 feedback loop is essential for anti-tumor immunity. *Nat Commun*. 2024;15(1).
106. Yu F, Xie D, Ng SS, et al. IFITM1 promotes the metastasis of human colorectal cancer via CAV-1. *Cancer Lett*. 2015;368(1):135-143.
107. Huang C, Zhou T, Ma L, Zhao S. IFI6 Downregulation Reverses Oxaliplatin Resistance of Colorectal Cancer Cells by Activating the ROS-Induced p38MAPK Signaling Pathway. *Biol Pharm Bull*. 2023;46(1):26-34.
108. Liu J, Chen H, Qiao G, et al. PLEK2 and IFI6, representing mesenchymal and immune-suppressive microenvironment, predicts resistance to neoadjuvant immunotherapy in esophageal squamous cell carcinoma. *Cancer Immunol Immunother*. 2023;72(4):881-893.

9. Publication IV: Deep proteomics characterization of enriched CD4+ T cells in colorectal cancer tumor microenvironment

Unpublished manuscript

Authors: Urbiola-Salvador, V., Miroszewska, D., Jabłońska, A., Duzowska, K., Drężek-Chyła, K., Zdrenka, M., Śrutek, E., Szyberg, Ł., Jankowski, M., Bała, D., Zegarski, W., Nowikiewicz, T., Makarewicz, W., Adamczyk, A., Ambicka, A., Przewoźnik, M., Harazin-Lechowicz, A., Ryś, J., Filipowicz, N., Piotrowski, A., Dumanski, JP., Chen, Z.

9.1. Introduction

Despite significant advances in the diagnosis and treatment of colorectal cancer (CRC), it remains the second deadliest and the third most common cancer worldwide¹. Recently developed immunotherapies, such as immune checkpoint blockade have revolutionized CRC treatment. However, CRC can develop resistance through alternative immunosuppressive mechanisms, which result in only a small proportion of CRC patients exhibiting complete responses to therapy². Notably, the tumor microenvironment (TME), which consists of CRC cells intermixed with immune and stromal cells, plays an essential role in CRC development, progression and immune evasion³. Therefore, a deeper understanding of the immune composition in CRC TME and the mechanisms underlying immune evasion are urgently needed.

Within the CRC TME, cancer-associated fibroblasts (CAFs) support tumor growth and metastasis as well as interact with immune cells through the release of pro-inflammatory and immunosuppressive mediators⁴. Among myeloid cells, M1 macrophages primarily contribute to anti-tumor activity, whereas M2 macrophages are associated with immunosuppression and tissue remodeling. M2 macrophages can recruit regulatory T cells (Treg) cells via CCL20 and Th2 cells via CCL17, CCL18, and CCL22 to the TME⁵. CD4+ T helper cell subsets are essential regulators of immune responses within CRC TME. By inducing multiple immunosuppressive mediators such as IL-10, immune checkpoint inhibitors (PD-1, TIM-3, and CTLA-4), Th2 and Tregs contribute to CRC immune evasion⁶. In contrast, Th1 cells can help cytotoxic CD8+ T cells to enhance anti-tumor activity and Th1 infiltration is linked to better CRC prognosis⁷. Importantly, metabolic reprogramming within the CRC TME by cancer and immune cells directly affects TME cell composition and promotes immunosuppressive mechanisms. This occurs through metabolic deprivation of amino acids, such as tryptophan and arginine and induced high adenosine levels via CD39/CD73, leading to the exhaustion of effector anti-tumor cells⁸.

Recent advances in mass spectrometry (MS)-based proteomics enable the quantification of thousands of proteins with high accuracy and sensitivity, providing valuable insights for clinical applications in colorectal cancer (CRC) research⁹. For instance, proteogenomics analyses resulted in identification of apoptosis dysregulation and increased proliferation, finding novel potential therapeutic targets. Interestingly, microsatellite instability sustained increasing glycolysis linked to the reduction of CD8+ T cells numbers within colon cancer TME⁹. Moreover, proteomic hypoxic signatures were linked to metabolic reprogramming and Epithelial-Mesenchymal Transition (EMT) together with TGFβ1 signaling¹⁰. Importantly, inferred immune score was associated with active MHCII antigen presentation, proteasome processing, FOXP3 and CD68 while immune “cold” tumors were characterized with poor survival¹⁰. Meanwhile, laser capture microdissection (LCM) combined with proteomics allows for Region of Interest (ROI) isolation to characterize their specific proteomes within cancer tissue¹¹. LCM combined with proteomics of epithelial and stromal regions from normal, adenoma, and CRC tissues demonstrated that stromal adenoma and CRC shared similar proteomic features characterized by active antigen presentation and higher proportions of CD4+ and CD8+ T cells¹¹. Recently, proteomics analysis of FACS-sorted CD4+ and CD8+ T cells from CRC and normal tissues unveiled that increased lipocalin-2 (LCN2) in CRC promotes T cell apoptosis via deregulation of iron efflux¹². Meanwhile, Huang et al.¹³ applied immunohistochemistry (IHC)

for LCM-based isolation of CAFs and hepatocellular carcinoma cells within the cancer tissue and Data-Independent Acquisition (DIA) proteomics demonstrated efficient isolation by representative CAF and cancer markers expression.

In this study, IHC of CD4 followed by macrodissection was applied to isolate ROIs enriched with CD4+ T cells and immune infiltration from CRC and normal-matched Formalin-Fixed Paraffin Embedded (FFPE) tissue samples. Deep (Data Independent Acquisition) DIA MS-based proteomics analysis was performed to determine protein changes involved in CRC development, progression, and associated immune infiltration within the ROIs. Several tumorigenic processes were altered, including cell cycle-associated pathways, key epigenetic and transcriptional regulators, and elevated levels of anti-apoptotic proteins. Importantly, we revealed a complex immune network within the CRC TME, characterized by cancer-associated inflammation and adaptive immune processes composed of pro-inflammatory and immunosuppressive mediators such as CD276 and PVR. Moreover, the CRC TME proteome also reflected a heterogeneous cell compositions with the co-existence of immunosuppressive M2 macrophages, Tregs, and CAFs as well as increased FGF2 and mast cell activators associated with CRC progression. Additionally, inferred Treg fractions were associated with high MHCII antigen presentation proteins, inflammatory proteins S100A8 and S100A9, and immunosuppressive IDO1 and ARG1.

Notably, the CRC TME exhibited metabolic reprogramming, with several immunosuppressive mechanisms involved simultaneously, including NT5E-derived adenosine signaling and the deprivation of tryptophan, taurine, and arginine. Furthermore, the novel immune-regulatory receptor mast cell expressed membrane protein 1 (MCEMP1) was associated with CRC and may play a role in the adhesion and migration of CRC infiltrating CD4+ T cells, especially Tregs.

9.2. Materials and methods

9.2.1. Study cohort and sample collection

23 CRC patients (mean age 59.2, range 42-75 years and 52% males) who had a positive colonoscopy and subsequently underwent CRC surgery were included in this study. 15 CRC patients had tumors with advanced stages according to the Union for International Cancer Control (UICC) Tumor Node Metastasis (TNM) classification. Malignant neoplasm was confirmed by a pathologist. Samples were obtained from 3P-Medicine Laboratory, Medical University of Gdansk and Bank of Biological Material at Masaryk Memorial Cancer Institute, Czech Republic. Tissue samples were collected after surgery, rinsed with PBS to remove blood, formalin-fixed and paraffin embedded. Tissue sections were stored at room temperature.

9.2.2. IHC, IF staining and ROI selection

For IHC staining, tissue sections of 5 µm thickness were deparaffinized and stained with anti-CD4 antibody (Abcam 133616) with subsequent detection with HRP/DAB Detection IHC kit (Abcam, ab64261) according to manufacturer's instructions. Slides were counterstained with hematoxylin (Sigma-Aldrich, GH5332) for 1 minute and mounted with Pertex® (Histolab, 00801-EX). Mounted slides were scanned with Axio Scan.Z1 (ZEISS, Oberkochen (Germany), digital images were uploaded to QuPath v.5.2. as Brightfield image (H-DAB), CD4+ cells were detected, and ROI areas were marked. Color deconvolution was performed with Estimate stain vectors command followed by Positive Cell Detection command to detect CD4+ cells with default parameters. For immunofluorescence analysis, FFPE tissues of 5 µm thickness were deparaffinized and stained with primary antibodies anti-MCEMP1 (Abcam, ab121447) and anti-CD3 (Biolegend, 300415), and secondary Alexa594 (Invitrogen, A-11012). Nuclei were stained with DAPI (ThermoFisher, D1306). Images were viewed in confocal microscope Leica TCS SP8, and recorded with Leica Application Suite X(3.5.2.18963) software. Images were processed in ImageJ (v. 1.54i).

9.2.3. Sample preparation for proteomics analysis

Selected ROIs were scraped from the glass slide and transferred to a Protein LowBind Eppendorf tube with 3 μ L of lysis buffer (4% SDS, 100 mM Tris-HCl pH 7.6 supplemented with protease and phosphoprotease inhibitors) per 10 nL of tissue. Samples were sonicated in an ultrasonicator Qsonica Q700 coupled with a cooler system (Qsonica, Newtown, CT, USA). Protein decrosslinking was performed by incubation in a thermoshaker for 1 h at 99 °C and 600 rpm. Protein concentrations were measured with the Pierce BCA Protein Assay Kit (Thermo Fisher) following manufacturer's instructions. Disulfide bonds were reduced with 50 mM DTT and an incubation at 95 °C for 5 min. Samples were prepared following the Filter Aided Sample Preparation (FASP) protocol¹⁴ in 10 kDa cut-off Microcon filters (Merck, Rahway, NJ, USA) with digestion using Sequencing Grade Modified Trypsin (Promega, Madison, WI, USA) at a protein:trypsin ratio of 1:50 overnight at 37 °C. After peptide elution, trypsin activity was quenched by adding trifluoroacetic acid at 0.1% final concentration. Peptide samples were desalted by STop And Go Extraction (STAGE) Tips protocol¹⁵ in Empore C18 extraction disks (CDS Analytical LLC, Oxford, PA, USA) and eluted with 60% acetonitrile (ACN)/1% acetic acid solution. Samples were dried using SpeedVac and stored at -20 °C until analysis.

9.2.4. High-pH reversed phase liquid chromatography (RPLC) fractionation

A pool sample was fractionated in a Gemini high pH C18 column (5 μ m, 4.6 x 250mm) coupled in a Shimadzu LC-20AB HPLC system by gradient of phase B (95% ACN, pH 9.8): 5% for 10 min, 5%-35% in 40 min, 35%-95% in 1 min, and 95% for 3 min with a flow rate of 1mL/min. Eluates were collected every minute and concatenated in 10 fractions.

9.2.5. LC-MS/MS analysis and MS data analysis

Peptide samples with spiked iRT peptides (Biognosys Inc, Newton, MA, USA) were injected into a Thermo UltiMate 3000 UHPLC liquid chromatograph with a trap column to enrich peptides coupled to a self-packed C18 column (150 μ m internal diameter, 1.8 μ m column size, 35cm column length). Peptides were separated by a gradient of phase B (98% ACN, 0.1% FA): 5% for 5 min, 5%-25% in 85 min, 25%-35% in 10 min, 35%-80% in 5 min, 80% for 10 min, 80%-5% in 5 min at a flow rate of 500 nL/min. Separated peptides were ionized with spray voltage 2kV and injected to a tandem mass spectrometer Fusion Lumos (Thermo Fisher Scientific, San Jose, CA, USA). Pool fractions were analyzed in DDA detection mode with 60K resolution MS scan (350-1500m/z) and MS AGC target of 3e6 with maximal injection time (MIT) 50ms by orbitrap mass analyzer that triggered the top 30 precursors. For MS/MS, resolution was 15K (200-2000 m/z) and AGC target was set to 1e5 with MIT 50 ms generated by HCD fragmentation with a normalized collision energy (NCE) of 30%. The dynamic exclusion was 30 s and MS/MS m/z start was fixed to 100. Precursors for MS/MS scan were with positive charge 2-6 and intensity over 2e4. Samples were analyzed in DIA detection mode with the same parameters as DDA, except the MS scan was 400-1500 m/z equally divided into 44 continuous windows and MS/MS resolution was 30K.

A hybrid spectral library was built with FragPipe (version 21.0) with the DIA_SpecLib workflow and default parameters including specific trypsin digestion¹⁶. *Homo sapiens* UniProtKB/Swiss-Prot database (Release 2024_02) was used as reference. Carbamidomethylation (C) was set as fixed modification. Variable modifications included oxidation (M), N-terminal acetylation, phosphorylation (STY), ubiquitination (K), pyroglutamic acid (QC), methylation (K), formylation (K), formaldehyde adduct (WYH), carbamylation (MLV), and dihydroxylation (WMH). DIA data quantification was performed with DIA-NN (version 1.8.2 beta 39) using the generated hybrid library with default parameters except protein inference was deactivated, while match between runs and peptidofrom scoring were used¹⁷.

9.2.6. Proteomics data processing, statistical and bioinformatics analysis

Proteomics data and statistical analysis was performed in RStudio (version 1.3.1093) (RStudio, PBC, Boston, MA, USA) with R (version 4.3.3) (R Foundation for Statistical Computing, Vienna, Austria).

Proteomics data report from DIA-NN was used as input and spectral features were filtered followed by data preprocessing with MSstats R package (version 4.8.7) with default parameters except imputation was deactivated. MSstats preprocessing mainly includes data filtering with low detection rates, logarithmic transformation, feature median center normalization, and Tukey Median Polish summarization to protein abundances¹⁸. MSstats mixed-linear model was applied to test significantly differentially expressed proteins (DEPs) between paired CRC and normal-matched tissue samples. Proteins were considered differentially expressed with a False Discovery Rate (FDR) < 0.05 cut-off that was controlled by Benjamini and Hochberg correction. General linear regression was applied to determine significantly expressed proteins between advanced CRC (T3-4) and early CRC TNM stages (T1-2) including tumor location and age as confounding factors. Spearman correlation analysis was applied to determine significantly correlated proteins with predicted Treg fractions with a p-value < 0.05 cut-off. CIBERSORT deconvolution of immune cell fractions¹⁹ was applied with the default LM22 signature matrix using IOBR R package (version 0.99.8) in absolute mode. Pathway enrichment analysis supported by active subnetworks was applied to determine enriched GO and KEGG terms from DEPs and selectively detected proteins or significantly correlated proteins with the pathfindR R package (version 2.3.0) based on the STRING protein-protein interaction database and FDR correction²⁰. Cytoscape (version 3.10.2) was used to generate protein networks from enriched term proteins based on STRING database. All the figure plots were generated with ggplot2 R package (version 3.4.3), except alluvial plot complemented with ggalluvial R package (version 0.12.5), Uniform Manifold Approximation and Projection (UMAP) plot that was created using the default pipeline using 20 Principal Components of Seurat R package (version 4.4.0), and heatmaps were generated with ComplexHeatmap R package (version 2.16.0) with z-score normalization.

9.3. Results

9.3.1. Deep DIA proteomics characterization of FFPE CRC and normal-matched tissues enriched with CD4+ T cells and immune infiltration

FFPE tissue samples with high immune lymphocyte infiltration were selected and stained with CD4 antibody to determine CD4 infiltration (Figure 9.1a, Appendix III Figure S1a). ROIs with high percentages of CD4 infiltration were isolated from CRC and normal matched tissue slides followed by protein extraction and sample preparation by FASP protocol for DIA LC-MS/MS proteomics analysis. As a result, 9249 protein groups, supported by spectra from 76448 peptides were included in the spectral library. Following data preprocessing and peptide summarization, 7983 protein groups were quantified across the cohort samples supported by 51789 peptides with an FDR < 0.01. While most of the protein groups were quantified in both cancerous and normal tissues, however, some were selectively expressed (Figure 9.1b, Appendix III Table S1). Among the 28 selectively expressed proteins in normal matched tissues, several were related to epithelial integrity, such as the mature absorptive cell marker BEST4²¹ and a Paneth-like secretory cell protein PLA2G10 which down-regulation is linked to CRC²². Similarly, a recently reported tumor suppressor ABCA8²³ was selectively detected in normal tissue together with proteins related to normal immune response and Peyer's patches integrity including CCR10 and CCL19 constitutively expressed in secondary lymphoid tissues to attract CCR7 expressing T cells and other immune cells. The absence of these proteins reflects the disruption of normal tissue integrity in CRC.

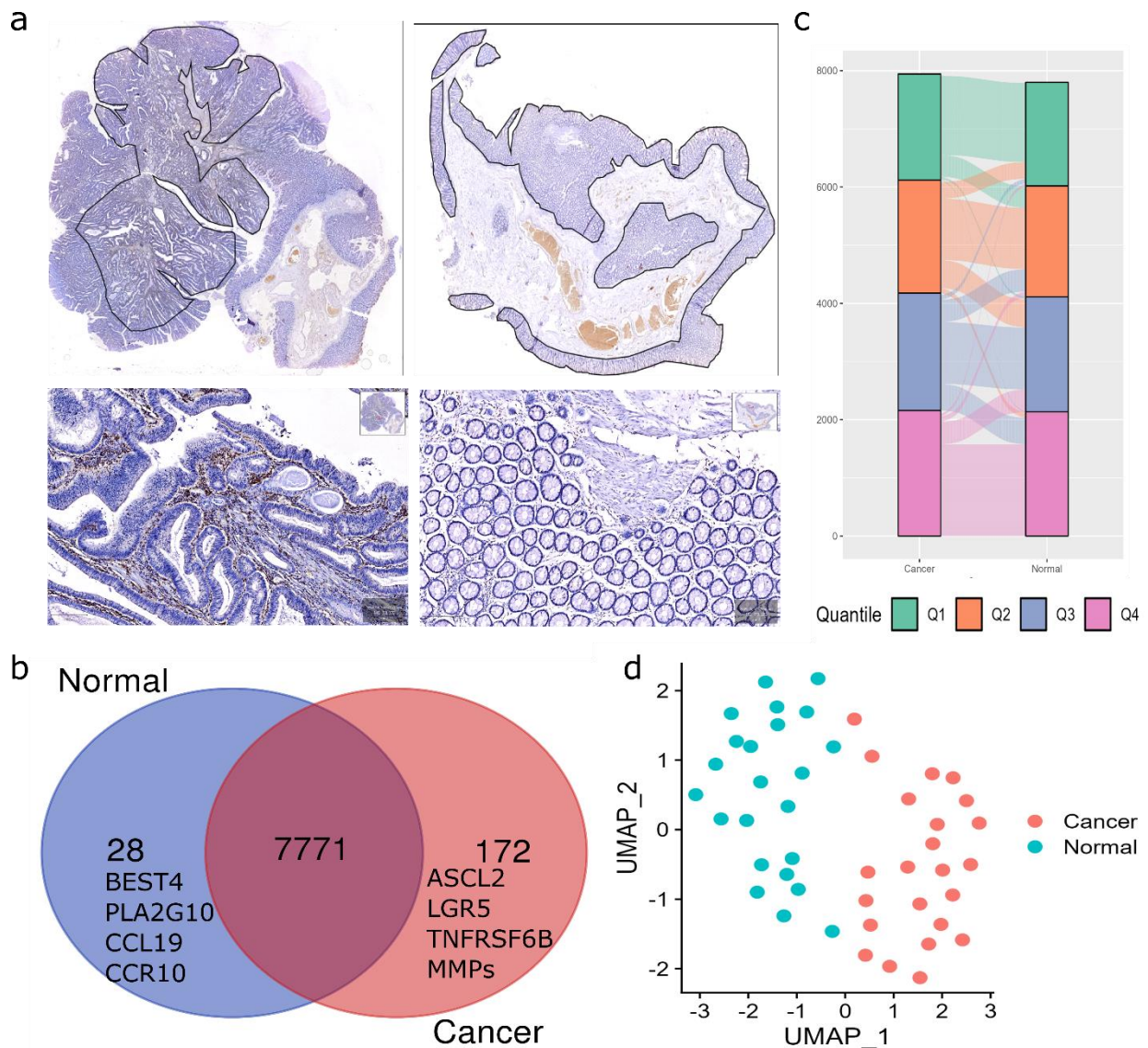


Figure 9.1. Deep proteomics characterization of C4⁺ T cell enriched CRC tissue and normal matched tissue. (a) CD4 IHC staining (DAB) of representative CRC and normal matched tissue (left and right) counterstained with hematoxylin. Brown color represents cells positive for CD4 expression and their corresponding magnifications with high CD4⁺ T cell infiltration. (b) Venn diagram of quantified proteins between both tissue types. (c) Alluvial plot of proteins commonly identified proteins in CRC and normal tissue divided in four quantiles according to their cumulative distribution of protein abundance mean. (d) UMAP plot of cancer and normal samples.

Among selectively detected proteins in CRC, ASCL2 and LGR5 were associated with CRC stem-like cells with metastatic capacities^{24,25}, cyclin CDKN2A, epigenetic regulators such as CTCF, and transcriptional factors such as MACC1 that may be involved in CRC epithelial mesenchymal transition (EMT)²⁶⁻²⁸. Other CRC selectively detected transcriptional factors included JUN, JUNB, DACH1 or DACH2 and the cell cycle regulator AURKA together with its transcriptional factor, a DNA-binding protein ARID3A²⁹. Also, extracellular matrix (ECM) remodelers were only found in CRC such as cathepsin K (CTSK), metalloproteinases MMP1, MMP11 and MMP12³⁰ as well as sulfatases, SULF1 and SULF2, involved in CRC progression^{31,32}. Proteins linked to apoptosis, such as death receptor 5 (TNFRSF10B), but at the same time the decoy receptor TNFRSF6B that protects against apoptosis, were also found selectively expressed in

tumor tissues. Interestingly, proteins involved in CRC metabolic rewiring, CRC stromal infiltration with associated CAFs, and innate immunity and inflammation were also identified only in CRC (Table 9.1).

Table 9.1 – Selected proteins involved in metabolic rewiring, stromal infiltration, immunity

Metabolic protein	Function
SULT2B1	Sulfotransferase involved in epidermal cholesterol and steroids metabolism. SULT2B1 facilitates CRC metastasis via SCD1-mediated lipid metabolism activation ³³
FOLR3	Folate receptor and other folic acid derivatives that mediates delivery of 5-methyltetrahydrofolate to the interior of cells
SLC6A6	Membrane protein that mediates sodium- and chloride-dependent transport of taurine
KYNU	Kynureninase is involved in the biosynthesis of NAD cofactors from tryptophan through the kynurenine pathway and mediates immunosuppression, a mechanism exploited in CRC via mainly tumor-associated macrophages and Tregs ³⁴
COL10A1/COL11A1	Chains of collagens type X and XI. TGF- β 1-SOX9 axis-inducible COL10A1 was associated with gastric cancer invasion and progression ³⁵
S100A12	Pro-inflammatory calcium-binding protein involved in mast cell degranulation, leukocyte recruitment, cytokine production, and regulation of leukocyte adhesion and migration. S100A12 is involved in inflammatory bowel disease (IBD) and CRC development ³⁶

Other immune related proteins were selectively detected such as C5AR1, a complement C5a receptor, cytolytic perforin PRF1, Interferon Induced Transmembrane Protein 3 (IFITM3), or chemoattractant cytokines CXCL10 and CCL20. Moreover, recently characterized proteins were also detected in CRC samples including C19orf53 that plays a role in metabolic imbalance and excessive cell proliferation³⁷ and C19orf59 defined as Mast Cell Expressed Membrane Protein 1 (MCEMP1).

To investigate the distribution of the cumulative abundance between cancerous and normal tissue, proteins were divided into four quantiles. The alluvial plot showed similar patterns of cumulative distribution, especially the most abundant proteins (Q1) were shared between cancer and normal including histones, keratins, tubulins, and other structural proteins as well as most of low-abundance proteins (Q3 and Q4). Importantly, several proteins are in different quantiles between cancerous and normal tissues, such as high abundance of adhesion proteins CEA Cell Adhesion Molecule (CEACAM) 6, an anoikis inhibitor, and CEACAM5 in CRC (Q1) compared to normal tissue (Q4) suggesting active CRC invasion^{38,39} (Figure 9.1c). Apart from selective detection of S100A12, other increased S100 proteins family in CRC included S100A8 and S100A9 that are also involved in cancer-associated inflammation. In addition, UMAP analysis showed that cancer and normal samples were grouped according to their protein abundance (Figure 9.1d). Collectively, DIA proteomics analysis of CRC and normal matched tissues enriched in CD4+ T cells and immune infiltration consistently quantified over 7900 protein groups. Selectively expressed proteins were detected, reflecting the CRC TME, including disrupted tissue integrity, oncogenic TFs, cell cycle proteins from uncontrolled CRC cell proliferation, ECM remodeling, metabolic rewiring, and prominent presence of pro-inflammatory proteins, cytokines and immunosuppressive mechanisms.

9.3.2. Protein changes in CRC TME reflects a complex network of immune processes with cell heterogeneity

To determine protein changes involved in CRC development within the TME enriched in CD4+ T cell infiltration and other immune cells, a mixed-general linear model was applied to compare protein abundances between paired tumor and normal-matched samples. 1954 protein groups were found increased and 607 with reduced levels in CRC (Figure 9.2a, Appendix III Tale S2). The most elevated protein in CRC was IGF2, which is a growth factor involved in cancer invasion secreted by CRC cells and CAFs. Additionally, elevated levels of COL12A1, tenascin C (TNC), Latent Transforming Growth Factor Beta Binding Protein 2 (LTBP2), SPARC, CD90 together with IGF2 suggested the presence of CAFs, which

promote cancer-associated inflammation in highly immune-infiltrated CRC regions ⁴⁰⁻⁴⁴. Similar to selectively detected proteins, the most elevated proteins in CRC included CRC stem cell markers such as OLFM4 and PROM1^{45,46}. Among reduced proteins in CRC, Trefoil Factor 3 (TFF3), Peptide-YY (PYY), and glucagon are crucial for intestine mucosa integrity and nutrient intake as well as multiple keratins and mucins reflecting the mucosa disruption of CRC. Supporting CRC tissue disruption, the lack of lamina propria is evident by reduced levels of desmin and dermatopontin (Figure 9.2).

Next, pathway enrichment analysis of GO and KEGG terms using DEPs and selectively expressed proteins was conducted to infer the biological processes involved in CRC TME. Both analyses revealed that the top terms were associated with splicing, RNA synthesis and translation, cell cycle, DNA repair, proteasome, and protein folding indicating that protein alterations reflected ongoing tumorigenic processes (Appendix III Figure S1b-c, Appendix III Table S3 and S4). For instance, oncogenes and proteins involved in CRC proliferation were elevated, including cyclins CDK1-2,5-7, MKI67, thymidine kinase 2 (TK2), G protein subunit gamma 4 (GNG4)⁴⁷, and G protein-coupled receptor, class C, group 5, member A (GPCR5A)⁴⁸ among others (Figure 9.2a). Moreover, tumor suppressors were also reduced in CRC such as chromogranin-A⁴⁹ and intelectin 1 (ITLN1) that can inhibit suppressive myeloid cells⁵⁰. Noteworthy, metabolic rewiring was observed in CRC protein changes with reduced oxidative phosphorylation and increased alternative pathways including amino acids metabolism, central carbon cancer metabolism, and purine metabolism (Figure S9.1d). At the same time, several hallmarks of cancer were enriched in CRC such as angiogenesis (FLT1, S100P and its regulator MACC1^{51, 52}), apoptotic deregulation, cell-matrix adhesion with ECM remodeling proteins (MMP10, MMP2, MMP9, NGAL, and ELN^{53,54}), and EMT with reduced EPCAM and increased SDBP (Figure 9.2a, 9.2b). Importantly, multiple proteins from enriched immune responses in CRC included innate immunity such as (defensins DEFA1 or DEFA3⁵⁵, azurocidin 1 (AZU1)⁵⁵, myeloperoxidase (MPO)⁵⁶, Macrophage Migration Inhibitory Factor (MIF), guanylate-binding protein 1 (GBP1), myeloid nuclear differentiation antigen (MNDA)⁵⁷, and anti-bacterial LBP and BPI (Figure 2a). Notably, the complement cascade was enriched in CRC with elevated levels of multiple components and regulators such as Factor H, CD55, and CD46 (Figure S9.1d). These results are in agreement with our previous LC-MS/MS proteomics analysis of CRC plasma samples in which several of these complement proteins were also elevated in plasma compared to healthy controls including C4B, C9 and C5 as well as other proteins such as LBP and ITIH4⁵⁸. Other enriched immune processes included type I IFN responses, IL1 response, IL12 production, monocyte and T cell chemotaxis, Fc gamma receptor, TGFB1 and NF-KB signaling pathways, antigen presentation (HLA-A,-B,-C and antigen processing proteins), immunosuppressor IL10 production pathway and several negative T cell regulators such as a PD-1 signaling mediator CSK binding protein (CBP)^{59,60}, CEACAM1, PTPRJ, GBP1, and immune checkpoints (PVR and CD276) (Figure 9.2a, 9.2b). In fact, other immunosuppressive protein elevated in CRC was 5'-Nucleotidase Ecto (NT5E) which converts ATP to immunosuppressive adenosine, inhibiting T cell activation⁶¹. Interestingly, lipocalin 2 (LCN2) was elevated in CRC, and recently, its immunosuppressive function in CRC via induction of T cell apoptosis from iron efflux deregulation was reported¹². High levels of nucleophosmin 3 (NPM3) may promote PD-L1-mediated immune escape in gastric cancer⁶². Here, we detected increased level of this protein in CRC.

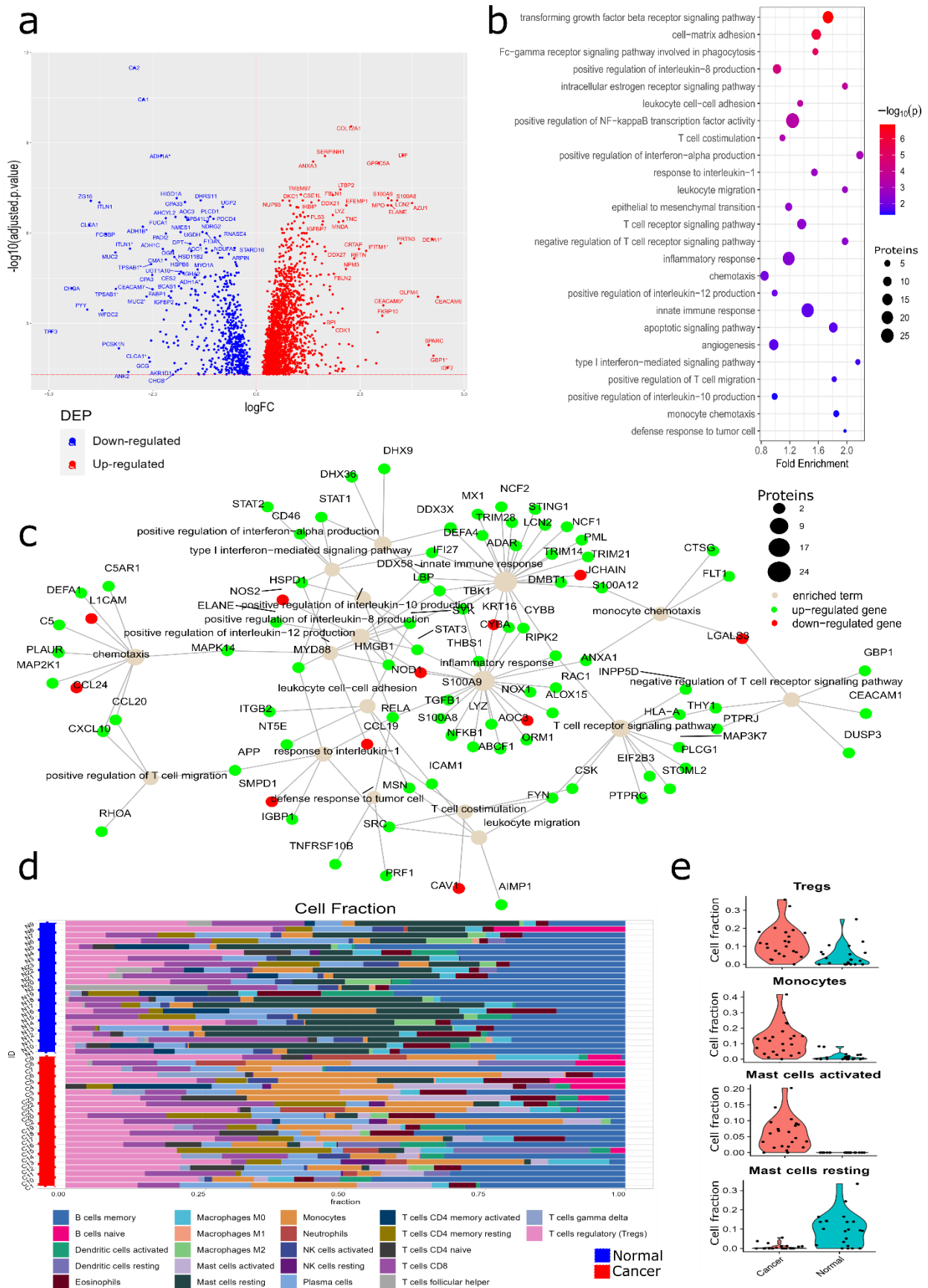


Figure 9.2. CRC TME enriched in CD4+ T cells and immune infiltration reflects a complex immune network. (a) Volcano plot of differentially expressed proteins (DEPs) between CRC and normal matched tissue with corresponding logarithmic fold changes and adjusted p-values (* indicates that the displayed protein is the first from a protein group).

(b) Bubble plot of selected GO-BP from DEPs between CRC and normal tissue. (c) Network of innate and adaptive immune processes within CRC TME inferred from DEPs present in the GO-BP terms. (d) Bar plot of CIBERSORT deconvolution results from cancer and normal tissues. Cell fractions are normalized to 1. (e) Violin plot of significantly changed cell fractions between cancer and normal tissues (all of them significant with adjusted p-value < 0.05).

Importantly, anti-tumor macrophage derived proteins were reduced, including FOLR2 and MARCKS^{63,64}, what indicates reduced levels of M1 macrophages within CRC TME. Regarding B cells, we found reduced levels of IgA, and JCHAIN in CRC which are required for intestinal immunity as well as reduced levels of protective proteins such as Fc Gamma Binding Protein (FCGBP) and zymogen 16 (ZG16) (Figure 2a). In contrast, IgGs, the BCR signaling transducer CD81 which facilitates clonal expansion and antibody production⁶⁵, and the IgM signal transducer Immunoglobulin Binding Protein 1 (IGBP1) were elevated in CRC. Another relevant reduced protein was Neural Cell Adhesion Molecule 1 (NCAM1), CD56, involved mainly in NK cell activation but also in T cells and B cells (Figure 9.2a). CIBERSORT cell fraction deconvolution was applied to infer the immune cellular composition in CRC TME and normal tissues. Cell fraction deconvolution revealed a complex mixture of immune cell types in both tissue types, including diverse T cell subsets, mast cells, myeloid cells, and B cells (Figure 9.2d). Importantly, CRC samples showed significantly elevated levels of inferred Treg, monocyte, and activated mast cells but reduced resting mast cells, suggesting an immunosuppressive TME in CRC compared to normal tissue (Figure 9.2e). Taken together, CRC tissue regions with high CD4+ T cell infiltration are marked by multiple cancer transformation pathways and hallmarks, including metabolic rewiring, cell stemness, and apoptosis. Simultaneously, an intricate network of innate and adaptive immune processes with proteins involved in cancer-associated inflammation and immunosuppressive mechanisms driven by Treg and monocytes/macrophages that may facilitate CRC immune evasion.

9.3.3. CRC progression is associated with mast cell activation, CAFs infiltration and antigen presentation alterations

CD4+ T cells and other immune cells are fundamental players within the TME in CRC progression and metastasis⁶⁶. To determine protein changes associated with CRC progression, general linear modelling was applied to compare between advanced CRC and early TNM stages. As a result, 215 proteins were increased in advanced stages and 300 were increased in early stages (Figure 9.3a, Appendix III Table S5). Altered protein levels along CRC progression were associated with multiple biological processes, such as HIF-1 signaling pathway, positive regulation of I-kappaB kinase/NF-kappaB signaling, cellular response to lipopolysaccharide, positive regulation of cell migration, ephrin receptor signaling pathway, and protein acetylation among others (Figure 9.3b, Appendix III Table S6, S7). The protein with highest fold change in late CRC stages was the secreted trypsin-like serine protease KLK6, that was previously reported being associated with poor CRC prognosis^{67,68} (Figure 9.3c). Notably, MUC13 previously associated with CRC progression, poor prognosis, and immunosuppressive TME⁶⁹. Here we found it was increased in advanced CRC along with its upregulation in cancer compared to normal tissue (Fig 9.3a, Appendix III Table S5). Several proteins involved in ribosome functionality were increased in advanced CRC along with higher levels of histones, which may reflect higher cell proliferation in advanced stages. At the same time, decreased levels of DNA repair proteins, MLH1 and ATM, and increased levels of key transcriptional factors, TCF20 and TMF1, involved in androgen receptor signaling, were found in advanced CRC. Metabolic alterations were also observed in CRC progression with elevated levels of glycosidases MAN2A2 and reduced MAN2A1, these changes were consistent with previous CRC studies⁷⁰. Another metabolic enzyme increased in late CRC was ADO (Fig. 9.3a, Appendix III Table S5), that converts cysteamine to hypotaurine, previously identified as a tumorigenic metabolic pathway in glioblastoma⁷¹.

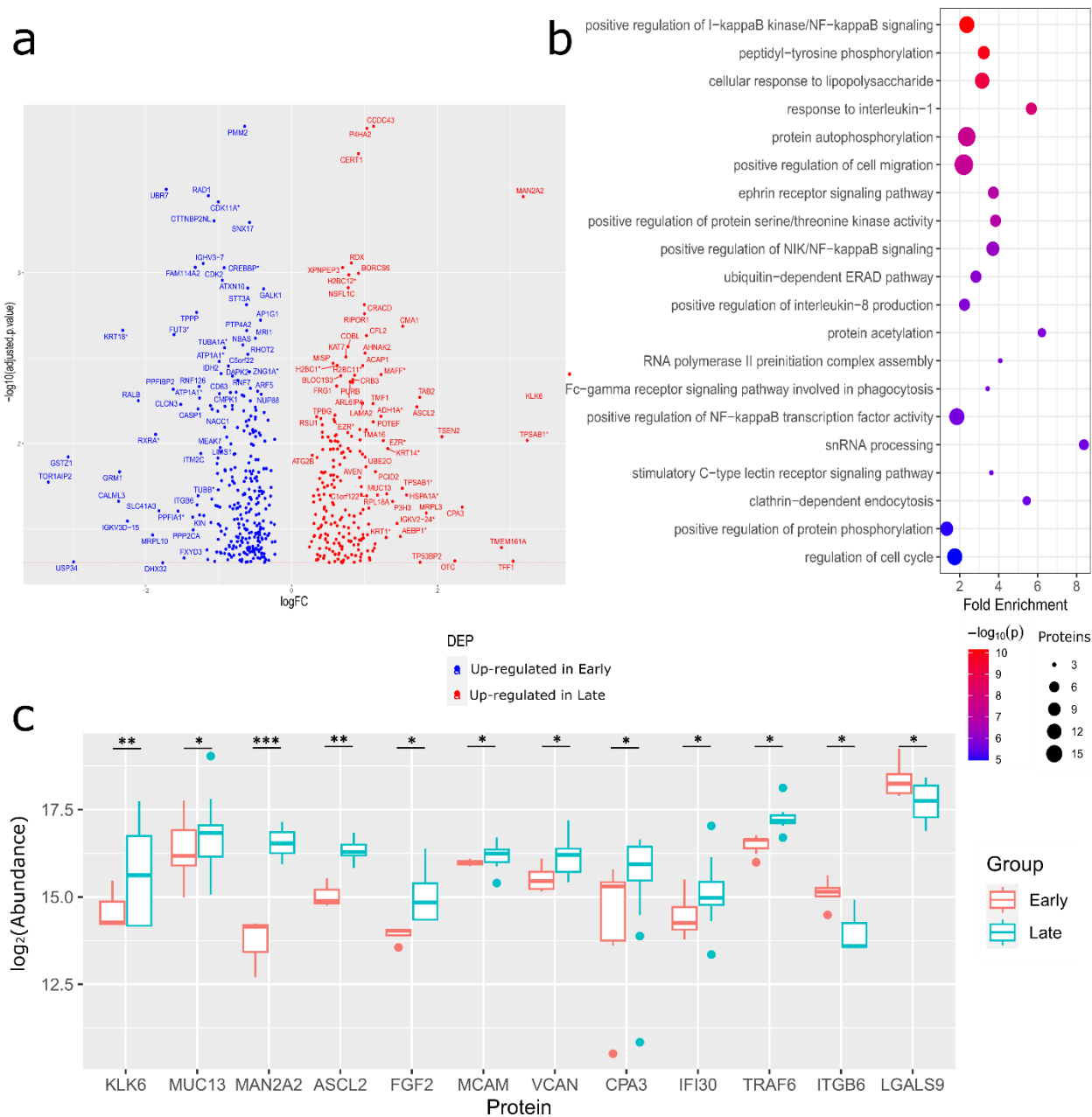


Figure 9.3. Protein changes within CRC TME associated with CRC progression. (a) Volcano plot of plot of differentially expressed proteins (DEPs) between advanced CRC and early TNM stages with corresponding logarithmic fold changes and adjusted p-values (* indicates that the displayed protein is the first from a protein group). (b) Bubble plot of selected GO-BP from significantly DEPs between advanced CRC and early stages. (c) Box and whisker plots of selected DEPs between early and late stages (* indicates p-value < 0.05, ** < 0.01, and *** < 0.001).

Interestingly, several altered proteins were likely derived from cancer-TME interactions and CRC heterogeneity. For instance, increased vimentin expression may indicate an active EMT phenotype whilst elevated ASCL2 and AVEN may indicate CRC stemness⁷² and anti-apoptotic signaling⁷³, respectively. Importantly, in advanced CRC stages, elevated TNC and FGF2 may be involved in cancer invasion and secreted mainly by CAFs⁷⁴ (Figure 9.3c). Presence of CAFs in samples with advanced CRC stages was further supported by elevated MCAM, which were associated with poor CRC prognosis and correlated with angiogenesis^{75,76}. ECM remodeling was also reflected in elevated levels of VCAN in advanced CRC, an ECM chondroitin sulfate proteoglycan that its proteolytic forms were previously associated with anti-tumor immunity against CRC while recently associated with T cell exhaustion depending on their glycosaminoglycan sulfation patterning in breast cancer^{77,78}. Importantly, mast cell activation markers,

TPSAB1 and TPSB2 as well as CPA3, which may be involved in cancer angiogenesis and tumorigenesis^{79,80} were increased in advanced CRC. Moreover, increased IFI30 and TRAF6 levels in samples of advanced stage CRC, could indicate ongoing antigen presentation processing⁸¹ and active immune response, respectively. Although, TRAF6 was previously correlated with lymphangiogenesis and lymph node metastasis in CRC as well as pro-inflammatory cytokine secretion in innate immune responses⁸² (Figure 9.3c).

On the other hand, early stages of the CRC were characterized by the elevation of ITGB6, FOLR2, and LGALS9, all indirectly involved in immunosuppression^{83,84} (Figure 9.3a, 9.3c). Noteworthy, MHC-I proteins (HLA-A,-C) were decreased with CRC progression (Figure 9.3a, 9.3c, Table S9.5), indicating a well-established mechanism of immune evasion⁸³.

Taken together, protein abundance changes associated with CRC progression suggested tumorigenic alteration within the TME including metabolic adaptations, EMT signatures, ECM remodeling with CAF-related proteins including FGF2, mast cell markers, and relevant immunosuppressive mechanisms including LGALS9 and reduction of MHC-I presentation.

9.3.4. Proteomic changes associated with Treg infiltration in CD4+ enriched CRC tissues

Increased Treg infiltration was observed in the comparison between CRC and normal tissue (Figure 9.2e). Considering the fundamental role of Treg infiltration in CRC immune evasion, Spearman correlation analysis was performed between CIBERSORT inferred Treg fractions and protein abundances along CRC tissues to determine potential protein associations with Tregs. This analysis revealed that 380 proteins were significantly positively correlated and 77 were negatively correlated with inferred Treg fractions (Figure 9.4a, Appendix III Table S8). Pathway enrichment analysis via active subnetworks of significantly correlated proteins demonstrated elevated oxidative phosphorylation with mitochondrial respiratory proteins (Figure 9.4b, Appendix III Table S9), that was reported to support Treg differentiation⁸⁵. Other enriched immune processes included proteasome processing and high MHCII antigen presentation, Fc-epsilon receptor signaling, TCR signaling and T cell cytotoxicity together with apoptosis regulation, cell-cell adhesion, and histone deacetylation (Figure 9.4b, Appendix III Table S9).

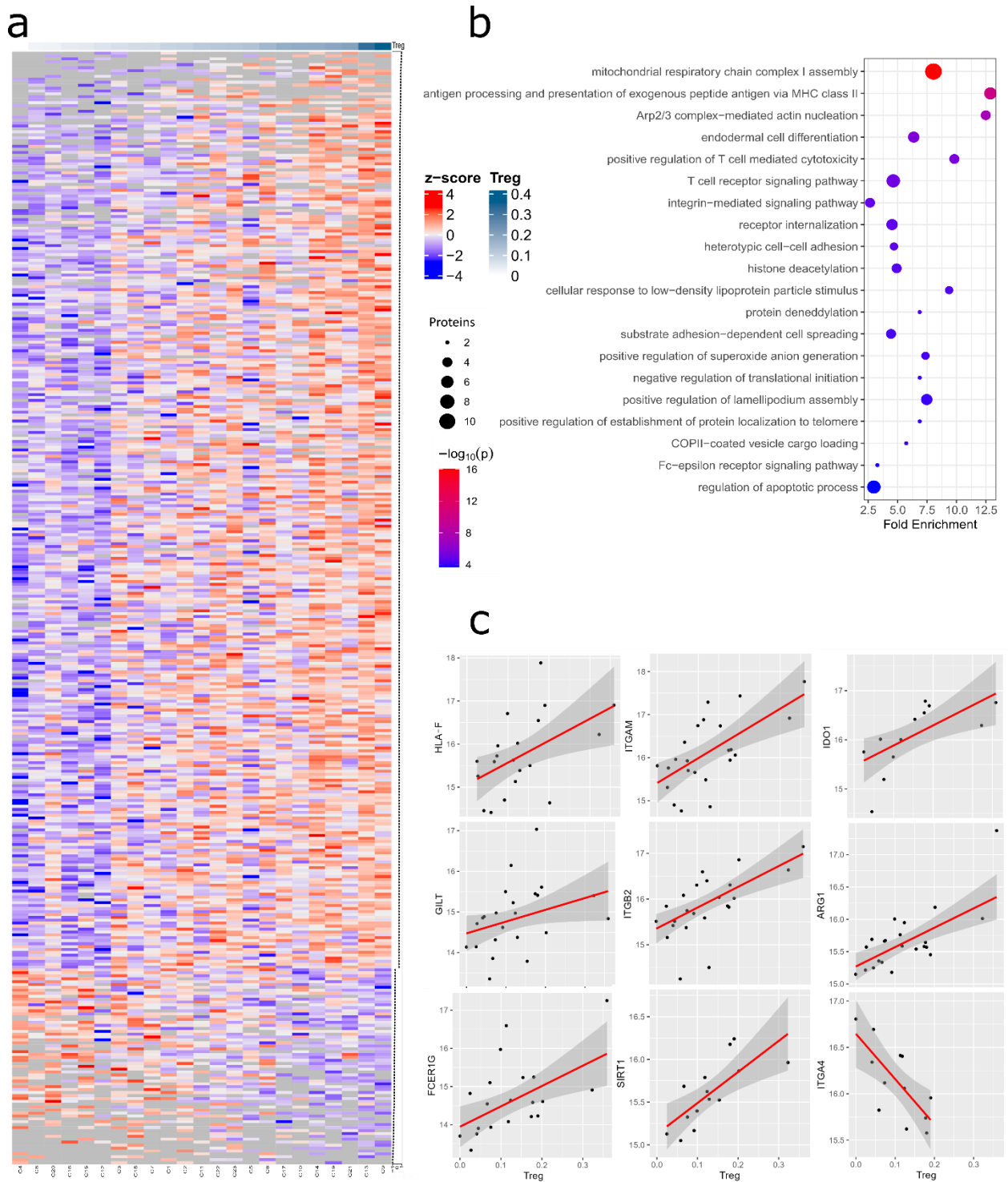


Figure 9.4. Treg fractions and associated protein changes. (a) Heatmap of significantly correlated proteins with Treg fractions order by decreasing rho value and samples order in increasing inferred Treg fraction with z-score normalization. (b) Bubble plot of selected GO-BP from significant correlated proteins with Treg fractions. (c) Scatter plots of selected significant correlated proteins with inferred Treg fractions and relative protein abundance.

High MHCII presentation, increasing MHC-I proteins HLA-A and HLA-F, immunoproteasome subunits PSMB8 and PSMB9, and MHC-I processing TAPBP and GILT may indicate the active interaction of innate and adaptive immune responses related to Treg presence in the CRC TME (Figure 9.4a, 9.4c, Appendix III Table S8). Increasing levels of integrins ITGAM and ITGB2 were associated with Treg fractions, both proteins were with reported function in innate immune complement-opsonized pathogens as well as T cell

migration^{86,87}. Similarly, FCER1G was linked to Treg content that could indicate the presence of mature regulatory DCs, a subset of highly immunosuppressive DCs with high IDO1 production and CXCL9 deregulation⁸⁸. In fact, IDO1 and ARG1 were positively correlated with Treg fractions, supporting an immunosuppressive metabolic rewiring within enriched CD4+ T cell CRC tissues with high Treg fractions^{89,90}. Increasing abundance of deacetylases SIRT1 and SIRT2 with Treg content may be associated with this immunosuppressive metabolic TME⁹¹. In contrast, ITGA4 was negatively correlated with Treg fractions. Low ITGA4 was reported to be associated with poor CRC prognosis and positively correlated with Th17 and immature DCs in CRC⁹². (Figure 9.4c). Taken together, Treg-linked protein changes within CRC TME are associated with antigen presentation with immunosuppressive phenotypes and metabolic alterations including tryptophan and arginine T cell deprivation.

9.3.5. CRC TME protein changes are associated with CD4+ T cell pro-inflammatory factors, CEACAMs and the novel chemotactic receptor MCEMP1

Our analysis revealed immune heterogeneity and the inflammatory and immunosuppressive processes within CRC TME enriched in CD4+ T cells and other immune cells. To precisely assess the expression changes in specific cell population, a complementary analysis of public datasets was performed. A scRNA-seq dataset from CRC and normal matched tissue of 72 CRC patients⁹³ were used to infer specific cell expression of detected protein changes. The selected protein changes identified in this proteomics analysis, were supported by scRNA-seq data among all CRC T-cells subsets as shown in Figure 5a. Interestingly, a tendency for higher fractions of LCN2 expressing Treg and CD8+CXCL13+ T cells was observed within CRC T cell subsets (Figure 9.5a). Another increased protein identified in CRC tissue CEACAM1 was found highly expressed in CRC infiltrating Tregs in scRNA-seq data (Fig 9.5a, 9.5b). Interestingly, the Gram-negative bactericidal BPI, only found in CRC tissues in this study, in scRNA-seq data it was mainly expressed by stem-like CRC cells and some macrophages/monocytes, suggesting a role in CRC TME. Among proteins associated with the CRC progression in this study, in scRNA-seq data FGF2 was mainly expressed by CAFs and CRC cells, GILT was mainly expressed by myeloid cells but also other cell types, and tryptases (TPSAB1, TPSB2) and CPA3 were mainly expressed by mast cells but also in epithelial and other immune cells (Figure 9.5a, Appendix III Figure S2a). From correlated proteins with inferred Treg fractions, ARG1 was only expressed from a minor portion of cells in this scRNA-seq dataset, mainly macrophage/granulocytes, low fraction of epithelial cells, and CRC infiltrating Treg and follicular helper T cells (T_{fh}) (Figure 9.5a, 9.5b, Appendix III Figure S2b). Next, a public proteomics dataset from sorted CD4+ and CD8+ T cells from CRC and normal-matched tissues¹², was analyzed to infer protein changes in CRC TME derived from T cells. First of all, we found elevated LCN2 levels in immune CRC TME (Figure 9.2a), which is in line with the main findings from Che et al.⁵³. Noteworthy, bioinformatics re-analysis demonstrated that, the recently characterized immune receptor MCEMP1, was consistently quantified in CD4+ and CD8+ T cells by proteomics and exhibited a trend for higher expression in tumor-infiltrating CD4+ T cells (paired t-test: logFC = 0.53, p-value = 0.06), but not in CD8+ T cells, suggesting a relevant role in CD4+ T cells within the CRC TME (Figure 9.5c). Similarly, scRNA-seq data confirmed MCEMP1 expression in several T-cells subsets as well as in monocyte/macrophages, and granulocytes with a high number of Tregs expressing MCEMP1 (Figure 9.5b, 9.5d, Appendix III Figure S2b). Consistently, immunofluorescence staining confirmed the co-expression of MCEMP1 and CD3⁺T-cells within CRC TME (Figure 9.5e).

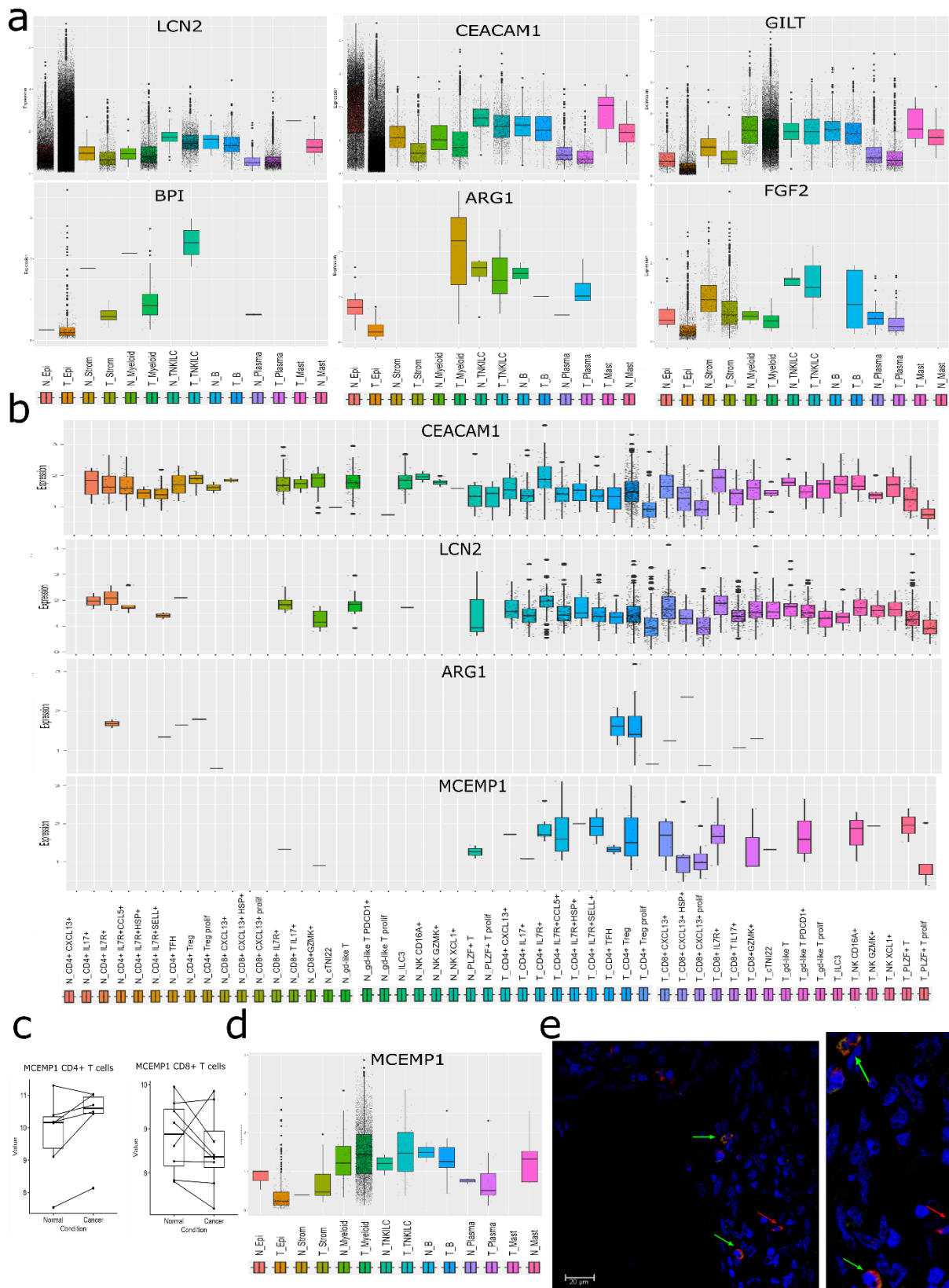


Figure 9.5. Protein changes are associated with specific cell components of CRC TME. (a) Box and whisker plots of normalized mRNA expression in scRNA-seq dataset from Pelka et al.⁹³ in main cell types separated by tumor and normal tissues. Each small black dot represents the gene expression of a single cell. (b) Box and whisker plots of normalized mRNA expression along T cell subtypes separated from CRC and normal tissue. (c) Paired box plots of normalized protein abundances of MCEMP1 between CRC-infiltrating CD4⁺ and CD8⁺ T cells and normal counterparts, respectively. (d) Box plot of MCEMP1 expression in scRNA-seq data. (e) IF staining of MCEMP⁺ CD3⁺ T-

cells in representative CRC samples. Green arrow double-positive MCEMP1+ and CD3+ T-cell, red arrow – single positive MCEMP1+ cell.

Taken together, our proteomics analysis revealed protein changes that may be associated with specific cell subsets within the TME, especially myeloid and T cells, many of which play a relevant role in tumor immunity and immunosuppression.

9.4. Discussion

Immune cell infiltration plays a crucial role within CRC TME via eliminating tumor cells or supporting tumor growth, invasion, and drug resistance among others⁵. In this study, deep DIA proteomics characterization of CRC and normal matched tissue enriched in CD4+ T cells and other immune cells was performed to determine protein changes within CRC TME. We analyzed the proteomics changes involved in CRC development, progression, and immune infiltration. CRC and normal-matched tissue samples were consistently different in their protein composition. Firstly, selectively detected proteins in CRC tissues revealed CRC tumorigenic processes with key epigenetic and transcriptional regulators. On the other hand, selective expression of a marker of absorptive cells, BEST4 in normal tissue, and CCL19, specific for secondary lymph nodes and previously associated with anti-tumor CD8+ T cells in TCGA datasets and breast cancer⁹⁴, demonstrated disrupted tissue integrity and reduction of anti-tumor CD8+ T cells in studied CRC tissue, respectively. Protein changes within TME CRC primarily reflected active cell cycle with DNA repair, RNA synthesis, spliceosome and protein refolding, all linked with high proliferation. Moreover, key CRC stem-cell markers such as ASCL2, involved in CRC progression, PROM1, and LGR5, for which CAR-T cell therapy are currently under development⁹⁵, were identified in CRC tissues. Other proteins, related to cancer hallmarks, were altered, such as FLT1 associated with angiogenesis and increasing microvessels in CRC⁹⁶, apoptosis deregulation with anti-apoptotic BCL2L1 and TNFRSF6B associated with poor CRC prognosis^{97,98} or EMT with EPCAM reduction and transcriptional factor MACC1 via HGF/MET signaling²⁸.

Importantly, protein expression patterns in CRC TME reflected changes in the cell composition. Although several key cellular markers were not detectable due to the heterogenous cellular populations in CRC TME and their low abundance, application of CIBERSORT enabled the deconvolution of cellular populations and estimation of cells fractions in bulk samples. Inferred immune cell fractions suggested an increased immunosuppressive environment compared to normal tissue reflected in higher fractions of Treg. Meanwhile, protein changes revealed cell composition changes linked to alterations in innate and adaptive immune responses. For instance, innate immune proteins dedicated to intestinal defense against pathogens such as ZG16 and FGCBP along with plasma-derived IgA were reduced, while B cells may be increased with high IgGs, CD81, and IGBP1 in CRC TME. Also, NK cell marker CD56 was reduced similarly to previous studies based on IHC staining⁹⁹. Among innate immune proteins, BPI was elevated in CRC tissues and in CRC stem-like and myeloid cells from scRNA dataset. BPI was previously reported to be associated with IBD as anti-angiogenic factor¹⁰⁰, however to the best of our knowledge, it was not studied in the context of CRC. BPI may play a role within TME infiltrated microbiota or can attenuate inflammation via competing with LBP¹⁰¹. Furthermore, complement cascade members are involved in tolerogenic cell death and immunosuppressive TME with recruitment of Treg, M2 macrophages, and myeloid-derived suppressor cells (MDSCs) what may be a reason for the elevated complement proteins in enriched CD4+ T cells TME¹⁰². Supporting this complement role in enriched CD4+ T cell TME, elevated soluble Factor H in CRC samples was reported to create anti-inflammatory responses while the negative complement regulators CD46 and CD55 are responsible for dampening the complement cascade¹⁰². Interestingly, increased mast cell activation markers (TPSAB1, TPSB2, and CPA3) in CRC were previously reported being associated with angiogenesis and tumorigenesis^{79,80}. However, the role of mast cells in CRC TME remains controversial and further research is needed¹⁰³.

Several CAF-related proteins were increased in CRC tissue, including CD90+ stromal cells that are main IL-6 producers, promoting cancer-associated inflammation⁴² and also can produce immunosuppressive NT5E¹⁰⁴. Furthermore, FGF2 is secreted mainly by CAFs but can also be produced in an autocrine manner by CRC cells as observed in the CRC scRNA-seq dataset^{105,106}. Moreover, increased levels of FGF2 were reported in IBD and FGF2 secretion is induced in Tregs to promote tissue repair in an IBD mice model¹⁰⁷, suggesting an immunosuppressive role in CRC progression. In this study, we reported a novel associations of FGF2 with CRC progression. Multiple myeloid related proteins were elevated, including GBP1 and GBP2, that are required for autophagosome maturation and activated by interferon type I and II stimulations. In fact, GBP1 was associated with immunosuppressive M2 macrophage phenotype in previous studies¹⁰⁸. Moreover, GBP1 can inhibit T cell activation by reducing IL-2 production via IFN γ ¹⁰⁹. Elevated levels of LCN2 together with lactotransferrin (LTF) may also counteract exacerbated inflammation as well as promote T-cell death via ferroptosis^{110,111}. Interestingly, high LCN2 expression in infiltrating Treg populations found in scRNA-seq data is according to the previous study that demonstrated Treg differentiation via LCN2 characterized by non-classical HLA-G expression *in vitro*¹¹², suggesting additional immunoregulatory functions of LCN2 within CRC TME. At the same time, PTPRJ was also increased in CRC while a recent proteomics study in circulating immune cells of CRC patients demonstrated that increasing PTPRJ levels are responsible of effector CD4+ T cell suppression along CRC progression¹¹³. Meanwhile, decreased levels of LGALS9 in advanced CRC in this study reinforces the recently proposed targeting of LGALS9 signaling as a treatment alternative, with promising results of anti-LGALS9 immunotherapy clinical trials in other types of solid tumors⁸⁴.

Increased levels of non-classical MHC-I class HLA-F, which was found to correlate with Tregs fractions, was reported to negatively regulate NK cells via alternative antigen presentation of a limited variety of peptides¹¹⁴ that may influence to the observed reduced CD56 marker in CRC tissues. In contrast, decreased FOLR2 in CRC compared with normal tissue and CRC progression may indicate the reduction of FOLR2+ macrophages. This population was previously identified to co-localized with CD8+ T cells in breast cancer, CRC, and other cancers as good prognostic factor⁶³. However, another scRNA-seq study showed FOLR2+ macrophages associated with Tregs and an immunosuppressive TME in invasive lung adenocarcinomas¹¹⁵. Therefore, further investigation is needed to unveil the role of this FOLR2+ macrophage subpopulation within the TME. Meanwhile, inferred Treg fractions were associated with oxidative phosphorylation and active antigen presentation from APCs including GILT, that was also increased in late CRC stages. GILT was previously linked to tolerogenic responses to breast cancer and melanoma tumor antigens via induction of Treg differentiation^{116,117}. A recent study reported that GILT was also associated with PD-L1 signaling in breast cancer¹¹⁸. This highlights the potential role of GILT in immune tolerance to CRC mediated by APCs.

Importantly, our data unveiled protein changes enriched in metabolic rewiring within CRC TME. Accumulated evidence demonstrated that metabolic alterations are responsible for immune evasion and immunosuppressive mechanisms¹¹⁹. In this study, multiple proteins involved in metabolic immunosuppression were reported including IDO1 correlation with inferred Treg together with increased KYNU and AHR, suggesting active tryptophan deprivation³⁴. Interestingly, SIRT1 and SIRT2 were correlated with Treg fractions and previous proteomics studies in cancer mice models determined that SIRT5 enhances Tregs⁹¹ while SIRT2 can promote T cell exhaustion¹²⁰. Apart from tryptophan metabolism, increased levels of the transporter SLC6A6 in CRC TME might be involved in a novel immunosuppressive mechanism through taurine deprivation, reported in lung cancer¹²¹. Previously, SCL6A6 overexpression was found in CRC tissues and associated with chemotherapy resistance *in vitro* and *in vivo*¹²². Further supported by increased ADO, a taurine intermediary producer, in advanced CRC as previously found via metabolomics in CRC tissue and serum¹²³. Another Treg-correlated metabolic enzyme, ARG1, was found associated with CD15+ bone-marrow derived cells in CRC and associated with poor prognosis^{124,125}. Recently, ARG1+ granulocytes and IDO1+ monocytes were analyzed in CRC and their spatial pattern distribution may be associated with CRC prognosis, however, immunosuppression was not addressed in

this tissue microarray multiplex IHC study ¹²⁶. In our study, ARG1 was positively correlated with Treg fractions and scRNA-seq confirmed its expression in myeloid cells as well as Treg and Tfol within CRC TME, suggesting effector T cell suppression via arginine deprivation.

For the first time, the novel chemotactic regulator MCEMP1 was selectively detected within the CRC TME. Our re-analysis of public CRC T cells proteomics data ¹² showed that increased MCEMP1 protein was detected in CD4+ T cells isolated from CRC tissue compared to normal tissue. Moreover, MCEMP1+ T cells presence in CRC tissue was confirmed by immunofluorescence. While scRNA-seq from CRC showed MCEMP1 expression mainly in CRC monocyte/macrophage, granulocytes, CRC stem-like cells, importantly, several T cells subsets also express MCEMP1, with a high fraction of Tregs. MCEMP1 was primarily found in mast cells in which can regulate proliferation within lungs ^{127,128}. Recently, TGFB1-mediated activation of MCEMP1 was found in classical monocytes and alveolar macrophages in which MCEMP1 regulates migration and adhesion ¹²⁹. A study in a mice sepsis model showed that MCEMP1 is upregulated in sepsis and promoted T cell apoptosis and inhibited their viability ¹³⁰. Interestingly, an *in silico* study in CRC mRNA data showed that FOXP3 and MCEMP1 were correlated with liver metastasis while in gastric cancer was included in a gene prognostic signature associated with Treg ^{131,132}. Further studies are needed to unveil MCEMP1 function in T cells, especially in infiltrating Treg within CRC TME as well as other immune cells.

This study was limited by the number of involved patients and limited tissue material, although robust proteomics analysis ensured deep proteome characterization of the CRC TME. Although bulk proteomics analysis of composed tissue samples limits to determine cell specific protein expression and their full spatial distribution, the usage of public proteomics and scRNA-seq datasets facilitated to infer the cell composition of the CRC TME. However, integration of multi-omics approaches with emerging single-cell proteomics and spatial proteomics will provide deeper understanding of CRC underlying immune responses.

In this study, deep proteomics analysis enable us characterized the immune regulatory network that included co-stimulatory and inhibitory signals reflecting the complexity of immune responses within CRC TME. Moreover, protein signatures linked to CRC progression and Treg content within CRC TME were found. Cancer-associated inflammation and immunosuppressive mechanisms are imbalanced with co-existence of multiple processes from exacerbated inflammation to immune checkpoints and metabolic deprivation immunosuppressive mechanisms. Moreover, proteomics changes within CRC TME enriched in CD4+ T cells and other immune cells reflected immune TME heterogeneity with higher inferred fractions of Tregs, monocytes, and activated mast cells. Our study unveiled novel immune regulators involved in CRC may facilitate the functional validation of immune-regulatory proteins for therapeutical application.

9.5. References

1. Bray, F. et al. Global cancer statistics 2022: GLOBOCAN estimates of incidence and mortality worldwide for 36 cancers in 185 countries. *CA Cancer J Clin* 74, 229–263 (2024).
2. Weng, J. et al. Exploring immunotherapy in colorectal cancer. *J Hematol Oncol* 15, 95 (2022).
3. Gallo, G., Vescio, G., De Paola, G. & Sammarco, G. Therapeutic Targets and Tumor Microenvironment in Colorectal Cancer. *J Clin Med* 10, 2295 (2021).
4. Kamali Zonouzi, S., Pezeshki, P. S., Razi, S. & Rezaei, N. Cancer-associated fibroblasts in colorectal cancer. *Clin Transl Oncol* 24, 757–769 (2022).
5. Zhang, Y., Rajput, A., Jin, N. & Wang, J. Mechanisms of Immunosuppression in Colorectal Cancer. *Cancers* 12, 3850 (2020).
6. Aristin Revilla, S., Kranenburg, O. & Coffey, P. J. Colorectal Cancer-Infiltrating Regulatory T Cells: Functional Heterogeneity, Metabolic Adaptation, and Therapeutic Targeting. *Front. Immunol.* 13, (2022).
7. DiToro, D. & Basu, R. Emerging Complexity in CD4+T Lineage Programming and Its Implications in Colorectal Cancer. *Front. Immunol.* 12, (2021).
8. Chen, X. et al. The effects of metabolism on the immune microenvironment in colorectal cancer. *Cell Death Discov.* 10, 1–11 (2024).
9. Vasaikar, S. et al. Proteogenomic Analysis of Human Colon Cancer Reveals New Therapeutic Opportunities. *Cell* 177, 1035–1049.e19 (2019).
10. Tanaka, A. et al. Proteogenomic characterization of primary colorectal cancer and metastatic progression identifies proteome-based subtypes and signatures. *Cell Reports* 43, (2024).
11. Yan, K. et al. The Comparable Microenvironment Shared by Colorectal Adenoma and Carcinoma: An Evidence of Stromal Proteomics. *Front Oncol* 12, 848782 (2022).
12. Che, R., Wang, Q., Li, M., Shen, J. & Ji, J. Quantitative Proteomics of Tissue-Infiltrating T Cells From CRC Patients Identified Lipocalin-2 Induces T-Cell Apoptosis and Promotes Tumor Cell Proliferation by Iron Efflux. *Molecular & Cellular Proteomics* 23, 100691 (2024).
13. Huang, P. et al. Spatial proteome profiling by immunohistochemistry-based laser capture microdissection and data-independent acquisition proteomics. *Anal Chim Acta* 1127, 140–148 (2020).
14. Wiśniewski, J. R. Filter Aided Sample Preparation – A tutorial. *Analytica Chimica Acta* 1090, 23–30 (2019).
15. Rappsilber, J., Mann, M. & Ishihama, Y. Protocol for micro-purification, enrichment, pre-fractionation and storage of peptides for proteomics using StageTips. *Nat Protoc* 2, 1896–1906 (2007).
16. Yu, F. et al. Analysis of DIA proteomics data using MSFragger-DIA and FragPipe computational platform. *Nat Commun* 14, 4154 (2023).
17. DIA-NN: neural networks and interference correction enable deep proteome coverage in high throughput | *Nature Methods*. <https://www.nature.com/articles/s41592-019-0638-x>.
18. MSstats Version 4.0: Statistical Analyses of Quantitative Mass Spectrometry-Based Proteomic Experiments with Chromatography-Based Quantification at Scale | *Journal of Proteome Research*. <https://pubs.acs.org/doi/10.1021/acs.jproteome.2c00834>.
19. Newman, A. M. et al. Determining cell type abundance and expression from bulk tissues with digital cytometry. *Nat Biotechnol* 37, 773–782 (2019).
20. Ulgen, E., Ozisik, O. & Sezerman, O. U. pathfindR: An R Package for Comprehensive Identification of Enriched Pathways in Omics Data Through Active Subnetworks. *Front. Genet.* 10, (2019).
21. Malonga, T., Vialaneix, N. & Beaumont, M. BEST4+ cells in the intestinal epithelium. *American Journal of Physiology-Cell Physiology* 326, C1345–C1352 (2024).
22. Schewe, M. et al. Secreted Phospholipases A2 Are Intestinal Stem Cell Niche Factors with Distinct Roles in Homeostasis, Inflammation, and Cancer. *Cell Stem Cell* 19, 38–51 (2016).
23. Yang, K. et al. Tumour suppressor ABCA8 inhibits malignant progression of colorectal cancer via Wnt/ β -catenin pathway. *Digestive and Liver Disease* 56, 880–893 (2024).
24. Li, R. et al. Single-cell transcriptomic analysis deciphers heterogenous cancer stem-like cells in colorectal cancer and their organ-specific metastasis. *Gut* 73, 470–484 (2024).
25. Defining the role of Lgr5+ stem cells in colorectal cancer: from basic research to clinical applications - PMC. <https://www.ncbi.nlm.nih.gov/pmc/articles/PMC5516356/>.
26. Shi, W.-K., Li, Y.-H., Bai, X.-S. & Lin, G.-L. The Cell Cycle-Associated Protein CDKN2A May Promotes Colorectal Cancer Cell Metastasis by Inducing Epithelial-Mesenchymal Transition. *Front. Oncol.* 12, (2022).
27. CTCF promotes colorectal cancer cell proliferation and chemotherapy resistance to 5-FU via the P53-Hedgehog axis - PMC. <https://www.ncbi.nlm.nih.gov/pmc/articles/PMC7485712/>.
28. Boardman, L. A. Overexpression of MACC1 leads to downstream activation of HGF/MET and potentiates metastasis and recurrence of colorectal cancer. *Genome Med* 1, 36 (2009).
29. Tang, J. et al. ARID3A promotes the development of colorectal cancer by upregulating AURKA. *Carcinogenesis* 42, 578–586 (2021).
30. Yu, J. et al. Comprehensive Analysis of the Expression and Prognosis for MMPs in Human Colorectal Cancer. *Front Oncol* 11, 771099 (2021).

31. Zhu, W. et al. SULF1 regulates malignant progression of colorectal cancer by modulating ARSH via FAK/PI3K/AKT/mTOR signaling. *Cancer Cell International* 24, 201 (2024).
32. Tao, Y., Han, T., Zhang, T. & Sun, C. Sulfatase-2 promotes the growth and metastasis of colorectal cancer by activating Akt and Erk1/2 pathways. *Biomedicine & Pharmacotherapy* 89, 1370–1377 (2017).
33. Che, G. et al. Sulfotransferase SULT2B1 facilitates colon cancer metastasis by promoting SCD1-mediated lipid metabolism. *Clinical and Translational Medicine* 14, e1587 (2024).
34. Ala, M. Tryptophan metabolites modulate inflammatory bowel disease and colorectal cancer by affecting immune system. *International Reviews of Immunology* 41, 326–345 (2022).
35. Li, T. et al. TGF- β 1-SOX9 axis-inducible COL10A1 promotes invasion and metastasis in gastric cancer via epithelial-to-mesenchymal transition. *Cell Death Dis* 9, 1–18 (2018).
36. Carvalho, A. et al. S100A12 in Digestive Diseases and Health: A Scoping Review. *Gastroenterology Research and Practice* 2020, 2868373 (2020).
37. Bertomeu, T. et al. A High-Resolution Genome-Wide CRISPR/Cas9 Viability Screen Reveals Structural Features and Contextual Diversity of the Human Cell-Essential Proteome. *Molecular and Cellular Biology* 38, e00302-17 (2018).
38. Gisina, A. et al. CEACAM5 overexpression is a reliable characteristic of CD133-positive colorectal cancer stem cells. *Cancer Biomark* 32, 85–98 (2021).
39. Zhao, D. et al. CEACAM6 expression and function in tumor biology: a comprehensive review. *Discov Onc* 15, 186 (2024).
40. Kasprzak, A. & Adamek, A. Insulin-Like Growth Factor 2 (IGF2) Signaling in Colorectal Cancer—From Basic Research to Potential Clinical Applications. *International Journal of Molecular Sciences* 20, 4915 (2019).
41. Drev, D. et al. Impact of Fibroblast-Derived SPARC on Invasiveness of Colorectal Cancer Cells. *Cancers* 11, 1421 (2019).
42. Huynh, P. T. et al. CD90+ stromal cells are the major source of IL-6, which supports cancer stem-like cells and inflammation in colorectal cancer. *International Journal of Cancer* 138, 1971–1981 (2016).
43. Li, M. et al. Proteomic analysis of stromal proteins in different stages of colorectal cancer establishes Tenascin-C as a stromal biomarker for colorectal cancer metastasis. *Oncotarget* 7, 37226–37237 (2016).
44. Giguelay, A. et al. The landscape of cancer-associated fibroblasts in colorectal cancer liver metastases. *Theranostics* 12, 7624–7639 (2022).
45. van der Flier, L. G., Haegbarth, A., Stange, D. E., van de Wetering, M. & Clevers, H. OLFM4 is a robust marker for stem cells in human intestine and marks a subset of colorectal cancer cells. *Gastroenterology* 137, 15–17 (2009).
46. Karim, B. O., Rhee, K.-J., Liu, G., Yun, K. & Brant, S. R. Prom1 function in development, intestinal inflammation, and intestinal tumorigenesis. *Front Oncol* 4, 323 (2014).
47. Liang, L. et al. GNG4 Promotes Tumor Progression in Colorectal Cancer. *Journal of Oncology* 2021, 9931984 (2021).
48. Zhou, H. & Rigoutsos, I. The emerging roles of GPRC5A in diseases. *Oncoscience* 1, 765–776 (2014).
49. Zhang X, Zhang H, Shen B, Sun XF. Chromogranin-A Expression as a Novel Biomarker for Early Diagnosis of Colon Cancer Patients. *Int J Mol Sci.* 2019 Jun 14;20(12), (2019).
50. Chen, L. et al. ITLN1 inhibits tumor neovascularization and myeloid derived suppressor cells accumulation in colorectal carcinoma. *Oncogene* 40, 5925–5937 (2021).
51. Zhou, H., Zhao, C., Shao, R., Xu, Y. & Zhao, W. The functions and regulatory pathways of S100A8/A9 and its receptors in cancers. *Front Pharmacol* 14, 1187741 (2023).
52. Schmid, F. et al. Calcium-binding protein S100P is a new target gene of MACC1, drives colorectal cancer metastasis and serves as a prognostic biomarker. *Br J Cancer* 127, 675–685 (2022).
53. Bauvois, B. & Susin, S. A. Revisiting Neutrophil Gelatinase-Associated Lipocalin (NGAL) in Cancer: Saint or Sinner? *Cancers* 10, 336 (2018).
54. Li, J. et al. Elastin is a key factor of tumor development in colorectal cancer. *BMC Cancer* 20, 217 (2020).
55. Sethi, M. K. et al. Quantitative proteomic analysis of paired colorectal cancer and non-tumorigenic tissues reveals signature proteins and perturbed pathways involved in CRC progression and metastasis. *J Proteomics* 126, 54–67 (2015).
56. Roncucci, L. et al. Myeloperoxidase-Positive Cell Infiltration in Colorectal Carcinogenesis as Indicator of Colorectal Cancer Risk. *Cancer Epidemiology, Biomarkers & Prevention* 17, 2291–2297 (2008).
57. Bottardi, S. et al. MNDA, a PYHIN factor involved in transcriptional regulation and apoptosis control in leukocytes. *Front. Immunol.* 15, (2024).
58. Urbiola-Salvador, V., Jabłońska, A., Miroszewska, D., Chen, Z. & Macur, K. Mass spectrometry proteomics characterization of plasma biomarkers for colorectal cancer associated with inflammation. *Biomarker Insights* 19, 11772719241257739 (2024).
59. Brdicka, T. et al. Phosphoprotein associated with glycosphingolipid-enriched microdomains (PAG), a novel ubiquitously expressed transmembrane adaptor protein, binds the protein tyrosine kinase csk and is involved in regulation of T cell activation. *J Exp Med* 191, 1591–1604 (2000).
60. Strazza, M., Azoulay-Alfaguter, I., Peled, M., Adam, K. & Mor, A. Transmembrane adaptor protein PAG is a mediator of PD-1 inhibitory signaling in human T cells. *Commun Biol* 4, 672 (2021).
61. Chen, S. et al. CD73: an emerging checkpoint for cancer immunotherapy. *Immunotherapy* 11, 983–997.
62. Wang, H. et al. Pumilio1 regulates NPM3/NPM1 axis to promote PD-L1-mediated immune escape in gastric cancer. *Cancer Letters* 581, 216498 (2024).
63. Nalio Ramos, R. et al. Tissue-resident FOLR2+ macrophages associate with CD8+ T cell infiltration in human breast cancer. *Cell* 185, 1189-1207.e25 (2022).

64. Bickeböllner, M. et al. Functional characterization of the tumor-suppressor MARCKS in colorectal cancer and its association with survival. *Oncogene* 34, 1150–1159 (2015).
65. Cherukuri, A. et al. B cell signaling is regulated by induced palmitoylation of CD81. *J Biol Chem* 279, 31973–31982 (2004).
66. Li, J., Chen, D. & Shen, M. Tumor Microenvironment Shapes Colorectal Cancer Progression, Metastasis, and Treatment Responses. *Front Med (Lausanne)* 9, 869010 (2022).
67. Petraki, C. et al. Evaluation and prognostic significance of human tissue kallikrein-related peptidase 6 (KLK6) in colorectal cancer. *Pathology - Research and Practice* 208, 104–108 (2012).
68. Vakrakou, A. et al. Kallikrein-related peptidase 6 (KLK6) expression in the progression of colon adenoma to carcinoma. *Biological Chemistry* 395, 1105–1117 (2014).
69. Sheng, Y. hua et al. MUC13 promotes the development of colitis-associated colorectal tumors via β -catenin activity. *Oncogene* 38, 7294–7310 (2019).
70. Wang, Y. et al. MAN2A1 predicts prognosis and progression through cancer-related pathways in colorectal cancer. *Transl Cancer Res* 11, 3686–3697 (2022).
71. Shen, D. et al. ADO/hypotaurine: a novel metabolic pathway contributing to glioblastoma development. *Cell Death Discov.* 7, 1–11 (2021).
72. Du, L. et al. High Vimentin Expression Predicts a Poor Prognosis and Progression in Colorectal Cancer: A Study with Meta-Analysis and TCGA Database. *BioMed Research International* 2018, 6387810 (2018).
73. Fan, D., Yang, M., Lee, H. J., Lee, J. H. & Kim, H. S. AVEN: a novel oncogenic biomarker with prognostic significance and implications of AVEN-associated immunophenotypes in lung adenocarcinoma. *Front. Mol. Biosci.* 10, (2023).
74. Ferguson, H. R., Smith, M. P. & Francavilla, C. Fibroblast Growth Factor Receptors (FGFRs) and Noncanonical Partners in Cancer Signaling. *Cells* 10, 1201 (2021).
75. Kobayashi, H. et al. The Origin and Contribution of Cancer-Associated Fibroblasts in Colorectal Carcinogenesis. *Gastroenterology* 162, 890–906 (2022).
76. Stalin, J. et al. Targeting of the NOX1/ADAM17 Enzymatic Complex Regulates Soluble MCAM-Dependent Pro-Tumorigenic Activity in Colorectal Cancer. *Biomedicines* 11, 3185 (2023).
77. Hope, C. et al. Versican-Derived Matrikines Regulate Batf3–Dendritic Cell Differentiation and Promote T Cell Infiltration in Colorectal Cancer. *The Journal of Immunology* 199, 1933–1941 (2017).
78. Hirani, P. et al. Versican Associates with Tumor Immune Phenotype and Limits T-cell Trafficking via Chondroitin Sulfate. *Cancer Research Communications* 4, 970–985 (2024).
79. de Souza Junior, D. A., Santana, A. C., da Silva, E. Z. M., Oliver, C. & Jamur, M. C. The Role of Mast Cell Specific Chymases and Trypsases in Tumor Angiogenesis. *BioMed Research International* 2015, 142359 (2015).
80. Atiakshin, D. et al. Carboxypeptidase A3—A Key Component of the Protease Phenotype of Mast Cells. *Cells* 11, 570 (2022).
81. West, L. C. & Cresswell, P. Expanding roles for GILT in immunity. *Curr Opin Immunol* 25, 103–108 (2013).
82. Guangwei, Z. et al. TRAF6 regulates the signaling pathway influencing colorectal cancer function through ubiquitination mechanisms. *Cancer Science* 113, 1393–1405 (2022).
83. Taylor, B. C. & Balko, J. M. Mechanisms of MHC-I Downregulation and Role in Immunotherapy Response. *Front. Immunol.* 13, (2022).
84. Lv, Y., Ma, X., Ma, Y., Du, Y. & Feng, J. A new emerging target in cancer immunotherapy: Galectin-9 (LGALS9). *Genes & Diseases* 10, 2366–2382 (2023).
85. Chen, X., Li, S., Long, D., Shan, J. & Li, Y. Rapamycin facilitates differentiation of regulatory T cells via enhancement of oxidative phosphorylation. *Cellular Immunology* 365, 104378 (2021).
86. DiScipio, R. G., Daffern, P. J., Schraufstatter, I. U. & Sriramarao, P. Human polymorphonuclear leukocytes adhere to complement factor H through an interaction that involves alphaMbeta2 (CD11b/CD18). *J Immunol* 160, 4057–4066 (1998).
87. Ostermann, G., Weber, K. S. C., Zernecke, A., Schröder, A. & Weber, C. JAM-1 is a ligand of the beta(2) integrin LFA-1 involved in transendothelial migration of leukocytes. *Nat Immunol* 3, 151–158 (2002).
88. Li, J. et al. Mature dendritic cells enriched in immunoregulatory molecules (mregDCs): A novel population in the tumour microenvironment and immunotherapy target. *Clinical and Translational Medicine* 13, e1199 (2023).
89. Mondanelli, G., Ugel, S., Grohmann, U. & Bronte, V. The immune regulation in cancer by the amino acid metabolizing enzymes ARG and IDO. *Current Opinion in Pharmacology* 35, 30–39 (2017).
90. Sieminska, I. & Baran, J. Myeloid-Derived Suppressor Cells in Colorectal Cancer. *Front. Immunol.* 11, (2020).
91. Wang, K. et al. SIRT5 Contributes to Colorectal Cancer Growth by Regulating T Cell Activity. *Journal of Immunology Research* 2020, 3792409 (2020).
92. Mo, J. et al. The early predictive effect of low expression of the ITGA4 in colorectal cancer. *J Gastrointest Oncol* 13, 265–278 (2022).
93. Pelka, K. et al. Spatially organized multicellular immune hubs in human colorectal cancer. *Cell* 184, 4734–4752.e20 (2021).
94. Gu, Q. et al. CCL19: a novel prognostic chemokine modulates the tumor immune microenvironment and outcomes of cancers. *Aging (Albany NY)* 15, 12369–12387 (2023).
95. Thompson, E. J. et al. Abstract 5545: Assessing LGR5 expression levels on colorectal cancer tissue samples for use in LGR5-targeting CAR-T cell therapy clinical trial. *Cancer Research* 83, 5545 (2023).
96. Zygoń, J., Szajewski, M., Kruszewski, W. J. & Rzepko, R. VEGF, Flt-1, and microvessel density in primary tumors as predictive factors of colorectal cancer prognosis. *Molecular and Clinical Oncology* 6, 243–248 (2017).

97. LAGOU, S., GRAPSA, D., SYRIGOS, N. & BAMIAS, G. The Role of Decoy Receptor DcR3 in Gastrointestinal Malignancy. *Cancer Diagn Progn* 2, 411–421 (2022).
98. Thomadaki, H. & Scorilas, A. BCL2 Family of Apoptosis-Related Genes: Functions and Clinical Implications in Cancer. *Critical Reviews in Clinical Laboratory Sciences* 43, 1–67 (2006).
99. Halama, N. et al. Natural Killer Cells are Scarce in Colorectal Carcinoma Tissue Despite High Levels of Chemokines and Cytokines. *Clinical Cancer Research* 17, 678–689 (2011).
100. Balakrishnan, A., Marathe, S. A., Joglekar, M. & Chakravorty, D. Bactericidal/permeability increasing protein: A multifaceted protein with functions beyond LPS neutralization. *Innate Immun* 19, 339–347 (2013).
101. Schultz, H. & Weiss, J. P. The bactericidal/permeability-increasing protein (BPI) in infection and inflammatory disease. *Clin Chim Acta* 384, 12–23 (2007).
102. Pio, R., Ajona, D., Ortiz-Espinosa, S., Mantovani, A. & Lambris, J. D. Complementing the Cancer-Immunity Cycle. *Front. Immunol.* 10, (2019).
103. Putro, E. et al. New Insight into Intestinal Mast Cells Revealed by Single-Cell RNA Sequencing. *International Journal of Molecular Sciences* 25, 5594 (2024).
104. Yu, M. et al. CD73 on cancer-associated fibroblasts enhanced by the A2B-mediated feedforward circuit enforces an immune checkpoint. *Nat Commun* 11, 515 (2020).
105. Knuchel, S., Anderle, P., Werfelli, P., Diamantis, E. & Rüegg, C. Fibroblast surface-associated FGF-2 promotes contact-dependent colorectal cancer cell migration and invasion through FGFR-SRC signaling and integrin $\alpha\beta 5$ -mediated adhesion. *Oncotarget* 6, 14300–14317 (2015).
106. Matsuda, Y., Ueda, J. & Ishiwata, T. Fibroblast Growth Factor Receptor 2: Expression, Roles, and Potential As a Novel Molecular Target for Colorectal Cancer. *Pathology Research International* 2012, 574768 (2012).
107. Song, X. et al. Growth Factor FGF2 Cooperates with Interleukin-17 to Repair Intestinal Epithelial Damage. *Immunity* 43, 488–501 (2015).
108. Honkala, A. T., Tailor, D. & Malhotra, S. V. Guanylate-Binding Protein 1: An Emerging Target in Inflammation and Cancer. *Front. Immunol.* 10, (2020).
109. Forster, F. et al. Guanylate binding protein 1-mediated interaction of T cell antigen receptor signaling with the cytoskeleton. *J Immunol* 192, 771–781 (2014).
110. Zhang, R., Kang, R. & Tang, D. Ferroptosis in gastrointestinal cancer: from mechanisms to implications. *Cancer Letters* 561, 216147 (2023).
111. Kruzel, M. L., Zimecki, M. & Actor, J. K. Lactoferrin in a Context of Inflammation-Induced Pathology. *Front. Immunol.* 8, (2017).
112. Manna, G. L. et al. Neutrophil Gelatinase-Associated Lipocalin Increases HLA-G+/FoxP3+ T-Regulatory Cell Population in an In Vitro Model of PBMC. *PLOS ONE* 9, e89497 (2014).
113. Zhu, W., Li, M., Wang, Q., Shen, J. & Ji, J. Quantitative Proteomic Analysis Reveals Functional Alterations of the Peripheral Immune System in Colorectal Cancer. *Molecular & Cellular Proteomics* 23, (2024).
114. Hazini, A., Fisher, K. & Seymour, L. Deregulation of HLA-I in cancer and its central importance for immunotherapy. *J Immunother Cancer* 9, e002899 (2021).
115. Xiang, C. et al. Single-cell profiling reveals the trajectory of FOLR2-expressing tumor-associated macrophages to regulatory T cells in the progression of lung adenocarcinoma. *Cell Death Dis* 14, 1–12 (2023).
116. Rausch, M. P. et al. GILT in Thymic Epithelial Cells Facilitates Central CD4 T Cell Tolerance to a Tissue-Restricted, Melanoma-Associated Self-Antigen. *J Immunol* 204, 2877–2886 (2020).
117. Rausch, M. P. & Hastings, K. T. GILT modulates CD4+ T-cell tolerance to the melanocyte differentiation antigen tyrosinase-related protein 1. *J Invest Dermatol* 132, 154–162 (2012).
118. Li, L. et al. IFI30 as a key regulator of PDL1 immunotherapy prognosis in breast cancer. *Int Immunopharmacol* 133, 112093 (2024).
119. Arner, E. N. & Rathmell, J. C. Metabolic programming and immune suppression in the tumor microenvironment. *Cancer Cell* 41, 421–433 (2023).
120. Hamaidi, I. et al. Sirt2 Inhibition Enhances Metabolic Fitness and Effector Functions of Tumor-Reactive T Cells. *Cell Metabolism* 32, 420–436.e12 (2020).
121. Cao, T. et al. Cancer SLC6A6-mediated taurine uptake transactivates immune checkpoint genes and induces exhaustion in CD8+ T cells. *Cell* 187, 2288–2304.e27 (2024).
122. Yasunaga, M. & Matsumura, Y. Role of SLC6A6 in promoting the survival and multidrug resistance of colorectal cancer. *Sci Rep* 4, 4852 (2014).
123. Mariani, F. & Roncucci, L. Role of the Vanins–Myeloperoxidase Axis in Colorectal Carcinogenesis. *International Journal of Molecular Sciences* 18, 918 (2017).
124. Miyoshi, K. et al. CD15+ Bone Marrow-derived Cells Are Regulators of Immune Response in ARG1-producing Colorectal Cancer Cells. *Anticancer Research* 42, 459–470 (2022).
125. Ma, Z. et al. Overexpression of Arginase-1 is an indicator of poor prognosis in patients with colorectal cancer. *Pathology - Research and Practice* 215, 152383 (2019).
126. Elomaa, H. et al. Quantitative Multiplexed Analysis of Indoleamine 2,3-Dioxygenase (IDO) and Arginase-1 (ARG1) Expression and Myeloid Cell Infiltration in Colorectal Cancer. *Modern Pathology* 37, 100450 (2024).

127. Li, K. et al. Identification and expression of a new type II transmembrane protein in human mast cells. *Genomics* 86, 68–75 (2005).
128. Choi, Y. J. et al. Lung-specific MCEMP1 functions as an adaptor for KIT to promote SCF-mediated mast cell proliferation. *Nat Commun* 14, 2045 (2023).
129. Cy, P. et al. Mast-cell expressed membrane protein-1 is expressed in classical monocytes and alveolar macrophages in idiopathic pulmonary fibrosis and regulates cell chemotaxis, adhesion, and migration in a TGF β -dependent manner. *American journal of physiology. Cell physiology* 326, (2024).
130. Chen, J.-X., Xu, X. & Zhang, S. Silence of long noncoding RNA NEAT1 exerts suppressive effects on immunity during sepsis by promoting microRNA-125-dependent MCEMP1 downregulation. *IUBMB Life* 71, 956–968 (2019).
131. Wang, Z. & Zhang, J. FOXP3 promotes colorectal carcinoma liver metastases by evaluating MMP9 expression via regulating S-adenosylmethionine metabolism. *Ann Transl Med* 8, 592 (2020).
132. Hu, G., Sun, N., Jiang, J. & Chen, X. Establishment of a 5-gene risk model related to regulatory T cells for predicting gastric cancer prognosis. *Cancer Cell International* 20, 433 (2020).

10. Publication V: Plasma protein changes reflect colorectal cancer development and associated inflammation

Published: (2023) *Frontiers in oncology*, 13, 1158261. <https://doi.org/10.3389/fonc.2023.1158261>

Authors: Urbiola-Salvador V, Jabłońska A, Miroszewska D, Huang Q, Duzowska K, Drężek-Chyta K, Zdrenka M, Śrutek E, Szylberg Ł, Jankowski M, Bała D, Zegarski W, Nowikiewicz T, Makarewicz W, Adamczyk A, Ambicka A, Przewoźnik M, Harazin-Lechowicz A, Ryś J, Filipowicz N, Piotrowski A, Dumanski JP, Li B, Chen Z.

10.1. Introduction

Colorectal cancer (CRC) is the third most common malignancy and the second most lethal cancer, causing 935,000 cancer-related deaths in 2020 (1). CRC prognosis depends mainly on the tumor stage, location, and time of detection. However, despite the huge progress in cancer research, a large number of CRC cases are diagnosed at the advanced stage where cancers are aggressive, malignant, and metastatic (2).

Currently, the most commonly used diagnostic tools for CRC screening and prevention include colonoscopy and flexible sigmoidoscopy, as well as the guaiac-based fecal occult blood test or the immunochemical fecal occult blood test, also known as the fecal immune test (3). These traditional stool-based tests have low sensitivity and specificity (4), while colonoscopy and sigmoidoscopy, despite the high sensitivity, have relatively low compliance, high cost, and are invasive which limits their efficacy in population screening programs (5). Therefore, alternative, non-invasive, and efficient screening strategies to improve the early detection of cancers are urgently needed. Until now, several potential blood-based protein biomarkers for CRC screening and cancer prevention have been reported, including methylated Septin9 (6), extracellular vesicle microRNAs (7), and cell-free circulating DNA (8), but all lack the sensitivity and/or specificity for use as a stand-alone marker.

Advances in proteomic-based technologies in the last decade have expanded the number of candidate biomarkers and led to a better comprehension of the CRC progression as well as the identification and characterization of related molecular signatures. The most recent advancement of Proximity Extension Assay (PEA) allows the quantification of over 3,000 proteins from low amounts of a sample by the combination of DNA-conjugated antibodies and next generation sequencing (9). Application of the PEA technology has led to the identification of carcinoembryonic antigen (CEA) as one of the best-studied blood-based prognostic biomarkers used in clinical practice (10–12). CEA is expressed in the embryonic endodermal epithelium, colorectal cancer, and other malignancies, such as inflammatory bowel disease (IBD), peptic ulcer, and pancreatitis (13). CEA is a promising plasma biomarker for the detection of CRC with high specificity and sensitivity (12, 14), however, due to the limited organ specificity (15), it is not the best sole biomarker for population based screening, yet it might be useful in CRC recurrence monitoring

(16) and metastasis (17). Currently, the trend in biomarkers discovery is to focus on the biomarker panels rather than on a single-target protein as the broader spectrum of the analysis may help to address the cancer prognosis and detection more precisely.

It was recently reported that two various multimarker panels consisting of five circulating proteins might be used as an efficient tool for the early and late-stage detection of CRC, including advanced adenomas, or in the prediction of overall survival in Germany and Chinese cohorts (18, 19). In a recent study, Harlid et al. (2021) showed that fibroblast growth factor 21 (FGF21) was associated with early, but not late stages of colon cancer, while pancreatic prohormone (PPY) was a promising biomarker for rectal cancer detection (20). However, neither FGF21 nor PPY could be used as stand-alone biomarkers for colon or rectal cancer but might be used as an efficient tool to discriminate between different subtypes of CRC. Therefore, there

is an urgent need for the identification of a reliable blood-based biomarker panel that would detect the early stages of CRC as well as assesses the prognosis at the population-based screening.

Both chronic inflammation, such as IBD, and sporadic, cancer associated inflammation are well-known as key factors in CRC progression and development. Inflammation alters the communication between a variety of cell types, including innate and adaptive immune cells, epithelial cells, and stem cells. These intricate networks of cytokines, growth factors, receptors, and other molecules interaction result in either a tumor-promoting or inhibiting environment (21). Thus, in the development of plasma biomarkers for CRC diagnosis, prognosis, and immunotherapy, the inflammatory status is essential.

The purpose of our study was to identify the protein expression changes in the plasma of CRC patients compared to healthy controls as well as between the early and late stages of CRC and inflammatory status. Therefore, an inflammation panel including 368 proteins was selected to be detected in this study. We hypothesized that CRC development, tumor stage, and inflammation-caused changes in protein level will be reflected in the circulating blood and as such, we would be able to obtain a panel of biomarkers with potential translation into clinics to improve patient care. In this study, we quantified the plasma protein profiles derived from 38 CRC patients and their age- and sex-matched 38 healthy subjects using the PEA technology and protein panels consisting of 368 oncology- and 368 inflammation-related protein biomarker candidates. We quantified 690 proteins, among which 78 differentially expressed proteins (DEPs), were elevated and 124 DEPs were reduced in patients with CRC. We found protein signatures associated with cytokine interactions, oncogenic signalling pathways, exacerbated apoptosis, as well as metabolism reprogramming. Additionally, we determined protein changes linked to cancer-associated inflammation and novel potential prognostic biomarkers associated with tumor stages. Linear regression model analysis revealed that carbonic anhydrase (CA11), a cluster of differentiation 276 (CD276), colony-stimulating factor 3 (CSF3), and interleukin 12 receptor subunit beta 1 (IL12RB1), were positively associated with inflammatory status, whilst amyloid beta precursor protein binding family B member 1 interacting protein (APBB1IP) and C-X-C motif chemokine ligand 6 (CXCL6) were negatively associated. Moreover, linear regression model analysis of tumor stage indicated high plasma levels of Fms-related tyrosine kinase 4 (FLT4), MANSC domain-containing protein 1 (MANSC1), and lysophosphatidic acid (LPA) phosphatase type 6 (ACP6), that could be used as potential prognostic biomarkers for advanced CRC. In contrast, high levels of interferon γ (IFNG), interleukin (IL)32, and IL17C in early CRC stages indicate that these proteins can discriminate between early and late stages, patients. Validation of these identified plasma protein changes with larger cohorts will facilitate the identification of potential novel diagnostic, prognostic biomarkers for CRC.

10.2. Methods

10.2.1. Study cohort

The study was retrospective and consisted of 38 patients who underwent CRC surgery (mean age: 66.7 ± 12.3 ; 42.1% male) between June 2019 and April 2021 and 38 age- and sex-matched healthy subjects. All CRC patients had a positive colonoscopy and pathology-confirmed malignant neoplasm of the rectum or colon. Among them, 63.2% (24/38) were diagnosed with late-stage CRC (III-IV) according to the Union for International Control TNM classification and 28.9% (11/38) had inflammation according to the pathologist assessment (Table 11.1). Samples collected from CRC patients and healthy subjects were obtained from the 3P-Medicine Laboratory, Medical University of Gdansk (22) and Biobank HARC, Medical University of Lodz, respectively. In order to validate the assay in an independent cohort, serum samples from 41 patients who underwent CRC surgery (mean age: 58.9 ± 10.1 ; 43.9% male) were obtained from the Bank of Biological Material at Masaryk Memorial Cancer Institute, Czech Republic. Supported by the project BBMRI.cz no. LM2023033. Whole blood samples were collected into sterile BD Vacutainer® K2EDTA tubes

during the day of the planned CRC resection, centrifuged, aliquoted plasma and serum, and stored at -80°C until use.

10.2.2. Protein profiling

Plasma proteins were analyzed using the multiplex PEA technology (Olink® Explore 384-Oncology and -Inflammation panel, Olink Proteomics, Uppsala, Sweden) (Supplementary Tables 1 and 2). Briefly, the PEA technology is a dual recognition approach based on matched pairs of oligonucleotide-labeled antibodies that bind to their target proteins. Once the target proteins are bound, the oligonucleotides brought into proximity, hybridize and are detected and quantified by using next-generation sequencing (9.20). PEA quantifies a large number of proteins (> 3,000) with good precision, using a minimal volume of plasma or serum samples, and without loss of specificity and sensitivity. The protein levels are presented in the normalized protein expression (NPX) values on a log2 scale. A high protein concentration corresponds to a high NPX value. For quality assessment and validation of the PEA technology, the protein level of ACP6 was measured by ELISA, while for CSF3, IFNG, IL6, CXCL9, and CCL23 were determined by using Luminex MAGPIX technology.

TABLE 10.1 Clinical characteristics of patients with CRC.

Patient	Age	Sex	Tumor stage	Inflammatory status
P1	49	F	Late	+
P2	77	F	Late	+
P5	71	M	Late	+
P6	77	F	Early	+
P7	85	F	Early	+
P9	72	M	Late	+
P10	62	M	Late	+
P11	56	F	Early	+
P12	80	M	Late	+
P13	38	F	Early	+
P14	89	F	Late	-
P15	73	F	Early	-
P16	76	F	Early	-
P17	42	M	Late	-
P18	61	M	Early	-
P19	62	F	Early	-
P20	76	M	Late	-
P21	56	F	Late	+
P22	50	F	Late	-
P23	42	M	Late	-
P24	53	F	Late	-
P25	75	M	Early	-
P27	60	M	Late	-
P28	63	F	Early	-
P29	67	F	Late	-
P30	83	M	Late	-
P31	73	M	Late	-
P32	63	M	Late	-
P35	73	F	Early	-
P36	64	F	Early	-
P37	68	F	Late	-
P38	61	M	Early	-
P39	80	M	Late	-
P40	77	F	Early	-
P41	73	F	Late	-
P42	63	F	Late	-
P43	79	F	Late	-
P44	67	M	Late	-

F, female; M, male; Early (I and II stages); Late (III and IV stages); -, non-inflammation; +, inflammation.

10.2.3. Statistical analyses

Almost all statistical analyses were performed in RStudio (version 1.3.1093) using R (version 4.0.3). First, proteins were filtered when the quality control was negative or the calculated NPX values were below the respective protein limit of detection (LOD) in at least 50% of samples from one of the study groups. The remaining NPX values below the LOD were imputed with the respective $LOD/\sqrt{2}$. Moderated t-test from the R package “limma” (version 3.46.0) was used to test differential protein abundance between CRC patients and healthy subjects. Additional analysis was performed using the general linear model regression approach with analysis of contrasts using the R package “emmeans” (version 1.6.2.1). A general linear model was fitted to the expression of each protein in all CRC patients using tumor stage and inflammation as independent variables, and sex as a confounding factor. The false discovery rate (FDR) was determined using the Benjamini & Hochberg correction. Proteins were considered differentially expressed when FDR adjusted p -value < 0.05. The built-in R function `cor.test` was used to calculate the point-biserial correlation between protein expression and tumor stage or inflammation status, the p -value < 0.05 was considered significant. Gene set enrichment analysis with Gene Ontology terms was performed using ClusterProfiler (version 4.6.0), while Kyoto Encyclopedia of Genes and Genomes (KEGG) pathway enrichment analysis *via* active subnetworks from STRING database was conducted using “pathfindR” (version 1.6.3), with FDR < 0.05. “ggplot2” (version 3.3.5) was used for graphics generation, excluding heatmaps that were generated using “ComplexHeatmap” (version 2.6.2). The hierarchical clustering (Euclidean distance) was implemented to visualize the patterns of DEPs among samples after the z-score transformation of NPX values; DEPs were split by k-means clustering. T test was used for the calculation of continuous variables (protein levels) by using GraphPad Prism version 9.0 (GraphPad Software Inc., San Diego, CA, USA).

10.3. Results

10.3.1. CRC development causes cytokine and oncogenic signaling pathway changes in plasma

To determine the changes in the protein profiles in peripheral blood caused by CRC development, we performed plasma protein analysis by using PEA technology. Out of the total 736 proteins from the Inflammation and Oncology Explore panels, after removing repetitions in the panels and after removal of proteins with low detection rates among the samples, 690 proteins were quantified. Among them, 78 proteins were elevated and 124 were reduced in the 38 CRC patients compared with their age- and sex-matched healthy controls (Figure 10.1A, Supplementary Figure 10.1A, and Supplementary Table 11.3). Of the elevated DEPs, dipeptidase 2 (DPEP2), hydroxyacylglutathione hydrolase (HAGH), and agouti-related neuropeptide (AGRP) as well as downregulated DEPs as neutrophil cytosolic factor 2 (NCF2), epidermal growth factor-like protein 7 (EGFL7), and ectonucleotide pyrophosphatase/phosphodiesterase family member 5 (ENPP5) were the DEPs with the most statistical difference. In line with previous studies which were carried out with different technologies for protein detection and quantification (17,23-28), high plasma levels of AGRP, FGF21, midkine (MDK), C-C motif chemokine ligand 20 (CCL20), IL6, and CSF3 as well as reduced ribonucleotide reductase regulatory TP53 inducible subunit M2B (RRM2B) on plasma level of CRC patients were also identified in our study. Importantly, we found novel protein changes including high levels of oncogenic proteins such as R-Spondin 3 (RSPO3) and secernin 1 (SCRN1) as well as low levels of tumor suppressors such as Ret proto-oncogene (RET) and Rho guanine nucleotide exchange factor 12 (ARHGEF12) in CRC patients. These results suggest the association between plasma protein levels and protein expression within the tumor microenvironment (TME).

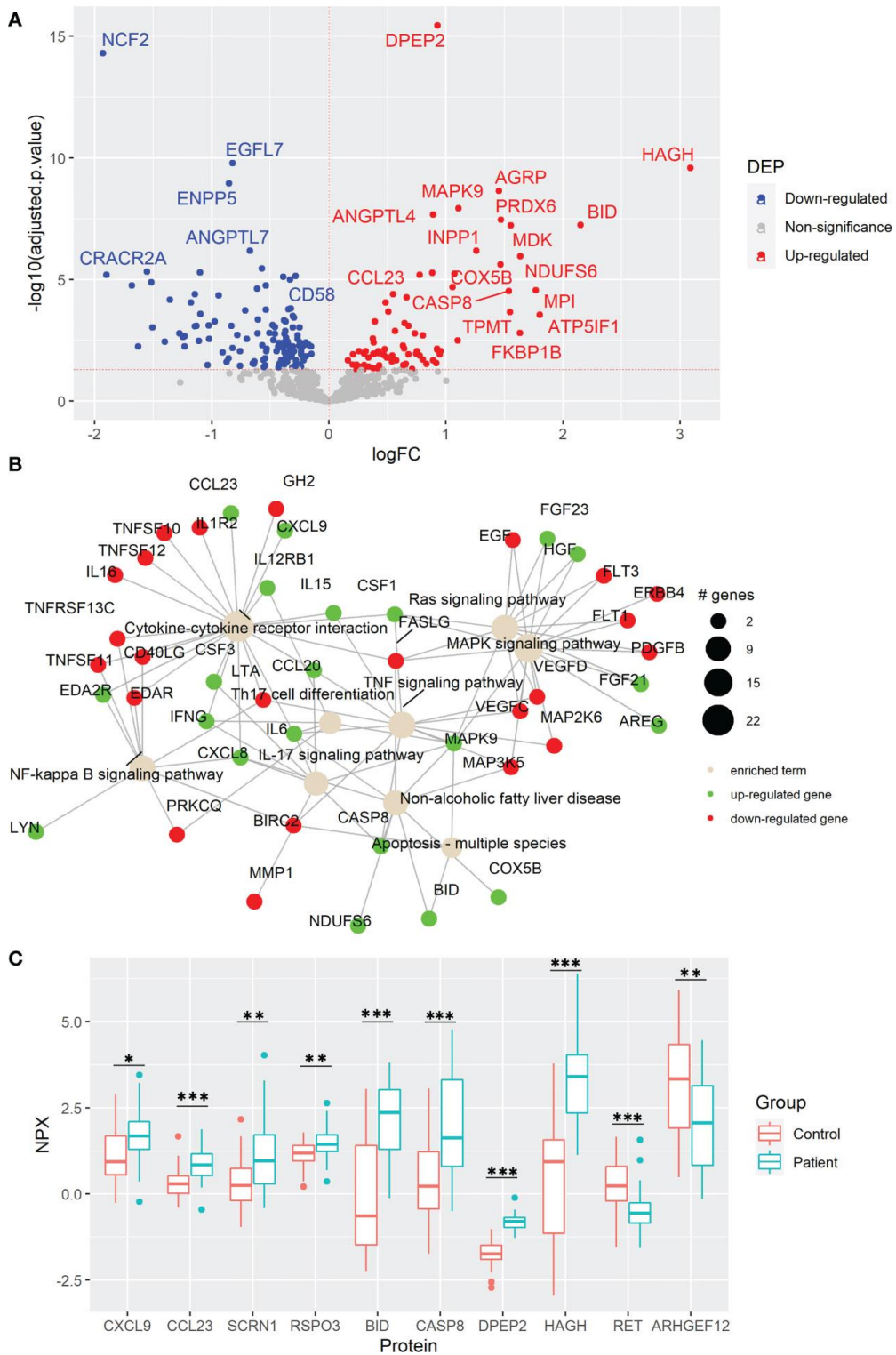


Figure 10.1 Colorectal cancer (CRC) development causes cytokine and oncogenic signaling pathway changes in plasma. (A) Volcano plot of statistical significance against fold-change of proteins between CRC patients and healthy controls. Dots indicate individual proteins and the red and blue dots represent significant up-regulation and down-regulation in patients, respectively. (B) Network of KEGG pathway enrichment analysis combined with STRING protein-protein interaction network analysis. Green and red proteins indicate significant up-regulation and down-regulation, respectively. (C) Box and whisker plots of selected DEPs not previously reported associated with CRC. * indicates statistically significant with an adjusted p-value < 0.05, ** indicates an adjusted p-value < 0.01, and *** indicates an adjusted p-value < 0.001. DEP, differentially expressed protein; FC, fold change, NPX; normalized protein expression.

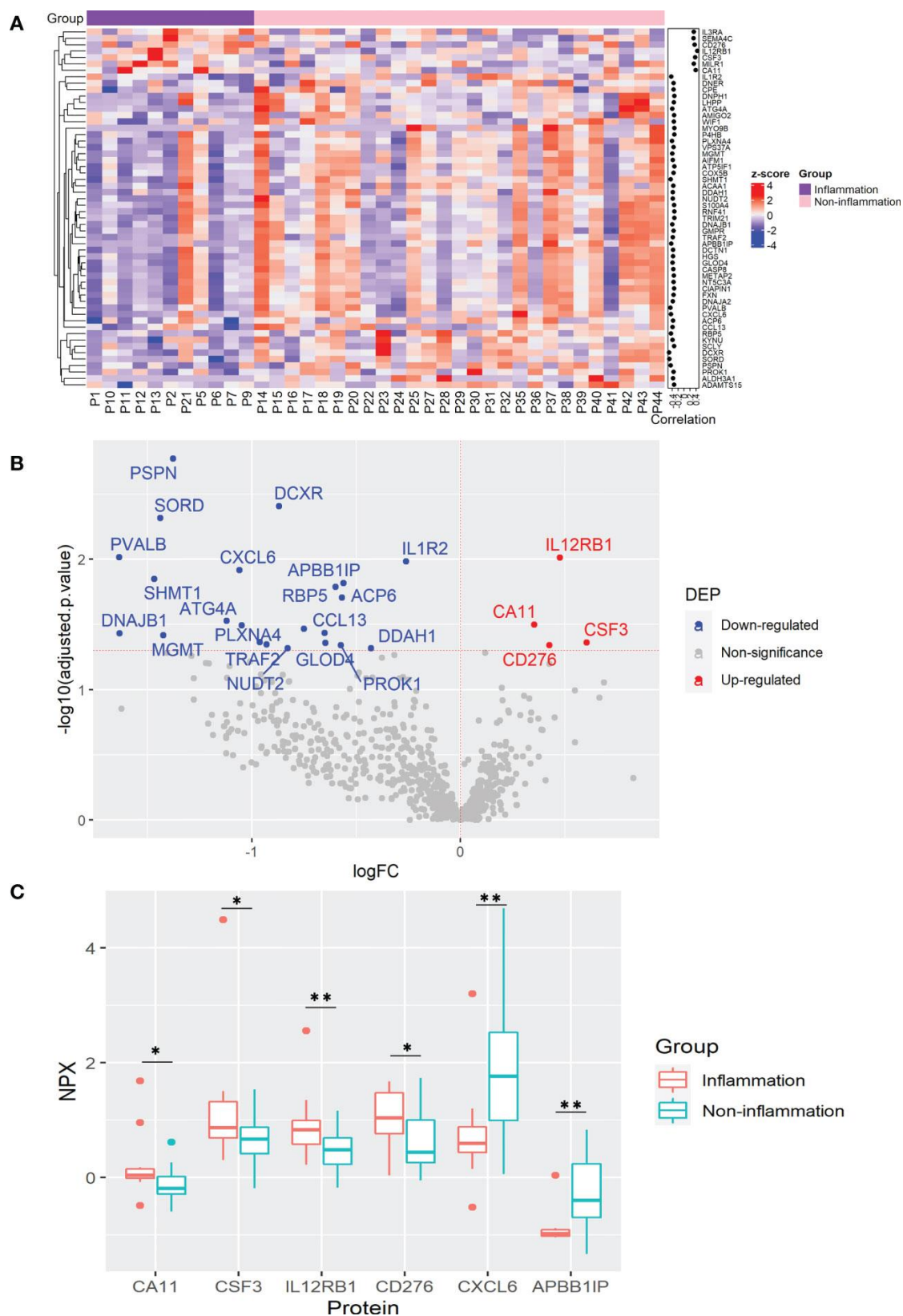
To investigate the involved pathways and the complex protein-protein interactions among these DEPs, KEGG enrichment analysis *via* active subnetworks was performed. Plasma protein changes were mainly associated with the cytokine-cytokine receptor interaction, including high plasma level of T-cell chemoattracting chemokine CXCL9 and the immune cell chemoattractant CCL23, as well as several signalling pathways including mitogen-activated protein kinase (MAPK), resistance to audiogenic seizures (Ras), tumor necrosis factor (TNF), nuclear factor kappa B (NF- κ B), and IL17 signalling pathways (Figures 11.1B, C, and Supplementary Table 4). Notably, proteins involved in Th17 cell differentiation were upregulated in CRC patients, suggesting an active role of this T-cell helper subtype in CRC development. Moreover, proteins related to non-fatty liver disease (NAFLD), a disease previously associated with CRC risk(29), were enriched (Figure 10.1B and Supplementary Tables 10.3, 10.4). At the same time, high levels of apoptosis-associated proteins, caspase-8 (CASP8) and BH3 interacting domain death agonist (BID) were discovered, with BID having the second highest fold change in the comparison (Figures 11.1A–C). To reveal possible mechanisms of cancer development, DEPs were further evaluated by using gene set enrichment analysis. This analysis revealed that the gene ontology terms including oxidative phosphorylation, aerobic respiration, respiratory electron transport chain, and ATP synthesis coupled electron transport in mitochondria were enriched in CRC patients (Appendix IV Supplementary Figure 1B and Appendix IV Supplementary Table5). Moreover, other metabolic proteins were highly elevated in CRC patients including HAGH and DPEP2 (Figure 10.1C) which may reflect the metabolism reprogramming due to CRC tumorigenesis, a well-known hallmark of cancer (30).

Next, to distinguish which of the protein changes were a consequence of an altered secretion from a certain type of cells and which were a result of destructed tissues or cells released during CRC tumorigenesis, from the 202 DEPs, 50 proteins were identified in the human blood secretome from Human Protein Atlas, including cytokines that modulate the immune responses within the TME, such as IFNG, IL6, IL15, CCL20, CXCL9, and CCL23 (Appendix IV Supplementary Table 6). Some of these cytokines were previously found with high plasma levels in CRC such as pro-inflammatory cytokine IL6 which is also required for Th17 differentiation (26), the pro-inflammatory MDK involved in multiple biological processes (17), and the chemoattractant of B- and T-cells CCL20 (25), whereas the detected IFNG is a well-recognized pro-inflammatory and antitumorigenic protein (31). Interestingly, the elevated plasma levels of the chemoattractant CXCL9 and CCL23 in CRC patients were reported for the first time in our study. These results suggest that plasma protein changes can reflect the variety of altered processes involved in tumorigenesis. Collectively, CRC development causes protein changes in plasma that are linked to several signalling pathways, cytokine interactions of underlying immune responses, and altered metabolism.

10.3.2. Cancer-associated inflammation alters the plasma protein expression in CRC patients

It is well-known that chronic inflammation may contribute to cancer development. To determine plasma protein changes related to inflammatory status in CRC patients, we analyzed DEPs among patients with and without inflammation (11 and 27 cases, respectively). Correlation analysis revealed 56 proteins significantly correlated with inflammation, among which 7 proteins, CA11, CD276, CSF3, IL3RA, IL12RB1, MILR1, and SEMA4C were positively correlated, while 46 proteins including ACP6, APBB1IP, CXCL6, and dicarbonyl and L-xylulose reductase (DCXR) were correlated negatively (Figure 10.2A and Appendix IV Supplementary Table 7). Among them, elevated IL12RB1 and reduced DCXR showed the highest correlation with inflammatory status (Figure 10. 2A and Appendix IV Supplementary Table 7). To confirm the association between protein expression and inflammation, a linear regression analysis was used to determine the differential expression of these proteins. As a result, 26 DEPs were identified which were significantly correlated in the previous analysis (Figure 10.2B and Appendix IV Supplementary Table 8).

Figure



10.2 Plasma protein changes induced by cancer-associated inflammation in CRC patients. (A) Heatmap of proteins with significant correlation with inflammation status. Protein expression is transformed with a z-score by row normalization and distributed by hierarchical clustering. The correlation coefficients (right) indicate a positive/negative correlation for each protein. (B) Volcano plot of statistical significance against fold-change of proteins between CRC patients with inflammation and without inflammation. Dots indicate individual proteins and the red and blue dots represent significant up-regulation and down-regulation in CRC patients with inflammation, respectively. (C) Box and whisker plots of selected DEPs not previously associated with cancer-related inflammation in CRC patients. *: adjusted p-value < 0.05, **: adjusted p-value < 0.01.

KEGG pathway enrichment analysis demonstrated that the DEPs were mainly assigned to cytokine-cytokine interaction, IL17 and Th17 cell differentiation, and Janus kinase (JAK)-signal transducer and activator of transcription (STAT) signalling pathways, as well as pentose and glucuronate conversion (Appendix IV Supplementary Table 9). It has been well documented that Th17 cells play an essential role in inflammation *via* the production of pro-inflammatory cytokines IL17A, IL17F, IL22, and IL21. Th17 cell activity is also associated with an increased risk of CRC tumorigenesis(32). Among the DEPs involved in the IL17, Th17 cell differentiation and JAK-STAT signalling pathways, elevated levels of CSF3 and reduced CXCL6 were previously found in the serum of CRC patients(27,33), while our study also demonstrates their association with cancer-associated inflammation (Figures 10.2A–C). Interestingly, CSF3 is involved in inflammation by inducing bone-marrow neutrophil differentiation and its high levels are related to CRC tumorigenesis (27). Moreover, we report, for the first time, the association of IL12RB1, CA11, CD276, and APBB1IP with cancer-associated inflammation (Figure 10.2C). Accordingly, IL12RB1 and CSF3 were detected with high plasma levels in the whole CRC patients compared with healthy controls (Figure 10.1A and Appendix IV Supplementary Table 3). It is worth noting that IL12RB1, CD276, and APBB1IP are involved in cancer surveillance, inhibition of T-cell mediated responses, and T-cell recruitment, respectively(34-36), whereas CA11 may induce proliferation and invasion of gastrointestinal tumors (37) (Figure 10.2C). In summary, these results suggest that inflammation in CRC patients can influence plasmatic protein levels. Furthermore, these proteins may be useful indicators of cancer-associated inflammation that may complicate the outcome of CRC patients.

10.3.3.Determination of potential plasma biomarkers associated with CRC stages

The main cause of a patient's death due to CRC is tumor growth and its increased invasiveness, resulting in metastasis. Therefore, it is crucial to find prognostic biomarkers for CRC progression. We determined the plasma protein changes associated with CRC advance by the comparison of patients with early (I and II) and late (III and IV) stages of CRC. The correlation analysis showed that 13 proteins, ACP6, CCL23, C-type lectin domain family 4 member G (CLEC4G), FLT4, IL1R2, IL6, MANSC1, marginal zone B and B1 cell-specific protein (MZB1), S100 calcium-binding protein A12 (S100A12), secretoglobin family 1A member 1 (SCGB1A1), SPARC-related modular calcium-binding protein 2 (SMOC2), thioredoxin domain containing 15 (TXNDC15), and WAP, follistatin/kazal, immunoglobulin, kunitz and netrin domain containing 2 (WFIKKN2) were positively correlated with tumor stage, whereas 7 proteins, including IFNG, IL32, integrin subunit alpha 11 (ITGA11), ITGAV, selectin P ligand (SELPLG), trefoil factor 2 (TFF2), and transmembrane serine protease 15 (TMPRSS15) were correlated negatively (Figure 10.3A). Among them, FLT4 showed the best prognostic performance for late-stage CRC with the highest correlation coefficient (Figure 10.3A and Supplementary Table 10.10). The elevated plasma FLT4, also named Vascular Endothelial Growth Factor Receptor 3 (VEGFR3) in the late stage of CRC may be associated with VEGF-mediated lymphangiogenesis and angiogenesis. Similarly to the analysis with inflammatory status, the regression analysis resulted in fewer DEPs than correlated proteins. This analysis revealed that ACP6, FLT4, and MANSC1 were elevated in the late stages of CRC, while IL17C, IL32, and IFNG were elevated in the early stages (Figures 11.3B, C, and Appendix IV Supplementary Table 11). Notably, the enzyme ACP6 which is involved in phospholipid metabolism by hydrolysis of LPA was negatively associated with inflammatory status, suggesting that ACP6 may play a role in both inflammation and CRC progression (Figure 10.3D).

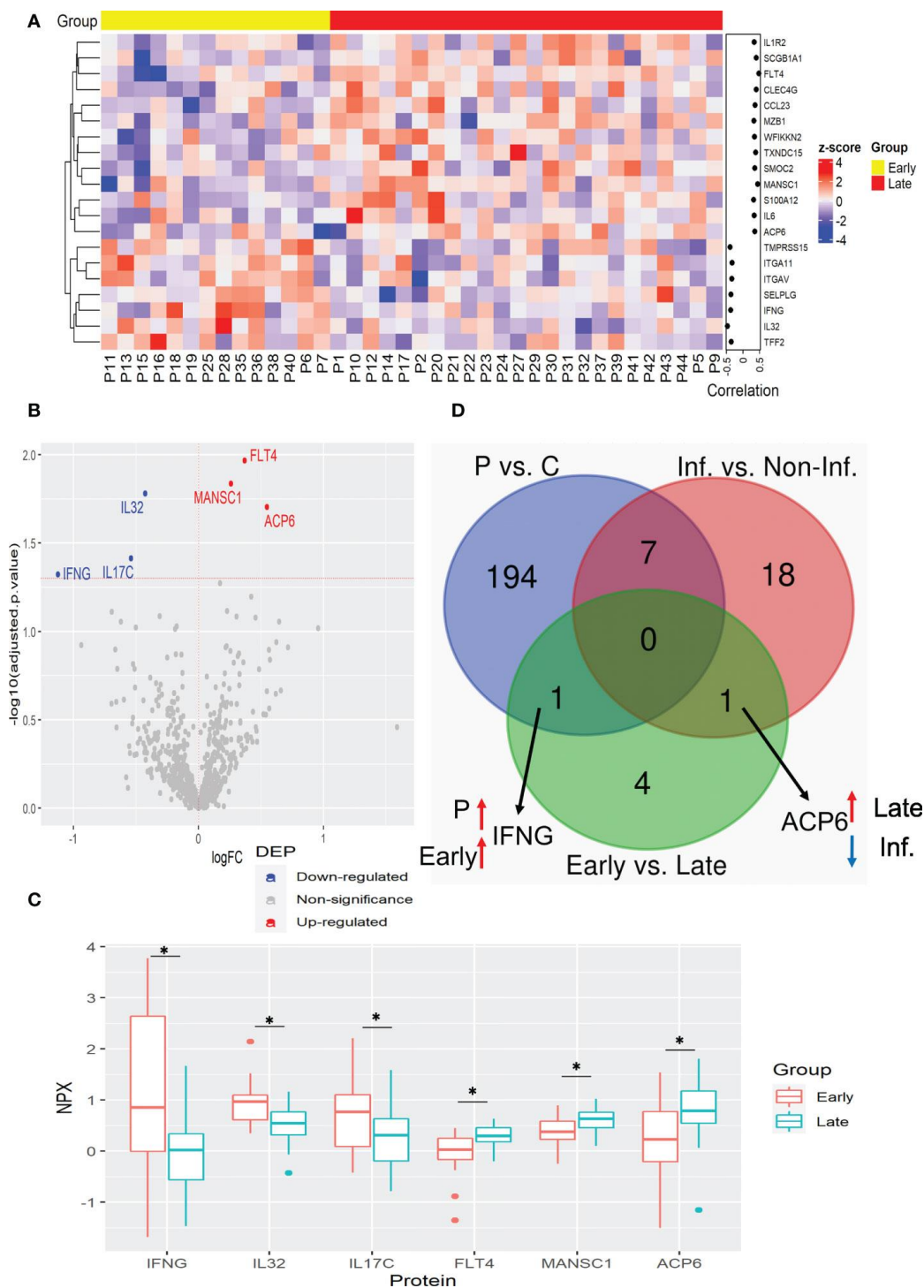


Figure 10.3 Plasma protein expression differences between early and late stages of CRC. (A) Heatmap of proteins with significant correlation with tumor stage. Protein expression is transformed with a z-score by row normalization and distributed by hierarchical clustering. The correlation coefficients (right) indicate a positive/negative correlation for each protein. (B) Volcano plot of statistical significance against fold-change of proteins between CRC patients with early tumor stage and with late tumor stage. Dots indicate individual protein and the red and blue dots represent significant up-regulation and down-regulation in CRC patients with late tumor stage, respectively. (C) Box and whisker plots of DEPs that are novel potential prognostic biomarkers associated with cancer stages in CRC patients. *: adjusted p-value < 0.05. (D) Venn diagram with the differentially expressed proteins for each comparison: CRC patients vs. control, Inflammation vs. Non-inflammation, and Early vs. Late. Black arrows indicate the proteins of interest that are in common between comparisons. Red and blue arrows indicate up-regulation and down-regulation for the specified group, respectively. C, control; Inf., inflammation; Non-Inf., non-inflammation; P, patient.

10.3.4. Validation of identified plasma protein changes with a different cohort

To validate some of the newly identified plasma protein changes in CRC patients, an independent cohort including 41 patients who underwent CRC surgery obtained from the Bank of Biological Material at Masaryk Memorial Cancer Institute, Czech Republic was used. Higher concentrations of IL6 and CSF3 among CRC patients than in healthy volunteers were confirmed in the validation stage of the study (Figure 10.4A). Importantly, increased secretion of IFNG, CXCL9 and CCL23 in the plasma of CRC patients compared to healthy subjects was detected in the validation cohort by Luminex (Figure 10.4A), suggesting that elevated plasma level of IFNG, CXCL9 and CCL23 might be served as a biomarker of CRC. Importantly, similar as detected by PEA (Figure 10.3B), the elevated level of ACP6 in late stage compared with early stage of CRC was confirmed in this cohort as well (Figure 10.4B). Taken together, these results indicate that ACP6 might be a potential prognostic marker for advanced CRC. Notably, MANSC1 and ACP6 have not been previously reported to be associated with CRC development. However, these findings need to be confirmed by using bigger validation cohort.

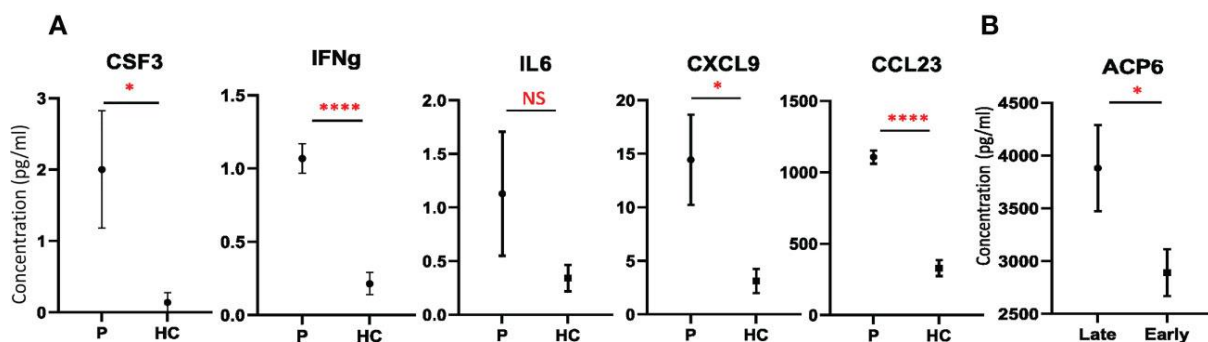


Figure 10.4. Validation of potential candidate biomarkers. (A) Plots with the concentrations of CSF3, IFNG, IL6, CXCL9, and CCL23 in CRC patients (P) and healthy controls (HC) (mean ± SEM) detected by Luminex. (B) Plot with the concentrations of ACP6 detected by ELISA in CRC patients with early and late stages, respectively (mean ± SEM). T test was used for statistical analysis. *: p-value < 0.05, ****: p-value < 0.0001, NS: non-significance.

10.4. Discussion

Cancer, including colorectal cancer, is the leading cause of death worldwide and the most devastating disease as the 21st century begins. Thus, there is an urgent need for the discovery and validation of reliable and efficient non-invasive biomarkers for early CRC detection and prognosis prediction, including biomarkers to detect cancer-associated inflammation. To determine plasma protein changes in CRC patients, by using PEA technology, we quantified 690 proteins, among which 202 were changed compared to healthy subjects.

Among the elevated cytokines in CRC patients, CXCL9 and CCL23 have been identified as novel potential biomarkers. The T-cell chemoattractant *CXCL9* was previously found elevated in CRC tissues compared to normal colon tissues and it was associated with tumor differentiation and invasion, lymph node and distant metastasis, as well as with vascular invasion (38). An enhanced expression of *CXCL9* in cancer tissue than healthy tissue was also observed in the second Chinese study, where *CXCL9* expression levels were associated with tumor stage and survival (39). Importantly, *CXCL9* may also recruit T-cells to the TME and exerts antitumor activity (40). The chemokine, *CCL23* has been found as a cytokine with both, pro- and anti-cancer properties. It can induce angiogenesis by activating C-C Motif Chemokine Receptor 1 (CCR1) on vascular endothelial cells and increase the proliferation of cancer cells, but also, it can promote immune infiltration (41). However, what type of immune cells and T-cells are attracted to the TME by *CCL23* and *CXCL9*, respectively, requires further studies. A strong elevation of *CCL23* protein was noticed in rectal cancer compared to non-rectal cancer consisting of ascending, transverse, and sigmoid colon (42), while *CCL23* expression was not detected in colon adenocarcinoma cells in a second study (43).

Interestingly, none of the previous studies reported high CXCL9 and CCL23 levels in the plasma of CRC patients.

Apart from cytokines, plasma levels of other immune-related proteins were changed in CRC patients compared to the healthy controls, such as DPEP2 and Peroxiredoxin 6 (PRDX6), which have not been previously reported as plasma diagnostic biomarkers. The protein expression of DPEP2, a dipeptidase involved in leukotriene metabolism, was recently found as a modulator of macrophage inflammatory responses, protecting mice against Coxsackievirus B3-induced viral myocarditis (44). Interestingly, DPEP1, the paralog of DPEP2 was up-regulated in CRC tissue at mRNA and protein levels and high DPEP1 expression was significantly correlated with cancer stage, location, and poorer prognosis (45), while no association of DPEP2 with CRC has been detected. Similarly, elevated PRDX6, a metabolic enzyme, may modulate inflammation and immune responses through the regulation of antioxidants and reactive oxygen species (46). It was suggested that PRDX6 may promote CRC invasiveness and aggressiveness by inducing an oxidizing TME (47). Importantly, we found two mediators of apoptosis, CASP8 and BID, which presented high plasma levels in CRC patients compared to healthy subjects, with BID having the second highest fold change. Recently, circulating CASP8 was identified with high expression in pre-operative serum samples of prostate cancer (48). BID, belonging to the B-cell lymphoma 2 (BCL-2) family, is a key regulator of apoptosis and a factor associated with CRC initiation and progression (49). It was found that high expression of proapoptotic BID was a predictor of overall survival in patients with CRC, whereas combined expression of BAD and BID was associated with disease-free survival rates and overall survival (50). However, further studies are needed to investigate whether the elevated plasma CASP8 and BID are associated with an exacerbated apoptosis of peripheral blood mononuclear cells (PBMC) among these patients, similarly as in the case of melanoma patients (51). Collectively, the altered cytokines and immune-related proteins suggest an active modulation of the immune system in CRC patients at the systemic level as well as a systemic inflammatory status.

It is well-known that several signalling pathways, such as Ras, NF- κ B, and MAPK are altered in CRC patients leading to oncogenesis (52), which was also confirmed in our study at a systemic level. Interestingly, several oncogenic proteins were elevated in plasma, such as SCRIN1 and RSPO3, whereas previous studies determine their overexpression in CRC tumor tissue (53, 54). SCRIN1 accelerates tumor progression by the regulation of exocytosis of matrix metalloproteinase-2/9 (MMP-2/9) (55), while RSPO3 is an oncogenic driver that causes CRC and extensive crypt hyperplasia, concomitantly stimulating stem cells and supportive niche cells (56). It was found that overexpression of *RSPO2* and *RSPO3* was presented by 4-10% of colon subjects (54) and recurrent R-spondin fusions in colon cancer activate the Wnt signaling and increase the tumorigenesis (57). Additionally, lower plasma levels of potential tumor suppressor proteins, such as RET and ARHGEF12 were detected in CRC patients. RET, is a transmembrane receptor tyrosine kinase and a receptor for the GDNF-family ligands, which downregulation in CRC tissue compared to healthy tissue was noticed (58). CRC patients with somatic RET mutations exhibited a lower incidence of liver metastasis but a higher incidence of peritoneal metastasis and more frequently exhibited mucinous histology (59). On the other hand, a germ-line or somatic RET mutation was linked with more intense and complete angiogenesis in patients with advanced medullary thyroid cancers (60). ARHGEF12, also known as leukemia-associated Rho guanine-nucleotide exchange factor (LARG), is underexpressed in CRC tissue and is associated with reduced cell proliferation and a slower migration rate in cancer cells (61). Moreover, it was found that ARHGEF12 regulates cell adhesion and structure morphogenesis in esophageal squamous cell carcinoma tissues (62) and plays a key role in erythroid regeneration after chemotherapy in acute lymphoblastic leukemia patients (63). These proteins can be potentially used as an oncogenic protein signature for CRC diagnosis in plasma. Apart from oncogenic pathways, NAFLD was also enriched in this cohort. Meta-analyses revealed that NAFLD was associated with an increased risk of gastrointestinal cancers (64) and colon cancers, especially in the right-sided colon (29).

More importantly, our data demonstrated the upregulation of Th17 cell differentiation in CRC patients. Th17 activity has been linked to CRC tumorigenesis and poor prognosis (65). It is well-known that chronic inflammation contributes to cancer development. We identified upregulation of IL12RB1 and CSF3 in Th17 differentiation and IL17 signaling, indicating their participation in CRC-related inflammation. It is worth noticing that CSF3 expression was previously found elevated in the serum of CRC patients (27). An increased gene expression of CSF3 was also observed in CRC tissue from two Consensus Molecular Subtypes (microsatellite instable immune and mesenchymal), where it was associated with regulators (e.g., CXCL5) of invasion (66). IL12RB1, a subunit of the interleukin 12 receptors is associated with tyrosine kinase 2 (TYK2), which plays a pivotal role in immunity to viral infection and cancer surveillance (34). It was found that elevated expression of tumor tissue IL12RB1 was associated with lung cancer progression (67), whereas its correlation with CRC development has not been reported. Moreover, IL12RB1 contributes to both the IL12- and IL23-signaling pathways and is involved in both Th1 and Th17 cell differentiation (68). A carbonic anhydrase, CA11, was also associated with inflammation which overexpression promotes the proliferation and invasion of gastrointestinal tumors without any previous association with CRC in plasma (37). Importantly, the immune checkpoint inhibitor CD276, also called B7-H3 was also linked to inflammation. CD276 was previously reported with high expression in CRC tissue and may contribute to the tumor evasion of T-cell mediated responses (35, 69) and has been already proposed as a target for immunotherapy (70). The overexpression of this immune checkpoint molecule in our study further indicates the importance of this protein in the personalized medicine and immune-checkpoint therapy aspect.

In contrast, the reduced plasma level of CXCL6 and APBB1IP in CRC patients with inflammation was observed in our study. It was recently found that low serum CXCL6 levels were associated with an increased risk of CRC development (33), while CXCL6 expression is not altered in CRC tissue (71). The APBB1IP is a Rap1-binding protein that acts as a regulator of leukocyte recruitment and pathogen clearance through complement-mediated phagocytosis (36). It was shown that expression of APBB1IP was correlated with the prognosis of various cancer types and its upregulation has been demonstrated as associated with increased immune cell infiltration, especially CD8⁺ T cells, natural killer (NK) cells, and immune regulators (36). Bioinformatics analyses revealed that *APBB1IP* may be used as a potential biomarker for osteosarcoma metastasis (72) and suggested its potential role in the evolutionary mechanisms of head and neck squamous cell carcinoma related to inflammation and TME (73). Moreover, cancer-related inflammation may cause the downregulation of APBB1IP decreasing the recruitment of leukocytes to the TME. In this study, for the first time, we reported the association of reduced plasma APBB1IP level with CRC and inflammation, suggesting that APBB1IP could be a potential biomarker for inflammation-associated CRC.

The next two elevated plasma proteins, MANSC1 and ACP6, identified in our study have never been suggested as associated with CRC risk. Expression of bone marrow *MANSC1* was detected in patients with different hematologic malignancies such as acute myeloid leukemia, myelodysplastic syndromes, and primary myelofibrosis, but no significant correlations between the expression of the gene and survival were observed (74). In contrast, an association between high expression of *MANSC1* and a positive prognosis for overall survival was found in patients with non-small cell lung cancer (75). A functional *MANSC1* Single Nucleotide Polymorphism has been also identified in patients with overall prostate cancer and non-advanced prostate cancer in a genome-wide association study (76). The metabolic enzyme ACP6 hydrolyzes LPA to monoacylglycerol and plays a role in regulating lipid metabolism in the mitochondria (77, 78). It has been recently demonstrated that overexpression of ACP6 in hepatocellular carcinoma tissue was positively correlated with clinical progression and worse overall survival of examined patients (77). On the other hand, decreased expression of ACP6 was found to contribute to increased cell mortality and disease progression in high-grade serous ovarian cancer and esophageal squamous cell carcinoma (78, 79). It was found that CRC cells have abnormal LPA receptor expression that may be associated with

enhanced proliferation, survival, and invasion of CRC cells (80). These results suggest that ACP6 may play a key role in oncogenesis. A positive correlation of plasma ACP6 with the advanced stage of CRC has been revealed for the first time in our study. Moreover, ACP6 was reduced in CRC patients with cancer-related inflammation. The function of ACP6 in cancer-related inflammation and CRC tumorigenesis needs to be further investigated.

More interestingly, three pro-inflammatory cytokines, IL32, IL17C, and IFNG, were increased in the early stages of CRC compared to late-stage patients in the Polish cohort. IL32 is an intracellular pluripotent cytokine, expressed in various cell types, which affects many cellular and physiological functions such as cell death and survival, angiogenesis, inflammation, and response to pathogens (81). Increased levels of IL32 were found in cancer tissue (82, 83), and primary CRC lymph nodes metastasis (84). Moreover, IL32 can stimulate NK and T-cell cytotoxicity against primary solid tumors, as well as increase T-cell infiltration (85). In our study, we observed increased circulating IL32 associated with the early tumor stage, indicating that IL32 may serve as a biomarker for the early stage of CRC. The second pro-inflammatory cytokine, IL17C, a member of the IL17 family, plays an essential role in immunopathology, autoimmune diseases, and cancer progression (86). It was found that IL17C is higher expressed in CRC tissue and induces tumor angiogenesis of intestinal endothelial cells *via* VEGFR2 production, subsequently enhancing cell invasion and migration of CRC cells (87, 88). Moreover, elevated levels of serum and tissue IL17C were observed in patients with active IBD, which can result in cancer progression (87). Among these patients, the production of IL17C is induced by the synergic effect of IL17A and TNF- α (89). Therefore, high circulating IL17C may be associated with tumorigenesis from IBD to early stages of CRC. Lasts of these cytokines, IFNG, is critical to both innate and adaptive immunity (90). IFNG was reduced in PBMC of patients with recurrent CRC, with the most significantly reduced expression in stage IV tumors (91). On contrary, the upregulation of *IFNG* mRNA in late-stage CRC tissue and peripheral blood of patients with CRC was observed in another study (92). IFNG is a well-established anti-tumor factor with controversial findings in CRC at mRNA and protein levels. Several studies did not find a significant association between circulating IFNG and CRC development (93–95). In contrast, our analysis showed high levels of IFNG in CRC patients supporting previous findings (31). Moreover, we found high levels of IFNG in the early stages of CRC, suggesting a higher anti-tumor activity of lymphocytes than in the late stages. Taken as a whole, these findings indicate that ACP6, FLT4, MANSC1, IFNG, IL17C, and IL32 may be used as promising prognostic biomarkers that distinguish early-stage from advanced CRC. Moreover, IFNG can be a potential biomarker for early detection of CRC due to its discrimination between early-stage patients with advanced CRC patients as well as healthy controls, which has not been reported before.

In this study, the application of PEA technology enabled us to detect 690 proteins from a low amount of plasma of CRC patients and healthy subjects. Despite the sensitivity and accuracy of PEA, this technology is limited by the availability and specificity of antibodies, and more importantly, the number of preselected proteins. Women are dominant in both study groups, which is different concerning the known population with CRC. We lacked information on family history, which is known as one of the best predictors of CRC risk. Future studies should be conducted to verify our results on a larger number of samples and by using PEA or other quantitative methods.

In conclusion, we identified plasma protein changes in CRC patients related to cytokine interactions, oncogenic pathways, Th17 activity, metabolism reprogramming, as well as cancer-related inflammation with potential usage in CRC diagnosis. We also validated in an independent cohort that ACP6 level was elevated in advanced CRC patients. Further study using larger cohort is needed to confirm whether FLT4, IFNG, IL17C, IL32, and MANSC1 may be used as potential prognostic biomarkers to discriminate early-stage and advanced CRC.

10.5. References

1. Sung H, Ferlay J, Siegel RL, Laversanne M, Soerjomataram I, Jemal A, et al. Global cancer statistics 2020: GLOBOCAN estimates of incidence and mortality worldwide for 36 cancers in 185 countries. *CA Cancer J Clin* (2021) 71:209–49. doi: 10.3322/caac.21660
2. Xi Y, Xu P. Global colorectal cancer burden in 2020 and projections to 2040. *Transl Oncol* (2021) 14:101174. doi: 10.1016/j.tranon.2021.101174
3. Ladabaum U, Dominitz JA, Kahi C, Schoen RE. Strategies for colorectal cancer screening. *Gastroenterology* (2020) 158:418–32. doi: 10.1053/J.GASTRO.2019.06.043
4. Nicholson BD, James T, East JE, Grimshaw D, Paddon M, Justice S, et al. Experience of adopting faecal immunochemical testing to meet the NICE colorectal cancer referral criteria for low-risk symptomatic primary care patients in Oxfordshire, UK. *Frontline Gastroenterol* (2019) 10:347–55. doi: 10.1136/flgastro-2018-101052
5. Young PE, Womeldorph CM. Colonoscopy for colorectal cancer screening. *J Cancer* (2013) 4:217. doi: 10.7150/JCA.5829
6. Lu D, Zhang Q, Li L, Luo X, Liang B, Lu Y, et al. Methylated Septin9 has moderate diagnostic value in colorectal cancer detection in Chinese population: a multicenter study. *BMC Gastroenterol* (2022) 22:232. doi: 10.1186/s12876-022-02313-x
7. Yang CK, Hsu HC, Liu YH, Tsai WS, Ma CP, Chen YT, et al. EV-miRome-wide profiling uncovers miR-320c for detecting metastatic colorectal cancer and monitoring the therapeutic response. *Cell Oncol* (2022) 45:621–38. doi: 10.1007/s13402-022-00688-3
8. Agah S, Akbari A, Talebi A, Masoudi M, Sarveazad A, Mirzaei A, et al. Quantification of plasma cell-free circulating DNA at different stages of colorectal cancer. *Cancer Invest* (2017) 35:625–32. doi: 10.1080/07357907.2017.1408814
9. Zhong W, Edfors F, Gummesson A, Bergström G, Fagerberg L, Uhlén M. Next generation plasma proteome profiling to monitor health and disease. *Nat Commun* (2021) 12:2493. doi: 10.1038/s41467-021-22767-z
10. Bhardwaj M, Weigl K, Tikk K, Benner A, Schrotz-King P, Brenner H. Multiplex screening of 275 plasma protein biomarkers to identify a signature for early detection of colorectal cancer. *Mol Oncol* (2020) 14:8–21. doi: 10.1002/1878-0261.12591
11. Mahboob S, Ahn SB, Cheruku HR, Cantor D, Rennel E, Fredriksson S, et al. A novel multiplexed immunoassay identifies CEA, IL-8 and prolactin as prospective markers for dukes' stages a-d colorectal cancers. *Clin Proteomics* (2015) 12:10. doi: 10.1186/s12014-015-9081-x
12. Thorsen SB, Lundberg M, Villablanca A, Christensen SLT, Belling KC, Nielsen BS, et al. Detection of serological biomarkers by proximity extension assay for detection of colorectal neoplasias in symptomatic individuals. *J Transl Med* (2013) 11:1–13. doi: 10.1186/1479-5876-11-253
13. Kankanala VL, Mukkamalla SKR. Carcinoembryonic antigen. Treasure Island (FL: StatPearls Publishing (2022)). Available at: <https://www.ncbi.nlm.nih.gov/books/NBK578172/>.
14. Chen H, Zucknick M, Werner S, Knebel P, Brenner H. Head-to-Head comparison and evaluation of 92 plasma protein biomarkers for early detection of colorectal cancer in a true screening setting. *Clin Cancer Res* (2015) 21:3318–26. doi: 10.1158/1078-0432.CCR-14-3051
15. Sekiguchi M, Matsuda T. Limited usefulness of serum carcinoembryonic antigen and carbohydrate antigen 19-9 levels for gastrointestinal and whole-body cancer screening. *Sci Rep* (2020) 10:18202. doi: 10.1038/s41598-020-75319-8
16. Ushigome M, Shimada H, Miura Y, Yoshida K, Kaneko T, Koda T, et al. Changing pattern of tumor markers in recurrent colorectal cancer patients before surgery to recurrence: serum p53 antibodies, CA19-9 and CEA. *Int J Clin Oncol* (2020) 25:622–32. doi: 10.1007/S10147-019-01597-6
17. Ji L, Gu L, Zhang X, Wang J. Evaluation of serum midkine and carcinoembryonic antigen as diagnostic biomarkers for rectal cancer and synchronous metastasis. *Transl Cancer Res* (2020) 9:2814–23. doi: 10.21037/TCR.2020.02.43
18. Chen H, Qian J, Werner S, Cuk K, Knebel P, Brenner H. Development and validation of a panel of five proteins as blood biomarkers for early detection of colorectal cancer. *Clin Epidemiol* (2017) 9:517–26. doi: 10.2147/CLEP.S144171
19. Sun X, Shu XO, Lan Q, Laszkowska M, Cai Q, Rothman N, et al. Prospective proteomic study identifies potential circulating protein biomarkers for colorectal cancer risk. *Cancers (Basel)* (2022) 14:3261. doi: 10.3390/cancers14133261
20. Harlid S, Harbs J, Myte R, Brunius C, Gunter MJ, Palmqvist R, et al. A two-tiered targeted proteomics approach to identify pre-diagnostic biomarkers of colorectal cancer risk. *Sci Rep* (2021) 11:5151. doi: 10.1038/s41598-021-83968-6
21. Terzić J, Grivnennikov S, Karin E, Karin M. Inflammation and colon cancer. *Gastroenterology* (2010) 138:2101–14. doi: 10.1053/J.GASTRO.2010.01.058
22. Filipowicz N, Drężek K, Horbacz M, Wojdak A, Szymanowski J, Rychlicka-Buniowska E, et al. Comprehensive cancer-oriented biobanking resource of human samples for studies of post-zygotic genetic variation involved in cancer predisposition. *PLoS One* (2022) 17:e0266111. doi: 10.1371/JOURNAL.PONE.0266111
23. Cui M, Zhao Y, Zhang Z, Zhao Y, Han S, Wang R, et al. IL-8, MSPa, MIF, FGF-9, ANG-2 and AgRP collection were identified for the diagnosis of colorectal cancer based on the support vector machine model. *Cell Cycle* (2021) 20:781–91. doi: 10.1080/15384101.2021.1903208
24. Qian J, Tikk K, Weigl K, Balavarca Y, Brenner H. Fibroblast growth factor 21 as a circulating biomarker at various stages of colorectal carcinogenesis. *Br J Cancer* (2018) 119:1374–82. doi: 10.1038/S41416-018-0280-X
25. Wang D, Yuan W, Wang Y, Wu Q, Yang L, Li F, et al. Serum CCL20 combined with IL-17A as early diagnostic and prognostic biomarkers for human colorectal cancer. *J Transl Med* (2019) 17:253. doi: 10.1186/s12967-019-2008-y
26. Xu J, Ye Y, Zhang H, Szmitkowski M, Mäkinen MJ, Li P, et al. Diagnostic and prognostic value of serum interleukin-6 in colorectal cancer. *Med (Baltimore)* (2016) 95:e2502. doi: 10.1097/MD.0000000000002502

27. Mroczko B, Groblewska M, Wereszczynska-Siemiatkowska U, Kedra B, Konopko M, Szmitkowski M. The diagnostic value of G-CSF measurement in the sera of colorectal cancer and adenoma patients. *Clin Chim Acta* (2006) 371:143–7. doi: 10.1016/J.CCA.2006.02.037
28. Mobarra N, Gholamalizadeh H, Abdulhussein KA, Raji S, Taheri Asl F, Mirvahabi MS, et al. Serum level and tumor tissue expression of ribonucleotide-diphosphate reductase subunit M2 b: a potential biomarker for colorectal cancer. *Mol Biol Rep* (2022) 49:3657–63. doi: 10.1007/s11033-022-07205-7
29. Lin XL, You FM, Liu H, Fang Y, Jin SG, Wang QL. Site-specific risk of colorectal neoplasms in patients with non-alcoholic fatty liver disease: a systematic review and meta-analysis. *PLoS One* (2021) 16:e0245921. doi: 10.1371/JOURNAL.PONE.0245921
30. Nenkov M, Ma Y, Gaßler N, Chen Y. Metabolic reprogramming of colorectal cancer cells and the microenvironment: implication for therapy. *Int J Mol Sci* (2021) 22:6262. doi: 10.3390/IJMS22126262
31. Crucitti A, Corbi M, Tomaiuolo PMC, Fanali C, Mazzari A, Lucchetti D, et al. Laparoscopic surgery for colorectal cancer is not associated with an increase in the circulating levels of several inflammation-related factors. *Cancer Biol Ther* (2015) 16:671–7. doi: 10.1080/15384047.2015.1026476
32. De Simone V, Pallone F, Monteleone G, Stolfi C. Role of TH17 cytokines in the control of colorectal cancer. *Oncoimmunology* (2013) 2:e26617. doi: 10.4161/ONCI.26617
33. Song M, Sasazuki S, Camargo MC, Shimazu T, Charvat H, Yamaji T, et al. Circulating inflammatory markers and colorectal cancer risk: a prospective case-cohort study in Japan. *Int J Cancer* (2018) 143:2767–76. doi: 10.1002/IJC.31821
34. Vielnascher RM, Hainzl E, Leitner NR, Rammerstorfer M, Popp D, Witalisz A, et al. Conditional ablation of TYK2 in immunity to viral infection and tumor surveillance. *Transgenic Res* (2014) 23:519–29. doi: 10.1007/S11248-014-9795-Y
35. Sun J, Chen LJ, Zhang GB, Jiang JT, Zhu M, Tan Y, et al. Clinical significance and regulation of the costimulatory molecule B7-H3 in human colorectal carcinoma. *Cancer Immunol Immunother* (2010) 59:1163–1171. doi: 10.1007/S00262-010-0841-1
36. Ge Q, Li G, Chen J, Song J, Cai G, He Y, et al. Immunological role and prognostic value of APBB1IP in pan-cancer analysis. *J Cancer* (2021) 12:595–610. doi: 10.7150/JCA.50785
37. Morimoto K, Nishimori I, Takeuchi T, Kohsaki T, Okamoto N, Taguchi T, et al. Overexpression of carbonic anhydrase-related protein XI promotes proliferation and invasion of gastrointestinal stromal tumors. *Virchows Arch* (2005) 447:66–73. doi: 10.1007/s00428-005-1225-3
38. Wu Z, Huang X, Han X, Li Z, Zhu Q, Yan J, et al. The chemokine CXCL9 expression is associated with better prognosis for colorectal carcinoma patients. *Biomed Pharmacother* (2016) 78:8–13. doi: 10.1016/J.BIOPHA.2015.12.021
39. Yu L, Yang X, Xu C, Sun J, Fang Z, Pan H, et al. Comprehensive analysis of the expression and prognostic value of CXC chemokines in colorectal cancer. *Int Immunopharmacol* (2020) 89:107077. doi: 10.1016/J.INTIMP.2020.107077
40. Tian Y, Wen C, Zhang Z, Liu Y, Li F, Zhao Q, et al. CXCL9-modified CAR T cells improve immune cell infiltration and antitumor efficacy. *Cancer Immunol Immunother* (2022) 71:2663–75. doi: 10.1007/S00262-022-03193-6
41. Korbecki J, Kojder K, Simińska D, Bohatyrewicz R, Gutowska I, Chlubek D, et al. CC chemokines in a tumor: a review of pro-cancer and anti-cancer properties of the ligands of receptors CCR1, CCR2, CCR3, and CCR4. *Int J Mol Sci* (2020) 21:8412. doi: 10.3390/IJMS21218412
42. Miyoshi H, Morishita A, Tani J, Sakamoto T, Fujita K, Katsura A, et al. Expression profiles of 507 proteins from a biotin label-based antibody array in human colorectal cancer. *Oncol Rep* (2014) 31:1277–81. doi: 10.3892/OR.2013.2935
43. Farquharson AJ, Steele RJ, Carey FA, Drew JE. Novel multiplex method to assess insulin, leptin and adiponectin regulation of inflammatory cytokines associated with colon cancer. *Mol Biol Rep* (2012) 39:5727–36. doi: 10.1007/S11033-011-1382-1
44. Yang X, Yue Y, Xiong S. Dpep2 emerging as a modulator of macrophage inflammation confers protection against CVB3-induced viral myocarditis. *Front Cell Infect Microbiol* (2019) 9:57. doi: 10.3389/FCIMB.2019.00057
45. Eisenach PA, Soeth E, Röder C, Klöppel G, Tepel J, Kalthoff H, et al. Dipeptidase 1 (DPEP1) is a marker for the transition from low-grade to high-grade intraepithelial neoplasia and an adverse prognostic factor in colorectal cancer. *Br J Cancer* (2013) 109:694–703. doi: 10.1038/BJC.2013.363
46. Patel P, Chatterjee S. Peroxiredoxin6 in endothelial signaling. *Antioxidants* (2019) 8:63. doi: 10.3390/ANTIOX8030063
47. Huang WS, Huang CY, Hsieh MC, Kuo YH, Tung SY, Shen CH, et al. Expression of PRDX6 correlates with migration and invasiveness of colorectal cancer cells. *Cell Physiol Biochem* (2018) 51:2616–30. doi: 10.1159/000495934
48. Liu S, Garcia-Marques F, Zhang CA, Lee JJ, Nolley R, Shen M, et al. Discovery of CASP8 as a potential biomarker for high-risk prostate cancer through a high-multiplex immunoassay. *Sci Rep* (2021) 11:7612. doi: 10.1038/s41598-021-87155-5
49. Ramesh P, Medema JP. BCL-2 family deregulation in colorectal cancer: potential for BH3 mimetics in therapy. *Apoptosis* (2020) 25:305–20. doi: 10.1007/S10495-020-01601-9
50. Sinicrope FA, Rego RL, Foster NR, Thibodeau SN, Alberts SR, Windschitl HE, et al. Proapoptotic bad and bid protein expression predict survival in stages II and III colon cancers. *Clin Cancer Res* (2008) 14:4128–33. doi: 10.1158/1078-0432.CCR-07-5160
51. Alecu M, Coman G, Dănilă L. High levels of sFas and PBMC apoptosis before and after excision of malignant melanoma—case report. *Roum Arch Microbiol Immunol* (2002) 61:267–73.
52. Mosnier JF, Airaud F, Métairie S, Volteau C, Bezieau S, Denis M. Mapping of colorectal carcinoma diseases with activation of wnt/beta-catenin signalling pathway using hierarchical clustering approach. *J Clin Pathol* (2022) 75:168–175. doi: 10.1136/JCLINPATH-2020-207144
53. Miyoshi N, Ishii H, Mimori K, Sekimoto M, Doki Y, Mori M. SCRN1 is a novel marker for prognosis in colorectal cancer. *J Surg Oncol* (2010) 101:156–9. doi: 10.1002/JSO.21459

54. Conboy CB, Velez-Reyes GL, Rathe SK, Abrahante JE, Temiz NA, Burns MB, et al. A. r-spondins 2 and 3 are overexpressed in a subset of human colon and breast cancers. *DNA Cell Biol* (2021) 40:70–9. doi: 10.1089/dna.2020.5585
55. Lin S, Jiang T, Yu Y, Tang H, Lu S, Peng Z, et al. Secernin-1 contributes to colon cancer progression through enhancing matrix metalloproteinase-2/9 exocytosis. *Dis Markers* (2015) 2015:230703. doi: 10.1155/2015/230703
56. Hilkens J, Timmer NC, Boer M, Ikink GJ, Schewe M, Sacchetti A, et al. RSPO3 expands intestinal stem cell and niche compartments and drives tumorigenesis. *Gut* (2017) 66:1095–105. doi: 10.1136/GUTJNL-2016-311606
57. Seshagiri S, Stawiski EW, Durinck S, Modrusan Z, Storm EE, Conboy CB, et al. Recurrent r-spondin fusions in colon cancer. *Nature* (2012) 488:660–4. doi: 10.1038/NATURE11282
58. Ashkboos M, Nikbakht M, Zarinfard G, Soleimani M. RET protein expression in colorectal Cancer ; an immunohistochemical assessment. *Asian Pac J Cancer Prev* (2021) 22:1019–23. doi: 10.31557/APJCP.2021.22.4.1019
59. Yang YZ, Hu WM, Xia LP, He WZ. Association between somatic RET mutations and clinical and genetic characteristics in patients with metastatic colorectal cancer. *Cancer Med* (2021) 10:8876–8882. doi: 10.1002/CAM4.4400
60. Verrienti A, Tallini G, Colato C, Boichard A, Checquolo S, Pecce V, et al. RET mutation and increased angiogenesis in medullary thyroid carcinomas. *Endocr Relat Cancer* (2016) 23:665–76. doi: 10.1530/ERC-16-0132
61. Ong DCT, Ho YM, Rudduck C, Chin K, Kuo W, Lie DKH, et al. LARG at chromosome 11q23 has functional characteristics of a tumor suppressor in human breast and colorectal cancer. *Oncogene* (2009) 28:4189–200. doi: 10.1038/onc.2009.266
62. Sha Y, Hong H, Cai W, Sun T. Single-cell transcriptomics of endothelial cells in upper and lower human esophageal squamous cell carcinoma. *Curr Oncol* (2022) 29:7680–94. doi: 10.3390/CURRONCOL29100607
63. Xie Y, Gao L, Xu C, Chu L, Gao L, Wu R, et al. ARHGEF12 regulates erythropoiesis and is involved in erythroid regeneration after chemotherapy in acute lymphoblastic leukemia patients. *Haematologica* (2020) 105:925–36. doi: 10.3324/HAEMATOL.2018.210286
64. Mantovani A, Petracca G, Beatrice G, Csermely A, Tilg H, Byrne CD, et al. Non-alcoholic fatty liver disease and increased risk of incident extrahepatic cancers: a meta-analysis of observational cohort studies. *Gut* (2022) 71:778–88. doi: 10.1136/GUTJNL-2021-324191
65. Razi S, Baradaran Noveiry B, Keshavarz-Fathi M, Rezaei N. IL-17 and colorectal cancer: from carcinogenesis to treatment. *Cytokine* (2019) 116:7–12. doi: 10.1016/j.cyto.2018.12.021
66. Saunders AM, Bender DE, Ray AL, Wu X, Morris KT. Colony-stimulating factor 3 signaling in colon and rectal cancers: immune response and CMS classification in TCGA data. *PLoS One* (2021) 16:e0247233. doi: 10.1371/JOURNAL.PONE.0247233
67. Li J, Zhang L, Zhang J, Wei Y, Li K, Huang L, et al. Interleukin 23 regulates proliferation of lung cancer cells in a concentration-dependent way in association with the interleukin-23 receptor. *Carcinogenesis* (2013) 34:658–66. doi: 10.1093/CARCIN/BGS384
68. Robinson RT. IL12Rβ1: the cytokine receptor that we used to know. *Cytokine* (2015) 71:348–59. doi: 10.1016/j.cyto.2014.11.018
69. Bin Z, Guangbo Z, Yan G, Huan Z, Desheng L, Xueguang Z. Overexpression of B7-H3 in CD133+ colorectal cancer cells is associated with cancer progression and survival in human patients. *J Surg Res* (2014) 188:396–403. doi: 10.1016/J.JSS.2014.01.014
70. Picarda E, Ohaegbulam KC, Zang X. Molecular pathways: targeting B7-H3 (CD276) for human cancer immunotherapy. *Clin Cancer Res* (2016) 22:3425–31. doi: 10.1158/1078-0432.CCR-15-2428
71. Rubie C, Frick V, Wagner M, Schuld J, Gräber S, Brittner B, et al. ELR+ CXC chemokine expression in benign and malignant colorectal conditions. *BMC Cancer* (2008) 8:178. doi: 10.1186/1471-2407-8-178
72. Liang J, Chen J, Hua S, Qin Z, Lu J, Lan C. Bioinformatics analysis of the key genes in osteosarcoma metastasis and immune invasion. *Transl Pediatr* (2022) 11:1656–70. doi: 10.21037/TP-22-402/
73. Sanati N, Iancu OD, Wu G, Jacobs JE, McWeeney SK. Network-based predictors of progression in head and neck squamous cell carcinoma. *Front Genet* (2018) 9:183. doi: 10.3389/fgene.2018.00183
74. Haferlach C, Bacher U, Kohlmann A, Schindela S, Alpermann T, Kern W, et al. CDKN1B, encoding the cyclin-dependent kinase inhibitor 1B (p27), is located in the minimally deleted region of 12p abnormalities in myeloid malignancies and its low expression is a favorable prognostic marker in acute myeloid leukemia. *Haematologica* (2011) 96:829–36. doi: 10.3324/HAEMATOL.2010.035584
75. Vastrad C, Vastrad B. Investigation into the underlying molecular mechanisms of non-small cell lung cancer using bioinformatics analysis. *Gene Rep* (2019) 15:100394. doi: 10.1016/J.GENREP.2019.100394
76. Haiman CA, Han Y, Feng Y, Xia L, Hsu C, Sheng X, et al. Genome-wide testing of putative functional exonic variants in relationship with breast and prostate cancer risk in a multiethnic population. *PLoS Genet* (2013) 9:e1003419. doi: 10.1371/JOURNAL.PGEN.1003419
77. Gao L, Xiong DD, Yang X, Li J, He RQ, Huang ZG, et al. The expression characteristics and clinical significance of ACP6, a potential target of nitidine chloride, in hepatocellular carcinoma. *BMC Cancer* (2022) 22:1–14. doi: 10.1186/s12885-022-10292-1
78. Chryplewicz A, Tienda SM, Nahotko DA, Peters PN, Lengyel E, Eckert, et al. Mutant p53 regulates LPA signaling through lysophosphatidic acid phosphatase type 6. *Sci Rep* (2019) 9:5195. doi: 10.1038/s41598-019-41352-5
79. Ando T, Ishiguro H, Kuwabara Y, Kimura M, Mitsui A, Kurehara H, et al. Expression of ACP6 is an independent prognostic factor for poor survival in patients with esophageal squamous cell carcinoma. *Oncol Rep* (2006) 15:1551–5. doi: 10.3892/or.15.6.1551
80. Lee SJ, Yun CC. Colorectal cancer cells – proliferation, survival and invasion by lysophosphatidic acid. *Int J Biochem Cell Biol* (2010) 42:1907–10. doi: 10.1016/J.BIOCEL.2010.09.021
81. Gautam A, Pandit B. IL32: the multifaceted and unconventional cytokine. *Hum Immunol* (2021) 82:659–67. doi: 10.1016/J.HUMIMM.2021.05.002
82. Shamoun L, Kolodziej B, Andersson RE, Dimberg J. Protein expression and genetic variation of IL32 and association with colorectal cancer in Swedish patients. *Anticancer Res* (2018) 38:321–8. doi: 10.21873/ANTICANRES.12225

83. Ozmen F, Erdem GO, Kulacoglu S, Ozmen M, Kansu E. Interleukin-21 and interleukin-32 gene expression levels and their relationship with clinicopathological parameters in colorectal cancer. *Ann Ital. Chir* (2022) 92:78–87.
84. Yang Y, Wang Z, Zhou Y, Wang X, Xiang J, Chen Z. Dysregulation of over-expressed IL-32 in colorectal cancer induces metastasis. *World J Surg Oncol* (2015) 13:146. doi: 10.1186/s12957-015-0552-3
85. Sloot YJE, Smit JW, Joosten LAB, Netea-Maier RT. Insights into the role of IL-32 in cancer. *Semin Immunol* (2018) 38:24–32. doi: 10.1016/J.SMIM.2018.03.004
86. Meehan EV, Wang K. Interleukin-17 family cytokines in metabolic disorders and cancer. *Genes (Basel)* (2022) 13:1643. doi: 10.3390/GENES13091643
87. Swedik S, Madola A, Levine A. IL-17C in human mucosal immunity: more than just a middle child. *Cytokine* (2021) 146:155641. doi: 10.1016/J.CYTO.2021.155641
88. Lee Y, Kim SJ, Choo J, Heo G, Yoo JW, Jung Y, et al. miR-23a-3p is a key regulator of IL-17C-Induced tumor angiogenesis in colorectal cancer. *Cells* (2020) 9:1363. doi: 10.3390/CELLS9061363
89. Friedrich M, Diegelmann J, Schaubert J, Auernhammer CJ, Brand S. Intestinal neuroendocrine cells and goblet cells are mediators of IL-17A-amplified epithelial IL-17C production in human inflammatory bowel disease. *Mucosal Immunol* (2015) 8:943–58. doi: 10.1038/MI.2014.124
90. Schroder K, Hertzog PJ, Ravasi T, Hume DA. Interferon-gamma: an overview of signals, mechanisms and functions. *J Leukoc Biol* (2004) 75:163–89. doi: 10.1189/JLB.0603252
91. Ganapathi SK, Beggs AD, Hodgson SV, Kumar D. Expression and DNA methylation of TNF, IFNG and FOXP3 in colorectal cancer and their prognostic significance. *Br J Cancer* (2014) 111:1581–9. doi: 10.1038/bjc.2014.477
92. Söylemez Z, Arikan ES, Solak M, Arikan Y, Tokyol Ç., Şeker H. Investigation of the expression levels of CPEB4, APC, TRIP13, EIF2S3, EIF4A1, IFNG, PIK3CA and CTNNB1 genes in different stage colorectal tumors. *Turkish J Med Sci* (2021) 51:661–74. doi: 10.3906/SAG-2010-18
93. Henry CJ, Sedjo RL, Rozhok A, Salstrom J, Ahnen D, Levin TR, et al. Lack of significant association between serum inflammatory cytokine profiles and the presence of colorectal adenoma. *BMC Cancer* (2015) 15:1–9. doi: 10.1186/s12885-015-1115-2
94. Farc O, Berindan-Neagoe I, Zaharie F, Budisan L, Zanoaga O, Cristea V. A role for serum cytokines and cell adhesion molecules in the non-invasive diagnosis of colorectal cancer. *Oncol Lett* (2022) 24:323. doi: 10.3892/ol.2022.13443
95. Ma Y, Zhang Y, Bi Y, He L, Li D, Wang D, et al. Diagnostic value of carcinoembryonic antigen combined with cytokines in serum of patients with colorectal cancer. *Med (Baltimore)* (2022) 101:e30787. doi: 10.1097/MD.00000000000030787

11. Publication VI: Mass Spectrometry Proteomics Characterization of Plasma Biomarkers for Colorectal Cancer Associated With Inflammation

Published: Biomarker Insights. 2024;19. doi:10.1177/11772719241257739

Authors: Urbiola-Salvador V, Jabłońska A, Miroszewska D, Kamysz W, Duzowska K, Drężek-Chyła K, Baber R, Thieme R, Gockel I, Zdrenka M, Śrutek E, Szyłberg Ł, Jankowski M, Bata D, Zegarski W, Nowikiewicz T, Makarewicz W, Adamczyk A, Ambicka A, Przewoźnik M, Harazin-Lechowicz A, Ryś J, Macur K, Czaplewska P, Filipowicz N, Piotrowski A, Dumanski JP, Chen Z

11.1. Introduction

Colorectal cancer (CRC) is the third most incident malignancy and the second most deadly cancer worldwide.¹ Despite the great advances in CRC treatment with recently developed immunotherapies, about 20% to 25% of diagnosed CRC patients present advanced cancer stages and metastasis that is linked to a 5 year survival rate lower than 10% and low therapeutic response.^{2,3} In contrast, diagnosis at early stages leads to reduced tumor-related mortality and a 90% 5 year survival rate after radical surgical resection.⁴ Apart from the disease stage at diagnosis, CRC prognosis depends on multiple factors such as location, genetic factors, molecular expression profiles, tumor immune infiltration, and inflammation.³ The low therapeutic response to immunotherapies such as immune checkpoint inhibitors may be caused by the influence of other non-targeted inflammatory and immunosuppressive mechanisms.⁵ Notably, cancer-associated inflammation is considered a well-established hallmark of cancer, especially in CRC.⁶ Inflammatory modulators including chemokines, cytokines, and growth factors influence the interactions between cancer cells and the tumor microenvironment driving tumor progression and the immune response.⁷ Moreover, CRC progression can promote systemic inflammation impacting other organs and facilitating metastasis.⁸

Currently, the gold standard for CRC prevention is colonoscopy complemented with fecal occult blood tests.⁹ However, colonoscopy is expensive and has poor patient compliance, due to its invasiveness and risks, while stool-based tests have low sensitivity and specificity.^{4,9} Therefore, alternative, non-invasive, cost-effective, and easily measurable CRC screening strategies are urgently needed. Mass spectrometry (MS)-based proteomics approaches have been successfully applied to determine blood-based biomarkers of CRC development and progression.⁴ MS-based proteomics characterization of low-abundance proteins in serum/plasma is limited by the high dynamic range of protein concentrations over 9 orders of magnitude with 99% of the total protein content from only 20 abundant proteins.¹⁰ However, the technological evolution of high-resolution MS instruments such as time-of-flight (TOF) or Orbitrap provides the possibility to discover blood-based biomarkers with high sensitivity and specificity.¹¹

Nowadays, the most common blood protein biomarker used in clinical CRC diagnosis is carcinoembryonic antigen (CEA), but its accuracy requires improvement.¹² Interestingly, untargeted tandem MS coupled with liquid chromatography (LC-MS/MS) proteomics strategies could discover novel potential CRC biomarkers that can be validated by using targeted MS techniques as well as antibody-based assays.⁴ For instance, proteomics analysis discovered that several SERPIN family members are altered in patients with CRC and adenomatous polyps which were validated as potential diagnostic biomarkers by ELISA.¹³ Moreover, plasma proteomics analysis combined with neural network classification identified 5

candidate biomarkers to distinguish between CRC stages.¹⁴ Another glycoproteomics study detected novel diagnostic biomarkers including elevated levels of complement C9 and fibronectin improved the diagnostic performance of a commercial CEA CRC biomarker.¹⁵ In addition, targeted proteomics analysis in a non-metastatic CRC cohort determined a 5 protein signature with efficient discrimination of CRC cases from healthy subjects.¹⁶ However, despite advances in CRC biomarker discovery and validation by proteomics, further studies are needed in larger cohorts to implement reliable biomarkers in clinical practice.

The aim of this study was to discover novel plasma protein signatures involved in CRC development and progression by untargeted LC-MS/MS proteomics analysis. Importantly, we identified significant changes in plasma protein levels associated with cholesterol metabolism, members of the SERPIN family as well as increased levels of complement cascade proteins in CRC patients versus healthy subjects. Furthermore, high complement C5 levels were confirmed in the validation cohort, being a potential diagnostic CRC biomarker. Plasma protein levels of 11 proteins, including complement C8A and serpin family A member 4 (SERPINA4) were linked to cancer-associated inflammation, while 4 proteins, including C8A and C4B, distinguished early from advanced CRC stages.

11.2. Materials and Methods

11.2.1. Study cohorts and design

This multi-center retrospective study included 36 patients with CRC surgery (age mean: 66.1 ± 11.6 years; 44.4% male) from June 2019 to April 2021 and 26 healthy subjects (age mean: 61.1 ± 10.5 years; 42.3% male) in the discovery cohort. Included patients were with positive colonoscopy and pathologist-confirmed malignant neoplasm. Patients with prior neoadjuvant therapy administration were excluded from the analysis. 69.4% (25 of 36) of diagnosed patients were with advanced CRC stages (III-IV) according to the Union for International Control of Cancer TNM classification and 30.5% (11 of 36) presented cancer-associated inflammation post-operatively assessed by pathologists. Blood samples of healthy subjects and CRC patients were obtained from Biobank HARC, Medical University of Łódź and the 3P-Medicine Laboratory, Medical University of Gdańsk.¹⁷ The independent validation cohort included 60 CRC patients (age mean: 61.8 ± 11.4 years; 51.7% male) without neoadjuvant therapy and 44 sex-and-age-matched healthy subjects. Serum samples were obtained from the Leipzig Medical Biobank, Germany and the Bank of Biological Material at Masaryk Memorial Cancer Institute, Czech Republic. The collection of whole blood samples was with sterile BD Vacutainer® K2EDTA tubes or Sarstedt S-Monovette® 2.7 mL, K3 EDTA (LMB) before the CRC resection followed by centrifugation, aliquoting, and storage at -80°C until use.

11.2.2. Sample preparation for mass spectrometry

Proteins were extracted from plasma samples with lysis buffer (1% SDS, 50 mM DTT, 100 mM Tris-HCl pH 8.0) (Merck KGaA, Darmstadt, Germany) containing phosphatase and protease inhibitors (Thermo Fisher Scientific, Waltham, MA, USA) followed by an incubation at 95°C for 10 minutes. Protein concentrations were determined at 280 nm in a µDrop plate with a Multiskan Thermo Nanodrop. Then, 100 µg of proteins were transferred to Microcon 10 kDa filters (Merck KGaA) and were processed based on the Filter Aided Sample Preparation (FASP) protocol.¹⁸ Briefly, 3 washes with 200 µl of urea buffer (8 M urea, 100 mM Tris-HCl pH 8.5) at 10 000 rcf for 20 minutes at room temperature (RT) were applied to the protein mixtures. Free cysteines were alkylated by incubation in the darkness for 20 minutes at RT with 55 mM iodoacetamide

(100 µl) in urea buffer (Merck KGaA). Samples were centrifuged at 10 000 rcf for 15 minutes and washed 3 times with urea (100 µl) and 2 times with digestion buffer (50 mM Tris-HCl pH 8.0). Afterward, the filters were transferred into new tubes and proteins were digested by incubation at 37°C with 1 µg of Sequencing Grade Modified Trypsin (Promega, Madison, WI, USA) in 60 µl of digestion buffer overnight. Then, the elution of peptides was performed with the same centrifugation conditions and washed 2 times with 125 and 100 µl digestion buffer. Next, 0.1% trifluoroacetic acid quenched trypsin activity. Peptide concentrations were measured as previously and 20 µg of peptides were desalted with STop And Go Extraction (STAGE) Tips¹⁹ in Empore C18 extraction disks (3M, Neuss, Germany). Peptides were eluted with 60% acetonitrile and 1% acetic acid. Desalted peptides were dried in a SpeedVac at 45°C and samples were in storage at -20°C until analysis.

11.2.3.LC-MS/MS analysis

LC-MS/MS analysis of prepared samples was performed with a TripleTOF 5600+ mass spectrometer (SCIEX, Framingham, MA, USA) and with an EksportMicroLC 200 Plus System (Eksigent, Redwood City, CA, USA). AB SCIEX Analyst TF 1.6 software was used to control the LC-MS/MS system. Samples were run in triplicates with 1.5 µg injected peptides in each technical replicate. Analyses were in a ChromXP C18CL column (3 µm, 120 Å, 150 mm × 0.3 mm) at 5 µl/minute and 35°C, for 60 minutes with an 11% to 35% acetonitrile gradient in 0.1% formic acid. TripleTOF 5600+ was set in data-dependent acquisition mode and the m/z range of the TOF MS survey scan was at 400 to 1200 Da with an accumulation time of 250 ms. The selection for collision-induced dissociation (CID) fragmentation was set to a maximum of top 20 precursor ions with +2 to +5 charges. The exclusion of precursor ions from reselection was for 5 seconds after 2 occurrences. Product ions spectra were acquired between 100 and 1800 Da with 50 ms accumulation time.

11.2.4.MS data analysis

Acquired raw SCIEX files were converted to mzML format with MSConvertGUI 3.0 and analyzed using PeaksStudio Xpro 10.6 software (Bioinformatics Solutions, Waterloo, ON, Canada). Peptide sequence search was against the *Homo sapiens* UniProtKB/Swiss-Prot database (release 2022_03) for trypsin digested peptides with maximum 3 missed cleavages per peptide. Carbamidomethylation was as fixed post-translational modification (PTM), whereas N-terminal acetylation and methionine oxidation as variable PTMs. Peptide and protein identification was with a <1% false discovery rate (FDR). Label-free quantification was performed based on the integration of the peptide areas under the curve (AUC).

11.2.5.Complement C5 validation

Complement C5 serum concentrations were quantified in the validation cohort by an ELISA kit with a coated antibody to human C5 (Abcam ab125963, Cambridge, UK) commercially available, following manufacturer's instructions.

11.2.6.Proteomics data and statistical analysis

Statistical analysis was performed with R (version 4.0.3) (R Foundation for Statistical Computing, Vienna, Austria) in RStudio (version 1.3.1093) (RStudio, PBC, Boston, MA, USA). Data preprocessing was performed by summarization of technical replicates with medians and logarithmic transformation of relative abundances. Proteins with missing values in over 50% of patients and 50% of healthy controls were filtered. Random forest imputation was applied to the remaining missing values with the "missForest" R package (version 1.5) followed by quantile normalization. Differences in protein levels between groups were

analyzed by the general linear model regression approach with contrast analysis with the “emmeans” R package (version 1.6.2.1). First, for each protein, a general linear model was generated to fit its expression to determine significant changes in CRC patients compared to healthy volunteers including age as a confounding factor. Then, for each protein expression, a general linear model was generated including only CRC patients with the independent variables inflammation and tumor stage while sex was considered a confounding factor. FDR control was applied with the Benjamini & Hochberg correction. Significant changes were considered with FDR-adjusted *P* value < .05. Point-biserial correlation of protein abundance with inflammation status or tumor stage was calculated with the built-in R function `cor.test` and correlation was significant with a *P* value < .05. Principal Component Analysis (PCA) was performed using `prcomp` built-in R function and PCA visualization using “factoextra” R package (version 1.0.7). Functional annotation of biological process and cellular component GO terms was performed by a 2-sided hypergeometric test with FDR correction using the Cytoscape `cluGO` plugin (version 2.5.7). Pathway enrichment analysis of KEGG terms supported by active subnetworks was applied with the R package “pathfindR” (version 1.6.3) using the STRING database and FDR correction. The generation of graphics was with the R package “ggplot2” (version 3.3.5), with the exception of heatmaps generation by the R package “ComplexHeatmap” (version 2.6.2). The construction of the protein network was with Cytoscape (version 3.8.2) using the STRING database and a 0.7 confidence cut-off.

11.3. Results

11.3.1. Identification and quantification of the plasma proteome of CRC patients using LC-MS/MS

To study the protein profile changes in blood involved in CRC development, we applied LC-MS/MS proteomics analysis to plasma samples of 36 CRC patients and 26 healthy controls. As a result, 322 proteins were identified with at least 1 unique peptide with FDR < .01, from which the majority of proteins were identified in both groups (Figure 11.1A; Appendix V Supplemental Table S1). Interestingly, IgGfC-binding protein (FCGBP), which is a mucin responsible for innate immune defense in the intestine and is associated with CRC metastasis by promoting cell adhesion, was only identified in CRC patients.²⁰ After filtering proteins with high % of missing values, 138 protein groups were quantified. The relative protein abundance was reproducible along technical replicates with high Pearson’s correlation coefficients (Figure 11.1B). LC-MS/MS analysis quantified proteins in a high dynamic range of concentrations from high-abundance albumin in the range of mg/mL to chemokines such as C-X-C motif chemokine ligand 7 (CXCL7) in the range of ng/mL (Figure 11.1C).

Functional annotation of the identified proteins determined that the majority were from the extracellular organelles, blood, and lipoprotein microparticles, as well as the vesicle/vacuolar lumen (Figure 11.2A). However, proteins from the plasma membrane, cytoplasm, and nucleus, such as histone H4, were also detected that may circulate in the peripheral blood due to tissue damage and cell turnover. (Appendix V Supplemental Table S2). Identified proteins were included in several biological processes such as blood coagulation, homeostasis, proteolysis, and several metabolic processes including cholesterol and fatty acid metabolism, vesicle-mediated transport, cell death as well as humoral immune and inflammatory responses (Figure 11.2B). Interestingly, over-represented biological process GO terms were associated with different humoral immune and inflammatory responses due to the presence of immunoglobulins, complement proteins, and some chemokines such as CXCL7 (Figure 11.2C; Appendix

V Supplemental Table S2). Overall, our proteomics analysis identified plasma proteins associated with different biological processes including immune responses and quantified 138 proteins in a high dynamic range of concentrations with high reproducibility.

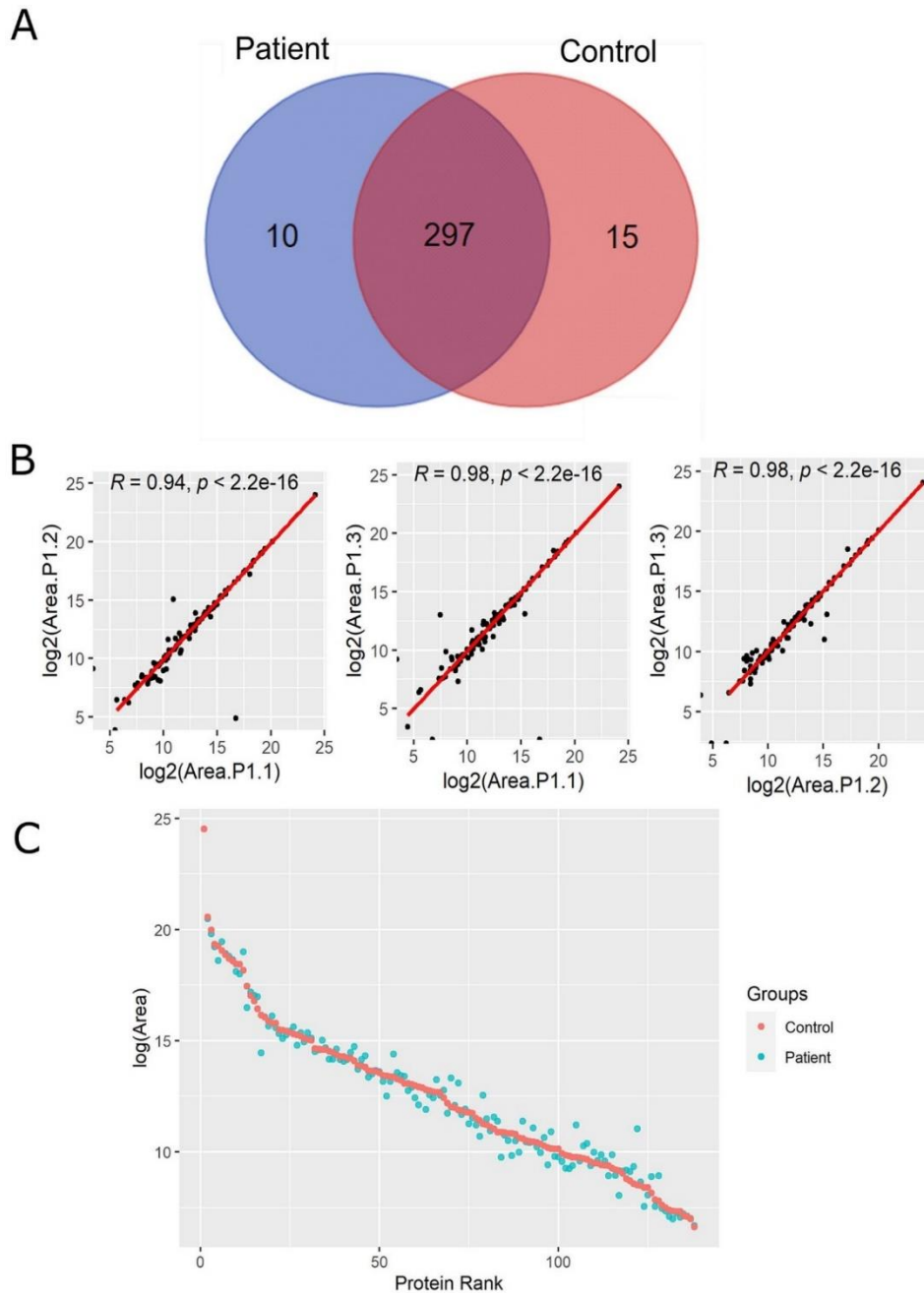


Figure 11.1. LC-MS/MS analysis of plasma proteome from CRC patients and healthy controls. (A) Venn diagram of identified proteins in CRC patients and healthy individuals. (B) Representative scatter plots of log-transformed areas for the 3 technical replicates from a CRC patient (P1) with their corresponding Pearson correlation coefficients and *P* values. (C) Abundance protein ranking plot with the mean of log-transformed areas from healthy subjects (red) and CRC patients (blue).

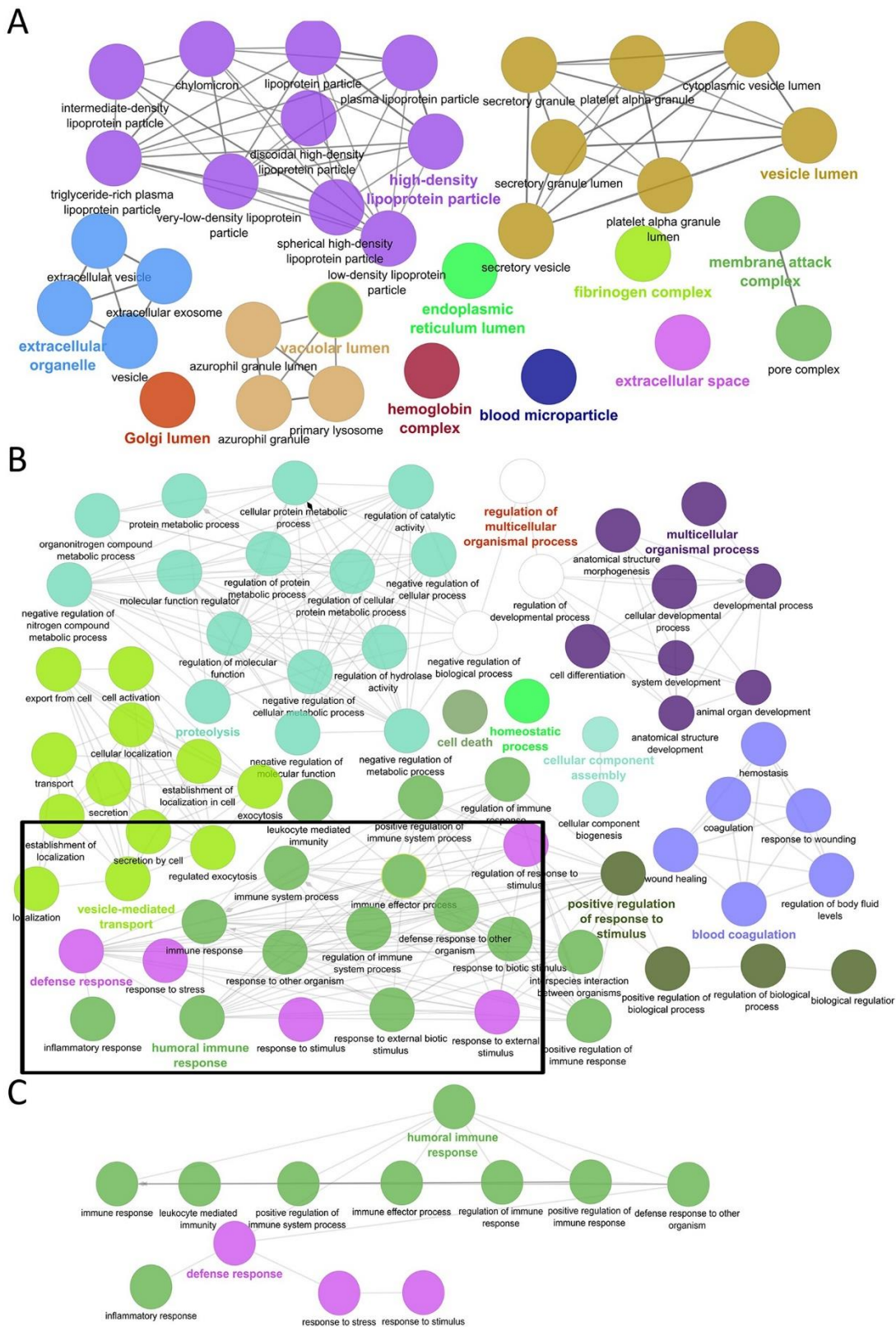


Figure 11.2. Functional annotation of the identified plasma proteins. (A) Interaction network of over-represented cellular component Gene Ontology (GO) terms with an organic layout. (B) Interaction network of over-represented GO terms of biological processes with an organic layout. (C) Amplification of the subnetwork of GO terms from immune and defense responses with a tree layout.

11.3.2. CRC development causes protein plasma changes associated with the complement cascade and cholesterol metabolism

To determine whether the plasma levels of quantified proteins differs in CRC patients versus healthy volunteers, PCA was performed. PCA showed a clear separation of plasma from CRC patients and healthy subjects, indicating that CRC development affects the protein plasma profiles in examined patients (Figure 11.3A). To unveil these protein changes, differential protein expression analysis was applied, resulting in 17 proteins with enhanced levels and 20 decreased proteins in CRC patients versus healthy volunteers (Figure 11.3B, Supplemental Table S11.3). Among the differentially expressed proteins (DEPs), inter-alpha-trypsin inhibitor heavy chain (ITIH)3, leucine-rich alpha-2-glycoprotein (A2GL), C9, and lipopolysaccharide-binding protein (LBP) showed the highest levels in CRC patients, while apolipoprotein (APO) A4, acid labile subunit (ALS), and kallikrein B1 (KLKB1) showed the lowest levels compared to healthy controls. ITIH3, a hyaluronan essential for multiple cellular processes, which transports and regulates hyaluronan turnover in the blood circulation, was found with the highest fold change. Unsupervised hierarchical clustering showed that these 37 DEPs separated CRC from control samples (Supplemental Figure S11.1). Pathway enrichment analysis of KEGG terms by active subnetworks revealed that complement and coagulation pathways were activated with elevated protein levels (C4B, C5, C1QB, and C9) in CRC patients (Figure 11.3C, Appendix V Supplemental Table S4). Moreover, cholesterol metabolism, vitamin digestion, and adsorption were down-regulated in CRC patients, involving 2 apolipoproteins, APOA2 and APOA4 (Figure 11.3B and C). Both APOA2 and APOA4 are associated with obesity and hypercholesterolemia that are independent risk factors for CRC development.^{21,22} Similarly, the STRING protein-protein interaction network showed the interaction between the complement proteins with elevated levels (Figure 11.3D). In addition, SERPINC1 was the most interconnected node linking complement proteins to other DEPs in the network. SERPINC1, also called antithrombin III, is the main inhibitor of blood coagulation which can attenuate inflammatory responses.²³ Collectively, our analysis indicates that development of CRC causes plasma protein changes which are associated with complement cascade and cholesterol metabolism.

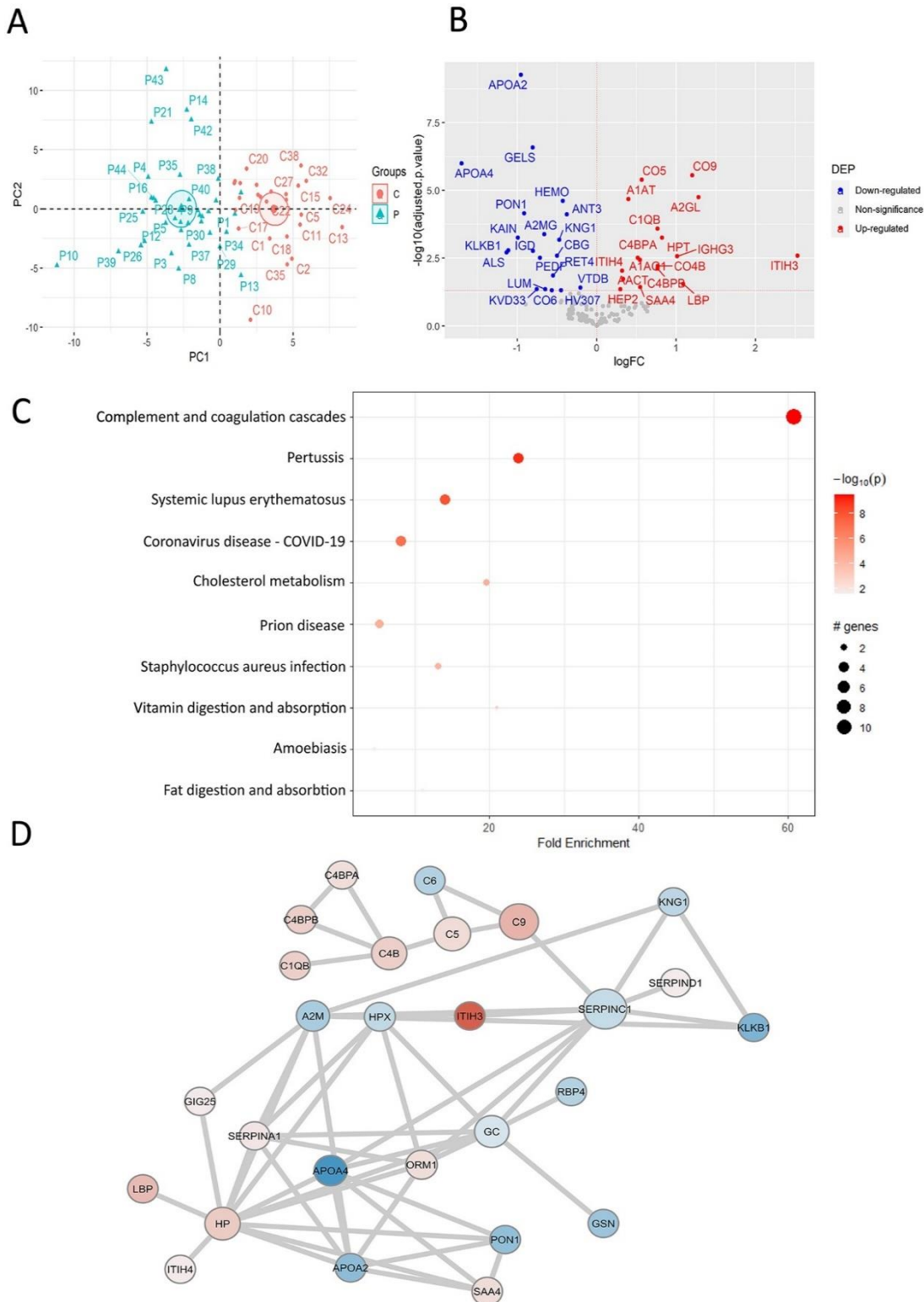


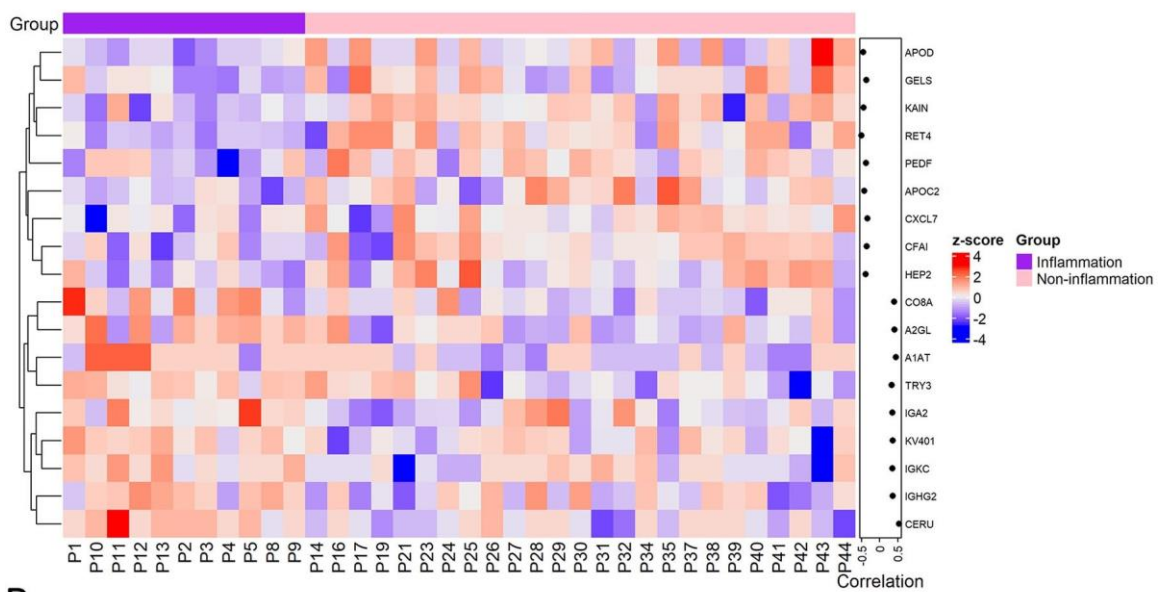
Figure 11.3. Colorectal cancer (CRC) development causes plasma protein changes involved in complement cascades and cholesterol metabolism. (A) Principal Component Analysis of CRC patients and healthy subjects using the relative abundances of all quantified proteins. (B) Volcano plot of statistical significance against fold-change of proteins between CRC patients and healthy individuals. Colored dots indicate statistically differentially expressed proteins (DEPs) calculated by the general linear model approach. (C) Dot plot of KEGG pathway enrichment combined with STRING protein-protein interaction network analysis from DEPs between CRC patients and healthy subjects. (D) Protein-protein interaction network of DEPs between CRC patients and healthy individuals from STRING database query with a 0.7 confidence cut-off. The size of nodes indicates the degree of connectivity of the nodes. The red and

blue dots/nodes represent up-regulation and down-regulation in CRC patients, respectively. FC, Fold Change; p, p-value; PC, Principal Component.

11.3.3. Plasma protein changes linked to cancer-associated inflammation in CRC patients

Inflammation is a well-established hallmark of cancer that influences CRC progression. To analyze protein changes in plasma associated with inflammatory status, the protein levels were compared between CRC patients with cancer-associated inflammation (11 of 36 cases) and without. First, correlation analysis determined significant correlation of 18 proteins with cancer-associated inflammation, including 9 proteins correlated positively such as C8A, A2GL, and ceruloplasmin (CERU), while another 9 proteins including retinol-binding protein 4 (RET4) were correlated negatively (Figure 11.4A, Appendix V Supplemental Table S5).

A



B

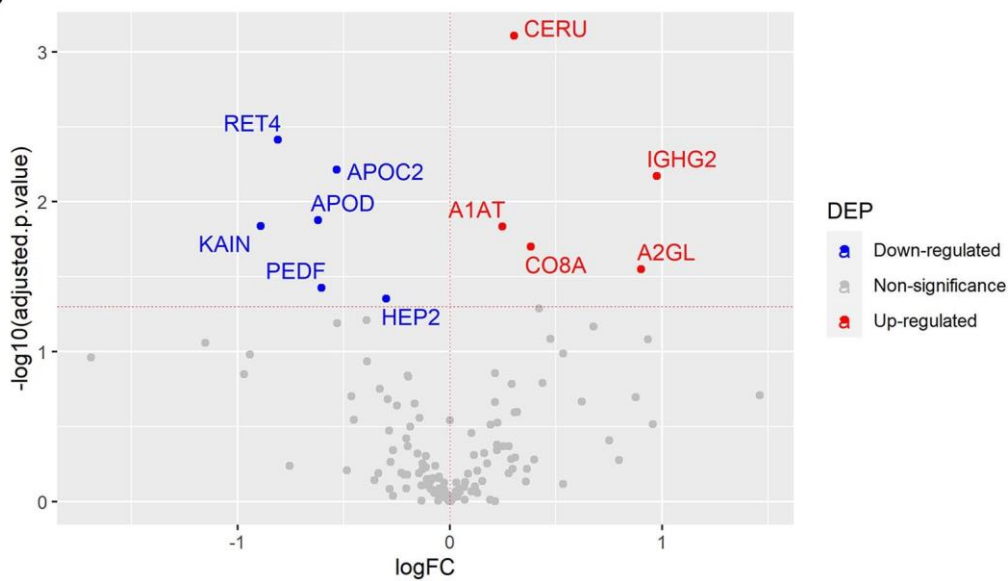


Figure 11.4. Plasma protein changes induced by cancer-associated inflammation in CRC patients. (A) Heatmap of proteins with significant correlation with inflammatory status. Protein expression is transformed with a z-score by row normalization and distributed by hierarchical clustering. The correlation coefficients (right) indicate a positive/negative correlation for each protein. (B) Volcano plot of statistical significance against fold-change of proteins between CRC patients with inflammation and without inflammation. Dots indicate individual proteins and the red and blue dots represent significant up-regulation and down-regulation in CRC patients with inflammation, respectively.

To determine the link between protein abundance and cancer-associated inflammation, the differential protein expression was evaluated by linear regression analysis. This analysis resulted in 11 DEPs that were previously identified with significant correlation (Figure 11.4B, Appendix V Supplemental Table S6). Some downregulated proteins were SERPIN family members, for example, SERPINA4 (KAIN) and SERPIND1 (HEP2). Noteworthy, SERPINA4 is an anti-angiogenic and anti-inflammatory agent that was decreased in CRC patients versus healthy volunteers and its downregulation was common in inflammatory processes as well as in cancer.²⁴ Additionally, C8A and immunoglobulin heavy constant gamma 2 (IGHG2) may be related to cancer-associated inflammation thus promoting an exacerbated immune response in these patients. Collectively, this analysis determined plasma protein signatures in CRC patients linked to cancer-associated inflammation.

11.3.4. Evaluation of plasma protein signatures linked to CRC stages

The main complication of CRC development is tumor progression and metastasis, resulting in increased CRC mortality. Therefore, CRC prognostic biomarkers are urgently needed. Plasma protein changes linked to CRC progression were determined by comparing protein levels in early-stage patients (I and II) versus late-patients (III and IV). Correlation analysis indicated that 5 proteins were correlated positively, while 6 proteins were correlated negatively (Figure 11.5A, Appendix V Supplemental Table S7). Among them, enhanced fibrinogen alpha chain (FIBA) levels in late CRC stages and their association with distant metastasis were previously reported.²⁵ Also, increased alpha-1-acid glycoprotein 2 (A1AG2) was linked to shorter survival rates in a CRC cohort.²⁶ Similar to the previous comparison, the regression analysis showed that only were 4 DEPs (Figure 11.5B, Appendix V Supplemental Table S8). Among them, C8A and C4B may play a relevant role in CRC progression, while the immunoglobulin IGHG2 may be associated with the immune response in CRC early stages by promoting inflammation as enhanced levels were linked to cancer-associated inflammation. Taken together, we found 4 potential biomarkers that can potentially discriminate early from late CRC stages.

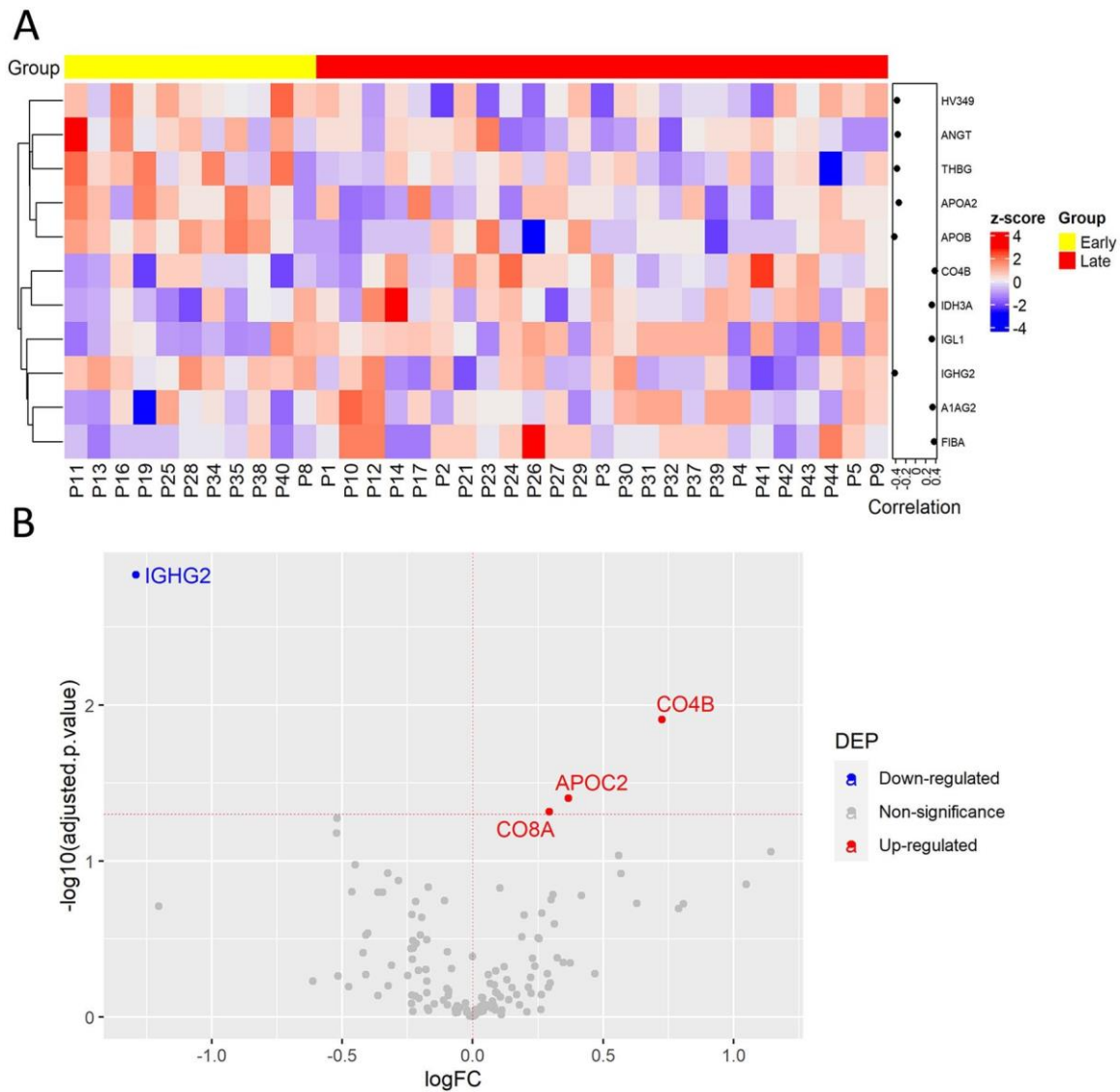


Figure 11.5. Plasma protein expression differences between early and late stages of CRC. (A) Heatmap of proteins with significant correlation with tumor stage. Protein expression is transformed with a z-score by row normalization and distributed by hierarchical clustering. The correlation coefficients (right) indicate a positive/negative correlation for each protein. (B) Volcano plot of statistical significance against fold-change of proteins between CRC patients with early tumor stage and with late tumor stage. Dots indicate individual proteins and the red and blue dots represent significant up-regulation and down-regulation in CRC patients with late tumor stage, respectively.

11.3.5. Complement protein C5 plasma levels are enhanced in CRC patients

Among the complement proteins, we found elevated C5 levels in plasma of CRC patients versus healthy volunteers by LC-MS/MS analysis (Figures 11.2B and 11.6A). To validate this finding, C5 concentrations were measured by ELISA in an independent validation cohort, including 60 CRC patients and 44 healthy subjects (Figure 11.6B). ELISA results confirmed LC-MS/MS findings. In fact, C5 proteolytic degradation promotes the release of the anaphylatoxin C5a that is an inflammatory mediator.²⁷ Noteworthy, a peptide from C5a was also enhanced in CRC patient's plasma (Figure 11.6C). Collectively, the enhanced plasma level of complement C5 is a novel promising biomarker for CRC diagnosis and may promote release of the pro-inflammatory C5a.

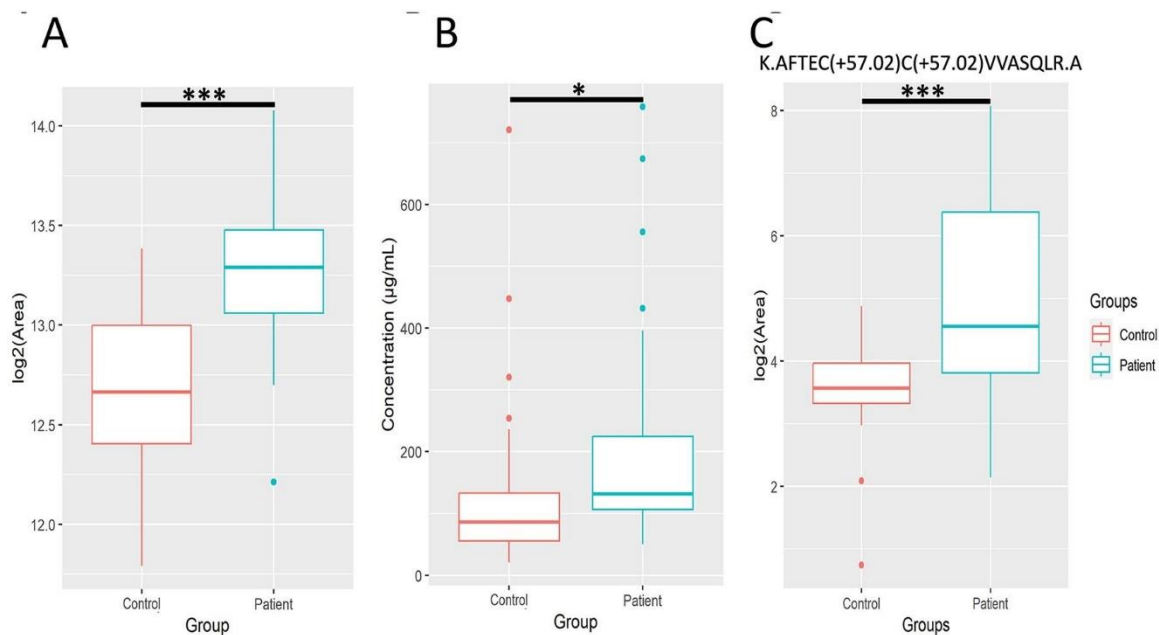


Figure 11.6. Complement protein C5 is a potential diagnostic biomarker for CRC. Box and whisker plots of (A) log-transformed areas of C5 in the discovery cohort calculated the significance by general linear model approach, (B) C5 concentrations measured by ELISA in the validation cohort calculated by Student t-test, and (C) log-transformed areas of a quantified peptide from C5a with the sequence AFTECCVVASQLR in the discovery cohort for CRC patients and healthy subjects calculated by Student t-test. * indicates statistical significance with a P value $< .05$, and *** indicates a P value $< .001$.

11.4. Discussion

In this study, we performed LC-MS/MS analysis to characterize the protein changes in plasma involved in CRC development by unbiased proteomics characterization of CRC patients and healthy individuals. Not only secreted proteins were detected but also released intracellular proteins from damaged tissues and cell turnover. Moreover, we quantified 138 proteins with high reproducibility and a high dynamic range of concentrations from ng/mL to mg/mL.

Several plasma proteins were identified with significant changes in CRC patients compared to healthy individuals. These findings were consistent with previously published data performed with LC-MS/MS as well as antibody-based techniques including ELISA and Western blot.^{13-16,28-30} For instance, ITIH3, the DEP with the highest fold change, was reported as increased in CRC patients' serum and serum of a CRC mice model,^{14,16,31} while another study showed opposite results.²⁸ Despite the role of ITIH3 in CRC development has not been determined yet, ITIH4 was found upregulated in CRC tissue versus normal-matched tissue and seems to be involved in the extracellular matrix remodeling and the systemic inflammatory response during CRC development.²⁸ Moreover, an increased level of several SERPIN family members was observed in the examined CRC cohort, which is consistent with previously reported data.^{13,29} Among them, SERPINC1 might play a central role in the systemic response to CRC as it is the most interconnected node in the protein-protein interaction network. Moreover, SERPINC1 downregulation may avoid its suppressive tumor activity and inhibit tumor angiogenesis and proliferation.¹³ Interestingly, another family member, SERPINF1 also revealed a link to cancer-associated inflammation. It was reported that this antiangiogenic

protein was downregulated in CRC tissue and sera and its low levels were associated with a poor survival prognosis.³⁰

Importantly, in this study, the increased level of the complement cascade and its components were found in CRC patients. This indicates that these proteins might play a relevant role in CRC development. Enhanced level of the complement proteins such as C9,¹⁵ complement component 4 binding protein alpha and beta (C4BPA and C4BPB)^{13,32} was previously reported in CRC patients while increased C1QB is novel. C1QB was found upregulated in tumor tissue versus normal-matched tissue but not in CRC patients' plasma.³³ Another novel complement protein with enhanced plasma level is C4B, which is a non-enzymatic component of C3/C5 convertases and was reported as upregulated in the serum of *Apc*^{Min/+} CRC mice versus wild-type mice.³¹ In our study, increased C4B was found in advanced-stage CRC patients, suggesting that this complement protein might play a key role in the disease progression. In addition to C4B, another member of the complement cascade, C8A, was also enhanced in the advanced stages of CRC patients. C8A is a key constituent of the membrane attack complex that regulates the pore formation in target cells and regulates the underlying innate and adaptive immune responses.²⁷ The high *C8a* expression was previously reported in CRC metastasis compared to the primary tumor which supports its potential role in CRC progression.³⁴ Moreover, the C8A level was also enhanced in patients with cancer-associated inflammation, suggesting that this complement protein is linked to the systemic inflammation promoted by CRC to facilitate metastasis from the primary tumor. More importantly, enhanced C5 was found in CRC patients' plasma, which was confirmed in the validation cohort. Increased C5 expression in colon tissue versus normal-matched tissue and its association with metastasis was recently reported in another study.³⁴ Proteomics analysis also revealed an enhanced level of a peptide corresponding to the C5A anaphylatoxin in examined CRC patients. Although there were no previous reports associating C5A with CRC, another complement anaphylatoxin, C3A, was proposed as a potential CRC diagnostic biomarker.³⁵ Moreover, several studies suggest that C5A may promote CRC tumorigenesis, metastasis, and immunosuppressive microenvironment within the tumor.³⁵⁻³⁷ However, further validation studies are needed to confirm the association between C5A plasma levels and CRC. Another enriched pathway in CRC patients was cholesterol metabolism, with 2 downregulated apolipoproteins APOA2 and APOA4, that were previously reported.³⁸ It was found that APOA2 polymorphisms were associated with CRC prognosis and might play a relevant role in disease development and progression.³⁹ These proteins were also related to metabolic syndrome which is a well-established CRC risk factor.⁴⁰

Interestingly, our analysis reported novel plasma protein changes associated with CRC development. For instance, serum amyloid A4 (SAA4), one of the major acute-phase reactants, was enhanced in CRC patients versus healthy individuals. The increased circulating levels of SAA have been linked to several inflammatory conditions including neoplasia.⁴¹ SAA4 was only detected in CRC tissue but not in normal tissue, suggesting a potential role in tumorigenesis.⁴² Another enhanced acute-phase response protein was LBP, which promotes cytokine release in response to bacterial lipopolysaccharide.⁴³ Noteworthy, our recently published study demonstrated the increased level of several pro-inflammatory cytokines in the same CRC cohort by proximity extension assay.⁴⁴ It was previously found that LBP polymorphisms were associated with CRC susceptibility⁴⁵ and high serum levels were associated with obesity.⁴⁶

Our analysis identified novel links between plasma protein levels in CRC patients and cancer-associated inflammation. The secreted glycoprotein A2GL, also called LRG1, was upregulated in CRC patients with positive inflammatory status and overall CRC patients versus healthy individuals.¹³ LRG1 was

also overexpressed in CRC tissue where it induced cancer proliferation.⁴⁷ Hence, it has been suggested that LRG1 plays an important role in CRC progression and may have an exacerbated pro-inflammatory effect in patients with cancer-associated inflammation due to its link to the acute-phase response.⁴⁸ Another enhanced protein in positive-inflammation CRC patients was CERU while higher levels in CRC patients versus healthy individuals were revealed in another study.⁴⁹ The metalloprotein CERU binds copper in plasma and is associated with inflammatory responses by promoting nitric oxide synthase activity and cytokine secretion.⁵⁰ On the contrary, this study found low levels of the retinol-binding protein 4 (RBP4), which is related to cancer-associated inflammation. Downregulation of RBP4 in CRC patients versus healthy individuals in serum and tumor tissue was previously reported.⁵¹ Other adipokines with antitumorogenic effects such as adiponectin (APOD) was also reduced in cancer patients and RBP4 may play a role in the reduction of inflammation.⁵² A lower level of APOD, a protein associated with cancer-associated inflammation, was also observed in our cohort. This blood transporter was inversely correlated with CRC tumorigenesis and was associated with early stages of CRC, however, further functional studies are needed to elucidate its role in CRC development.⁵³

A comparison early-stage and late-stage CRC patients revealed 4 potential biomarkers associated with cancer progression, including C4B, C8A, APOC2, and IGHG2. The lipoprotein metabolism regulator, APOC2, was found elevated in advanced stages of cancer for the first time, while it was previously described as a potential biomarker of CRC development.¹⁴ On the contrary, IGHG2 plasma levels were increased in CRC early stages and in patients with cancer-associated inflammation. The *IGHG2* expression was previously detected enhanced in cancer tissues of CRC patients but not in plasma.⁵⁴ Further analysis in larger cohorts will validate our findings to determine the suitability of these potential biomarkers to predict the cancer stage and the association with inflammation.

By using LC-MS/MS proteomics analysis, we quantified 138 plasma proteins in CRC patients and healthy subjects. However, the high dynamic range of proteins limited the quantification of proteins with low abundance. Moreover, due to the relatively low number of patients in the discovery CRC cohort, further validation of the novel potential biomarkers in a larger validation cohort by targeted MS techniques or other quantitative methods such as antibody-based strategies is required. The discovery cohort was also limited by the higher percentage of women, while CRC incidence is higher in men. Finally, CRC family history information and molecular expression profiles of the tumor were missing, which are relevant factors in CRC development and progression.

In this study, LC-MS/MS plasma proteomics application in CRC patients identified novel protein signatures compared to healthy subjects including complement proteins as well as proteins such as SAA4 and LBP associated with pro-inflammatory conditions. Importantly, we confirmed the enhanced levels of C5 in patients of a validation cohort as a potential diagnostic biomarker of CRC. Moreover, several proteins were linked to cancer-associated inflammation and tumor stages that may be prognostic biomarkers after further validation in larger cohorts to apply them in clinics to improve patient care.

11.5. References

1. Sung H, Ferlay J, Siegel RL, et al. Global Cancer Statistics 2020: GLOBOCAN estimates of incidence and mortality worldwide for 36 cancers in 185 countries. *CA Cancer J Clin.* 2021;71:209-249
2. Cervantes A, Adam R, Roselló S, et al. Metastatic colorectal cancer: ESMO Clinical Practice Guideline for diagnosis, treatment and follow-up. *Ann Oncol.* 2023;34:10-32.
3. Xi Y, Xu P. Global colorectal cancer burden in 2020 and projections to 2040. *Transl Oncol.* 2021;14:101174
4. Martins BAA, de Bulhões GF, Cavalcanti IN, et al. Biomarkers in colorectal cancer: the role of translational proteomics research. *Front Oncol.* 2019;9:1284.
5. Jenkins RW, Barbie DA, Flaherty KT. Mechanisms of resistance to immune checkpoint inhibitors. *Br J Cancer.* 2018;118:9-16.
6. Sirniö P, Väyrynen JP, Mutt SJ, et al. Systemic inflammation is associated with circulating cell death released keratin 18 fragments in colorectal cancer. *Oncoimmunology.* 2020;9:1783046.
7. Terzić J, Grivennikov S, Karin E, Karin M. Inflammation and colon cancer. *Gastroenterology.* 2010;138:2101-2114.e5.
8. Ladabaum U, Dominitz JA, Kahi C, et al. Strategies for colorectal cancer screening. *Gastroenterology.* 2020;158:418-432.
9. Young PE, Womeldorph CM. Colonoscopy for colorectal cancer screening. *J Cancer.* 2013;4:217-226.
10. Anderson NL, Anderson NG. The human plasma proteome: history, character, and diagnostic prospects. *Mol Cell Proteomics.* 2002;1:845-867.
11. Zhao Y, Xue Q, Wang M, et al. Evolution of mass spectrometry instruments and techniques for blood proteomics. *J Proteome Res.* 2023;22:1009-1023.
12. Kankanala VL, Mukkamalla SKR. Carcinoembryonic Antigen. StatPearls Publishing;2022. Accessed May 11, 2023. <https://www.ncbi.nlm.nih.gov/books/NBK578172/>
13. Peltier J, Roperch JP, Audebert S, et al. Quantitative proteomic analysis exploring progression of colorectal cancer: Modulation of the serpin family. *J Proteomics.* 2016;148:139-148.
14. Ahn SB, Sharma S, Mohamedali A, et al. Potential early clinical stage colorectal cancer diagnosis using a proteomics blood test panel. *Clin Proteomics.* 2019;16:1-20.
15. Chantaraamporn J, Champattanachai V, Khongmanee A, et al. Glycoproteomic analysis reveals aberrant expression of complement c9 and fibronectin in the plasma of patients with colorectal cancer. *Proteomes.* 2020;8:26.
16. Ivancic MM, Megna BW, Sverchokov Y, et al. Noninvasive detection of colorectal carcinomas using serum protein biomarkers. *J Surg Res.* 2020;246:160-169.
17. Filipowicz N, Drężek K, Horbacz M, et al. Comprehensive cancer-oriented biobanking resource of human samples for studies of post-zygotic genetic variation involved in cancer predisposition. *PLoS One.* 2022;17:e0266111.
18. Wiśniewski JR. Filter aided sample preparation – a tutorial. *Anal Chim Acta.* 2022;190:23-30.
19. Rappsilber J, Mann M, Ishihama Y. Protocol for micro-purification, enrichment, pre-fractionation and storage of peptides for proteomics using StageTips. *Nat Protoc.* 2007;2:1896-1906.
20. Liu Q, Niu X, Li Y, et al. Role of the mucin-like glycoprotein FCGBP in mucosal immunity and cancer. *Front Immunol.* 2022;13:863317.
21. Domínguez-Reyes T, Astudillo-López CC, Salgado-Goytia L, et al. Interaction of dietary fat intake with APOA2, APOA5 and LEPR polymorphisms and its relationship with obesity and dyslipidemia in young subjects. *Lipids Health Dis.* 2015;14:106.
22. Carmena-Ramon R, Ascaso JF, Real JT, et al. Genetic variation at the ApoA-IV gene locus and response to diet in familial hypercholesterolemia. *Arterioscler Thromb Vasc Biol.* 1998;18:1266-1274.
23. Hepner M, Karlaftis V. Antithrombin. *Methods Mol Biol.* 2013;992:355-364.
24. Sun HM, Mi YS, Yu FD, et al. SERPINA4 is a novel independent prognostic indicator and a potential therapeutic target for colorectal cancer. *Am J Cancer Res.* 2016;6:1636.
25. Tang L, Liu K, Wang J, et al. High preoperative plasma fibrinogen levels are associated with distant metastases and impaired prognosis after curative resection in patients with colorectal cancer. *J Surg Oncol.* 2010;102:428-432.
26. Gao F, Zhang X, Wang S, Zheng C. Prognostic impact of plasma ORM2 levels in patients with stage II colorectal cancer. *Ann Clin Lab Sci.* 2014;44:388-393.
27. Merle NS, Church SE, Fremeaux-Bacchi V, et al. Complement system part I—molecular mechanisms of activation and regulation. *Front Immunol.* 2015;6:262.
28. Jiang X, Bai XY, Li B, et al. Plasma inter-alpha-trypsin inhibitor heavy chains H3 and H4 serve as novel diagnostic biomarkers in human colorectal cancer. *Dis Markers.* 2019;2019:5069614.
29. Wågsäter D, Löfgren S, Zar N, et al. Pigment epithelium-derived factor expression in colorectal cancer patients. *Cancer Invest.* 2010;28:872-877.
30. Ji D, Li M, Zhan T, et al. Prognostic role of serum AZGP1, PEDF and PRDX2 in colorectal cancer patients. *Carcinogenesis.* 2013;34:1265-1272.
31. Ivancic MM, Huttlin EL, Chen X, et al. Candidate serum biomarkers for early intestinal cancer using 15N metabolic labeling and quantitative proteomics in the ApcMin/+ mouse. *J Proteome Res.* 2013;12:4152-4166.
32. Battistelli S, Stefanoni M, Lorenzi B, et al. Coagulation factor levels in non-metastatic colorectal cancer patients. *Int J Biol Markers.* 2018;23:36-41.
33. Yang Q, Roehrl MH, Wang JY. Proteomic profiling of antibody-inducing immunogens in tumor tissue identifies PSMA1, LAP3, ANXA3, and maspin as colon cancer markers. *Oncotarget.* 2018;9:3996-4019.

34. Chang H, Jin L, Xie P, et al. Complement C5 is a novel biomarker for liver metastasis of colorectal cancer. *J Gastrointest Oncol.* 2022;13:2351-2365.
35. Ajona D, Ortiz-Espinosa S, Pio R. Complement anaphylatoxins C3a and C5a: emerging roles in cancer progression and treatment. *Semin Cell Dev Biol.* 2019;85:153-163.
36. Ding P, Xu Y, Li L, et al. Intracellular complement C5a/C5aR1 stabilizes β -catenin to promote colorectal tumorigenesis. *Cell Rep.* 2022;39:110851.
37. Piao C, Zhang WM, Li TT, et al. Complement 5a stimulates macrophage polarization and contributes to tumor metastases of colon cancer. *Exp Cell Res.* 2018;366:127-138.
38. Voronova V, Glybochko P, Svistunov A, et al. Diagnostic value of combinatorial markers in colorectal carcinoma. *Front Oncol.* 2020;10:832.
39. Vargas T, Moreno-Rubio J, Herranz J, et al. Genes associated with metabolic syndrome predict disease-free survival in stage II colorectal cancer patients. A novel link between metabolic dysregulation and colorectal cancer. *Mol Oncol.* 2014;8:1469-1481.
40. Esposito K, Chiodini P, Capuano A, et al. Colorectal cancer association with metabolic syndrome and its components: a systematic review with meta-analysis. *Endocrine.* 2013;44:634-647.
41. Buck M, Gouwy M, Wang J, et al. Structure and expression of different serum amyloid A (SAA) variants and their concentration-dependent functions during host insults. *Curr Med Chem.* 2016;23:1725-1755.
42. Michaeli A, Finci-Yeheskel Z, Dishon S, et al. Serum amyloid A enhances plasminogen activation: implication for a role in colon cancer. *Biochem Biophys Res Commun.* 2008;368:368-373.
43. Heumann D, Gallay P, Betz-Corradin S, et al. Competition between bactericidal/permeability-increasing protein and lipopolysaccharide-binding protein for lipopolysaccharide binding to monocytes. *J Infect Dis.* 1993;167:1351-1357.
44. Urbiola-Salvador V, Jabłońska A, Miroszewska D, et al. Plasma protein changes reflect colorectal cancer development and associated inflammation. *Front Oncol.* 2023;13:1158261.
45. Chen R, Luo FK, Wang YL, et al. LBP and CD14 polymorphisms correlate with increased colorectal carcinoma risk in Han Chinese. *World J Gastroenterol.* 2011;17:2326-2331.
46. González-Sarrías A, Núñez-Sánchez MA, Ávila-Gálvez MA, et al. Consumption of pomegranate decreases plasma lipopolysaccharide-binding protein levels, a marker of metabolic endotoxemia, in patients with newly diagnosed colorectal cancer: a randomized controlled clinical trial. *Food Funct.* 2018;9:2617-2622.
47. Zhou Y, Zhang X, Zhang J, et al. LRG1 promotes proliferation and inhibits apoptosis in colorectal cancer cells via RUNX1 activation. *PLoS One.* 2017;12:e0175122.
48. Shirai R, Hirano F, Ohkura N, et al. Up-regulation of the expression of leucine-rich α 2-glycoprotein in hepatocytes by the mediators of acute-phase response. *Biochem Biophys Res Commun.* 2009;382:776-779.
49. Nayak SB, Bhat VR, Upadhyay D, et al. Copper and ceruloplasmin status in serum of prostate and colon cancer patients. *Indian J Physiol Pharmacol.* 2003;47:108-110.
50. Linder MC. Ceruloplasmin and other copper binding components of blood plasma and their functions: an update. *Metallomics.* 2016;8:887-905.
51. Fei W, Chen L, Chen J, et al. RBP4 and THBS2 are serum biomarkers for diagnosis of colorectal cancer. *Oncotarget.* 2017;8:92254-92264.
52. Raucci R, Rusolo F, Sharma A, Colonna G, Castello G, Costantini S. Functional and structural features of adipokine family. *Cytokine.* 2013;61:1-14.
53. Kopylov AT, Stepanov AA, Malsagova KA, et al. Revelation of proteomic indicators for colorectal cancer in initial stages of development. *Molecules.* 2020;25:619.
54. Boncheva VB, Linnebacher M, Kdimati S, et al. Identification of the antigens recognised by colorectal cancer patients using sera from patients who exhibit a Crohn's-like lymphoid reaction. *Biomolecules.* 2022;12:1058.

12. Publication VII: Proteomics approaches to characterize the immune responses in cancer

Published: (2022) *Biochimica et biophysica acta. Molecular cell research*, 1869(8), 119266.
<https://doi.org/10.1016/j.bbamcr.2022.119266>

Authors: Urbiola-Salvador V, Miroszewska D, Jabłonska A, Quereshi T, Chen Z.

12.1. Introduction

In 2020, according to the International Agency for Research on Cancer, over 19 million new cases and 10 million deaths caused by cancer were estimated to occur worldwide. Breast, lung, and colorectal cancer (CRC) were assigned as the most commonly occurring types of cancer [1]. There are many known risk factors of cancer, both independent from lifestyle e.g., genetic predisposition or random DNA mutation, and lifestyle dependent such as tobacco smoking habits, lack of exercise and obesity, exposure to radiation, or poor diet [2]. Despite some differences in the mortality rate due to cancer between developed and developing countries, undeniably this issue concerns the global population [1]. For some types of cancers, inflammation is associated with tumor development, either as a cause or a consequence of ongoing tumor growth. Regardless of the origin, the inflammation and immune cells in the tumor microenvironment (TME) play an important role in cancer development [3], [4]. Helper T (Th) cells, essential moderators of the immune response, exhibit a dual role in cancer progression and immunity. The cluster of differentiation (CD)4+ T cells orchestrate immune responses against tumors and can differentiate into different subsets within TME [5]. Th1 lymphocytes, as the main producers of interferon- γ (IFN- γ), play the major role in anti-tumor response by activating innate immune cells such as macrophages and natural killer (NK) cells, promoting proinflammatory phenotype of macrophages, and inducing expression of major histocompatibility complex (MHC) class II on the surface of antigen-presenting cells (APCs). In addition, Th1, via the production of IFN- γ , induce the differentiation of cytotoxic CD8+ T cells and inhibit T regulatory lymphocytes (Tregs) function [6]. Th2 lymphocytes are the key players in host immunity and tissue repair signaling. Signatory cytokines produced by Th2 cells, interleukin (IL)-4, IL-5, IL-9, and IL-13, participate in B cell proliferation and immunoglobulin E (IgE) production. They are also associated with the pathological states of chronic inflammation e.g., asthma [7]. Their role in cancer clearance has been linked with the recruitment of eosinophils, neutrophils, and macrophages at tumor sites via IL-4 signalling [8].

Another subset of CD4+ T cells, Th17, are the main producers of IL-17 and play a key role in the host defense against pathogens, especially in the gut [9]. Th17 cells have been linked with the induction of a protumor environment [10], however, preclinical and clinical studies demonstrate that Th17 cells contribute to the recruitment of effector cells such as neutrophils to TME [11]. Therefore, the role of Th17 in cancer progression remains controversial and requires further studies [12]. On the other hand, Treg cells are a subpopulation of T cells that are engaged in sustaining immunological self-tolerance and homeostasis. They can suppress and downregulate the immune response, as such, they participate in promoting the tumor favorable conditions [9], [13]. Moreover, Treg cells' phenotypic plasticity facilitates the conversion to different subsets with superior immunosuppressive activity such as IL-17 producing Treg and latent-associated peptide (LAP)+ Treg cells [14]. More recently, other novel T cell subsets such as Th9, Th22, and follicular Th cells have been suggested to affect the TME with controversial effects, regarding their anti-tumor or protumor activity [15], [16]. Despite the great advance in cancer immunology in the last few years, a better understanding of the TME heterogeneity and the complexity of immune cell interactions is needed.

Cancer immunotherapy with monoclonal antibodies (mAbs) that block the interaction of programmed cell death protein 1 (PD-1) with its ligand PD-L1 has shown clinical response in a wide range

of solid and hematological cancers [17]. However, only a minority of patients exhibit dramatic positive responses. The low response rate can be linked to other immunosuppressive mechanisms and an array of factors affecting immunotherapy effectiveness such as tumor genomic instability, immune phenotype, level of inflammation, microbiome, T cell memory, or even sunlight exposure [18]. Therefore, a comprehensive understanding of the role of T cells in TME is needed to discover novel targets and biomarkers for the effective treatment of cancer.

High-dimensional and high-throughput techniques are promising tools in unraveling this issue [19]. Omics-based strategies such as transcriptomics have been applied to uncover the immune surveillance mechanisms and immune profiling in various cancer types [20], [21], [22], [23]. However, the knowledge about the mechanism of gene regulation at the posttranscriptional, translational, and posttranslational levels is still limited. Poor levels of concordance between changes in protein abundance and mRNA expression have been reported, especially in CD4+ T cells [24], [25]. Therefore, with steady progress in proteomics technology, proteomics analyses can provide a more comprehensive view of T cells' fate in cancer progression through simultaneous detection, identification, and quantification of thousands of proteins in a single study. In particular, tandem mass spectrometry (MS) coupled with liquid chromatography (LC-MS/MS) provides an integrated system for proteomics analysis with improved sensitivity and moderate throughput [26], [27].

Nowadays, two basic proteomics strategies are commonly used in cancer research: MS-based and antibody-based. Bottom-up proteomics is currently the predominant MS-based strategy, which is applied to discovery research aiming at the deep identification of a given proteome in an exploratory and unbiased manner. In contrast, antibody-based strategies are widely used in targeted approaches, which can detect preselected proteins from a given sample, ideally, with high sensitivity, selectivity, quantitative accuracy, and reproducibility. However, antibody-based approaches are limited by the number of proteins that can be detected simultaneously and the availability of antibodies. MS-based strategies can potentially detect hundreds or thousands of proteins to establish novel biomarkers, potential drug targets, and other research efforts [28]. So far, neither of the two strategies has achieved the detection of the whole proteome. In this review, we focus on different proteomics approaches, including antibody-based and MS-based strategies, for immune characterization of cancer states with an emphasis on CD4+ T cells. Finally, we will present novel single-cell proteomics approaches with great potential in cancer immunology.

12.2. A brief overview of proteomics

Proteomics is a large-scale analysis of the sum of proteins from an organism, tissue, cell, or biofluid [29]. Clinical proteomics aims at understanding how their abundance, expression, localization, posttranslational modifications (PTMs), and molecular interactions cause disease to improve patient care [30]. Various protein identification techniques have been applied to study proteins involved in cancer formation and progression such as flow cytometry (FC), mass cytometry (MC or CyTOF; cytometry by time-of-flight) [31], [32], and immunohistochemistry (IHC) [33]. However, these strategies are limited by their multiplexing capacity and the availability and quality of specific antibodies [27].

Bottom-up proteomics is currently a predominant strategy that utilizes protein digestion before MS analysis. The general sample preparation workflow in bottom-up proteomics (Fig. 12.1) consists of protein extraction, solubilization with detergents, reduction of disulfide bonds, alkylation of free cysteines, and lastly enzymatic digestion (normally trypsin) conducted in-solution or filter-aided. Then, obtained peptides are desalted with reversed phase C18 tips [34], [35]. This workflow can be combined with fractionation steps at protein and peptide levels with different biochemical approaches such as two-dimensional electrophoresis (2-DE), strong cation exchange, or enrichment of peptides with PTMs (e.g., phosphorylation, acetylation, glycosylation) [36]. The resulting mixtures of peptides are identified and quantified in the mass spectrometer by the analysis of mass-to-charge ratios of molecular ions.

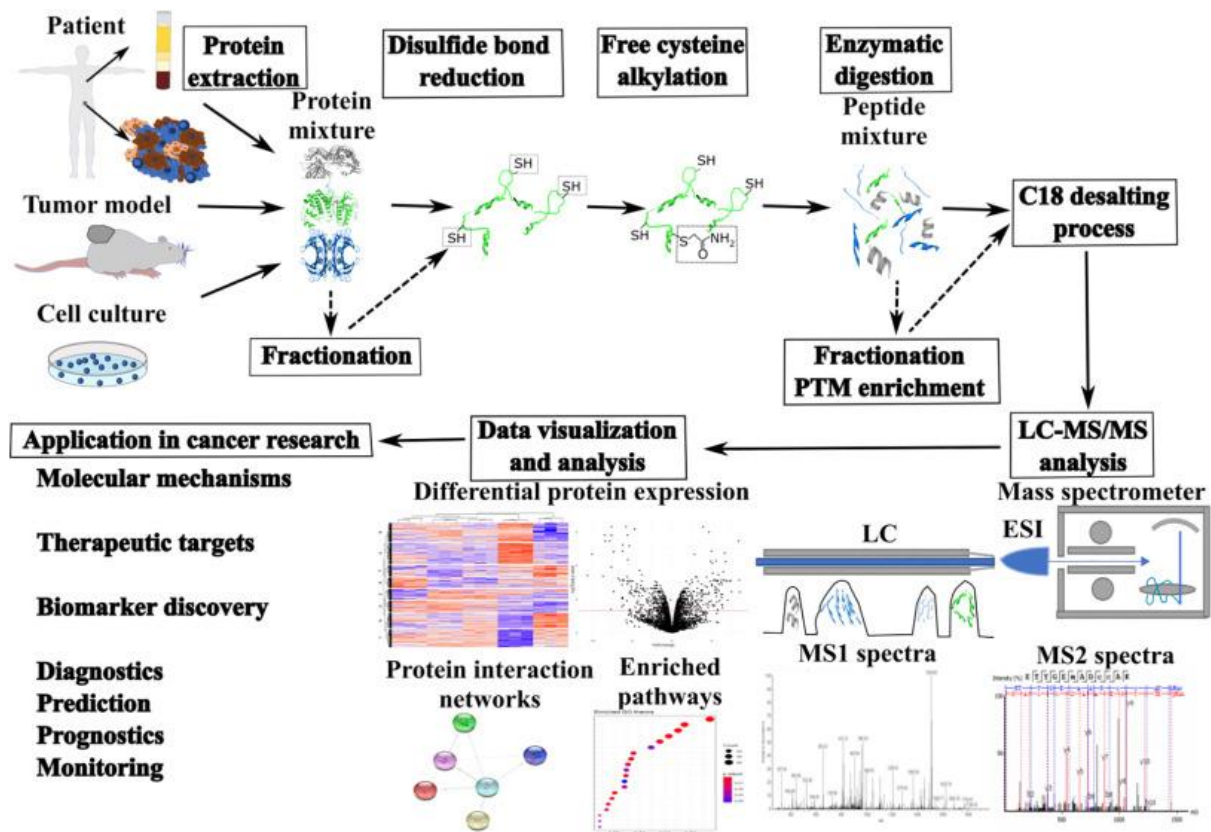


Figure 12.1. Bottom-up proteomics workflow. Protein mixtures are extracted from patient samples, tumor model samples, or cell culture. Proteins are solubilized, disulfide bonds are reduced, free cysteines are alkylated, and proteins are digested with enzymes. Alternatively, proteins and peptides can be fractionated or enriched in posttranslational modifications (PTMs). Peptide mixture is desalted with reversed phase C18 tips and prepared for tandem mass spectrometry coupled with liquid chromatography (LC-MS/MS) analysis. LC separates peptides that are ionized by electrospray ionization (ESI) and analyzed in the mass spectrometer, generating MS1 and MS2 spectra. Data visualization and analysis allow the identification and quantification of differentially expressed proteins as well as the identification of enriched pathways and protein interaction networks. Proteomics analysis has several applications in cancer research such as the discovery of underlying molecular mechanisms, therapeutic targets, and biomarkers as well as improvement of diagnostics, prediction, prognostic, and therapy monitoring.

LC-MS/MS has revolutionized proteomics because of the great advances in reproducibility, high resolution, high mass accuracy, improvement of scanning modes, and excellent sensitivity. The combination of nano-LC technology or capillary electrophoresis with electrospray ionization (ESI) enables the identification and quantification of thousands of proteins from one single injection in high-resolution mass spectrometers [27], [37], [38]. This progress in clinical proteomics accelerates the study of the underlying mechanisms of cancer as well as biomarkers discovery and, at the same time, improves diagnostic, prediction, prognostic, and monitoring efficacy of novel immunotherapies [26], [39], [40].

MS Imaging is a cutting-edge technology that incorporates matrix-assisted laser desorption/ionization time-of-flight (MALDI-TOF) with micrometer laser beams that shed on frozen or Formalin Fixed Paraffin-Embedded (FFPE) tissue samples. Each laser-excited spot generates ionized proteins/peptides which are generally identified by MALDI-TOF. Thus, tissue images are generated via a raster scan in which each spot is associated with its mass spectrum, providing the spatial distribution and relative abundance of the analytes over the entire tissue section [41]. MS Imaging is mostly non-destructive and can be combined with histological staining to study regions of interest or digital PCR [42], [43]. This technique can resolve the complexity of spatial protein patterns and other biomolecules (lipids, glycans, and metabolites) within the TME in an untargeted manner [44], [45], [46], [47]. Interestingly, recent technical advances in laser resolution enable the measurement of analytes at the single-cell level [48].

However, its wider application is currently limited by the required heavy instrumentation, non-standardized workflows, and its suboptimal quantification capability [49].

Another approach is top-down proteomics that identifies intact proteins by the combination of different protein separation techniques with LC-MS/MS, where the proteins are ionized and subsequently fragmented. However, the sensitivity is about 100-fold lower than bottom-up proteomics with lesser proteomic coverage and throughput due to its lower efficiency to fragment intact proteins [50], [51].

12.3. MS-based proteomics approaches applied to study immune responses in cancer

Upregulation of immune checkpoints (IC) such as cytotoxic T cell antigen-4 (CTLA-4) and PD-1 molecules within the TME is considered as the major immunosuppressive mechanism that inhibits effector T cell functions [52]. Apart from that, the TME is enriched in soluble factors such as tumor growth factor- β (TGF- β), IL-10, and CD73-derived adenosine which potently suppress T cell anti-tumor functions and promote the conversion of naïve CD4+ T cells into Tregs [53], [54]. Moreover, metabolic restriction of T cells by nutrient competition from tumor cells inhibits effector T cell anti-tumor functions [55]. MS-based discovery proteomics can contribute to elucidating the most relevant proteins, molecular mechanisms, and pathways involved in immunosuppression, which will lead to the identification of novel targets for potential immunotherapy. This section describes various MS-based proteomics approaches and their application in the analysis of the immune responses in cancer by characterization of T cells, the tumor-infiltrating lymphocytes (TILs) as well as biofluids in mice models and clinics.

12.3.1. The potential of MS-based proteomics approaches in preclinical cancer model studies for discovery research

Preclinical studies in mice models are an essential milestone towards novel therapeutic strategies in humans as well as to uncover molecular mechanisms involved in the disease progression. Despite the great potential of proteomics to discover novel therapeutic targets, proteomics analysis has not been broadly applied in mice models in the research field of cancer immunology. Interestingly, a few bottom-up proteomics studies exemplify its ability to characterize T cells originating from spleen and lymph nodes in cancer mice models, providing novel insights in this field. For instance, proteomics analysis of T cells in a mice model of colitis-associated colorectal cancer (CAC) demonstrated that sirtuin 5 (SIRT5) downregulates numerous proteins related to the T cell receptor signaling pathway and enhances immunosuppressive Treg cell differentiation. However, further studies are needed to evaluate the broader role of SIRT5 in cancer immunotherapy. In addition, bottom-up proteomics analysis can be applied to reveal PTMs involved in tumor immunosuppression. MS-based proteomic analysis of SIRT2-immunoprecipitated proteins and acetyl-lysine peptides demonstrated that SIRT2 suppresses key metabolic enzymes by deacetylation in T cells, promoting a T cell exhausted phenotype. These findings were validated in melanoma and lung cancer mice models as well as in vitro in T cells originating from healthy donors and TILs isolated from non-small cell lung cancer patients, which revealed that pharmacologic inhibition of SIRT2 can enhance cancer immunotherapies [56]. Interestingly, the sirtuins family has been associated with cancer progression and metastasis through different mechanisms [57], [58], [59]. Application of bottom-up proteomics in an arginase 2 (*Arg2*)^{-/-} T-cell-specific knock-out in CRC and melanoma xenograft models discovered the immunosuppressive function of mitochondrial ARG2 in CD8+ T cells. *Arg2*-deficient CD8+ T cells were synergized with PD-1 blockade, unveiling the potential application of ARG2 inhibition as novel immunotherapy [60]. Bottom-up proteomics has also been applied to study the immune response to treatment in a breast cancer mice model. Shotgun MS analysis of mice serum revealed that cryo-thermal therapy induces acute phase response with IL-6 activation, promoting Th1 anti-tumor activity [61].

Application of shotgun proteomics in hyperactive platelets derived from CAC mice revealed an increased level of protumor serum amyloid A (SAA) proteins, suggesting a novel target to treat CAC patients at early clinical stages, or even to prevent cancer development [62]. Also, bottom-up proteomics analyzed extracellular vesicles (EVs) from tumor-associated macrophages (TAMs) derived from a CRC mouse model. Surprisingly, TAM-EVs possessed a proteomic signature that was associated with inflammation and immune response through Th1/M1 macrophage polarization [63]. Both studies show the broad application of MS-based proteomics in the analysis of innate immune cells which influence the cancer immune response.

The abovementioned studies show the potential application of MS-based proteomics in preclinical cancer mice models to understand molecular mechanisms involved in immunosuppression, in the studies on the effect of therapies at the protein level as well as in the discovery of novel therapeutic targets for immunotherapy. However, instead of inferring their activity from peripheral blood, further proteomics analysis of TILs will provide more valuable information of T cell functions within the TME.

12.3.2. MS-based proteomics application in clinical studies to characterize cancer immune responses

The advancement of shotgun MS-proteomics enables better characterization of TILs in clinical samples. First step towards this goal was the development of the simple and integrated spin tip-based proteomics technology (termed SISPROT) combined with laser-capture microdissection technology (LCM) [64]. LCM-SISPROT provided spatial proteome profiling of cancer cells, enterocytes, lymphocytes, and smooth muscle cells of both normal and CRC tissue obtained from the same patient. Each cell type possessed an individual proteomic signature such as immune processes enrichment in lymphocytes. Interestingly, the spatial proteomic composition from the same cell type showed expression fluctuations across micrometer spatial distance which highlights the heterogeneity of TME [64]. This proof-of-concept study demonstrates the technical advancement towards high-throughput proteomics characterization of TILs. The next step is the application of LCM combined with shotgun proteomics in studies of clinical importance. For instance, this approach has been recently applied to compare the proteomes of microdissected TILs from 3 metastatic melanoma patient samples (IFN- γ -high, lymphocyte activation gene-3 (LAG-3)-high, and none), showing that only the IFN- γ -high sample was enriched in different inflammatory pathways [65].

It is well known that tumor-secreted factors and exosomes enrich immunosuppressive cells within the tumor-draining lymph nodes, leading to defective local T cell priming [66], [67]. Further characterization of the tumor-draining lymph node cellular and protein composition is needed to release T cell inhibition and to develop potential immunotherapy. MS-based proteomics has been recently applied to characterize the pathophysiology of perfused breast cancer patient-derived axillary lymph nodes (ALNs) sustained *ex vivo* using normothermic perfusion [68]. Neutrophil degranulation and extracellular matrix degradation pathways were enriched in metastatic ALNs compared to reactive ALNs. Similar results of enriched pathways were observed in metastatic lymph nodes from pancreatic ductal adenocarcinoma and prostate cancer [69], [70]. These studies demonstrate that MS-based proteomics is a powerful tool to characterize biofluids such as perfusates from tissue, facilitating the protein characterization of lymph nodes. MS-based shotgun proteomics analysis has also been applied to study the cellular composition of tumor-draining lymph nodes, such as Treg cells from Sentinel Nodes (SN) compared to non-SN Tregs in bladder cancer patients [71]. It was found that SN-resident Tregs were enriched in growth and immune signaling pathways with IL-16 playing a central role. Moreover, Treg cells *in vitro* exposition to tumor secretome increased the IL-16 processing into its bioactive form through caspase-3 activation, reinforcing Treg suppressive capacity [71].

Currently, MS imaging has been applied to study the protein heterogeneity as well as spatial pattern in multiple solid tumors, focusing on sub-histological classification as well as the discovery of new candidate biomarkers [72], [73], [74], [75]. In breast cancer patients' samples, MS imaging revealed a correlation between high intra-tumor heterogeneity, high level of TILs, and better prognosis [76]. These

findings suggest that unveiling the proteome heterogeneity is crucial for defining the extent of cellular heterogeneity within the TME. In recent years, MS imaging has been approved as a powerful tool to characterize immune cell population changes and to identify protein signatures in response to immunotherapy. Berghmans et al. [77] used MS imaging to measure anti-PD-L1 immunotherapy response in non-small cell lung cancer patients. Downstream analysis and IHC validation demonstrated that neutrophil defensins-1, -2, -3 are predictive biomarkers associated with a positive immunotherapy response. Indeed, *in vitro* experiments showed that these defensins activate immune cells against cancer cells. Importantly, MS imaging can be combined with LCM and subsequent bottom-up/top-down proteomics to facilitate the identification of putative proteins within the TME [78], [79]. This combination revealed that the proteomes from TME cell subpopulations are associated with unique molecular signatures in breast cancer [78]. This proof-of-concept study demonstrates that the combination of proteomics approaches can reveal TME proteomics heterogeneity.

Top-down proteomics has not been widely applied to cancer immunological research but several studies exemplify the potential of this technique. Generally, top-down proteomics is combined with bottom-up proteomics or MS imaging. On one hand, top-down/bottom-up proteomics has been used to identify potential biomarkers in prostate cancer [80] and pediatric brain cancers [81], [82], [83] as well as to investigate the proteome landscape of breast cancer patient-derived mouse xenograft models [84]. Bottom-up proteomics has a higher coverage of the proteome, while top-down facilitates the identification of proteoforms with specific PTMs. These studies highlight the benefit of the integration of both approaches. On the other hand, combination of top-down proteomics and MS imaging can identify the spatial patterns of protein products from alternative Open Reading Frames within the TME. This integrative approach can detect potential biomarkers that were not considered before. Interestingly, top-down proteomics also facilitates the identification of protein complexes [85], novel quaternary structures [86], and tumor mutant proteoforms [87].

In summary, MS-based proteomics has been widely applied in cancer immunology research. Studies have approved that novel insights into the current understanding of tumor-mediated immunosuppression have been gained by using these technologies. Systematic untargeted proteome characterization of different T cell subsets, other cell subtypes within the TME, and biofluids will facilitate the discovery of novel biomarkers and therapeutic targets to overcome tumor-mediated suppression of effector T cell activation.

Despite these great advances, several technical challenges must be addressed. MS-proteomics does not provide the full sequence of a protein but rather relies on the identification of unique peptides from a protein. Its sensitivity is limited by the number of acquired spectra to identify a specific peptide [88]. However, an average of 75% of collected spectra can remain unidentified [89]. This lack of sensitivity limits the dynamic range of mass spectrometers as well as the identification of low abundant proteins, especially in clinical samples such as serum, in which the dynamic range can overpass 10 orders of magnitude [90]. Once a peptide is correctly identified, another challenge is the identification of different isoforms of the protein, called proteoforms. These proteoforms are generated by posttranscriptional processing and PTMs, yielding multiple proteoforms from the same canonical amino acid sequence [91]. Despite the development of PTMs enrichment strategies, identification of modified peptides arises more complications due to their lower abundance, lower ionization and fragmentation efficiency, inaccurate mass determination, confusion with the assignment of residue substitutions, and uncertainty in the PTM site assignment [92], [93]. Lastly, the high cost of MS instrumentation as well as the level of expertise required to perform MS-proteomics hinders its wider usage.

12.4. Antibody-based technologies to characterize immune responses in cancer

MS-based proteomics is widely used in discovery proteomics while antibody-based approaches are the most widely chosen for targeted proteomics, although the number of simultaneously detected proteins is limited. One of the main challenges in cancer immunology is to find novel biomarkers to guide the choice of therapeutic strategies to maximize patient benefit. Predictive biomarkers for immunotherapy require a more holistic approach with panels of biomarkers to identify the underlying biology and complexity of the tumor immune response [94]. Recently developed antibody-based detection techniques can detect from tens to hundreds of proteins simultaneously, being a powerful tool to identify these panels of biomarkers. Multiplex immunoassays utilize antibodies as anchors that are immobilized on a solid surface or the surface of beads. In both, the protein of interest is bound to the specific antibody. This technology enables simultaneous detection and quantitation of tens of proteins. It is a powerful tool, especially for the detection of secreted proteins, such as cytokines and growth factors from a limited amount of biological and clinical materials. For example, this technique was applied to study the correlation between 59 serum-derived proteins and response to immunotherapy in gastrointestinal cancers. As a result, protein signatures characterized by higher levels of IC molecules, namely PD-L1, CD28, immunoglobulin and mucin domain 3 (TIM-3), LAG-3, and CTLA-4, correlated with better prognosis and higher response, being a promising panel of predictive biomarkers [95]. In addition to detecting proteins from serum or plasma samples, recently, this technique has been applied to characterize inflammation-involved proteins in CRC tumors and matched normal tissues, providing a panel of 32 biomarkers differentially expressed in CRC tumors [96].

Another antibody-based technology, Proximity Extension Assay (PEA) further extends the number of detected proteins from tens to hundreds and even thousands. The technology is based on target-specific antibodies conjugated with unique complementary DNA. The antibody pairs targeting one protein bind to the target and a barcoded DNA duplex is formed, which is amplified by qPCR or next-generation sequencing (NGS), allowing quantification of up to 3072 proteins [97], [98]. In a recent study, the oncology panel of PEA with 92 cancer-related proteins was utilized to identify potential circulating tumor biomarkers for meningioma. The pathway analysis revealed upregulation of immunomodulatory proteins such as CD69, CC motif chemokine 24 (CCL24), IL-24, CCL9, and B-cell activating factor (BAFF) [99]. In another study, the PEA immune-oncology panel was applied to study the serum/plasma proteomic profiles of pancreatic neuroendocrine neoplasms patients. Many well-known immune regulators, such as CCL3, IL-7, IL-10, CCL20, were significantly elevated in patients compared to healthy controls, whereas FAS ligand (FASLG) was downregulated [100]. The PEA technology has shown a promising potential to detect chemokine variability within metastatic melanoma patients subjected to anti-PD-1 therapy [101]. Likewise, it has also been used to assess the immune profile of chronic lymphocytic leukemia patients undergoing different treatments. [102]. PEA analysis of 29 CRC tumors using the immune-oncology panel resulted in only 9 tumors clustered together in unsupervised hierarchical clustering, which revealed the intra-tumor TME heterogeneity [103]. PEA technology possesses a validated specificity and sensitivity (sub-pg/ml) which allows multiplexed protein detection, consuming a minimal amount of sample. Further progress will have a powerful impact on the discovery of new diagnostic, predictive, prognostic, and monitoring biomarkers as well as on the understanding of the proteome of cancer patients [104].

Moreover, other antibody-based proteomics techniques, such as Reverse Phase Protein Arrays (RPPA) [105] and chip array cDNA-based Nucleic Acid Programmable Protein Array (NAPPA) [106] have been applied in cancer immunology research. RPPA has been used to correlate the tumor heterogeneity and immune response in melanoma patients [107], while NAPPA to analyze tumor autoantibodies in CRC patients [108]. However, antibody-based approaches are limited by the availability and the specificity of antibodies that implies cross-reactivity. Another disadvantage is the variability

between batches, especially when the antibody is produced in a new population of antibody-producing animals [109]. Most importantly, these approaches only detect limited numbers of preselected proteins.

12.5. Emerging single-cell proteomics applied to characterize the immune TME

The interplay between cancer cells and their microenvironment plays an important role in many cancer-related biological processes, including progression, metastasis, drug resistance as well as immune response. These complex cellular interactions of the TME and cancer cells are driven by cell heterogeneity [110], [111]. Therefore, to develop more effective immune therapies, it is fundamental to understand the interaction between immune and cancer cells. Single-cell protein measurements rather than a conventional bulk analysis can provide more precise information on this heterogeneity. This section reviews the different single-cell proteomics strategies applied or with potential application in cancer immunity and immune cell characterization. The following section includes a short description of antibody-based approaches, MS-based approaches, and multi-omics strategies applied to cancer immunity at the single-cell level.

12.5.1. Antibody-based approaches

For the past 30 years, FC has become the ‘gold standard’ in marker analysis at the single-cell level. Despite its popularity, this method is limited to a low number of markers for simultaneous analysis due to overlapping fluorescence spectra [112], [113]. A recently developed modification of traditional FC, full spectrum flow cytometry (FSFC) overcomes the issue of overlapping fluorescence spectra of fluorophore-conjugated antibodies, as the detection and measurement include an entire fluorescence spectrum. This enables the simultaneous detection of up to 64 proteins [114]. This technique has been applied to characterize specific cells populations within the TME. For instance, FSFC with over 30 markers found a tumor favorable environment formation caused by arginine-metabolizing myeloid cells co-localized with CD4+ T cells of unconventional phenotype in neuroblastoma mice models [115]. FSFC was applied to characterize the immune cells populations in syngeneic melanoma, breast, ovarian, and CRC cancer models with the focus on Tim-3 as a focal molecule [116]. Comparable higher cytolytic activity of Tim-3+PD-1+CD8+ TILs lead researchers to conduct the validation of combined treatment with Tim-3/PD-1 mAbs which indicated an enhanced anti-tumor effect [116].

By the combination of features of FC and MS, MC (CyTOF) has been developed to overcome the limitations of simultaneous analysis of up to 100 proteins at the single-cell level. In this method, cells are stained with metal isotope-tagged antibodies and separated in a mass cytometer, followed by TOF analysis of isotopes mass ratio in the analyzed samples. MC has been successfully applied in the study of the immune signature and immune response in cancer and exhibits potential in the discovery of novel cell populations in different types of cancer [117], [118], [119], [120], [121], [122], [123], [124], [125]. For example, MC and RNA-seq analysis of tumor and peripheral blood mononuclear cells (PBMC) of CRC patients revealed that exhausted T cells are induced and recruited by the TME at all stages of the tumor development, demonstrating the link between immunosuppressive TME and the lack of immunotherapy response [117]. This study demonstrated the superiority of MC analysis of TME over RNA-seq to characterize the single-cell proteome state. Interestingly, another CyTOF study identified a novel specific population of effector Tregs with protective function in CRC tumors [118]. In glioblastoma (GBM), MC provided data confirming the inter- and intra-tumor heterogeneity of glioma-associated macrophages (GAM). Moreover, the proportion of GAMs was decreased and exhausted T cells and Tregs were increased in recurrent tumors, contributing to the immunosuppressive environment [119]. In xenografts GBM models, MC was utilized as a comparative tool of immune landscape between tumor-silent and tumor-active models revealing distinct differences in the cells profiles [120]. Additionally, cell barcoding in MC enables sample multiplexing which is a very useful option when dealing with valuable clinical samples and low

amounts of murine tissue samples. Recently, MC has been successfully applied in high-throughput clinical analysis, where multiple samples have been analyzed with more than 35+ isotope tags [121].

Further advances in antibody-based proteomics utilize the combination of already established antibodies properties and application with microchips or microfluidics to perform proteomic analysis in isolated single cells. Single-cell barcode chips (SCBC) separate single cells in microchambers and secreted or intracellular proteins are captured on an antibody array. Then, captured proteins undergo the staining and quantification with the corresponding biotinylated antibodies and fluorescent streptavidin [126]. Advances in this technology led to the development of a commercial platform that quantifies a panel of 40 key secreted proteins from a single, viable cell [127]. Among other applications, this platform was used to study the heterogeneity of CD8+ TILs in metastatic melanoma patients [128].

Multiplexed in situ targeting (MIST) technology uses microbeads hybridized with antibodies conjugated to single-stranded DNA. Once the secreted target proteins are captured, an ELISA assay with the usage of a second, complementary DNA-conjugated antibody is performed [129]. Both technologies, SCBC and MIST, have to compromise the multiplex capacity and detection sensitivity, i.e. increasing the number of different antibodies can increase the multiplexing capacity but, in parallel, decrease the amounts of particular antibodies used, decreasing the sensitivity [130]. Antibody barcoding with cleavable DNA (ABCD) is the next technology that improves multiplexing capacity by utilizing antibodies linked to a unique DNA barcode via a photocleavable linker. DNA barcodes are released after incubation by UV exposition and are quantified by fluorescence hybridization [131]. Moreover, ABCD allows simultaneous analysis of hundreds of proteins from cancer cells and it was applied to characterize lung cancer cells from minimally invasive fine-needle aspirates [132].

TME heterogeneity does not only rely on the different cell types but also their spatial distribution and cell-cell interactions [133]. Whereas previous techniques analyze proteins in isolated single cells, the next antibody-based strategies are focused on comprehensive protein profiling in their natural spatial contexts. Multiplex immunofluorescence (mIF) is based on cycles of antibody staining, imaging, and antibody removal in tissue slides. This method allows the simultaneous identification of several immune markers in the same cell providing data about both the expression and location of target proteins (Fig. 13.2A). A combination of tissue microarrays with mIF has been optimized (e.g., for TME immune profiling) [134]. Gerdes et al. [33] applied mIF to analyze 61 proteins in CRC, revealing extensive tumor heterogeneity. Recently, mIF has been used to unveil the immune heterogeneity within the TME of melanoma and breast cancer ALNs [65], [68].

Since the specific intracellular localization of the proteins is essential to performing their biological function(s), while localization abnormality may severely disrupt biological processes causing disease, characterization of protein expression as well as its localization in a high resolution is needed. Single-cell spatial proteomics aims at solving this problem in a comprehensive manner (reviewed in [135], [136]). An mIF technique called Multi-Epitope Ligand Cartography (MELC) uses an automated microscopic robot that allows multiplexed protein characterization at subcellular level. In a pioneering work, MELC was applied to identify changes in key immune function-related proteins in CRC tissue at subcellular level [137]. In this study, 1930 clusters of proteins distinguished CRC from healthy tissue, and CRC tissue was enriched in T cells with altered T cell adhesion and NK cells with high nuclear factor-kappa B (NF- κ B) expression. Later, Bhattacharya et al. [138] used Toponome Imaging System, a similar mIF strategy, to compare CRC with a normal colon. 5708 clusters of proteins that are specific to colon cancer were identified, showing that CRC has a unique higher-order toponomy signature.

Since the application of mIF techniques carries a risk of damaging the epitopes' integrity, oligonucleotide conjugated antibodies alternatives have been explored [139], [140], [141]. CO-Detection by indEXing (CODEX) iteratively visualizes targets through in situ polymerization-based indexing procedure with oligonucleotide-conjugated barcodes and dNTPs analogs tethered to fluorophores (Fig. 13.2B) [142]. CODEX has been applied to study the immune TME of CRC with 56 markers, showing the

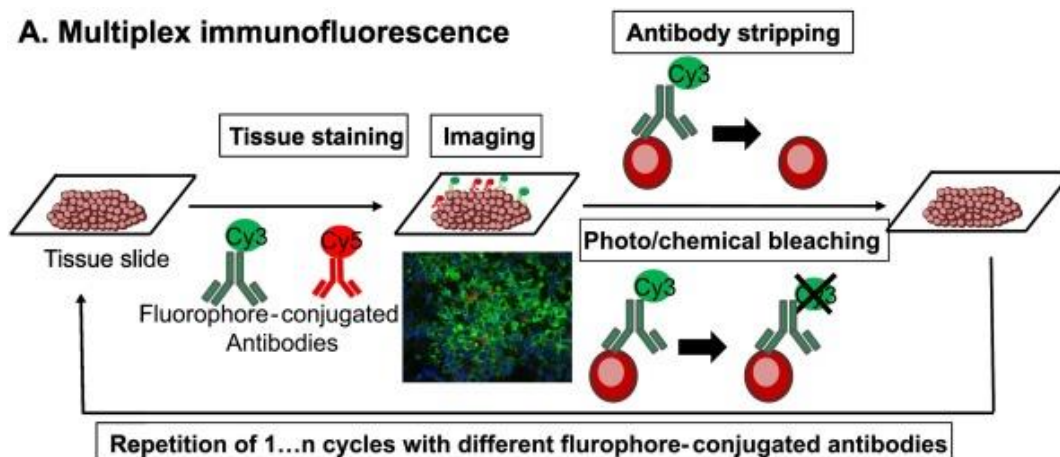
importance of the spatial distribution and cell neighborhoods in CRC [143]. Despite the recent advances in multiplexed analysis, it was found that oligonucleotides negatively affect the specificity and the binding affinity of antibodies. To avoid this interference, other alternatives are used e.g., removable antibodies with fluorophores linked by an azido group [144].

In the context of cancer immunology, imaging mass cytometry (IMC) and multiplexed ion beam imaging (MIBI) are powerful tools to assess the complexity of the TME and networks of cell-cell interactions in their spatial context within the tissue. IMC is a technology that combines CyTOF (MC) and imaging to analyze proteins in situ (Fig. 12.2C). First, the tissue slide is stained with a panel of metal conjugated antibodies and then the stained tissue is converted to a stream of particles pixel-to-pixel by a laser. Next, the mass spectrometer determines and quantifies the metal isotopes linked to the antibodies in each particle and, finally, a computational algorithm combines the MS data of each pixel with its coordination information to generate a two-dimensional image [145]. IMC not only provides information on single-cell proteomics but also on the localization of the particular protein in the tissue and constructs the cellular interaction within the TME. This methodology gives additional data potentially relevant in the context of prognosis or treatment. IMC analysis with 35 biomarkers of patients' breast tumors samples, together with available survival data, yielded high-dimensional images providing information on the complexity of organization of tumor and stromal cells, their location within the tissue, and distinct phenotypes of tumor cells. This study led to the proposal of novel breast cancer subgroups closely related to the particular patient's prognosis [146]. IMC was also used to explore the TME of different cancer types including Hodgkin lymphoma, and CRC, in which tertiary lymphoid structures in CRC were found to have abundant forkhead box P3 (FoxP3)+ Treg expression, demonstrating its potential for immune profiling in tumors [147].

The second technology, MIBI is a variation of IMC which operates an ion beam to release metal ion reporters, therefore increasing its multiplexing capacity to more than 100 targets at once [148]. An interesting application of MIBI is single-cell metabolic regulome profiling, which enables to study the composition of the metabolic regulome in combination with phenotypic identity with more than 110 antibodies against metabolite transporters, metabolic enzymes, or regulatory modifications. The study revealed the metabolic heterogeneity and spatial organization of CD8+ T cells in CRC, including subsets expressing the T cell exhaustion-associated molecules CD39 and PD-1, indicating their exclusion from the tumor-immune boundary [149]. Undeniably, IMC and MIBI are superior methods to fluorescence-based technologies because they detect simultaneously targeted proteins with a higher dynamic range avoiding staining/stripping cycles that can compromise epitope integrity [150]. However, their disadvantage is the availability of the number of antibodies conjugated with metal isotopes suitable for FFPE and fresh frozen tissue staining [151].

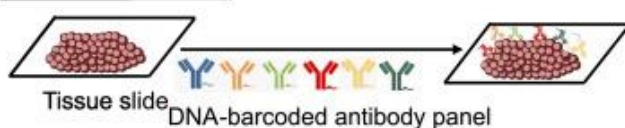
In summary, the bottleneck of single-cell measurements with antibodies is the limit of sensitivity, which stems from the molecular shot noise, limiting accurate quantification to the low attomolar (aM) range, as well as the quality of the antibody [152].

A. Multiplex immunofluorescence

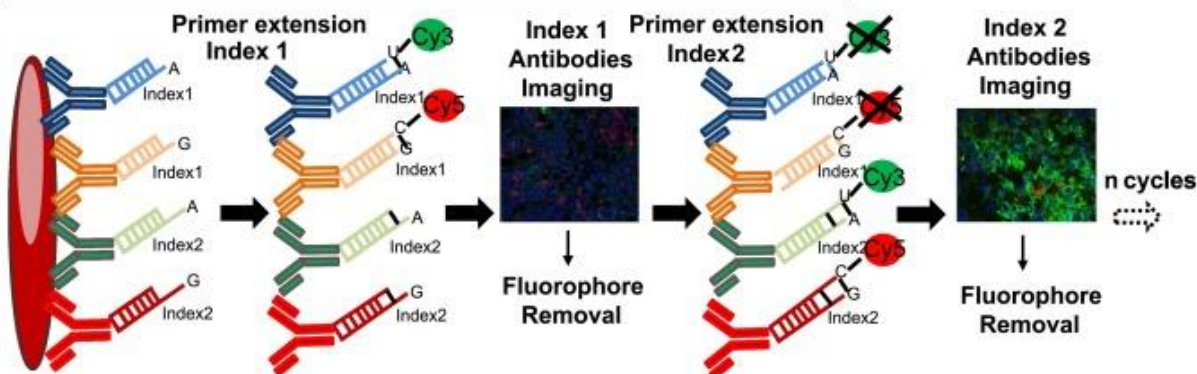


B. CO-Detection by indEXing (CODEX)

1. Tissue staining

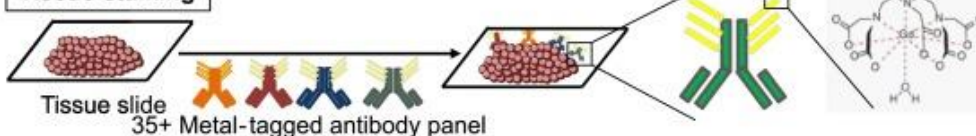


2. Revealing by primer extension, imaging, fluorophore removal cycles

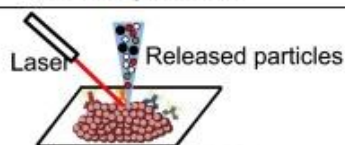


C. Imaging Mass Cytometry (IMC) and Multiplexed Ion Beam Imaging (MIBI)

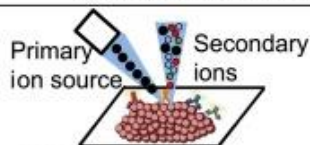
Tissue staining



IMC: Ablation of tissue with laser beam releases particles



MIBI: Rastering of tissue with primary ion beam releases secondary ions



Pixel-based quantification of ions by Time-of-Flight (TOF) mass spectrometry

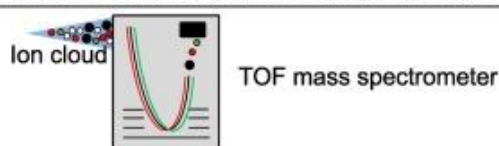


Figure 12.2. Schematic representation of single-cell spatial proteomics approaches. (A) Multiplex immunofluorescence (mIF), (B) CO-Detection by indEXing (CODEX), (C) imaging mass cytometry (IMC) and multiplexed ion beam imaging (MIBI).

12.5.2. Single-cell MS-based approaches

Unbiased single-cell MS-based proteomics approaches are currently in development, being a promising alternative that can overcome the limitation of antibody-based approaches, potentially leading to an increased number of detected proteins [153]. However, single-cell MS analysis must overcome additional challenges apart from the abovementioned for bulk MS proteomics. Proteins cannot be amplified as nucleic acids. Thus, one of the major challenges is the delivery of peptides to the mass spectrometer taking into account the low protein content of a single cell. Single-cell sample preparation requires miniaturization and automation to reduce protein losses and increases their concentration [154]. Single cells are separated by FACS or other alternative techniques and subsequently, protein extraction and digestion are performed in reduced volumes (1 μ l/cell or lower). Different strategies of sample preparation have been successfully developed such as nanodroplet processing in one pot for trace samples (nanoPOTS) [155], oil-air droplets [156], or minimal ProteOmic sample Preparation (mPOP) based on freeze-heat cycles [157]. Moreover, peptide separation in the LC column and its corresponding ESI must be miniaturized with flow rates at low-nanoliter-per-minute or even picoliter-per-minute range. Therefore, the inner diameter of nanoLC columns is reduced from 75 μ m to 30 μ m which in consequence improves single-cell proteome coverage [158].

Importantly, single-cell MS analysis needs an increase in peptide sequence identification as well as in its multiplexing capacity to analyze the proteome from thousands of cells at an affordable cost [153]. A great advance has recently been achieved with an approach called Single Cell ProtEomics by mass spectrometry (SCoPE-MS) [159]. SCoPE-MS prepares the sample by mPOP and adds an isobarically labeled carrier (e.g., the proteome of 100 cells) with tandem mass tags [160]. The usage of a proteomic carrier mitigates sample losses, facilitates peptide sequence identification, and increases the multiplexing capacity with a limit of 12 single-cell proteomes in one run due to the limited tandem mass tags available. With such technological development, SCoPE-MS found its application in heterogeneity studies. SCoPE-MS quantified 3042 proteins in 1490 single monocytes and macrophages, suggesting that heterogeneity of macrophages may emerge without the participation of polarizing cytokines [161]. Moreover, SCoPE-MS quantified 1500 proteins from 152 cells from three acute myeloid leukemia (AML) cell lines, revealing functionally distinct differences between the three cell clusters [162], [163]. Additionally, the combination of nanoPOTS and SCoPE-MS quantified around 1000 proteins per cell of 3000 FACS-sorted cells from an AML culture model. It allowed resolving AML heterogeneity at a single-cell level along different hierarchical stages of differentiation [164].

Further improvements will be achieved through innovations in sample preparation and peptide separation, hardware advances of mass spectrometers as well as innovative acquisition and interpretation methods. These improvements will facilitate increased coverage of single-cell proteomes as well as the sensitivity and confidence of peptide sequence identification, revolutionizing cancer immunology [165].

12.5.3. Single-cell multi-omics strategies

For precision oncology, to deeply and comprehensively understand the complexity of the TME, in addition to proteomics, an integration of multi-omics data at the individual cell level with the molecular landscape of each cell is needed [166], [167]. Proteogenomics approaches combine bulk MS-based proteomics with genomics and transcriptomics. This strategy has been applied to several cancer types, providing novel insights into somatic mutation consequences at the protein level as well as neoantigens discovery for immunotherapy [168], [169], [170], [171]. However, the genomic and proteomic data integration at the single-cell level is currently in development. Recently, a pioneering study designed DAb-seq which allows analysis of 49 DNA targets and 23 protein markers by the combination of DNA barcodes conjugated to antibodies and multiplex PCR. Although this technology requires an increase in its multiplexing capacity, it demonstrated the heterogeneous interactions of somatic mutations and protein expression in AML single cells [172].

On the other hand, there are some techniques designed to link mRNA and antibody based protein analysis in single-cell approaches. Proximity Ligation Assay for RNA (PLAYR) is a method that uses FC/MC for simultaneous analysis of target proteins stained with antibodies and RNA. PLAYR probe pairs hybridize their targets and then the insert and backbone are hybridized and ligated to the probes. After rolling circle amplification, labeled oligonucleotides bind the insert regions for detection and quantification [173]. Recently, this method has been used to demonstrate intra-clonal heterogeneity in chronic lymphocytic leukemia cells [174]. Cellular indexing of transcriptomes and epitopes by sequencing (CITE-seq) and its sister technology RNA expression and protein sequencing (REAP-seq) combine DNA-conjugated antibodies with scRNA-seq [175], [176]. The difference is that CITE-seq uses biotinylated antibodies whereas REAP-seq uses antibodies covalently bonded to aminated DNA sequences. These methods integrate cellular surface protein and transcriptome measurements into single-cell readout. CITE-seq provides a more detailed characterization of cellular phenotypes compared to scRNA-seq alone and allows simultaneous protein expression and transcriptome profiling of thousands of single cells (Fig. 13.3). CITE-seq may also show quantitative differences in marker expression between subsets e.g., expression difference of CD8a between NK and T cells [176]. A CITE-seq panel of 157 antibodies was applied to immunophenotype breast cancer patients. 18 clusters of T cells and innate lymphoid cells (ILCs) were found with different proportions among clinical subtypes. Interestingly, IC molecules were also differentially expressed among breast cancer subtypes. These findings may lead to personalized immunotherapy strategies for each subtype [177]. Moreover, it was found that CITE-seq can be combined with single-cell sequencing assay for transposase-accessible chromatin (scATAC-seq) and used to study the RNA expression, surface proteins, and chromatin accessibility at the single-cell level. Granja et al. [178] applied such strategy to find distinct and shared molecular mechanisms of leukemia. Among the challenges for both technologies (CITE-seq and REAP-seq), the efficiency of cell captures must be increased, the system requires total automation, and the multiplex detection must be extended to intracellular proteins which is currently limited to a reduced number of proteins [179], [180]. Recently, SURface-protein Glycan And RNA-seq (SUGAR-seq) has been designed to enable the detection and analysis of N-linked glycosylation, extracellular epitopes, and the transcriptome at the single-cell level. SUGAR-seq is an extension of CITE-seq in which glycans are captured with a biotinylated lectin and subsequently detected using an anti-biotin mAb conjugated to a DNA-barcode. Integrated SUGAR-seq and glycoproteome analysis identified TILs with unique N-glycan profiles as cellular T cell subsets with the altered epigenetic and functional state in CRC and melanoma mice models [181].

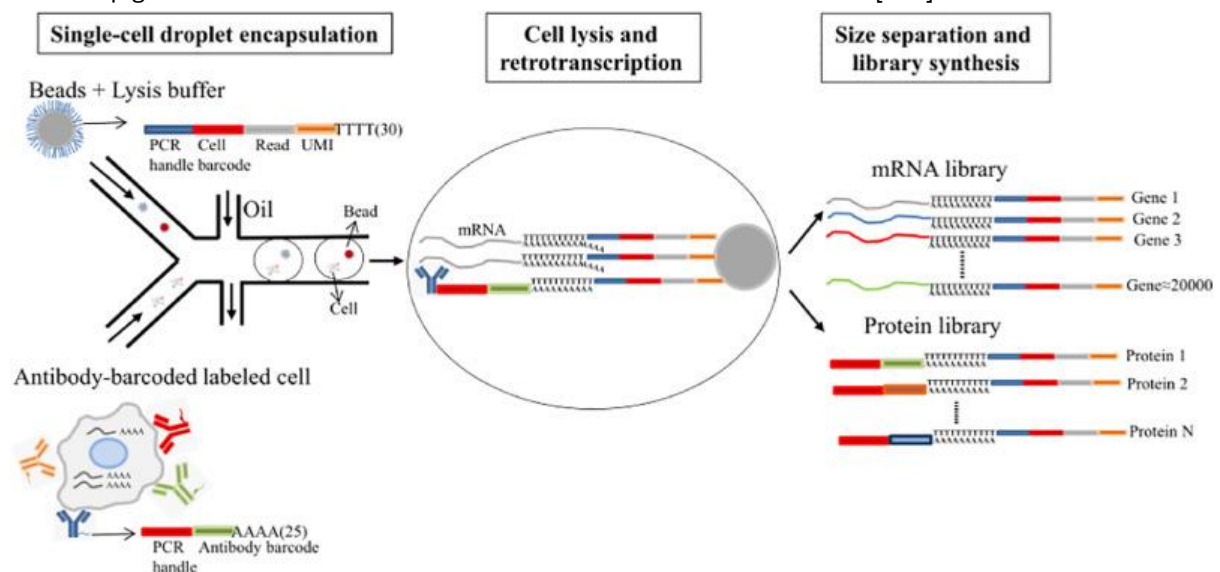


Fig. 12.3. Schematic representation of CITE-seq and REAP-seq. Antibody-barcoded labeled cells are mixed in a microfluidic system in which each droplet contains a cell, beads with the PCR adapters with the corresponding cell barcodes, and lysis buffer. After cell lysis within the droplet, mRNA and DNA barcodes from antibodies are hybridized with PCR adapters. Subsequent retrotranscription

generates cDNAs and droplets are disrupted. Upon disruption, the respective cDNAs for mRNAs and proteins are separated by size. These synthesized libraries are sequenced, providing the single-cell expression profiles of mRNA and targeted proteins.

Zhang et al. [182] combined scRNA-seq and mIF to study the immune TME of CRC patients. They found that TILs showed an exhausted phenotype compared to T cells originating from normal tissue and peripheral blood. Moreover, they identified a population of Th1-like cells that were enriched in microsatellite instability (MSI) CRC, providing a possible explanation for MSI patients' good response to anti-PD-1 immunotherapy. Finally, de Vries et al. [183] combined MC with 36 markers, FC, scRNA-seq, and mIF to analyze T cells from CRC, matched associated lymph nodes, healthy mucosa, and peripheral blood. Different phenotypes of CD8+/ $\gamma\delta$ T cell and CD4+ memory T cells were observed in each examined tissue. Interestingly, an innate lymphoid cell (ILC) population was enriched in CRC tissues with high expression of cytotoxic molecules. Additionally, this ILC population correlated with the presence of tumor-resident cytotoxic, helper, and $\gamma\delta$ T cells with similar activated profiles. This study not only sheds some light on the complexity of lymphocytes composition dependent on the sample type but also demonstrates that multi-omics data integration provides much more data and in-depth analysis, which otherwise would not be obtained.

12.6. Conclusions and future perspectives

Despite the great advances in cancer immunology and the development of immunotherapy, the patients' response rate remains a clinical challenge. Understanding the complexity of TME and immunosuppression mechanisms may lead to design of more effective cancer immunotherapies. Proteomics is a powerful approach to accelerate the studies on immune responses in cancer. MS-based proteomics can uncover novel insights into molecular mechanisms and potential therapeutic targets, while the application of antibody-based proteomics approaches does not require specialized expertise as in MS and is widely applied as a tool to characterize selected proteins and discover new clinical biomarkers. However, both approaches possess limitations and technical challenges that complicate the characterization of the whole proteome of biological systems, especially to differentiate between proteoforms.

Emerging single-cell proteomics approaches will revolutionize our understanding of the complex cellular networks within the TME and interactions between cancer and immune cells. Several technologies have been recently developed with the potential for comprehensive proteomic characterization that facilitates the deep profiling of immune responses in cancer at the single-cell level. Novel technical solutions will provide higher sensitivity and higher resolution at the subcellular and molecular level [184], [185], [186]. Importantly, a new era in proteomics was born with single-molecule protein sequencing based on fluorescence-mediated in situ protein identification [187], [188] as well as nanopores [189], [190]. Further technical development of these next-generation proteomics approaches will ideally enable the whole proteome characterization and unveil the distribution of proteoforms at the single-cell level.

In summary, together with the technological advancements in single-cell analysis, progress in a holistic system of multi-omics approaches and data analysis is needed. To date, it was found that a combination of different 'omics' data with single-cell proteomics, may provide information on cancer origin, progression, and prognosis, which could remain undiscovered if were analyzed separately. It is well-recognized that a comprehensive approach to TME composition is crucial in personalized therapy and efficient treatment. In this review, we have discussed examples of immune heterogeneity studies of TME in cancer, focusing on both MS-based bulk/antibody-based and single-cell analysis (Table 1). Moreover, we reviewed emerging single-cell proteomic analysis methods with examples of the combination of multi-omics studies, which we believe become widely applied in cancer research in the future.

Table 12.1

Summary of the presented emerging single-cell proteomics techniques divided by approaches type and with their corresponding advantages and disadvantages.

Type	Technique	Advantages	Disadvantages
Antibody-based approaches	Full spectrum flow cytometry (FSFC)	Up to 64 of markers analyzed simultaneously Possibility to use dyes with close peak emission, if the full spectra of fluorescence significantly differs	Increased need for a larger number of antibodies combined with dyes suitable for full spectrum detection Reproducibility (increased number of parameters analyzed simultaneously increases the number of factors influencing the outcome of the experiment) Requires specialized device
	Mass cytometry (MC or cytometry of time-of-flight; CyTOF)	Up to 100 of markers analyzed simultaneously in comparison to fluorescence methods Low background noise Multiplexing capacity crucial for the analysis of valuable samples	Infeasible to recover living cells after analysis Longer analysis time Requires specialized device
	Single-cell barcode chips (SCBC)	Dynamic range (up to 10,000 cells analyzed) Possibility to analyze proteins originating from cell-surface, cytoplasm or secreted Cells can be recovered for further analysis	Requires big number of barcoded antibodies Specificity of antibody binding might be hindered by oligonucleotides
	Multiplexed in situ targeting (MIST)	Potential to detect hundreds of proteins	Multiplexing vs. sensitivity – increase in the number of microbeads decreases the sensitivity
	Antibody barcoding with cleavable DNA (ABCD)	High multiplexing capacity due to infinite number of DNA barcodes can be discriminated	Low sample throughput May not detect low-expression proteins
	Multiplexed ImmunoFluorescence (mIF)	Unmodified primary antibodies can be used for this method Allows the detection for several markers at once Relatively short assay time No need for specialized equipment apart from fluorescence microscope	Incomplete removal of antibodies can interfere with the signal detection in subsequent staining cycle Risk of damaging the epitopes during the stripping step
	Multi-Epitope Ligand Cartography (MELC)	Allows the detection of up to 50 epitopes at once High resolution	Requires specialized device Long sampling time
	Toponome Imaging System	Allows the analysis of up to 100 proteins in a single cell	Requires specialized device
	CO-Detection by indEXing (CODEX)	Detection of up to 40 proteins Can provide information on relative abundance of the detected markers in spatial context	Specificity of antibody binding might be hindered by oligonucleotides Relatively long scanning time
	Imaging mass cytometry (IMC)	Up to 40 markers can be detected Provides spatial context	High cost of the analysis Availability of isotope-tagged antibodies Sample is destroyed during detection Time of the data acquisition and analysis Requires specialized device
MS-based approaches	Multiplexed ion beam imaging (MIBI)	Higher detection capacity (up to 100 markers)	High cost of the analysis Availability of isotope-tagged antibodies Sample is destroyed during detection Time of the data acquisition
	Single Cell Proteomics by mass spectrometry (SCOPE-MS)	High throughput and accurate quantification Decreased sample losses Increased identification of peptide sequences	Low accuracy (when comparing the abundance of proteins) Requires special device
Multi-omics approaches	Proximity Ligation Assay for RNA (PLAYR)	Possibility to analyze both mRNA and protein expression levels High throughput	Need to apply FC or MC to obtain the results Limited to the detection of 40 markers due to the availability of the suitable antibodies Multiple probes required to detect one transcript
	Cellular indexing of transcriptomes and epitopes by sequencing (CITE-seq)	Can detect a protein even in the case when corresponding mRNA is of low abundance	Cell capturing efficiency needs to be increased Requires total automation Multiplex detection must be extended to intracellular proteins which is currently limited to a reduced number of proteins
	RNA expression and protein sequencing (REAP-seq)	Can detect a protein even in the case when corresponding mRNA is of low abundance	Cell capturing efficiency needs to be increased Requires total automation Multiplex detection must be extended to intracellular proteins which is currently limited to a reduced number of proteins
	SURface-protein Glycan And RNA-seq (SUGAR-seq)	Can analyze N-linked glycosylation, extracellular epitopes, and the transcriptome at the single-cell level	Similar limitations as for CITE-seq and REAP-seq Biased detection of glycans – detection depends on the type of lectin used in the assay

12.7. References

- [1] H. Sung, J. Ferlay, R.L. Siegel, M. Laversanne, I. Soerjomataram, A. Jemal, F. Bray, Global cancer statistics 2020: GLOBOCAN estimates of incidence and mortality worldwide for 36 cancers in 185 countries, *CA. Cancer J. Clin.* 71 (2021) 209–249, <https://doi.org/10.3322/caac.21660>.
- [2] S. Wu, W. Zhu, P. Thompson, Y.A. Hannun, Evaluating intrinsic and non-intrinsic cancer risk factors, *Nat. Commun.* 91 (9) (2018) 1–12, <https://doi.org/10.1038/s41467-018-05467-z>.
- [3] F. Colotta, P. Allavena, A. Sica, C. Garlanda, A. Mantovani, Cancer-related inflammation, the seventh hallmark of cancer: links to genetic instability, *Carcinogenesis* 30 (7) (2009) 1073–1081, <https://doi.org/10.1093/CARCIN/BGP127>.
- [4] A. Mantovani, P. Allavena, A. Sica, F. Balkwill, Cancer-related inflammation, *Nature* 454 (2008) 436–444, <https://doi.org/10.1038/nature07205>.
- [5] B. Sun, Y. Zhang, Overview of orchestration of CD4+ T cell subsets in immune responses, in: *Adv. Exp. Med. Biol.*, Springer New York LLC, 2014, pp. 1–13, https://doi.org/10.1007/978-94-017-9487-9_1.
- [6] F. Castro, A.P. Cardoso, R.M. Gonçalves, K. Serre, M.J. Oliveira, Interferon- gamma at the crossroads of tumor immune surveillance or evasion, *Front. Immunol.* 9 (847) (2018), <https://doi.org/10.3389/FIMMU.2018.00847>.
- [7] J.A. Walker, A.N.J. McKenzie, TH2 cell development and function, *Nat. Rev. Immunol.* 18 (2) (2018) 121–133, <https://doi.org/10.1038/nri.2017.118>.
- [8] J.I. Ellyard, L. Simson, C.R. Parish, Th2-mediated anti-tumour immunity: friend or foe? *Tissue Antigens* 70 (1) (2007) 1–11, <https://doi.org/10.1111/J.1399-0039.2007.00869.X>.
- [9] H.M. Knochelmann, C.J. Dwyer, S.R. Bailey, S.M. Amaya, D.M. Elston, J. M. Mazza-McCrann, C.M. Paulos, When worlds collide: Th17 and Treg cells in cancer and autoimmunity, *Cell. Mol. Immunol.* 15 (5) (2018) 458–469, <https://doi.org/10.1038/s41423-018-0004-4>.
- [10] J. Zhao, X. Chen, T. Herjan, X. Li, The role of interleukin-17 in tumor development and progression, *J. Exp. Med.* 217 (1) (2020), e20190297, <https://doi.org/10.1084/JEM.20190297>.
- [11] S. Razi, B. Baradaran Noveiry, M. Keshavarz-Fathi, N. Rezaei, IL-17 and colorectal cancer: from carcinogenesis to treatment, *Cytokine* 116 (2019) 7–12, <https://doi.org/10.1016/j.cyto.2018.12.021>.
- [12] S.R. Bailey, M.H. Nelson, R.A. Himes, Z. Li, S. Mehrotra, C.M. Paulos, Th17 cells in cancer: the ultimate identity crisis, *Front. Immunol.* 5 (2014), 276, <https://doi.org/10.3389/FIMMU.2014.00276>.
- [13] Y. Ohue, H. Nishikawa, Regulatory T (Treg) cells in cancer: can treg cells be a new therapeutic target? *Cancer Sci.* 110 (7) (2019) 2080, <https://doi.org/10.1111/CAS.14069>.
- [14] K.A. Ward-Hartstonge, R.A. Kemp, Regulatory T-cell heterogeneity and the cancer immune response, *Clin. Transl. Immunol.* 6 (9) (2017), e154, <https://doi.org/10.1038/cti.2017.43>.
- [15] G. Cui, TH9, TH17, and TH22 cell subsets and their main cytokine products in the pathogenesis of colorectal cancer, *Front. Oncol.* 9 (2019) 1002, <https://doi.org/10.3389/fonc.2019.01002>.
- [16] H.F. Hetta, A. Elkady, R. Yahia, A.K. Meshall, M.M. Saad, M.A. Mekky, I.M.S. Al-Kadmy, T follicular helper and T follicular regulatory cells in colorectal cancer: a complex interplay, *J. Immunol. Methods* 480 (2020), 112753, <https://doi.org/10.1016/j.jim.2020.112753>.
- [17] W. Zou, J.D. Wolchok, L. Chen, PD-L1 (B7–H1) and PD-1 pathway blockade for cancer therapy: mechanisms, response biomarkers, and combinations, *Sci. Transl. Med.* 8 (328) (2016), 328rv4, <https://doi.org/10.1126/SCITRANSLMED.AAD7118>.
- [18] D.S. Chen, I. Mellman, Elements of cancer immunity and the cancer-immune set point, *Nat.* 541 (2017) 321–330, <https://doi.org/10.1038/nature21349>.
- [19] M. Binnewies, E.W. Roberts, K. Kersten, V. Chan, D.F. Fearon, M. Merad, L. M. Coussens, D.I. Gabrilovich, S. Ostrand-Rosenberg, C.C. Hedrick, R. H. Vonderheide, M.J. Pittet, R.K. Jain, W. Zou, T.K. Howcroft, E.C. Woodhouse, R.A. Weinberg, M.F. Krummel, Understanding the tumor immune microenvironment (TIME) for effective therapy, *Nat. Med.* 24 (5) (2018) 541–550, <https://doi.org/10.1038/s41591-018-0014-x>.
- [20] K. Chang, M.W. Taggart, L. Reyes-Urbe, E. Borrás, E. Riquelme, R.M. Barnett, G. Leoni, F. Anthony San Lucas, M.T. Catanese, F. Mori, M.G. Diodoro, Y. Nancy You, E.T. Hawk, J. Roszik, P. Scheet, S. Kopetz, A. Nicosia, E. Scarselli, P. M. Lynch, F. McAllister, E. Vilar, Immune profiling of premalignant lesions in patients with Lynch syndrome, in: *JAMA Oncol.*, American Medical Association, 2018, pp. 1085–1092, <https://doi.org/10.1001/jamaoncol.2018.1482>.
- [21] X. Yang, Q. Qi, Y. Pan, Q. Zhou, Y. Wu, J. Zhuang, J. Xu, M. Pan, S. Han, Single-cell analysis reveals characterization of infiltrating T cells in moderately differentiated colorectal cancer, *Front. Immunol.* 11 (2021), 620196, <https://doi.org/10.3389/fimmu.2020>.
- [22] A.C. Hopkins, M. Yarchoan, J.N. Durham, E.C. Yusko, J.A. Rytlewski, H.S. Robins, D.A. Laheru, D.T. Le, E.R. Lutz, E.M. Jaffee, T cell receptor repertoire features associated with survival in immunotherapy-treated pancreatic ductal adenocarcinoma, *JCI Insight* 3 (13) (2018), e122092, <https://doi.org/10.1172/JCI.INSIGHT.122092>.
- [23] A. Sharma, E. Merritt, X. Hu, A. Cruz, C. Jiang, H. Sarkodie, Z. Zhou, J. Malhotra, G.M. Riedlinger, S. De, Non-genetic intra-tumor heterogeneity is a major predictor of phenotypic heterogeneity and ongoing evolutionary dynamics in lung tumors, *Cell Rep.* 29 (8) (2019) 2164–2174.e5, <https://doi.org/10.1016/J.CELREP.2019.10.045>.
- [24] I. Mohammad, K. Nousiainen, S.D. Bhosale, I. Starskaia, R. Moulder, A. Rokka, F. Cheng, P. Mohanasundaram, J.E. Eriksson, D.R. Goodlett, H. Lähdesmäki, Z. Chen, Quantitative proteomic characterization and comparison of T helper 17 and induced regulatory T cells, *PLoS Biol.* 16 (5) (2018), e2004194, <https://doi.org/10.1371/journal.pbio.2004194>.

- [25] C. Cenik, E.S. Cenik, G.W. Byeon, F. Grubert, S.I. Candille, D. Spacek, B. Alsallakh, H. Tilgner, C.L. Araya, H. Tang, E. Ricci, M.P. Snyder, Integrative analysis of RNA, translation, and protein levels reveals distinct regulatory variation across humans, *Genome Res.* 25 (11) (2015) 1610–1621, <https://doi.org/10.1101/gr.193342.115>.
- [26] M. Ludvigsen, L. Thortlacius-Ussing, H. Vorum, M.P. Moyer, M.T. Stender, O. Thortlacius-Ussing, B. Honoré, Proteomic characterization of colorectal cancer cells versus normal-derived colon mucosa cells: approaching identification of novel diagnostic protein biomarkers in colorectal cancer, *Int. J. Mol. Sci.* 21 (10) (2020), 3466, <https://doi.org/10.3390/ijms21103466>.
- [27] A. Macklin, S. Khan, T. Kislinger, Recent advances in mass spectrometry based clinical proteomics: applications to cancer research, *Clin. Proteomics* 17 (17) (2020) 1–25, <https://doi.org/10.1186/s12014-020-09283-w>.
- [28] K. Carbonara, M. Andonovski, J.R. Coorssen, Proteomes are of proteoforms: embracing the complexity, *Proteomes* 9 (3) (2021) 38, <https://doi.org/10.3390/PROTEOMES9030038>.
- [29] T.R. Shah, A. Misra, Proteomics, in: *Challenges Deliv. Ther. Genomics Proteomics*, 2011, pp. 387–427, <https://doi.org/10.1016/B978-0-12-384964-9.00008-6>.
- [30] N.M. Verrills, Clinical proteomics: present and future prospects, *Clin. Biochem. Rev.* 27 (2) (2006) 99–116.
- [31] C.R. Scurrah, A.J. Simmons, K.S. Lau, Single-cell mass cytometry of archived human epithelial tissue for decoding cancer signaling pathways, *Methods Mol. Biol.* 1884 (2019) 215–229, https://doi.org/10.1007/978-1-4939-8885-3_15.
- [32] A.J. Simmons, C.R. Scurrah, E.T. McKinley, C.A. Herring, J.M. Irish, M. K. Washington, R.J. Coffey, K.S. Lau, Impaired coordination between signaling pathways is revealed in human colorectal cancer using single-cell mass cytometry of archival tissue blocks, *Sci. Signal.* 9 (449) (2016), rs11, <https://doi.org/10.1126/SCISIGNAL.AAH4413>.
- [33] M.J. Gerdes, C.J. Sevinsky, A. Sood, S. Adak, M.O. Bello, A. Bordwell, A. Can, A. Corwin, S. Dinn, R.J. Filkins, D. Hollman, V. Kamath, S. Kaanumalle, K. Kenny, M. Larsen, M. Lazare, Q. Li, C. Lowes, C.C. McCulloch, E. McDonough, M. C. Montalto, Z. Pang, J. Rittscher, A. Santamaria-Pang, B.D. Sarachan, M.L. Seel, A. Seppo, K. Shaikh, Y. Sui, J. Zhang, F. Ginty, Highly multiplexed single-cell analysis of formalin-fixed, paraffin-embedded cancer tissue, *Proc. Natl. Acad. Sci. U. S. A.* 110 (29) (2013) 11982–11987, <https://doi.org/10.1073/pnas.1300136110>.
- [34] R.L. Gundry, M.Y. White, C.I. Murray, L.A. Kane, Q. Fu, B.A. Stanley, J.E. Van Eyk, Preparation of proteins and peptides for mass spectrometry analysis in a bottom-up proteomics workflow, *Curr. Protoc. Mol. Biol.* (88) (2009) 10.25.1–10.25.23, <https://doi.org/10.1002/0471142727.MB1025S88>.
- [35] J.R. Wiśniewski, Filter aided sample preparation – a tutorial, *Anal. Chim. Acta* 1090 (2019) 23–30, <https://doi.org/10.1016/J.ACA.2019.08.032>.
- [36] L. Ly, V.C. Wasinger, Protein and peptide fractionation, enrichment and depletion: tools for the complex proteome, *Proteomics* 11 (4) (2011) 513–534, <https://doi.org/10.1002/PMIC.201000394>.
- [37] C. Wichmann, F. Meier, S.V. Winter, A.-D. Brunner, J. Cox, M. Mann, MaxQuant. Live enables global targeting of more than 25,000 peptides, *Mol. Cell. Proteomics* 18 (5) (2019) 982–994, <https://doi.org/10.1074/MCP.TIR118.001131>.
- [38] J.-J. Hao, X. Zhi, Y. Wang, Z. Zhang, Z. Hao, R. Ye, Z. Tang, F. Qian, Q. Wang, J. Zhu, Comprehensive proteomic characterization of the human colorectal carcinoma reveals signature proteins and perturbed pathways, *Sci. Rep.* 7 (7) (2017) 1–15, <https://doi.org/10.1038/srep42436>.
- [39] B.A.A. Martins, G.F. de Bulhoes, I.N. Cavalcanti, M.M. Martins, P.G. de Oliveira, A.M.A. Martins, Biomarkers in colorectal cancer: the role of translational proteomics research, *Front. Oncol.* 9 (2019) 1284, <https://doi.org/10.3389/FONC.2019.01284>.
- [40] M.A. MacMullan, Z.S. Dunn, N.A. Graham, L. Yang, P. Wang, Quantitative proteomics and metabolomics reveal biomarkers of disease as potential immunotherapy targets and indicators of therapeutic efficacy, *Theranostics* 9 (25) (2019) 7872–7888, <https://doi.org/10.7150/THNO.37373>.
- [41] M. Stoeckli, P. Chaurand, D.E. Hallahan, R.M. Caprioli, Imaging mass spectrometry: a new technology for the analysis of protein expression in mammalian tissues, *Nat. Med.* 7 (4) (2001) 493–496, <https://doi.org/10.1038/86573>.
- [42] M. Aichler, A. Walch, MALDI imaging mass spectrometry: current frontiers and perspectives in pathology research and practice, *Lab. Investig.* 95 (4) (2015) 422–431, <https://doi.org/10.1038/labinvest.2014.156>.
- [43] D. Kazdal, R. Longuespée, S. Dietz, R. Casadonte, K. Schwamborn, A.L. Volckmar, J. Kriegsmann, K. Kriegsmann, M. Fresnais, A. Stenzinger, H. Sülthmann, A. Warth, M. Kriegsmann, Digital PCR after MALDI-mass spectrometry imaging to combine proteomic mapping and identification of activating mutations in pulmonary adenocarcinoma, *PROTEOMICS – Clin.Appl.* 13 (1) (2019), e1800034, <https://doi.org/10.1002/PRCA.201800034>.
- [44] K. Erich, K. Reinle, T. Müller, B. Munteanu, D.A. Sammour, I. Hinsenkamp, T. Gutting, E. Burgermeister, P. Findeisen, M.P. Ebert, J. Krijgsveld, C. Hopf, Spatial distribution of endogenous tissue protease activity in gastric carcinoma mapped by MALDI mass spectrometry imaging, *Mol. Cell. Proteomics* 18 (1) (2019) 151–161, <https://doi.org/10.1074/mcp.RA118.000980>.
- [45] T.W. Powers, B.A. Neely, Y. Shao, H. Tang, D.A. Troyer, A.S. Mehta, B.B. Haab, R. R. Drake, MALDI imaging mass spectrometry profiling of N-glycans in formalin-fixed paraffin embedded clinical tissue blocks and tissue microarrays, *PLoS One* 9 (9) (2014), e106255, <https://doi.org/10.1371/JOURNAL.PONE.0106255>.
- [46] M.R.L. Paine, J. Liu, D. Huang, S.R. Ellis, D. Trede, J.H. Kobarg, R.M.A. Heeren, F. Fernandez, T.J. MacDonald, Three-dimensional mass spectrometry imaging identifies lipid markers of medulloblastoma metastasis, *Sci. Rep.* 9 (1) (2019), 2205, <https://doi.org/10.1038/s41598-018-38257-0>.
- [47] S. Lou, B. Balluff, A.H.G. Cleven, J.V.M.G. Bovée, L.A. McDonnell, Prognostic metabolite biomarkers for soft tissue sarcomas discovered by mass spectrometry imaging, *J. Am. Soc. Mass Spectrom.* 28 (2) (2017) 376–383, <https://doi.org/10.1007/s13361-016-1544-4>.

- [48] M.J. Taylor, J.K. Lukowski, C.R. Anderton, Spatially resolved mass spectrometry at the single cell: recent innovations in proteomics and metabolomics, *J. Am. Soc. Mass Spectrom.* 32 (4) (2021) 872–894, <https://doi.org/10.1021/JASMS.0C00439>.
- [49] M. Ahmed, G. Broeckx, G. Baggerman, K. Schildermans, P. Pauwels, A.H. Van Craenenbroeck, A. Dendooven, Next-generation protein analysis in the pathology department, *J. Clin. Pathol.* 73 (1) (2020) 1–6, <https://doi.org/10.1136/JCLINPATH-2019-205864>.
- [50] W. Timp, G. Timp, Beyond mass spectrometry, the next step in proteomics, *Sci. Adv.* 6 (2) (2020), eaax8978, <https://doi.org/10.1126/sciadv.aax8978>.
- [51] H. Steen, M. Mann, The abc's (and xyz's) of peptide sequencing, *Nat. Rev. Mol. Cell Biol.* 59 (5) (2004) 699–711, <https://doi.org/10.1038/nrm1468>.
- [52] S.H. Baumeister, G.J. Freeman, G. Dranoff, A.H. Sharpe, in: *Coinhibitory pathways in immunotherapy for cancer* 34, 2016, pp. 539–573, <https://doi.org/10.1146/ANNUREV-IMMUNOL-032414-112049>.
- [53] B. Allard, S. Aspeslagh, S. Garaud, F.A. Dupont, C. Solinas, M. Kok, B. Routy, C. Sotiriou, J. Stagg, L. Buisseret, Immunology-101: overview of major concepts and translational perspectives, *Semin. Cancer Biol.* 52 (2) (2018) 1–11, <https://doi.org/10.1016/J.SEMCANCER.2018.02.005>.
- [54] D.H. Munn, V. Bronte, Immune suppressive mechanisms in the tumor microenvironment, *Curr. Opin. Immunol.* 39 (2016) 1–6, <https://doi.org/10.1016/J.COI.2015.10.009>.
- [55] C.H. Chang, J. Qiu, D. O'Sullivan, M.D. Buck, T. Noguchi, J.D. Curtis, Q. Chen, M. Gindin, M.M. Gubin, G.J.W. Van Der Windt, E. Tonc, R.D. Schreiber, E. J. Pearce, E.L. Pearce, Metabolic competition in the tumor microenvironment is a driver of cancer progression, *Cell* 162 (6) (2015) 1229–1241, <https://doi.org/10.1016/J.CELL.2015.08.016>.
- [56] I. Hamaidi, L. Zhang, N. Kim, M.H. Wang, C. Iclozan, B. Fang, M. Liu, J. M. Koomen, A.E. Berglund, S.J. Yoder, J. Yao, R.W. Engelman, B.C. Creelan, J. R. Conejo-Garcia, S.J. Antonia, J.J. Mul' e, S. Kim, Sirt2 inhibition enhances metabolic fitness and effector functions of tumor-reactive T cells, *Cell Metab.* 32 (3) (2020) 420–436.e12, <https://doi.org/10.1016/j.cmet.2020.07.008>.
- [57] F. Cheng, L. Su, C. Yao, L. Liu, J. Shen, C. Liu, X. Chen, Y. Luo, L. Jiang, J. Shan, J. Chen, W. Zhu, J. Shao, C. Qian, SIRT1 promotes epithelial–mesenchymal transition and metastasis in colorectal cancer by regulating Fra-1 expression, *Cancer Lett.* 375 (2) (2016) 274–283, <https://doi.org/10.1016/J.CANLET.2016.03.010>.
- [58] L. Shi, H. Yan, S. An, M. Shen, W. Jia, R. Zhang, L. Zhao, G. Huang, J. Liu, SIRT5- mediated deacetylation of LDHB promotes autophagy and tumorigenesis in colorectal cancer, *Mol. Oncol.* 13 (2) (2019) 358–375, <https://doi.org/10.1002/1878-0261.12408>.
- [59] B. Wang, Y. Ye, X. Yang, B. Liu, Z. Wang, S. Chen, K. Jiang, W. Zhang, H. Jiang, H. Mustonen, P. Puolakkainen, S. Wang, J. Luo, Z. Shen, SIRT2-dependent IDH1 deacetylation inhibits colorectal cancer and liver metastases, *EMBO Rep.* 21 (4) (2020), e48183, <https://doi.org/10.15252/EMBR.201948183>.
- [60] A.A. Martí i Líndez, I. Dunand-Sauthier, M. Conti, F. Gobet, N. Núñez, J. T. Hannich, H. Riezman, R. Geiger, A. Piersigilli, K. Hahn, S. Lemeille, B. Becher, T. de Smedt, S. Hugues, W. Reith, Mitochondrial arginase-2 is a cell-autonomous regulator of CD8+ T cell function and antitumor efficacy, *JCI Insight* 4 (24) (2019), e132975, <https://doi.org/10.1172/jci.insight.132975>.
- [61] T. Xue, P. Liu, Y. Zhou, K. Liu, L. Yang, R.L. Moritz, W. Yan, L.X. Xu, Interleukin-6 induced “Acute” phenotypic microenvironment promotes Th1 anti-tumor immunity in cryo-thermal therapy revealed by shotgun and parallel reaction monitoring proteomics, *Theranostics.* 6 (6) (2016) 773–794, <https://doi.org/10.7150/thno.14394>.
- [62] L. Servais, O. Wera, J. Dibato Epoh, C. Delierneux, N. Bouznad, S. Rahmouni, G. Mazzucchelli, D. Baiwir, P. Delvenne, P. Lancellotti, C. Oury, Platelets contribute to the initiation of colitis-associated cancer by promoting immunosuppression, *J. Thromb. Haemost.* 16 (4) (2018) 762–777, <https://doi.org/10.1111/jth.13959>.
- [63] C. Cianciaruso, T. Beltraminelli, F. Duval, S. Nassiri, R. Hamelin, A. Mozes, H. Gallart-Ayala, G. Ceada Torres, B. Torchia, C.H. Ries, J. Ivanisevic, M. De Palma, Molecular profiling and functional analysis of macrophage-derived tumor extracellular vesicles, *Cell Rep.* 27 (10) (2019) 3062–3080.e11, <https://doi.org/10.1016/j.celrep.2019.05.008>.
- [64] R. Xu, J. Tang, Q. Deng, W. He, X. Sun, L. Xia, Z. Cheng, L. He, S. You, J. Hu, Y. Fu, J. Zhu, Y. Chen, W. Gao, A. He, Z. Guo, L. Lin, H. Li, C. Hu, R. Tian, Spatial- resolution cell type proteome profiling of cancer tissue by fully integrated proteomics technology, *Anal. Chem.* 90 (9) (2018) 5879–5886, <https://doi.org/10.1021/ACS.ANALCHEM.8B00596>.
- [65] F. Maria Bosisio, A. Antoranz, Y. Van Herck, M. Maria Bolognesi, L. Marcelis, C. Chinello, J. Wouters, F. Magni, L. Alexopoulos, M. Stas, V. Boecxstaens, O. Bechter, G. Cattoretto, J. Van Den Oord, Functional heterogeneity of lymphocytic patterns in primary melanoma dissected through single-cell multiplexing, *eLife* 9 (2020), e53008, <https://doi.org/10.7554/eLife.53008>. [66] S.A. Stacker, S.P. Williams, T. Karnezis, R. Shayan, S.B. Fox, M.G. Achen, Lymphangiogenesis and lymphatic vessel remodelling in cancer, *Nat. Rev. Cancer* 14 (3) (2014) 159–172, <https://doi.org/10.1038/nrc3677>.
- [67] L.C. Dieterich, K. Ikenberg, T. Cetintas, K. Kapaklikaya, C. Hutmacher, M. Detmar, Tumor-associated lymphatic vessels upregulate PDL1 to inhibit T-cell activation, *Front. Immunol.* 8 (2017) 66, <https://doi.org/10.3389/fimmu.2017.00066>.
- [68] J. Stevenson, R. Barrow-McGee, L. Yu, A. Paul, D. Mansfield, J. Owen, N. Woodman, R. Natrajan, S. Haider, C. Gillett, A. Tutt, S.E. Pinder, J. Choudary, K. Naidoo, Proteomics of REPLICANT perfusate detects changes in the metastatic lymph node microenvironment, *NPJ Breast Cancer* 7 (1) (2021) 24, <https://doi.org/10.1038/s41523-021-00227-7>.
- [69] A.K. Müller, M. Föll, B. Heckelmann, S. Kiefer, M. Werner, O. Schilling, M.L. Binossek, C.A. Jilg, V. Drendel, Proteomic characterization of prostate cancer to distinguish nonmetastasizing and metastasizing primary tumors and lymph node metastases, *Neoplasia (United States)*. 20 (2) (2018) 140–151, <https://doi.org/10.1016/j.neo.2017.10.009>.
- [70] K. Naidoo, R. Jones, B. Dmitrovic, N. Wijesuriya, H. Kocher, I.R. Hart, T. Crnogorac-Jurcevic, Proteome of formalin-fixed paraffin-embedded pancreatic ductal adenocarcinoma and lymph node metastases, *J. Pathol.* 226 (5) (2012) 756–763, <https://doi.org/10.1002/path.3959>.

- [71] D. Krantz, M. Mints, M. Winerdal, K. Riklund, D. Rutishauser, R. Zubarev, A. A. Zirakhzadeh, F. Alamdari, M. Johansson, A. Sherif, O. Winqvist, IL-16 processing in sentinel node regulatory T cells is a factor in bladder cancer immunity, *Scand. J. Immunol.* 92 (6) (2020), e12926, <https://doi.org/10.1111/SJI.12926>.
- [72] M. Kriegsmann, R. Casadonte, J. Kriegsmann, H. Dienemann, P. Schirmacher, J. H. Kobarg, K. Schwamborn, A. Stenzinger, A. Warth, W. Weichert, Reliable entity subtyping in non-small cell lung cancer by matrix-assisted laser desorption/ionization imaging mass spectrometry on formalin-fixed paraffinembedded tissue specimens, *Mol. Cell. Proteomics* 15 (10) (2016) 3081–3089, <https://doi.org/10.1074/mcp.M115.057513>.
- [73] R. Casadonte, M. Kriegsmann, A. Perren, G. Baretton, S.O. Deininger, K. Kriegsmann, T. Welsch, C. Pilarsky, J. Kriegsmann, Development of a class prediction model to discriminate pancreatic ductal adenocarcinoma from pancreatic neuroendocrine tumor by MALDI mass spectrometry imaging, *PROTEOMICS – Clin.Appl.* 13 (1) (2019) e1800046, <https://doi.org/10.1002/PRCA.201800046>.
- [74] L. Phillips, A.J. Gill, R.C. Baxter, Novel prognostic markers in triple-negative breast cancer discovered by MALDI-mass spectrometry imaging, *Front. Oncol.* 9 (2019) 379, <https://doi.org/10.3389/fonc.2019.00379>.
- [75] S. Meding, U. Nitsche, B. Balluff, M. Elsner, S. Rauser, C. Schöne, M. Nipp, M. Maak, M. Feith, M.P. Ebert, H. Friess, R. Langer, H. Höfler, H. Zitzelsberger, R. Rosenberg, A. Walch, Tumor classification of six common cancer types based on proteomic profiling by MALDI imaging, *J. Proteome Res.* 11 (3) (2012) 1996–2003, <https://doi.org/10.1021/pr200784p>.
- [76] M. Gawin, A. Kurczyk, J. Niemiec, A. Stanek-Widera, A. Grela-Wojewoda, A. Adamczyk, M. Biskup-Frużyńska, J. Polańska, P. Widtak, Intra-tumor heterogeneity revealed by mass spectrometry imaging is associated with the prognosis of breast cancer, *Cancers (Basel)* 13 (17) (2021) 4349, <https://doi.org/10.3390/cancers13174349>.
- [77] E. Berghmans, J. Jacobs, C. Deben, C. Hermans, G. Broeckx, E. Smits, E. Maes, J. Raskin, P. Pauwels, G. Baggerman, Mass spectrometry imaging reveals neutrophil defensins as additional biomarkers for anti-PD-(L)1 immunotherapy response in NSCLC patients, *Cancers* 12 (4) (2020) 863, <https://doi.org/10.3390/CANCERS12040863>.
- [78] D. Alberts, C. Pottier, N. Smargiasso, D. Baiwir, G. Mazzucchelli, P. Delvenne, M. Kriegsmann, D. Kazdal, A. Warth, E. De Pauw, R. Longuespée, MALDI imaging-guided microproteomic analyses of heterogeneous breast tumors—a pilot study, *PROTEOMICS – Clin.Appl.* 12 (1) (2018) 1700062, <https://doi.org/10.1002/PRCA.201700062>.
- [79] E. Berghmans, G. Van Raemdonck, K. Schildermans, H. Willems, K. Boonen, E. Maes, I. Mertens, P. Pauwels, G. Baggerman, MALDI mass spectrometry imaging linked with top-down proteomics as a tool to study the non-small-cell lung cancer tumor microenvironment, *Methods Protoc.* 2 (2) (2019) 44, <https://doi.org/10.3390/MPS2020044>.
- [80] K. Davalieva, S. Kiprijanovska, I.M. Kostovska, S. Stavridis, O. Stankov, S. Komina, G. Petrussevska, M. Polenakovic, Comparative proteomics analysis of urine reveals down-regulation of acute phase response signaling and LXR/RXR activation pathways in prostate cancer, *Proteomes* 6 (1) (2018) 1, <https://doi.org/10.3390/PROTEOMES6010001>.
- [81] L. Massimi, C. Martelli, M. Caldarelli, M. Castagnola, C. Desiderio, Proteomics in pediatric cystic craniopharyngioma, *Brain Pathol.* 27 (3) (2017) 370–376, <https://doi.org/10.1111/BPA.12502>.
- [82] C. Martelli, R. Serra, I. Inserra, D.V. Rossetti, F. Iavarone, F. Vincenzoni, M. Castagnola, A. Urbani, G. Tamburrini, M. Caldarelli, L. Massimi, C. Desiderio, Investigating the protein signature of adamantinomatous craniopharyngioma pediatric brain tumor tissue: towards the comprehension of its aggressive behavior, *Dis. Markers* 2019 (2019), 3609789, <https://doi.org/10.1155/2019/3609789>.
- [83] D.V. Rossetti, L. Massimi, C. Martelli, F. Vincenzoni, S. Di Silvestre, G. Scorpio, G. Tamburrini, M. Caldarelli, A. Urbani, C. Desiderio, Ependymoma pediatric brain tumor protein fingerprinting by integrated mass spectrometry platforms: a pilot investigation, *Cancers* 12 (3) (2020) 674, <https://doi.org/10.3390/CANCERS12030674>.
- [84] I. Ntai, R.D. LeDuc, R.T. Fellers, P. Erdmann-Gilmore, S.R. Davies, J. Rumsey, B. P. Early, P.M. Thomas, S. Li, P.D. Compton, M.J.C. Ellis, K.V. Ruggles, D. Fenyó, E.S. Boja, H. Rodriguez, R.R. Townsend, N.L. Kelleher, Integrated bottom-up and top-down proteomics of patient-derived breast tumor xenografts, *Mol. Cell. Proteomics* 15 (1) (2016) 45–56, <https://doi.org/10.1074/MCP.M114.047480>.
- [85] O.S. Skinner, N.A. Haverland, L. Fornelli, R.D. Melani, L.H.F. Do Vale, H. S. Seckler, P.F. Doubleday, L.F. Schachner, K. Szrenti, N.L. Kelleher, P. D. Compton, Top-down characterization of endogenous protein complexes with native proteomics, *Nat. Chem. Biol.* 14 (1) (2017) 36–41, <https://doi.org/10.1038/nchembio.2515>.
- [86] W.I. Deighan, V.J. Winton, R.D. Melani, L.C. Anderson, J.P. McGee, L. F. Schachner, D. Barnidge, D. Murray, H.D. Alexander, D.S. Gibson, M.J. Deery, F. P. McNicholl, J. McLaughlin, N.L. Kelleher, P.M. Thomas, Development of novel methods for non-canonical myeloma protein analysis with an innovative adaptation of immunofixation electrophoresis, native top-down mass spectrometry, and middle-down de novo sequencing, *Clin. Chem. Lab. Med.* 59 (4) (2021) 653–661, <https://doi.org/10.1515/cclm-2020-1072>.
- [87] I. Ntai, L. Fornelli, C.J. DeHart, J.E. Hutton, P.F. Doubleday, R.D. LeDuc, A.J. van Nispen, R.T. Fellers, G. Whiteley, E.S. Boja, H. Rodriguez, N.L. Kelleher, Precise characterization of KRAS4b proteoforms in human colorectal cells and tumors reveals mutation/modification cross-talk, *Proc. Natl. Acad. Sci. U. S. A.* 115 (16) (2018) 4140–4145, <https://doi.org/10.1073/pnas.1716122115>.
- [88] K.A. Resing, N.G. Ahn, Proteomics strategies for protein identification, *FEBS Lett.* 579 (4) (2005) 885–889, <https://doi.org/10.1016/J.FEBSLET.2004.12.001>.
- [89] J. Griss, Y. Perez-Riverol, S. Lewis, D.L. Tabb, J.A. Dianes, N. Del-Toro, M. Rurik, M. Walzer, O. Kohlbacher, H. Hermjakob, R. Wang, J.A. Vizcano, Recognizing millions of consistently unidentified spectra across hundreds of shotgun proteomics datasets, *Nat. Methods* 13 (13) (2016) 651–656, <https://doi.org/10.1038/nmeth.3902>.
- [90] P.E. Geyer, L.M. Holdt, D. Teupser, M. Mann, Revisiting biomarker discovery by plasma proteomics, *Mol. Syst. Biol.* 13 (9) (2017) 942, <https://doi.org/10.15252/MSB.20156297>.

- [91] P.R. Jungblut, B. Thiede, H. Schlüter, Towards deciphering proteomes via the proteoform, protein speciation, moonlighting and protein code concepts, *J. Proteome* 134 (2016) 1–4, <https://doi.org/10.1016/J.JPROT.2016.01.012>.
- [92] Y. Zhang, B.R. Fonslow, B. Shan, M.C. Baek, J.R. Yates, Protein analysis by shotgun/bottom-up proteomics, *Chem. Rev.* 113 (4) (2013) 2343–2394, <https://doi.org/10.1021/CR3003533>.
- [93] M.S. Kim, J. Zhong, A. Pandey, Common errors in mass spectrometry-based analysis of post-translational modifications, *Proteomics* 16 (5) (2016) 700–714, <https://doi.org/10.1002/PMIC.201500355>.
- [94] A. Cesano, S. Warren, Bringing the next generation of immuno-oncology biomarkers to the clinic, *Biomedicine* 6 (1) (2018) 14, <https://doi.org/10.3390/BIOMEDICINES6010014>.
- [95] C. Zhao, L. Wu, D. Liang, H. Chen, S. Ji, G. Zhang, K. Yang, Y. Hu, B. Mao, T. Liu, Y. Yu, H. Zhang, J. Xu, Identification of immune checkpoint and cytokine signatures associated with the response to immune checkpoint blockade in gastrointestinal cancers, *Cancer Immunol. Immunother.* 70 (9) (2021) 2669–2679, <https://doi.org/10.1007/S00262-021-02878-8>.
- [96] V. Calu, A. Ionescu, L. Stanca, O.I. Geicu, F. Iordache, A.M. Pisoschi, A.I. Serban, L. Bilteanu, Key biomarkers within the colorectal cancer related inflammatory microenvironment, *Sci. Reports* 11 (1) (2021) 1–14, <https://doi.org/10.1038/s41598-021-86941-5>.
- [97] M. Lundberg, A. Eriksson, B. Tran, E. Assarsson, S. Fredriksson, Homogeneous antibody-based proximity extension assays provide sensitive and specific detection of low-abundant proteins in human blood, *Nucleic Acids Res.* 39 (15) (2011), e102, <https://doi.org/10.1093/NAR/GKR424>.
- [98] W. Zhong, F. Edfors, A. Gummeson, G. Bergström, L. Fagerberg, M. Uhlén, Next generation plasma proteome profiling to monitor health and disease, *Nat. Commun.* 12 (1) (2021) 1–12, <https://doi.org/10.1038/s41467-021-22767-z>.
- [99] E.P. Erkan, T. Ströbel, C. Dorfer, M. Sonntagbauer, A. Weinhäusel, N. Saydam, O. Saydam, Circulating tumor biomarkers in meningiomas reveal a signature of equilibrium between tumor growth and immune modulation, *Front. Oncol.* 9 (2019) 1031, <https://doi.org/10.3389/FONC.2019.01031>.
- [100] A.S. Ali, A. Perren, C. Lindskog, S. Welin, H. Sorbye, M. Gronberg, E.T. Janson, “ Candidate protein biomarkers in pancreatic neuroendocrine neoplasms grade 3, *Sci. Rep.* 10 (1) (2020) 1–9, <https://doi.org/10.1038/s41598-020-67670-7>.
- [101] H. Kasanen, M. Hernberg, S. Mäkelä, O. Brück, S. Juteau, L. Kohtamäki, M. Ilander, S. Mustjoki, A. Kreutzman, Age-associated changes in the immune system may influence the response to anti-PD1 therapy in metastatic melanoma patients, *Cancer Immunol. Immunother.* 69 (5) (2020) 717–730, <https://doi.org/10.1007/S00262-020-02497-9>.
- [102] M. Eltahir, E. Fletcher, L. Dynesius, J.L. Jarblad, M. Lord, I. Laurén, M. Zekarias, X. Yu, M.S. Cragg, C. Hammarström, K.H. Levedahl, M. Höglund, G. Ullenhag, M. Mattsson, S.M. Mangsbo, Profiling of donor-specific immune effector signatures in response to rituximab in a human whole blood loop assay using blood from CLL patients, *Int. Immunopharmacol.* 90 (2021), 107226, <https://doi.org/10.1016/J.INTIMP.2020.107226>.
- [103] S.S. Árnadóttir, T.B. Mattesen, S. Vang, M.R. Madsen, A.H. Madsen, N.J. Birkbak, J.B. Bramsen, C.L. Andersen, Transcriptomic and proteomic intra-tumor heterogeneity of colorectal cancer varies depending on tumor location within the colorectum, *PLoS One* 15 (12) (2020), e0241148, <https://doi.org/10.1371/JOURNAL.PONE.0241148>.
- [104] L. Wik, N. Nordberg, J. Broberg, J. Björkstén, E. Assarsson, S. Henriksson, “ I. Grundberg, E. Pettersson, C. Westerberg, E. Liljeroth, A. Falck, M. Lundberg, Proximity extension assay in combination with next-generation sequencing for high-throughput proteome-wide analysis, *Mol. Cell. Proteomics* 20 (2021), 100168, <https://doi.org/10.1016/j.mcpro.2021.100168>.
- [105] C. Coarfa, S.L. Grimm, K. Rajapakshe, D. Perera, H.-Y. Lu, X. Wang, K. R. Christensen, Q. Mo, D.P. Edwards, S. Huang, Reverse-phase protein array: technology, application, data processing, and integration, *J. Biomol. Tech.* 32 (1) (2021) 15–29, <https://doi.org/10.7171/JBT.2021-3202-001/-/DC1>.
- [106] P. Díez, M. González-González, L. Lourido, R.M. Dégano, N. Ibarrola, J. Casado-Vela, J. LaBaer, M. Fuentes, NAPPA as a real new method for protein microarray generation, *Microarrays* 4 (2) (2015) 214–227, <https://doi.org/10.7171/jbt.2021-3202-001>.
- [107] Z. Lin, X. Meng, J. Wen, J.M. Corral, D. Andreev, K. Kachler, G. Schett, X. Chen, A. Bozec, Intratumor heterogeneity correlates with reduced immune activity and worse survival in melanoma patients, *Front. Oncol.* 10 (2020), 596493, <https://doi.org/10.3389/fonc.2020.596493>.
- [108] M. González-González, J.M. Sayagués, L. Muñoz-Bellvís, C.E. Pedreira, M.L.R. de Campos, J. García, J.A. Alcázar, P.F. Braz, B.L. Galves, L.M. González, O. Bengoechea, M.D.M. Abad, J.J. Cruz, L. Bellido, E. Fonseca, P. Díez, P. Juanes-Velasco, A. Landeira-Viñuela, Q. Lecrevisse, E. Montalvillo, R. Góngora, O. Blanco, J.M. Sánchez-Santos, J. Labaer, A. Orfao, M. Fuentes, Tracking the antibody immunome in sporadic colorectal cancer by using antigen self-assembled protein arrays, *Cancers (Basel)* 13 (11) (2021), 2718, <https://doi.org/10.3390/cancers13112718>.
- [109] A. Bradbury, A. Plückerthun, Reproducibility: standardize antibodies used in research, *Nature* 518 (7537) (2015) 27–29, <https://doi.org/10.1038/518027a>.
- [110] F. Runa, S. Hamalian, K. Meade, P. Shisgal, P.C. Gray, J.A. Kelber, Tumor microenvironment heterogeneity: challenges and opportunities, *Curr. Mol. Biol. Rep.* 3 (4) (2017) 218–229, <https://doi.org/10.1007/s40610-017-0073-7>.
- [111] R.E. Vickman, D.V. Faget, P. Beachy, D. Beebe, N.A. Bhowmick, E. Cukierman, W. M. Deng, J.G. Granneman, J. Hildesheim, R. Kalluri, K.S. Lau, E. Lengyel, J. Lundeberg, J. Moscat, P.S. Nelson, K. Pietras, K. Politi, E. Pure, R. Scherz-Shouval, M.H. Sherman, D. Tuveson, A.T. Weeraratna, R.M. White, M.H. Wong, E. C. Woodhouse, Y. Zheng, S.W. Hayward, S.A. Stewart, Deconstructing tumor heterogeneity: the stromal perspective, *Oncotarget* 11 (40) (2020) 3621–3632, <https://doi.org/10.18632/ONCOTARGET.27736>.
- [112] C.K. Sanders, J.R. Mourant, Advantages of full spectrum flow cytometry 18, 2013, <https://doi.org/10.1117/1.JBO.18.3.037004>.
- [113] S. Schmutz, M. Valente, A. Cumano, S. Novault, Spectral cytometry has unique properties allowing multicolor analysis of cell suspensions isolated from solid tissues, *PLoS One* 11 (8) (2016), e0159961, <https://doi.org/10.1371/JOURNAL.PONE.0159961>.

- [114] D.L. Bonilla, G. Reinin, E. Chua, Full spectrum flow cytometry as a powerful technology for cancer immunotherapy research, *Front. Mol. Biosci.* 7 (2021), 612801, <https://doi.org/10.3389/FMOLB.2020.612801>.
- [115] L.A. van de Velde, E. Kaitlynn Allen, J.C. Crawford, T.L. Wilson, C.S. Guy, M. Russier, L. Zeitler, A. Bahrami, D. Finkelstein, S. Pelletier, S. Schultz-Cherry, P. G. Thomas, P.J. Murray, Neuroblastoma formation requires unconventional CD4 T cells and arginase-1-dependent myeloid cells, *Cancer Res.* 81 (19) (2021) 5047–5059, <https://doi.org/10.1158/0008-5472.CAN-21-0691>.
- [116] M. Yang, W. Du, L. Yi, S. Wu, C. He, W. Zhai, C. Yue, R. Sun, A.V. Menk, G. M. Delgoffe, J. Jiang, B. Lu, Checkpoint molecules coordinately restrain hyperactivated effector T cells in the tumor microenvironment 9, 2020, <https://doi.org/10.1080/2162402X.2019.1708064>.
- [117] J. Di, M. Liu, Y. Fan, P. Gao, Z. Wang, B. Jiang, X. Su, Phenotype molding of T cells in colorectal cancer by single-cell analysis, *Int. J. Cancer* 146 (8) (2020) 2281–2295, <https://doi.org/10.1002/ijc.32856>.
- [118] S.E. Norton, K.A. Ward-Hartstonge, J.L. McCall, J.K.H. Leman, E.S. Taylor, F. Munro, M.A. Black, B.F. de St, H.M. Groth, R.A.Kemp McGuire, High-dimensional mass cytometric analysis reveals an increase in effector regulatory T cells as a distinguishing feature of colorectal tumors, *J. Immunol.* 202 (6) (2019) 1871–1884, <https://doi.org/10.4049/JIMMUNOL.1801368>.
- [119] W. Fu, W. Wang, H. Li, Y. Jiao, R. Huo, Z. Yan, J. Wang, S. Wang, J. Wang, D. Chen, Y. Cao, J. Zhao, Single-cell atlas reveals complexity of the immunosuppressive microenvironment of initial and recurrent glioblastoma, *Front. Immunol.* 11 (2020) 835, <https://doi.org/10.3389/FIMMU.2020.00835>.
- [120] J.K. Khalsa, N. Cheng, J. Keegan, A. Chaudry, J. Driver, W.L. Bi, J. Lederer, K. Shah, Immune phenotyping of diverse syngeneic murine brain tumors identifies immunologically distinct types, *Nat. Commun.* 11 (1) (2020) 3912, <https://doi.org/10.1038/s41467-020-17704-5>.
- [121] E.M. Thrash, K. Kleinsteinuber, E.S. Hathaway, M. Nazzaro, E. Haas, F.S. Hodi, M. Severgnini, High-throughput mass cytometry staining for immunophenotyping clinical samples, *STAR Protoc.* 1 (2) (2020), 100055, <https://doi.org/10.1016/j.XPRO.2020.100055>.
- [122] E. Friebel, K. Kapolou, S. Unger, N.G. Núñez, S. Utz, E.J. Rushing, L. Regli, M. Weller, M. Greter, S. Tugues, M.C. Neidert, B. Becher, Single-cell mapping of human brain cancer reveals tumor-specific instruction of tissue-invading leukocytes, *Cell* 181 (7) (2020) 1626–1642.e20, <https://doi.org/10.1016/j.cell.2020.04.055>.
- [123] M. Wierz, B. Janji, G. Berchem, E. Moussay, J. Paggetti, High-dimensional mass cytometry analysis revealed microenvironment complexity in chronic lymphocytic leukemia 7, 2018, <https://doi.org/10.1080/2162402X.2018.1465167>.
- [124] S. Chevrier, J.H. Levine, V.R.T. Zanotelli, K. Silina, D. Schulz, M. Bacac, C.H. Ries, L. Ailles, M.A.S. Jewett, H. Moch, M. van den Broek, C. Beisel, M.B. Stadler, C. Gedye, B. Reis, D. Pe'er, B. Bodenmiller, An immune atlas of clear cell renal cell carcinoma, *Cell* 169 (4) (2017) 736–749, <https://doi.org/10.1016/j.cell.2017.04.016>.
- [125] J. Wagner, M.A. Rapsomaniki, S. Chevrier, T. Anzeneder, C. Langwieder, A. Dykgers, M. Rees, A. Ramaswamy, S. Muenst, S.D. Soysal, A. Jacobs, J. Windhager, K. Silina, M. van den Broek, K.J. Dedes, M. Rodríguez Martínez, W. P. Weber, B. Bodenmiller, A single-cell atlas of the tumor and immune ecosystem of human breast cancer, *Cell* 177 (5) (2019) 1330–1345, <https://doi.org/10.1016/j.cell.2019.03.005>.
- [126] C. Ma, R. Fan, H. Ahmad, Q. Shi, B. Comin-Anduix, T. Chodon, R.C. Koya, C. C. Liu, G.A. Kwong, C.G. Radu, A. Ribas, J.R. Heath, A clinical microchip for evaluation of single immune cells reveals high functional heterogeneity in phenotypically similar T cells, *Nat. Med.* 17 (6) (2011) 738–743, <https://doi.org/10.1038/nm.2375>.
- [127] Y. Lu, Q. Xue, M.R. Eisele, E.S. Sulistijo, K. Brower, L. Han, E.A.D. Amir, D. Pe'er, K. Miller-Jensen, R. Fan, Highly multiplexed profiling of single-cell effector functions reveals deep functional heterogeneity in response to pathogenic ligands, *Proc. Natl. Acad. Sci. U. S. A.* 112 (7) (2015) E607–E615, <https://doi.org/10.1073/pnas.1416756112>.
- [128] A. Diab, S. Tykodi, G. Daniels, M. Maio, B. Curti, K. Lewis, S. Jang, E. Kalinka, I. Puzanov, A. Spira, D. Cho, S. Guan, E. Puente, U. Hoch, S. Currie, T. Nguyen, W. Lin, M. Tagliaferri, J. Zalevsky, M. Sznol, M. Hurwitz, Progression-free survival and biomarker correlates of response with BEMPEG plus NIVO in previously untreated patients with metastatic melanoma: results from the PIVOT-02 study, *J. Immunother. Cancer* 8 (2020), <https://doi.org/10.1136/JITC-2020-SITC2020.0420>.
- [129] P. Zhao, S. Bhowmick, J. Yu, J. Wang, Highly multiplexed single-cell protein profiling with large-scale convertible DNA-antibody barcoded arrays, *Adv. Sci.* 5 (9) (2018) 1800672, <https://doi.org/10.1002/adv.201800672>.
- [130] T. Pham, A. Tyagi, Y. Wang, J. Guo, Single-cell proteomic analysis, *WIREs Mech. Dis.* 13 (2021), e1503, <https://doi.org/10.1002/wsbm.1503>.
- [131] S.S. Agasti, M. Liong, V.M. Peterson, H. Lee, R. Weissleder, Photocleavable DNA barcode-antibody conjugates allow sensitive and multiplexed protein analysis in single cells, *J. Am. Chem. Soc.* 134 (45) (2012) 18499–18502, <https://doi.org/10.1021/ja307689w>.
- [132] A.V. Ullal, V. Peterson, S.S. Agasti, S. Tuang, D. Juric, C.M. Castro, R. Weissleder, Cancer cell profiling by barcoding allows multiplexed protein analysis in fine-needle aspirates, *Sci. Transl. Med.* 6 (219) (2014), 219ra9, <https://doi.org/10.1126/scitranslmed.3007361>.
- [133] Y. Yuan, Spatial heterogeneity in the tumor microenvironment, *Cold Spring Harb. Perspect. Med.* 6 (8) (2016), a026583, <https://doi.org/10.1101/cshperspect.a026583>.
- [134] E.R. Parra, J. Zhai, A. Tamegnon, N. Zhou, R.K. Pandurengan, C. Barreto, M. Jiang, D.C. Rice, C. Creasy, A.A. Vaporciyan, W.L. Hofstetter, A.S. Tsao, I. I. Wistuba, B. Sepesi, C. Haymaker, Identification of distinct immune landscapes using an automated nine-color multiplex immunofluorescence staining panel and image analysis in paraffin tumor tissues, *Sci. Rep.* 11 (1) (2021) 4530, <https://doi.org/10.1038/s41598-021-83858-x>.
- [135] E. Lundberg, G.H.H. Borner, Spatial proteomics: a powerful discovery tool for cell biology, *Nat. Rev. Mol. Cell Biol.* 20 (5) (2019) 285–302, <https://doi.org/10.1038/s41580-018-0094-y>.

- [136] I. Paul, C. White, I. Turcinovic, A. Emili, Imaging the future: the emerging era of single-cell spatial proteomics, *FEBS J.* 288 (24) (2021) 6990–7001, <https://doi.org/10.1111/febs.15685>.
- [137] U. Berndt, L. Philipsen, S. Bartsch, B. Wiedenmann, D.C. Baumgart, M. Hämmerle, A. Sturm, Systematic high-content proteomic analysis reveals substantial immunologic changes in colorectal cancer, *Cancer Res.* 68 (3) (2008) 880–888, <https://doi.org/10.1158/0008-5472.CAN-07-2923>.
- [138] S. Bhattacharya, G. Mathew, E. Ruban, D.B.A. Epstein, A. Krusche, R. Hillert, W. Schubert, M. Khan, Toponome imaging system: in situ protein network mapping in normal and cancerous colon from the same patient reveals more than five-thousand cancer specific protein clusters and their subcellular annotation by using a three symbol code, *J. Proteome Res.* 9 (12) (2010) 6112–6125, <https://doi.org/10.1021/pr100157p>.
- [139] D.Y. Duose, R.M. Schweller, W.N. Hittelman, M.R. Diehl, Multiplexed and reiterative fluorescence labeling via DNA circuitry, *Bioconjug. Chem.* 21 (12) (2010) 2327–2331, <https://doi.org/10.1021/bc100348q>.
- [140] R.J. Giedt, D. Pathania, J.C.T. Carlson, P.J. McFarland, A.F. del Castillo, D. Juric, R. Weissleder, Single-cell barcode analysis provides a rapid readout of cellular signaling pathways in clinical specimens, *Nat. Commun.* 9 (1) (2018) 4550, <https://doi.org/10.1038/s41467-018-07002-6>.
- [141] P. Zrazhevskiy, X. Gao, Quantum dot imaging platform for single-cell molecular profiling, *Nat. Commun.* 4 (2013) 1619, <https://doi.org/10.1038/ncomms2635>. [142] Y. Goltsev, N. Samusik, J. Kennedy-Darling, S. Bhate, M. Hale, G. Vazquez, S. Black, G.P. Nolan, Deep profiling of mouse splenic architecture with CODEX multiplexed imaging, *Cell* 174 (4) (2018) 968–981.e15, <https://doi.org/10.1016/j.cell.2018.07.010>.
- [143] C.M. Schürch, S.S. Bhate, G.L. Barlow, D.J. Phillips, L. Noti, I. Zlobec, P. Chu, S. Black, J. Demeter, D.R. McIlwain, N. Samusik, Y. Goltsev, G.P. Nolan, Coordinated cellular neighborhoods orchestrate antitumoral immunity at the colorectal cancer invasive front, *Cell* 182 (5) (2020) 1341–1359.e19, <https://doi.org/10.1016/j.cell.2020.07.005>.
- [144] M. Mondal, R. Liao, L. Xiao, T. Eno, J. Guo, Highly multiplexed single-cell in situ protein analysis with cleavable fluorescent antibodies, *Angew. Chem. Int. Ed.* 56 (10) (2017) 2636–2639, <https://doi.org/10.1002/anie.201611641>.
- [145] C. Giesen, H.A.O. Wang, D. Schapiro, N. Zivanovic, A. Jacobs, B. Hattendorf, P. J. Schöffler, D. Grolimund, J.M. Buhmann, S. Brandt, Z. Varga, P.J. Wild, D. Günther, B. Bodenmiller, Highly multiplexed imaging of tumor tissues with subcellular resolution by mass cytometry, *Nat. Methods* 11 (2014) 417–422, <https://doi.org/10.1038/nmeth.2869>.
- [146] H.W. Jackson, J.R. Fischer, V.R.T. Zanotelli, H.R. Ali, R. Mechera, S.D. Soysal, H. Moch, S. Muenst, Z. Varga, W.P. Weber, B. Bodenmiller, The single-cell pathology landscape of breast cancer, *Nature* 578 (2020) 615–620, <https://doi.org/10.1038/s41586-019-1876-x>.
- [147] M. Singh, P. Chaudhry, E. Gerdtsen, A. Maoz, W. Cozen, J. Hicks, P. Kuhn, S. Gruber, I. Siddiqi, A. Merchant, Highly multiplexed imaging mass cytometry allows visualization of tumor and immune cell interactions of the tumor microenvironment in FFPE tissue sections, *Blood* 130 (1) (2017), https://doi.org/10.1182/BLOOD.V130.SUPPL_1.2751.2751, 2751–2751.
- [148] M. Angelo, S.C. Bendall, R. Finck, M.B. Hale, C. Hitzman, A.D. Borowsky, R. M. Levenson, J.B. Lowe, S.D. Liu, S. Zhao, Y. Natkunam, G.P. Nolan, Multiplexed ion beam imaging of human breast tumors, *Nat. Med.* 20 (2014) 436–442, <https://doi.org/10.1038/nm.3488>.
- [149] F.J. Hartmann, D. Mrdjen, E. McCaffrey, D.R. Glass, N.F. Greenwald, A. Bharadwaj, Z. Khair, S.G.S. Verberk, A. Baranski, R. Baskar, W. Graf, D. Van Valen, J. Van den Bossche, M. Angelo, S.C. Bendall, Single-cell metabolic profiling of human cytotoxic T cells, *Nat. Biotechnol.* 39 (2) (2020) 186–197, <https://doi.org/10.1038/s41587-020-0651-8>.
- [150] H. Baharlou, N.P. Canete, A.L. Cunningham, A.N. Harman, E. Patrick, Mass cytometry imaging for the study of human diseases—applications and data analysis strategies, *Front. Immunol.* 10 (2019), 2657, <https://doi.org/10.3389/fimmu.2019.02657>.
- [151] F. Maibach, H. Sadozai, S.M. Seyed Jafari, R.E. Hunger, M. Schenk, Tumor-infiltrating lymphocytes and their prognostic value in cutaneous melanoma, *Front. Immunol.* 11 (2020) 2105, <https://doi.org/10.3389/fimmu.2020.02105>.
- [152] C.F. Woolley, M.A. Hayes, P. Mahanti, S. Douglass Gilman, T. Taylor, Theoretical limitations of quantification for noncompetitive sandwich immunoassays, *Anal. Bioanal. Chem.* 407 (28) (2015) 8605–8615, <https://doi.org/10.1007/S00216-015-9018-2>.
- [153] N. Slavov, Single-cell protein analysis by mass spectrometry, *Curr. Opin. Chem. Biol.* 60 (2021) 1–9, <https://doi.org/10.1016/j.cbpa.2020.04.018>.
- [154] R.T. Kelly, Single-cell proteomics: progress and prospects, *Mol. Cell. Proteomics* 19 (11) (2020) 1739–1748, <https://doi.org/10.1074/mcp.R120.002234>.
- [155] Y. Zhu, P.D. Piehowski, R. Zhao, J. Chen, Y. Shen, R.J. Moore, A.K. Shukla, V. A. Petyuk, M. Campbell-Thompson, C.E. Mathews, R.D. Smith, W.J. Qian, R. T. Kelly, Nanodroplet processing platform for deep and quantitative proteome profiling of 10–100 mammalian cells, *Nat. Commun.* 9 (1) (2018), 882, <https://doi.org/10.1038/s41467-018-03367-w>.
- [156] Z.Y. Li, M. Huang, X.K. Wang, Y. Zhu, J.S. Li, C.C.L. Wong, Q. Fang, Nanoliter-scale oil-air-droplet chip-based single cell proteomic analysis, *Anal. Chem.* 90 (8) (2018) 5430–5438, <https://doi.org/10.1021/acs.analchem.8b00661>.
- [157] H. Specht, G. Harmange, D.H. Perlman, E. Emmott, Z. Niziolek, B. Budnik, N. Slavov, Automated sample preparation for high-throughput single-cell proteomics, *BioRxiv* (2018), 399774, <https://doi.org/10.1101/399774>.
- [158] Y. Cong, Y. Liang, K. Motamedchaboki, R. Huguette, T. Truong, R. Zhao, Y. Shen, D. Lopez-Ferrer, Y. Zhu, R.T. Kelly, Improved single-cell proteome coverage using narrow-bore packed nanoLC columns and ultrasensitive mass spectrometry, *Anal. Chem.* 92 (3) (2020) 2665–2671, <https://doi.org/10.1021/acs.analchem.9b04631>.
- [159] B. Budnik, E. Levy, G. Harmange, N. Slavov, SCoPE-MS: mass spectrometry of single mammalian cells quantifies proteome heterogeneity during cell differentiation, *Genome Biol.* 19 (1) (2018), 161, <https://doi.org/10.1186/s13059-018-1547-5>.

- [160] A. Thompson, J. Schäfer, K. Kuhn, S. Kienle, J. Schwarz, G. Schmidt, T. Neumann, C. Hamon, Tandem mass tags: a novel quantification strategy for comparative analysis of complex protein mixtures by MS/MS, *Anal. Chem.* 75 (8) (2003) 1895–1904, <https://doi.org/10.1021/ac0262560>.
- [161] H. Specht, E. Emmott, A.A. Petelski, R. Gray Huffman, D.H. Perlman, M. Serra, P. Kharchenko, A. Koller, N. Slavov, Single-cell mass-spectrometry quantifies the emergence of macrophage heterogeneity, *BioRxiv* (2019), 665307, <https://doi.org/10.1101/665307>.
- [162] C.F. Tsai, R. Zhao, S.M. Williams, R.J. Moore, K. Schultz, W.B. Chrisler, L. Pasa-Tolic, K.D. Rodland, R.D. Smith, T. Shi, Y. Zhu, T. Liu, An improved boosting to amplify signal with isobaric labeling (iBASIL) strategy for precise quantitative single-cell proteomics, *Mol. Cell. Proteomics* 19 (5) (2020) 828–838, <https://doi.org/10.1074/mcp.RA119.001857>.
- [163] S.M. Williams, A.V. Liyu, C.F. Tsai, R.J. Moore, D.J. Orton, W.B. Chrisler, M. J. Gaffrey, T. Liu, R.D. Smith, R.T. Kelly, L. Pasa-Tolic, Y. Zhu, Automated coupling of nanodroplet sample preparation with liquid chromatography-mass spectrometry for high-throughput single-cell proteomics, *Anal. Chem.* 92 (15) (2020) 10588–10596, <https://doi.org/10.1021/acs.analchem.0c01551>.
- [164] E.M. Schoof, B. Furtwängler, N. Üresin, N. Rapin, S. Savickas, C. Gentil, E. Lechman, U. auf dem Keller, J.E. Dick, B.T. Porse, *Nat. Commun.* 121 (12) (2021) 1–15, <https://doi.org/10.1038/s41467-021-23667-y>.
- [165] N. Slavov, Driving single cell proteomics forward with innovation, *J. Proteome Res.* 20 (11) (2021) 4915–4918, <https://doi.org/10.1021/ACS.JPROTEOME.1C00639>.
- [166] N.L. de Vries, A. Mahfouz, F. Koning, N.F.C.C. de Miranda, Unraveling the complexity of the cancer microenvironment with multidimensional genomic and cytometric technologies, *Front. Oncol.* 10 (2020) 1254, <https://doi.org/10.3389/fonc.2020.01254>.
- [167] M. Efremova, R. Vento-Tormo, J.-E. Park, S.A. Teichmann, K.R. James, Immunology in the era of single-cell technologies, *Annu. Rev. Immunol.* 38 (2020) 727–757, <https://doi.org/10.1146/annurev-immunol-090419-020340>.
- [168] P. Mertins, D.R. Mani, K.V. Ruggles, M.A. Gillette, K.R. Clauser, P. Wang, X. Wang, J.W. Qiao, S. Cao, F. Petralia, E. Kawaler, F. Mundt, K. Krug, Z. Tu, J. T. Lei, M.L. Gatza, M. Wilkerson, C.M. Perou, V. Yellapantula, K. Huang, C. Lin, M.D. McLellan, P. Yan, S.R. Davies, R.R. Townsend, S.J. Skates, J. Wang, B. Zhang, C.R. Kinsinger, M. Mesri, H. Rodriguez, L. Ding, A.G. Paulovich, D. Fenyo, M.J. Ellis, S.A. Carr, Proteogenomics connects somatic mutations to signalling in breast cancer, *Nat.* 534 (2016) 55–62, <https://doi.org/10.1038/nature18003>.
- [169] Y. Zhu, L.M. Orre, H.J. Johansson, M. Huss, J. Boekel, M. Vesterlund, A. Fernandez-Woodbridge, R.M.M. Branca, J. Lehtio, Discovery of coding regions in the human genome by integrated proteogenomics analysis workflow, *Nat. Commun.* 9 (2018) 903, <https://doi.org/10.1038/s41467-018-03311-y>.
- [170] S. Vasaikar, C. Huang, X. Wang, V.A. Petyuk, S.R. Savage, B. Wen, Y. Dou, Y. Zhang, Z. Shi, O.A. Arshad, M.A. Gritsenko, L.J. Zimmerman, J.E. McDermott, T.R. Clauss, R.J. Moore, R. Zhao, M.E. Monroe, Y.-T. Wang, M.C. Chambers, R.J. C. Slebos, K.S. Lau, Q. Mo, L. Ding, M. Ellis, M. Thiagarajan, C.R. Kinsinger, H. Rodriguez, R.D. Smith, K.D. Rodland, D.C. Liebler, T. Liu, B. Zhang, A. Pandey, A. Paulovich, A. Hoofnagle, D.R. Mani, D.W. Chan, D.F. Ransohoff, D. Fenyo, D. L. Tabb, D.A. Levine, E.S. Boja, E. Kuhn, F.M. White, G.A. Whiteley, H. Zhu, H. Zhang, I.-M. Shih, J. Bavarva, J. Whiteaker, K.A. Ketchum, K.R. Clauser, K. Ruggles, K. Elburn, L. Hannick, M. Watson, M. Oberti, M. Mesri, M.E. Sanders, M. Borucki, M.A. Gillette, M. Snyder, N.J. Edwards, N. Vatanian, P.A. Rudnick, P. B. McGarvey, P. Mertins, R.R. Townsend, R.R. Thangudu, R.C. Rivers, S.H. Payne, S.R. Davies, S. Cai, S.E. Stein, S.A. Carr, S.J. Skates, S. Madhavan, T. Hiltke, X. Chen, Y. Zhao, Y. Wang, Z. Zhang, Proteogenomic analysis of human colon cancer reveals new therapeutic opportunities, *Cell* 177 (4) (2019) 1035–1049. e19, <https://doi.org/10.1016/j.CELL.2019.03.030>.
- [171] H. Zhang, T. Liu, Z. Zhang, S.H. Payne, B. Zhang, J.E. McDermott, J.-Y. Zhou, V. A. Petyuk, L. Chen, D. Ray, S. Sun, F. Yang, L. Chen, J. Wang, P. Shah, S.W. Cha, P. Aiyetan, S. Woo, Y. Tian, M.A. Gritsenko, T.R. Clauss, C. Choi, M.E. Monroe, S. Thomas, S. Nie, C. Wu, R.J. Moore, K.-H. Yu, D.L. Tabb, D. Fenyo, V. Bafna, Y. Wang, H. Rodriguez, E.S. Boja, T. Hiltke, R.C. Rivers, L. Sokoll, H. Zhu, I.-M. Shih, L. Cope, A. Pandey, B. Zhang, M.P. Snyder, D.A. Levine, R.D. Smith, D. W. Chan, K.D. Rodland, S.A. Carr, M.A. Gillette, K.R. Klauser, E. Kuhn, D.R. Mani, P. Mertins, K.A. Ketchum, R. Thangudu, S. Cai, M. Oberti, A.G. Paulovich, J. R. Whiteaker, N.J. Edwards, P.B. McGarvey, S. Madhavan, P. Wang, D.W. Chan, A. Pandey, I.-M. Shih, H. Zhang, Z. Zhang, H. Zhu, L. Cope, G.A. Whiteley, S.J. Skates, F.M. White, D.A. Levine, E.S. Boja, C.R. Kinsinger, T. Hiltke, M. Mesri, R.C. Rivers, H. Rodriguez, K.M. Shaw, S.E. Stein, D. Fenyo, T. Liu, J. E. McDermott, S.H. Payne, K.D. Rodland, R.D. Smith, P. Rudnick, M. Snyder, Zhao, X. Chen, D.F. Ransohoff, A.N. Hoofnagle, D.C. Liebler, M.E. Sanders, Y. Shi, R.J.C. Slebos, D.L. Tabb, B. Zhang, L.J. Zimmerman, Y. Wang, S.R. Davies, L. Ding, M.J.C. Ellis, R.R. Townsend, Integrated proteogenomic characterization of human high-grade serous ovarian cancer, *Cell* 166 (3) (2016) 755–765, <https://doi.org/10.1016/j.CELL.2016.05.069>.
- [172] B. Demaree, C.L. Delley, H.N. Vasudevan, C.A.C. Peretz, D. Ruff, C.C. Smith, A. R. Abate, Joint profiling of DNA and proteins in single cells to dissect genotype- phenotype associations in leukemia, *Nat. Commun.* 12 (2021) 1–10, <https://doi.org/10.1038/s41467-021-21810-3>.
- [173] A.P. Frei, F.A. Bava, E.R. Zunder, E.W.Y. Hsieh, S.Y. Chen, G.P. Nolan, P. F. Gherardini, Highly multiplexed simultaneous detection of RNAs and proteins in single cells, *Nat. Methods* 13 (2016) 269–275, <https://doi.org/10.1038/nmeth.3742>.
- [174] A.D. Duckworth, P.F. Gherardini, M. Sykorova, F. Yasin, G.P. Nolan, J.R. Slupsky, N. Kalakonda, Multiplexed profiling of RNA and protein expression signatures in individual cells using flow or mass cytometry, *Nat. Protoc.* 14 (2019) 901–920, <https://doi.org/10.1038/s41596-018-0120-8>.
- [175] V.M. Peterson, K.X. Zhang, N. Kumar, J. Wong, L. Li, D.C. Wilson, R. Moore, T. K. Mcclanahan, S. Sadekova, J.A. Klappenbach, Multiplexed quantification of proteins and transcripts in single cells, *Nat. Biotechnol.* 35 (2017) 936–939, <https://doi.org/10.1038/nbt.3973>.

- [176] M. Stoeckius, C. Hafemeister, W. Stephenson, B. Houck-Loomis, P. K. Chattopadhyay, H. Swerdlow, R. Satija, P. Smibert, Simultaneous epitope and transcriptome measurement in single cells, *Nat. Methods* 14 (2017) 865–868, <https://doi.org/10.1038/nmeth.4380>.
- [177] S.Z. Wu, G. Al-Eryani, D.L. Roden, S. Junankar, K. Harvey, A. Andersson, A. Thennavan, C. Wang, J.R. Torpy, N. Bartonicek, T. Wang, L. Larsson, D. Kaczorowski, N.I. Weisenfeld, C.R. Uyttingco, J.G. Chew, Z.W. Bent, C.-L. Chan, V. Gnanasambandapillai, C.-A. Dutertre, L. Gluch, M.N. Hui, J. Beith, A. Parker, E. Robbins, D. Segara, C. Cooper, C. Mak, B. Chan, S. Warriar, F. Ginhoux, E. Millar, J.E. Powell, S.R. Williams, X.S. Liu, S. O’Toole, E. Lim, J. Lundeberg, C. M. Perou, A. Swarbrick, A single-cell and spatially resolved atlas of human breast cancers, *Nat. Genet.* 53 (9) (2021) 1334–1347, <https://doi.org/10.1038/s41588-021-00911-1>.
- [178] J.M. Granja, S. Klemm, L.M. McGinnis, A.S. Kathiria, A. Mezger, M.R. Corces, B. Parks, E. Gars, M. Liedtke, G.X.Y. Zheng, H.Y. Chang, R. Majeti, W.J. Greenleaf, Single-cell multiomic analysis identifies regulatory programs in mixed-phenotype acute leukemia, *Nat. Biotechnol.* 37 (2019) 1458–1465, <https://doi.org/10.1038/s41587-019-0332-7>.
- [179] H. Chung, C.N. Parkhurst, E.M. Magee, D. Phillips, E. Habibi, F. Chen, B. Yeung, J. Waldman, D. Artis, A. Regev, Simultaneous single cell measurements of intranuclear proteins and gene expression, *BioRxiv* (2021), 2021.01.18.427139, <https://doi.org/10.1101/2021.01.18.427139>.
- [180] Y. Katzenelenbogen, F. Sheban, A. Yalin, I. Yofe, D. Svetlichnyy, D.A. Jaitin, C. Bornstein, A. Moshe, H. Keren-Shaul, M. Cohen, S.Y. Wang, B. Li, E. David, T. M. Salame, A. Weiner, I. Amit, Coupled scRNA-seq and intracellular protein activity reveal an immunosuppressive role of TREM2 in cancer, *Cell* 182 (4) (2020) 872–885.e19, <https://doi.org/10.1016/j.cell.2020.06.032>.
- [181] C.J. Kearney, S.J. Vervoort, K.M. Ramsbottom, I. Todorovski, E.J. Lelliott, M. Zethoven, L. Pijpers, B.P. Martin, T. Semple, L. Martelotto, J.A. Trapani, I. A. Parish, N.E. Scott, J. Oliaro, R.W. Johnstone, SUGAR-seq enables simultaneous detection of glycans, epitopes, and the transcriptome in single cells, *Sci. Adv.* 7 (8) (2021) 3610, <https://doi.org/10.1126/sciadv.abe3610>.
- [182] L. Zhang, X. Yu, L. Zheng, Y. Zhang, Y. Li, Q. Fang, R. Gao, B. Kang, Q. Zhang, J. Y. Huang, H. Konno, X. Guo, Y. Ye, S. Gao, S. Wang, X. Hu, X. Ren, Z. Shen, W. Ouyang, Z. Zhang, Lineage tracking reveals dynamic relationships of T cells in colorectal cancer, *Nature* 564 (2018) 268–272, <https://doi.org/10.1038/s41586-018-0694-x>.
- [183] N.L. De Vries, V. Van Unen, M.E. Ijsselsteijn, T. Abdelaal, R. Van Der Breggen, A. Farina Sarasqueta, A. Mahfouz, K.C.M.J. Peeters, T. Hollt, B.P.F. Lelieveldt, F. Koning, N.F.C.C. De Miranda, High-dimensional cytometric analysis of colorectal cancer reveals novel mediators of antitumour immunity, *Gut* 69 (2020) 691–703, <https://doi.org/10.1136/gutjnl-2019-318672>.
- [184] M.P. Blundell, S.L. Sanderson, T.A. Long, Flow cytometry as an important tool in proteomic profiling, *Methods Mol. Biol.* 2261 (2021) 213–227, https://doi.org/10.1007/978-1-0716-1186-9_13.
- [185] G. Holzner, B. Mateescu, D. van Leeuwen, G. Cereghetti, R. Dechant, S. Stavrakis, A. deMello, High-throughput multiparametric imaging flow cytometry: toward diffraction-limited sub-cellular detection and monitoring of sub-cellular processes, *Cell Rep.* 34 (10) (2021), 108824, <https://doi.org/10.1016/j.celrep.2021.108824>.
- [186] S.K. Saka, Y. Wang, J.Y. Kishi, A. Zhu, Y. Zeng, W. Xie, K. Kirli, C. Yapp, M. Cicconet, B.J. Beliveau, S.W. Lapan, S. Yin, M. Lin, E.S. Boyden, P.S. Kaeser, G. Pihan, G.M. Church, P. Yin, Immuno-SABER enables highly multiplexed and amplified protein imaging in tissues, *Nat. Biotechnol.* 37 (2019) 1080–1090, <https://doi.org/10.1038/s41587-019-0207-y>.
- [187] J. Swaminathan, A.A. Boulgakov, E.T. Hernandez, A.M. Bardo, J.L. Bachman, J. Marotta, A.M. Johnson, E.V. Anslyn, E.M. Marcotte, Highly parallel single-molecule identification of proteins in zeptomole-scale mixtures, *Nat. Biotechnol.* 36 (2018) 1076–1091, <https://doi.org/10.1038/nbt.4278>.
- [188] A. Emili, M. McLaughlin, K. Zagorovsky, J.B. Olsen, S.S. Sidhu, Protein Sequencing Method And Reagents, US9566335B1, 2017.
- [189] H. Ouldali, K. Sarthak, T. Ensslen, F. Piguet, P. Manivet, J. Pelta, J.C. Behrends, A. Aksimentiev, A. Oukhaled, Electrical recognition of the twenty proteinogenic amino acids using an aerolysin nanopore, *Nat. Biotechnol.* 38 (2020) 176–181, <https://doi.org/10.1038/s41587-019-0345-2>.
- [190] N. Drachman, M. LePoitevin, H. Szapary, B. Wiener, W. Maulbetsch, D. Stein, A nanopore ion source delivers single amino acid and peptide ions directly into the gas phase, *BioRxiv* (2021), 2021.08.15.456243, <https://doi.org/10.1101/2021.08.15.456243>.

III. Conclusions

The meticulous investigation of T cells, hold yet not entirely unlocked, potential for clinical application in IBD and CRC. There are studies indicating that some bacteria strains can regulate the pathogenic Th17 population as in Lecesse et al. showed *Lactobacillus* and *Bifidobacterium* to reduce production of pro-inflammatory cytokines in patients with UC²³⁸. Hence, understanding how microbiota affects the T-cells populations is vital. Immunodeficient mice which underwent adoptive T-cells transfer from immunocompetent mice develop colitis to the different degree depending on the microbiota composition present in the environment.

Mice maintained in the housing conditions where *H. hepaticus*, *H. typhlonius*, or *Klebsiella oxytoca* were detected exhibited severe colitis, elevated levels of serum IFN- γ and IL17 and increased levels of IFN- γ CD4⁺ and IL17⁺ CD4⁺ T-cells, whilst mice held in different conditions all were positive for IFN- γ CD4⁺ T-cells, what highlights the crucial role of Th17 in the development of colitis upon microbiota changes. In addition, the reduction of the diversity of gut microbiota was also linked with more severe T-cells dependent colitis.

Publication II utilized chemically induced colitis model to investigate the role of USP28 on T-cells. Ubiquitin-specific peptidase 28 (USP28) belongs to Ubiquitin-Specific Protease family of deubiquitinates^{239,240}. In this study, knockout of USP28 led to the increased suppressor functions in Tregs by STAT5 action as STAT5 is vital for i.e FOXP3 expression¹⁷². Furthermore, USP28 was revealed to participated in induction of IL22/STAT5 axis affecting the T-cells activation what indirectly links USP28 to changes in interleukins expression²⁴¹. There are multiple post translational modifications that directly or indirectly influence the Th17/Treg balance, hence this study provides new evidence aiding the deciphering the control mechanism of Tregs population.

Local niche of cellular components and expressed proteins is highly altered during tumorigenesis. Hence, publication III focused on deciphering TME in CRC in the attempt to decode immune cells signature within the tumor. Heterogenic environment and the complexity of immune cells communication hinders investigations on potential reliable targets for therapy to improve patients outcome. In this study, several interferon and TP53-related genes exhibited different expression patterns depending on the location along the invasive trajectory and interactions between, SPP1 macrophages, T-regs, and epithelial cancer cells. Furthermore, pseudotime analysis of the TLS structures development showed upregulation of SIT1, negative regulator of T-cells, comparing to normal lymph nodes, suggesting potentially tumor-enabling conditions induced within the TLSs, however the exact role SIT1 in the CRC context requires further studies.

Publication IV, complemented spatial transcriptomics analysis of T helper cells, by high resolution proteomic technology, characterization of protein profiles in CD4 enriched CRC patients' tissues. This analysis revealed showed high contents of CAFs, Tregs, M2 macrophages, and mast cells contributing to the immunosuppressive environment, highlighting the importance of deciphering complex TME composition for the effective treatment. For example, predicted Tregs fraction were correlated with IDO1, ARG1, or SIRT1 and SIRT2 all linked to the immunosuppressive function of Tregs. Moreover, SIRT2 was found to be differentially expressed in TLSs, comparing to normal lymph node, in the previous spatial transcriptomics studies what indicates the that SIRT2 might play an important role in CRC-associated Tregs. This analysis identified several new proteins with significance in shaping the TME such as NPM3 linked with immune evasion or MCEMP1, identified as upregulated in CRC tissue, found to play potentially a role in migration of Tregs. Simultaneously, the analysis revealed upregulation of proteins associated with inflammation such as S100A8 and S100A9, what highlight the complexity of suppressive and inflammatory signaling linked to the CD4 cells infiltration.

Lastly, tumorigenesis leads to the changes in plasma proteins expression, reflected in publications V and VI. Publication V, performed with PEA technology on CRC and healthy controls serum samples revealed potential new CRC biomarkers. Among identified DEPs, for the first time CXCL9 AND CCL23, T-cells chemoattractant, were found upregulated in serum of CRC patients comparing to healthy

controls. Furthermore, levels of IFN- γ , which induces CXCL9 expression, were found to be elevated in early-stage of CRC in this study what might suggest the link between IFN- γ and CXCL9 in the cancer progression²⁴². All 3 proteins were validated and showed significant upregulation in the independent cohort of CRC vs normal what indicates their high potential for becoming a CRC serum biomarker. Confirmed elevated levels of IFN- γ and interferon-induced CXCL9 at plasma levels, highlight the relevance of interferon-induced genes participation in CRC progression observed in ST study. At the same time CSF3, involved in Th17 differentiation pathway, was found to be upregulated in CRC serum of patients with inflammation status and further validated in the independent cohort. CSF3 is a pro-inflammatory cytokine that may promote angiogenesis and it was found to be upregulated in the serum samples of CRC patients with inflammation²⁴³.

Furthermore, publication VI revealed significant upregulation of complement cascade protein C4B in the patients with inflammatory status, and together with C8A showed significant upregulation in the late stages of CRC. Members of acute-phase proteins such as SAA4 and LBP, together with proposed A2GL were upregulated in CRC serum patients, with A2GL being selectively upregulated in patients with assigned inflammation status²⁴⁴. At the same time, C5 upregulated in CRC patients samples, was additionally validated in the independent cohort indicating its potential biomarker for CRC detection potential.

Collectively, this study yielded new potential biomarkers for CRC diagnosis and revealed CRC-associated changes in the expression of proteins linked to the immune response. However, for the clinical application of these findings further studies are required, including studies on larger cohorts and application of multi-omics technologies to understand the role of immune cells, including T-cells, in orchestrating the immune response during tumorigenesis. Emerging new, single-cell, high throughput technologies, several described in publication VII, as well as development of spatial technologies aiming at single-cell resolution, as recently announced VisiumHD are needed to accelerate translational potential of these findings²⁴⁵.

IV. Literature

1. Morgan E, Arnold M, Gini A, et al. Global burden of colorectal cancer in 2020 and 2040: Incidence and mortality estimates from GLOBOCAN. *Gut*. 2023;72(2):338-344.
2. Bray Bsc F, Laversanne J, Mathieu, Hyuna J, et al. Global cancer statistics 2022: GLOBOCAN estimates of incidence and mortality worldwide for 36 cancers in 185 countries. *CA Cancer J Clin*. 2024;74(3):229-263.
3. World Health Organization. (2019). International statistical classification of diseases and related health problems (10th rev.). Accessed June 18, 2024. <https://icd.who.int/browse10/2019/en>
4. Bogaert J, Prenen H. Molecular genetics of colorectal cancer. *Ann Gastroenterol*. 2014;27(1):9-14.
5. Jaspersion KW, Tuohy TM, Neklason DW, Burt RW. Hereditary and Familial Colon Cancer. *Gastroenterology*. 2010;138(6):2044-2058.
6. Arends MJ. Pathways of colorectal carcinogenesis. *Appl Immunohistochem Mol Morphol AIMM*. 2013;21(2):97-102.
7. Steinke-Lange V, Holinski-Feder E. Lynch Syndrome (Hereditary Nonpolyposis Colorectal Cancer). *Gastroenterologie*. 2024;19(1):50-59.
8. Zhang X, Zhang W, Cao P. Advances in CpG Island Methylator Phenotype Colorectal Cancer Therapies. *Front Oncol*. 2021;11:629390.
9. Mulet-Margalef N, Linares J, Badia-Ramentol J, et al. Challenges and Therapeutic Opportunities in the dMMR/MSI-H Colorectal Cancer Landscape. *Cancers (Basel)*. 2023;15(4):1022.
10. Guinney J, Dienstmann R, Wang X, et al. The consensus molecular subtypes of colorectal cancer. *Nat Med*. 2015;21(11):1350-1356.
11. Hoorn S Ten, De Back TR, Sommeijer DW, Vermeulen L. Clinical Value of Consensus Molecular Subtypes in Colorectal Cancer: A Systematic Review and Meta-Analysis. *J Natl Cancer Inst*. 2022;114(4):503-516.
12. Li Y, Yao Q, Zhang L, et al. Immunohistochemistry-Based Consensus Molecular Subtypes as a Prognostic and Predictive Biomarker for Adjuvant Chemotherapy in Patients with Stage II Colorectal Cancer. *Oncologist*. 2020;25(12):e1968-e1979.
13. Shah SC, Itzkowitz SH. Colorectal Cancer in Inflammatory Bowel Disease: Mechanisms and Management. *Gastroenterology*. 2022;162(3):715-730.e3.
14. McDowell C, Farooq U, Haseeb M. Inflammatory Bowel Disease. *StatPearls*. Published August 4, 2023. Accessed September 9, 2024. <https://www.ncbi.nlm.nih.gov/books/NBK470312/>
15. Eaden JA, Abrams KR, Mayberry JF. The risk of colorectal cancer in ulcerative colitis: a meta-analysis. *Gut*. 2001;48(4):526-535.
16. De Mattos BRR, Garcia MPG, Nogueira JB, et al. Inflammatory Bowel Disease: An Overview of Immune Mechanisms and Biological Treatments. *Mediators Inflamm*. 2015;2015:49301.
17. Gude SS, Veeravalli RS, Vejandla B, Gude SS, Venigalla T, Chintagumpala V. Colorectal Cancer Diagnostic Methods: The Present and Future. *Cureus*. 2023;15(4):e37622.
18. Program badań przesiewowych raka jelita grubego. Narodowy Fundusz Zdrowia. Accessed June 20, 2024. <https://www.nfz.gov.pl/dla-pacjenta/programy-profilaktyczne/program-badan-przesiewowych-raka-jelita-grubego/>
19. Rosen RD, Sapra A. TNM Classification. In *StatPearls*. (Treasure Island (FL): StatPearls Publishing, 2024)
20. Amin MB, Edge SB, Greene FL, et al. *AJCC Cancer Staging Manual*. 8th ed. Springer Cham; 2017.
21. Akkoca AN, Yanik S, Özdemir ZT, et al. TNM and Modified Dukes staging along with the demographic characteristics of patients with colorectal carcinoma. *Int J Clin Exp Med*. 2014;7(9):2828-2835.
22. Ueno H, Kajiwara Y, Shimazaki H, et al. New criteria for histologic grading of colorectal cancer. *Am J Surg Pathol*. 2012;36(2):193-201.
23. Fischer AH, Jacobson KA, Rose J, Zeller R. Hematoxylin and Eosin Staining of Tissue and Cell Sections. *Cold Spring Harb Protoc*. 2008;(2008):pdb.prot4986.
24. Bressenot A, Cahn V, Danese S, Peyrin-Biroulet L. Microscopic features of colorectal neoplasia in inflammatory bowel diseases. *World J Gastroenterol*. 2014;20(12):3164-3172.
25. Magaki S, Hojat SA, Wei B, So A, Yong WH. An Introduction to the Performance of Immunohistochemistry. *Biobanking*. (Yong W, ed.). Humana Press, New York, NY; 2019.
26. Lemos Garcia J, Rosa I, Saraiva S, et al. Routine Immunohistochemical Analysis of Mismatch Repair Proteins in Colorectal Cancer—A Prospective Analysis. *Cancers (Basel)*. 2022;14(15).
27. Malka D, Lièvre A, André T, Taieb J, Ducreux M, Bibeau F. Immune scores in colorectal cancer: Where are we? *Eur J Cancer*. 2020;140:105-118.
28. Alwers E, Kather JN, Kloor M, et al. Validation of the prognostic value of CD3 and CD8 cell densities analogous to the Immunoscore® by stage and location of colorectal cancer: an independent patient cohort study. *J Pathol Clin Res*. 2023;9(2):129-136.
29. Bankhead P, Loughrey MB, Fernández JA, et al. QuPath: Open source software for digital pathology image analysis. *Sci Rep*. 2017;7(1):16878.
30. Mao R, Krautscheid P, Graham RP, et al. Genetic testing for inherited colorectal cancer and polyposis, 2021 revision: a technical standard of the American College of Medical Genetics and Genomics (ACMG). *Genet Med*. 2021;23(10):1807-1817.

31. Guerrero RM, Labajos VA, Ballena SL, et al. Targeting BRAF V600E in metastatic colorectal cancer: where are we today? *Ecancermedicalscience*. 2022;(16):1489.
32. Dong Q, Chen C, Hu Y, et al. Clinical application of molecular residual disease detection by circulation tumor DNA in solid cancers and a comparison of technologies: review article. *Cancer Biol Ther*. 2023;24(1):2274123.
33. Kasi PM, Aushev VN, Ensor J, et al. Circulating tumor DNA (ctDNA) for informing adjuvant chemotherapy (ACT) in stage II/III colorectal cancer (CRC): Interim analysis of BESPOKE CRC study. *J Clin Oncol*. 2024;42:9-9.
34. Yaeger R, Chatila WK, Lipsyc MD, et al. Clinical sequencing defines the genomic landscape of metastatic colorectal cancer. *Cancer Cell*. 2018;33(1):125-136.e3.
35. Cheng DT, Mitchell TN, Zehir A, et al. Memorial Sloan Kettering-integrated mutation profiling of actionable cancer targets (MSK-IMPACT): A hybridization capture-based next-generation sequencing clinical assay for solid tumor molecular oncology. *J Mol Diagnostics*. 2015;17(3):251-264.
36. U.S. Food and Drug Administration. (2023, September 29). FDA unveils streamlined path to authorization for tumor profiling tests alongside its latest product action. FDA. Accessed September 9, 2024. <https://www.fda.gov/news-events/press-announcements/fda-unveils-streamlined-path-authorization-tumor-profiling-tests-alongside-its-latest-product-action>
37. Kopetz S, Tabernero J, Rosenberg R, et al. Genomic Classifier ColoPrint Predicts Recurrence in Stage II Colorectal Cancer Patients More Accurately Than Clinical Factors. *Oncologist*. 2015;20(2):127-133.
38. Barnell EK, Wurtzler EM, La Rocca J, et al. Multitarget Stool RNA Test for Colorectal Cancer Screening. *JAMA*. 2023;330(18):1760-1768.
39. Study Details | Colorectal Cancer and Pre-Cancerous Adenoma Non-Invasive Detection Test Study | ClinicalTrials.gov. Accessed September 9, 2024. <https://clinicaltrials.gov/study/NCT04739722>
40. FDA Approves ColoSense™ - Geneoscopy's Noninvasive Multi-target Stool RNA (mt-sRNA) Colorectal Cancer Screening Test - Geneoscopy - Transforming Gastrointestinal Health.
41. Cheng M, Jiang Y, Xu J, et al. Spatially resolved transcriptomics: a comprehensive review of their technological advances, applications, and challenges. *J Genet Genomics*. 2023;50(9):625-640.
42. Ståhl PL, Salmén F, Vickovic S, et al. Visualization and analysis of gene expression in tissue sections by spatial transcriptomics. *Science* (80-). 2016;353(6294):78-82.
43. Visium Spatial Gene Expression - 10x Genomics. Accessed September 9, 2024. <https://www.10xgenomics.com/products/spatial-gene-expression>
44. Amaral P, Carbonell-Sala S, De La Vega FM, et al. The status of the human gene catalogue. *Nat* 2023 6227981. 2023;622(7981):41-47.
45. Bandura DR, Baranov VI, Ornatsky OI, et al. Mass cytometry: technique for real time single cell multitarget immunoassay based on inductively coupled plasma time-of-flight mass spectrometry. *Anal Chem*. 2009;81(16):6813-6822.
46. Spitzer MH, Nolan GP. Mass Cytometry: Single Cells, Many Features. *Cell*. 2016;165(4):780.
47. Le Rochais M, Hemon P, Pers JO, Uguen A. Application of High-Throughput Imaging Mass Cytometry Hyperion in Cancer Research. *Front Immunol*. 2022;13:859414.
48. Ijsselstein ME, van der Breggen R, Sarasqueta AF, Koning F, de Miranda NFCC. A 40-marker panel for high dimensional characterization of cancer immune microenvironments by imaging mass cytometry. *Front Immunol*. 2019;10(OCT):484562.
49. Highly Multiplexed Imaging Mass Cytometry Allows Visualization of Tumor and Immune Cell Interactions of the Tumor Microenvironment in FFPE Tissue Sections. *Blood*. 2017;130:2751.
50. Tran M, Su A, Lee H, et al. 665 Spatial single-cell analysis of colorectal cancer tumour using multiplexed imaging mass cytometry. *J Immunother Cancer*. 2020;8:A399.1-A399.
51. Zhang T, Lv J, Tan Z, et al. Immunocyte profiling using single-cell mass cytometry reveals EpCAM+ CD4+ T cells abnormal in colon cancer. *Front Immunol*. 2019;10(JULY):462927.
52. Bodenmiller B. Multiplexed Epitope-Based Tissue Imaging for Discovery and Healthcare Applications. *Cell Syst*. 2016;2(4):225-238.
53. Merritt CR, Ong GT, Church SE, et al. Multiplex digital spatial profiling of proteins and RNA in fixed tissue. *Nat Biotechnol*. 2020;38(5):586-599.
54. Wang N, Wang R, Li X, et al. Tumor Microenvironment Profiles Reveal Distinct Therapy-Oriented Proteogenomic Characteristics in Colorectal Cancer. *Front Bioeng Biotechnol*. 2021;9.
55. Pelka K, Hofree M, Chen JH, et al. Spatially organized multicellular immune hubs in human colorectal cancer. *Cell*. 2021;184(18):4734-4752.e20.
56. Gubin MM, Vesely MD. Cancer Immunoediting in the Era of Immuno-oncology. *Clin Cancer Res*. 2022;28(18):3917-3928.
57. Lasek W. Cancer immunoediting hypothesis: history, clinical implications and controversies. *Cent J Immunol*. 2022;47(2):168-174.
58. Tang S, Ning Q, Yang L, Mo Z, Tang S. Mechanisms of immune escape in the cancer immune cycle. *Int Immunopharmacol*. 2020;86:106700.
59. Abbas AK, Lichtman AH, Pillai S, Baker DL, Abbas AK. *Cellular and Molecular Immunology*. 10th ed. Elsevier; 2021.
60. Marshall JS, Warrington R, Watson W, Kim HL. *An introduction to immunology and immunopathology*. Allergy, Asthma Clin Immunol. 2018;14(2):1-10.
61. Silva MT. When two is better than one: macrophages and neutrophils work in concert in innate immunity as complementary and cooperative partners of a myeloid phagocyte system. *J Leukoc Biol*. 2010;87(1):93-106.

62. Kovtun A, Messerer DAC, Scharffetter-Kochanek K, Huber-Lang M, Ignatius A. Neutrophils in Tissue Trauma of the Skin, Bone, and Lung: Two Sides of the Same Coin. *J Immunol Res.* 2018;2018(1):8173983.
63. Yu P, Zhang X, Liu N, Tang L, Peng C, Chen X. Pyroptosis: mechanisms and diseases. *Signal Transduct Target Ther* 2021 6(1):1-21.
64. Watford WT, Moriguchi M, Morinobu A, O'Shea JJ. The biology of IL-12: Coordinating innate and adaptive immune responses. *Cytokine Growth Factor Rev.* 2003;14(5):361-368.
65. Wang H, Tian T, Zhang J. Tumor-Associated Macrophages (TAMs) in Colorectal Cancer (CRC): From Mechanism to Therapy and Prognosis. *Int J Mol Sci.* 2021;22(16).
66. Krystel-Whittemore M, Dileepan KN, Wood JG. Mast cell: A multi-functional master cell. *Front Immunol.* 2016;6:165675.
67. Yokoyama WM. Natural killer cell immune responses. *Immunol Res.* 2005;32(1-3):317-325.
68. Vivier E, Raulet DH, Moretta A, et al. Innate or Adaptive Immunity? The Example of Natural Killer Cells. *Science (80-).* 2011;331(6013):44-49.
69. Dunkelberger JR, Song WC. Complement and its role in innate and adaptive immune responses. *Cell Res.* 2009;20(1):34-50.
70. Wright SD, Reddy PA, Jong MTC, Erickson BW. C3bi receptor (complement receptor type 3) recognizes a region of complement protein C3 containing the sequence Arg-Gly-Asp. *Proc Natl Acad Sci.* 1987;84(7):1965-1968.
71. Marshall JS, Warrington R, Watson W, Kim HL. An introduction to immunology and immunopathology. *Allergy, Asthma Clin Immunol.* 2018;14(2):1-10.
72. Kang SM, Compans RW. Host Responses from Innate to Adaptive Immunity after Vaccination: Molecular and Cellular Events. *Mol Cells.* 2009;27(1):5-14.
73. Bullen M, Heriot GS, Jamrozik E. Herd immunity, vaccination and moral obligation. *J Med Ethics.* 2023;49(9):636-641.
74. Ramírez J, Lukin K, Hagman J. From hematopoietic progenitors to B cells: mechanisms of lineage restriction and commitment. *Curr Opin Immunol.* 2010;22(2):177-184.
75. Pieper K, Grimbacher B, Eibel H. B-cell biology and development. *J Allergy Clin Immunol.* 2013;131(4):959-971.
76. Übelhart R, Werner M, Jumaa H. Assembly and Function of the Precursor B-Cell Receptor. *Curr Top Microbiol Immunol.* 2015;393:3-25.
77. Pieper K, Grimbacher B, Eibel H. B-cell biology and development. *J Allergy Clin Immunol.* 2013;131(4):959-971.
78. Liu X, Zhao Y, Qi H. T-independent antigen induces humoral memory through germinal centers. *J Exp Med.* 2022;219(3):e20210527.
79. Hoffman W, Lakkis FG, Chalasani G. B Cells, Antibodies, and More. *Clin J Am Soc Nephrol.* 2016;11(1):137-154.
80. Wen Y, Jing Y, Yang L, et al. The regulators of BCR signaling during B cell activation. *Blood Sci.* 2019;1(2):119-129.
81. Hamid MHBA, Cespedes PF, Jin C, et al. Unconventional human CD61 pairing with CD103 promotes TCR signaling and antigen-specific T cell cytotoxicity. *Nat Immunol.* 2024;25(5):834-846.
82. Manning BD, Cantley LC. AKT/PKB Signaling: Navigating Downstream. *Cell.* 2007;129(7):1261-1274.
83. Janeway CA, Travers P, Walport M, Shlomchik MJ. *Immunobiology - the Immune System in Health and Disease.* 5th ed. Garland Publishing, New York; 2001.
84. Market E, Papavasiliou FN. V(D)J Recombination and the Evolution of the Adaptive Immune System. *PLoS Biol.* 2003;1(1):e16.
85. Qi Y, Zhang R, Lu Y, Zou X, Yang W. Aire and Fezf2, two regulators in medullary thymic epithelial cells, control autoimmune diseases by regulating TSAs: Partner or complements? *Front Immunol.* 2022;13:948259.
86. Ribot JC, Lopes N, Silva-Santos B. $\gamma\delta$ T cells in tissue physiology and surveillance. *Nat Rev Immunol* 2020 214. 2020;21(4):221-232.
87. Shah K, Al-Haidari A, Sun J, Kazi JU. T cell receptor (TCR) signaling in health and disease. *Signal Transduct Target Ther* 2021 6(1):1-26.
88. Macián F, López-Rodríguez C, Rao A. Partners in transcription: NFAT and AP-1. *Oncogene.* 2001;20(19):2476-2489.
89. Pollizzi KN, Powell JD. Regulation of T cells by mTOR: The known knowns and the known unknowns. *Trends Immunol.* 2015;36(1):13-20.
90. Ciesielska-Figlon K, Lisowska KA. The Role of the CD28 Family Receptors in T-Cell Immunomodulation. *Int J Mol Sci.* 2024;25(2):1274.
91. Chen L, Flies DB. Molecular mechanisms of T cell co-stimulation and co-inhibition. *Nat Rev Immunol.* 2013;13(4):227-242.
92. Cruz-Tapias P, Castiblanco J, Anaya JM. *Autoimmunity: From Bench to Bedside - Major Histocompatibility Complex: Antigen Processing and Presentation.* El Rosario University Press; 2013.
93. Hewitt EW. The MHC class I antigen presentation pathway: strategies for viral immune evasion. *Immunology.* 2003;110(2):163-169.
94. Lin A, Yan WH. The Emerging Roles of Human Leukocyte Antigen-F in Immune Modulation and Viral Infection. *Front Immunol.* 2019;MAY 10(10):964.
95. Beltrami S, Rizzo S, Strazzabosco G, et al. Non-classical HLA class I molecules and their potential role in viral infections. *Hum Immunol.* 2023;84(8):384-392.
96. Zakharova MY, Belyanina TA, Sokolov A V., Kiselev IS, Mamedov AE. The Contribution of Major Histocompatibility Complex Class II Genes to an Association with Autoimmune Diseases. *Acta Naturae.* 2019;11(4):4-12.

97. Liu S, Wei S, Sun Y, Xu G, Zhang S, Li J. Molecular Characteristics, Functional Definitions, and Regulatory Mechanisms for Cross-Presentation Mediated by the Major Histocompatibility Complex: A Comprehensive Review. *Int J Mol Sci.* 2024;25(1):196.
98. Ciechanover A, Schwartz AL. The ubiquitin-proteasome pathway: The complexity and myriad functions of proteins death. *Proc Natl Acad Sci U S A.* 1998;95(6):2727-2730.
99. Blum JS, Wearsch PA, Cresswell P. Pathways of Antigen Processing. *Annu Rev Immunol.* 2013;31:443-473.
100. Roche PA, Furuta K. The ins and outs of MHC class II-mediated antigen processing and presentation. *Nat Rev Immunol.* 2015;15(4):203.
101. Garstka MA, Neeffjes J. How to target MHC class II into the MHC compartment. *Mol Immunol.* 2013;55(2):162-165.
102. Koh CH, Lee S, Kwak M, Kim BS, Chung Y. CD8 T-cell subsets: heterogeneity, functions, and therapeutic potential. *Exp Mol Med* 2023 5511. 2023;55(11):2287-2299.
103. McBride JA, Striker R. Imbalance in the game of T cells: What can the CD4/CD8 T-cell ratio tell us about HIV and health? *PLoS Pathog.* 2017;13(11):e1006624.
104. Annunziato F, Cosmi L, Liotta F, Maggi E, Romagnani S. Human T helper type 1 dichotomy: origin, phenotype and biological activities. *Immunology.* 2015;144(3):343-351.
105. Mills CD, Kincaid K, Alt JM, Heilman MJ, Hill AM. M-1/M-2 Macrophages and the Th1/Th2 Paradigm. *J Immunol.* 2000;164(12):6166-6173.
106. Cella M, Scheidegger D, Palmer-Lehmann K, Lane P, Lanzavecchia A, Alber G. Ligation of CD40 on dendritic cells triggers production of high levels of interleukin-12 and enhances T cell stimulatory capacity: T-T help via APC activation. *J Exp Med.* 1996;184(2):747-752.
107. Hsieh CS, Macatonia SE, Tripp CS, Wolf SF, O'Garra A, Murphy KM. Development of TH1 CD4+ T cells through IL-12 produced by Listeria-induced macrophages. *Science.* 1993;260(5107):547-549.
108. IGF Does Not Drive Th1 Development but Synergizes with IL-12 for Interferon- γ Production and Activates IRAK and NF κ B. *Immunity.* 1997;7(4):571-581.
109. Smeltz RB, Chen J, Ehrhardt R, Shevach EM. Role of IFN- γ in Th1 Differentiation: IFN- γ Regulates IL-18R α Expression by Preventing the Negative Effects of IL-4 and by Inducing/Maintaining IL-12 Receptor β 2 Expression. *J Immunol.* 2002;168(12):6165-6172.
110. Bacon CM, McVicar DW, Ortaldo JR, Rees RC, O'Shea JJ, Johnston JA. Interleukin 12 (IL-12) induces tyrosine phosphorylation of JAK2 and TYK2: differential use of Janus family tyrosine kinases by IL-2 and IL-12. *J Exp Med.* 1995;181(1):399-404.
111. Good SR, Thieu VT, Mathur AN, et al. Temporal induction pattern of STAT4 target genes defines potential for Th1 lineage-specific programming. *J Immunol.* 2009;183(6):3839.
112. Hu X, Ivashkiv LB. Cross-regulation of Signaling and Immune Responses by IFN- γ and STAT1. *Immunity.* 2009;31(4):539.
113. Christie D, Zhu J. Transcriptional Regulatory Networks for CD4 T Cell Differentiation. *Curr Top Microbiol Immunol.* 2014;381:125-172.
114. Romagnani S. Th1/Th2 Cells. *Inflamm Bowel Dis.* 1999;5(4):285-294.
115. León B. T Cells in Allergic Asthma: Key Players Beyond the Th2 Pathway. *Curr Allergy Asthma Rep.* 2017;17(7).
116. Ko H, Kim CJ, Im SH. T Helper 2-Associated Immunity in the Pathogenesis of Systemic Lupus Erythematosus. *Front Immunol.* 2022;13:866549.
117. Lack of IL-4-induced Th2 response and IgE class switching in mice with disrupted Stat6 gene. *Nature.* 1996;380(6575):630-633.
118. Maier E, Duschl A, Horejs-Hoec J. STAT6-dependent and -independent mechanisms in Th2 polarization. *Eur J Immunol.* 2012;42(11):2827-2833.
119. Liao W, Schones DE, Oh J, et al. Priming for T helper type 2 differentiation by interleukin 2-mediated induction of IL-4 receptor α chain expression. *Nat Immunol.* 2008;9(11):1288-1296.
120. Zhu J, Cote-Sierra J, Guo L, Paul WE. Stat5 activation plays a critical role in Th2 differentiation. *Immunity.* 2003;19(5):739-748.
121. Osawa E, Nakajima A, Fujisawa T, et al. Predominant T helper type 2-inflammatory responses promote murine colon cancers. *Int J Cancer.* 2006;118(9):2232-2236.
122. Ziegler A, Heidenreich R, Braumuller H, et al. EpCAM, a human tumor-associated antigen promotes Th2 development and tumor immune evasion. *Blood.* 2009;113(15):3494-3502.
123. Luo W, Weisel F, Shlomchik MJ. B Cell Receptor and CD40 Signaling Are Rewired for Synergistic Induction of the c-Myc Transcription Factor in Germinal Center B Cells. *Immunity.* 2018;48(2):313-326.e5.
124. Nurieva RI, Chung Y, Martinez GJ, et al. Bcl6 mediates the development of T follicular helper cells. *Science.* 2009;325(5943):1001-1005.
125. Johnston RJ, Poholek AC, DiToro D, et al. Bcl6 and Blimp-1 are reciprocal and antagonistic regulators of T follicular helper cell differentiation. *Science.* 2009;325(5943):1006-1010.
126. Yu D, Rao S, Tsai LM, et al. The transcriptional repressor Bcl-6 directs T follicular helper cell lineage commitment. *Immunity.* 2009;31(3):457-468.
127. Breitfeld D, Ohl L, Kremmer E, et al. Follicular B Helper T Cells Express Cxc Chemokine Receptor 5, Localize to B Cell Follicles, and Support Immunoglobulin Production. *J Exp Med.* 2000;192(11):1545.

128. Goenka R, Barnett LG, Silver JS, et al. Cutting Edge: Dendritic Cell-Restricted Antigen Presentation Initiates the Follicular Helper T Cell Program but Cannot Complete Ultimate Effector Differentiation. *J Immunol.* 2011;187(3):1091-1095.
129. Choi J, Crotty S. Bcl6-Mediated Transcriptional Regulation of Follicular Helper T cells (TFH). *Trends Immunol.* 2021;42(4):336.
130. Choi YS, Eto D, Yang JA, Lao C, Crotty S. Cutting edge: STAT1 is required for IL-6-mediated Bcl6 induction for early follicular helper cell differentiation. *J Immunol.* 2013;190(7):3049-3053.
131. Choi YS, Kageyama R, Eto D, et al. ICOS Receptor Instructs T Follicular Helper Cell versus Effector Cell Differentiation via Induction of the Transcriptional Repressor Bcl6. *Immunity.* 2011;34(6):932-946.
132. Crotty S. Follicular Helper CD4 T Cells (TFH). *Annu Rev Immunol.* 2011;29(1):621-663.
133. Crotty S. T Follicular Helper Cell Differentiation, Function, and Roles in Disease. *Immunity.* 2014;41(4):529-542.
134. Oliveira YLDC, Oliveira LM, Cirilo TM, Fujiwara RT, Bueno LL, Dolabella SS. T follicular helper cells: Their development and importance in the context of helminthiasis. *Clin Immunol.* 2021;231:108844.
135. Bindea G, Mlecnik B, Tosolini M, et al. Spatiotemporal dynamics of intratumoral immune cells reveal the immune landscape in human cancer. *Immunity.* 2013;39(4):782-795.
136. Yao Z, Painter SL, Fanslow WC, et al. Human IL-17: a novel cytokine derived from T cells. *J Immunol.* 1995;155(12):5483-5486.
137. Harrington LE, Hatton RD, Mangan PR, et al. Interleukin 17-producing CD4+ effector T cells develop via a lineage distinct from the T helper type 1 and 2 lineages. *Nat Immunol.* 2005;6(11):1123-1132.
138. Park H, Li Z, Yang XO, et al. A distinct lineage of CD4 T cells regulates tissue inflammation by producing interleukin 17. *Nat Immunol.* 2005;6(11):1133-1141.
139. Zambrano-Zaragoza JF, Romo-Martínez EJ, Durán-Avelar MDJ, García-Magallanes N, Vibanco-Pérez N. Th17 Cells in Autoimmune and Infectious Diseases. *Int J Inflam.* 2014;2014:651503.
140. Langrish CL, Chen Y, Blumenschein WM, et al. IL-23 drives a pathogenic T cell population that induces autoimmune inflammation. *J Exp Med.* 2005;201(2):233-240.
141. Oppmann B, Lesley R, Blom B, et al. Novel p19 protein engages IL-12p40 to form a cytokine, IL-23, with biological activities similar as well as distinct from IL-12. *Immunity.* 2000;13(5):715-725.
142. Aggarwal S, Ghilardi N, Xie MH, De Sauvage FJ, Gurney AL. Interleukin-23 promotes a distinct CD4 T cell activation state characterized by the production of interleukin-17. *J Biol Chem.* 2003;278(3):1910-1914.
143. Ferber IA, Brocke S, Taylor-Edwards C, et al. Mice with a disrupted IFN-gamma gene are susceptible to the induction of experimental autoimmune encephalomyelitis (EAE). *J Immunol.* 1996;156(1):5-7.
144. Zhang GX, Gran B, Yu S, et al. Induction of experimental autoimmune encephalomyelitis in IL-12 receptor-beta 2-deficient mice: IL-12 responsiveness is not required in the pathogenesis of inflammatory demyelination in the central nervous system. *J Immunol.* 2003;170(4):2153-2160.
145. Veldhoen M, Hocking RJ, Atkins CJ, Locksley RM, Stockinger B. TGFbeta in the context of an inflammatory cytokine milieu supports de novo differentiation of IL-17-producing T cells. *Immunity.* 2006;24(2):179-189.
146. Wilson NJ, Boniface K, Chan JR, et al. Development, cytokine profile and function of human interleukin 17-producing helper T cells. *Nat Immunol.* 2007;8(9):950-957.
147. Acosta-Rodríguez E V., Napolitani G, Lanzavecchia A, Sallusto F. Interleukins 1beta and 6 but not transforming growth factor-beta are essential for the differentiation of interleukin 17-producing human T helper cells. *Nat Immunol.* 2007;8(9):942-949.
148. Garbers C, Aparicio-Siegmund, Samadhi Rose-John S. The IL-6/gp130/STAT3 signaling axis: recent advances towards specific inhibition. *Curr Opin Immunol.* 2015;34:75-82.
149. Wei L, Laurence A, Elias KM, O'Shea JJ. IL-21 is produced by Th17 cells and drives IL-17 production in a STAT3-dependent manner. *J Biol Chem.* 2007;282(48):34605-34610.
150. Durant L, Watford WT, Ramos HL, et al. Diverse Targets of the Transcription Factor STAT3 Contribute to T Cell Pathogenicity and Homeostasis. *Immunity.* 2010;32(5):605-615.
151. Martinez GJ, Zhang Z, Reynolds JM, et al. Smad2 positively regulates the generation of Th17 cells. *J Biol Chem.* 2010;285(38):29039-29043.
152. Malhotra N, Robertson E, Kang J. SMAD2 is essential for TGF beta-mediated Th17 cell generation. *J Biol Chem.* 2010;285(38):29044-29048.
153. Martinez GJ, Zhang Z, Chung Y, et al. Smad3 differentially regulates the induction of regulatory and inflammatory T cell differentiation. *J Biol Chem.* 2009;284(51):35283-35286.
154. Yang L, Anderson DE, Baecher-Allan C, et al. IL-21 and TGF-beta are required for differentiation of human TH17 cells. *Nature.* 2008;454(7202):350-352.
155. Qin H, Wang L, Feng T, et al. TGF-beta promotes Th17 cell development through inhibition of SOCS3. *J Immunol.* 2009;183(1):97-105.
156. Ghoreschi K, Laurence A, Yang XP, et al. Generation of Pathogenic Th17 Cells in the Absence of TGF-beta Signaling. *Nature.* 2010;467(7318):967-971.
157. Kebir H, Ifergan I, Alvarez JI, et al. Preferential recruitment of interferon-gamma-expressing TH17 cells in multiple sclerosis. *Ann Neurol.* 2009;66(3):390-402.
158. Atarashi K, Tanoue T, Ando M, et al. Th17 Cell Induction by Adhesion of Microbes to Intestinal Epithelial Cells Article Th17 Cell Induction by Adhesion of Microbes to Intestinal Epithelial Cells. *Cell.* 2015;163:367-380.

159. Ivanov II, Frutos R de L, Manel N, et al. Specific microbiota direct the differentiation of IL-17-producing T-helper cells in the mucosa of the small intestine. *Cell Host Microbe*. 2008;4(4):337-349.
160. Goto Y, Panea C, Nakato G, et al. Segmented filamentous bacteria antigens presented by intestinal dendritic cells drive mucosal Th17 cell differentiation. *Immunity*. 2014;40(4):594-607.
161. Woo V, Eshleman EM, Hashimoto-Hill S, et al. Commensal segmented filamentous bacteria-derived retinoic acid primes host defense to intestinal infection. *Cell Host Microbe*. 2021;29(12):1744-1756.e5.
162. Garidou L, Pomié C, Klopp P, et al. The Gut Microbiota Regulates Intestinal CD4 T Cells Expressing ROR γ t and Controls Metabolic Disease. *Cell Metab*. 2015;22(1):100-112.
163. Xu D, Liu H, Komai-Koma M, et al. CD4+CD25+ Regulatory T Cells Suppress Differentiation and Functions of Th1 and Th2 Cells, Leishmania major Infection, and Colitis in Mice. *J Immunol*. 2003;170(1):394-399.
164. Lim HW, Hillsamer P, Banham AH, Kim CH. Cutting Edge: Direct Suppression of B Cells by CD4+CD25+ Regulatory T Cells. *J Immunol*. 2005;175(7):4180-4183.
165. S S, N S, M A, M I, M T. Immunologic self-tolerance maintained by activated T cells expressing IL-2 receptor alpha-chains (CD25). Breakdown of a single mechanism of self-tolerance causes various autoimmune diseases. *J Immunol*. 1995;155(3):1151-1164.
166. Hori S, Nomura T, Sakaguchi S. Control of regulatory T cell development by the transcription factor Foxp3. *Science*. 2003;299(5609):981-985.
167. Borna S, Meffre E, Bacchetta R. FOXP3 deficiency, from the mechanisms of the disease to curative strategies. *Immunol Rev*. 2024;322(1):244-258.
168. Noval Rivas M, Chatila TA. Regulatory T cells in allergic diseases. *J Allergy Clin Immunol*. 2016;138(3):639-652.
169. Wyss L, Stadinski BD, King CG, et al. Affinity for self antigen selects Treg cells with distinct functional properties. *Nat Immunol*. 2016;17(9):1093-1101.
170. Haribhai D, Lin W, Edwards B, et al. A Central Role for Induced Regulatory T Cells in Tolerance Induction in Experimental Colitis. *J Immunol*. 2009;182(6):3461.
171. Lio CWJ, Hsieh CS. A Two-Step Process for Thymic Regulatory T Cell Development. *Immunity*. 2008;28(1):100-111.
172. Harris F, Berdugo YA, Tree T. IL-2-based approaches to Treg enhancement. *Clin Exp Immunol*. 2023;211(2):149-163.
173. Takimoto T, Wakabayashi Y, Sekiya T, et al. Smad2 and Smad3 Are Redundantly Essential for the TGF- β -Mediated Regulation of Regulatory T Plasticity and Th1 Development. *J Immunol*. 2010;185(2):842-855.
174. Harris F, Berdugo YA, Tree T. Smad2 role in mesoderm formation, left-right patterning and craniofacial development. *Nature*. 2023;393(6687):786-790.
175. Bonniaud P, Margetts PJ, Ask K, Flanders K, Gaudie J, Kolb M. TGF- β and Smad3 Signaling Link Inflammation to Chronic Fibrogenesis. *J Immunol*. 2005;175(8):5390-5395.
176. Chen Q, Kim YC, Laurence A, Punkosdy GA, Shevach EM. IL-2 controls the stability of Foxp3 expression in TGF-beta-induced Foxp3+ T cells in vivo. *J Immunol*. 2011;186(11):6329-6337.
177. Tone Y, Furuuchi K, Kojima Y, Tykocinski ML, Greene MI, Tone M. Smad3 and NFAT cooperate to induce Foxp3 expression through its enhancer. *Nat Immunol*. 2008;9(2):194-202.
178. Xu L, Kitani A, Stuelten C, McGrady G, Fuss I, Strober W. Positive and Negative Transcriptional Regulation of the Foxp3 Gene is Mediated by Access and Binding of the Smad3 Protein to Enhancer I. *Immunity*. 2010;33(3):313-325.
179. Figliuolo da Paz VR, Jamwal DR, Kiela PR. Intestinal Regulatory T Cells. *Adv Exp Med Biol*. 2021;1278:141.
180. Iwata M, Hirakiyama A, Eshima Y, Kagechika H, Kato C, Song SY. Retinoic acid imprints gut-homing specificity on T cells. *Immunity*. 2004;21(4):527-538.
181. Païdassi H, Acharya M, Zhang A, et al. Preferential Expression of Integrin α v β 8 Promotes Generation of Regulatory T Cells by Mouse CD103+ Dendritic Cells. *Gastroenterology*. 2011;141(5):1813.
182. Schmidt A, Oberle N, Krammer PH. Molecular Mechanisms of Treg-Mediated T Cell Suppression. *Front Immunol*. 2012;Mar 21(3):51.
183. Kuehn HS, Ouyang W, Lo B, et al. Immune dysregulation in human subjects with heterozygous germline mutations in CTLA4. *Science (80-)*. 2014;345(6204):1623-1627.
184. Schubert D, Bode C, Kenefeck R, et al. Autosomal dominant immune dysregulation syndrome in humans with CTLA4 mutations. *Nat Med*. 2014;20(12):1410-1416.
185. Tivol EA, Borriello F, Schweitzer AN, Lynch WP, Bluestone JA, Sharpe AH. Loss of CTLA-4 leads to massive lymphoproliferation and fatal multiorgan tissue destruction, revealing a critical negative regulatory role of CTLA-4. *Immunity*. 1995;3(5):541-547.
186. Boasso A, Herbeuval JP, Hardy AW, Winkler C, Shearer GM. Regulation of indoleamine 2,3-dioxygenase and tryptophanyl-tRNA-synthetase by CTLA-4-Fc in human CD4+ T cells. *Blood*. 2005;105(4):1574-1581.
187. Fallarino F, Grohmann U, Vacca C, et al. T cell apoptosis by kynurenines. *Adv Exp Med Biol*. 2003;527:183-190.
188. Stone TW, Williams RO. Modulation of T cells by tryptophan metabolites in the kynurenine pathway. *Trends Pharmacol Sci*. 2023;44(7):442-456.
189. Wu D, Zhu Y. Role of kynurenine in promoting the generation of exhausted CD8+ T cells in colorectal cancer. *Am J Transl Res*. 2021;13(3):1535-1547.
190. Huang CT, Workman CJ, Flies D, et al. Role of LAG-3 in Regulatory T Cells. *Immunity*. 2004;21(4):503-513.

191. Maruhashi T, Sugiura D, Okazaki IM, Okazaki T. LAG-3: from molecular functions to clinical applications. *J Immunother Cancer*. 2020;8(2):1014.
192. Pandiyan P, Zheng L, Ishihara S, Reed J, Lenardo MJ. CD4+CD25+Foxp3+ regulatory T cells induce cytokine deprivation-mediated apoptosis of effector CD4+ T cells. *Nat Immunol*. 2007;8(12):1353-1362.
193. Chinen T, Kannan AK, Levine AG, et al. An essential role for the IL-2 receptor in Treg cell function. *Nat Immunol* 2016 1711. 2016;17(11):1322-1333.
194. Kryczek I, Wei S, Zou L, et al. Cutting edge: induction of B7-H4 on APCs through IL-10: novel suppressive mode for regulatory T cells. *J Immunol*. 2006;177(1):40-44.
195. Jarnicki AG, Lysaght J, Todryk S, Mills KHG. Suppression of antitumor immunity by IL-10 and TGF-beta-producing T cells infiltrating the growing tumor: influence of tumor environment on the induction of CD4+ and CD8+ regulatory T cells. *J Immunol*. 2006;177(2):896-904.
196. Grossman WJ, Verbsky JW, Barchet W, Colonna M, Atkinson JP, Ley TJ. Human T regulatory cells can use the perforin pathway to cause autologous target cell death. *Immunity*. 2004;21(4):589-601.
197. Yu X, Harden K, Gonzalez LC, et al. The surface protein TIGIT suppresses T cell activation by promoting the generation of mature immunoregulatory dendritic cells. *Nat Immunol*. 2009;10(1):48-57.
198. Joller N, Lozano E, Burkett PR, et al. Treg cells expressing the co-inhibitory molecule TIGIT selectively inhibit pro-inflammatory Th1 and Th17 cell responses. *Immunity*. 2014;40(4):569-581.
199. Dupage M, Bluestone JA. Harnessing the plasticity of CD4+ T cells to treat immune-mediated disease. *Nat Rev Immunol*. 2016;16(3):149-163.
200. Zhou L, Lopes JE, Chong MMW, et al. TGF-beta-induced Foxp3 inhibits TH17 cell differentiation by antagonizing RORgamma function. *Nature*. 2008;453(7192):236-240.
201. Zhou L, Lopes JE, Chong MMW, et al. TGF-beta-induced Foxp3 inhibits T(H)17 cell differentiation by antagonizing RORgamma function. *Nature*. 2008;453(7192):236-240.
202. Tsun A, Chen Z, Li B. Romance of the three kingdoms: RORgamma allies with HIF1alpha against FoxP3 in regulating T cell metabolism and differentiation. *Protein Cell*. 2011;2(10):778-781.
203. Massoud AH, Charbonnier LM, Lopez D, Pellegrini M, Phipatanakul W, Chatila TA. An asthma-associated IL4R variant exacerbates airway inflammation by promoting conversion of regulatory T cells to TH17-like cells. *Nat Med*. 2016;22(9):1013-1022.
204. Kimura A, Kishimoto T. IL-6: Regulator of Treg/Th17 balance. *Eur J Immunol*. 2010;40(7):1830-1835.
205. Jung MK, Kwak JE, Shin EC. IL-17A-Producing Foxp3+ Regulatory T Cells and Human Diseases. *Immune Netw*. 2017;17(5):276-286.
206. Kim BS, Lu H, Ichiyama K, et al. Generation of RORgamma+ antigen-specific T regulatory 17 (Tr17) cells from Foxp3+ precursors in autoimmunity. *Cell Rep*. 2017;21(1):195-207.
207. Kleinewietfeld M, Hafler DA. The plasticity of human Treg and Th17 cells and its role in autoimmunity. *Semin Immunol*. 2013;25(4):305-312.
208. Omenetti S, Pizarro TT. The Treg/Th17 Axis: A Dynamic Balance Regulated by the Gut Microbiome. *Front Immunol*. 2015;6:17.
209. Turula H, Wobus CE. The Role of the Polymeric Immunoglobulin Receptor and Secretory Immunoglobulins during Mucosal Infection and Immunity. *Viruses*. 2018;10(5):237.
210. Cao AT, Yao S, Gong B, Elson CO, Cong Y. Th17 cells upregulate polymeric Ig receptor and intestinal IgA and contribute to intestinal homeostasis. *J Immunol*. 2012;189(9):4666-4673.
211. Chen L, Ruan G, Cheng Y, Yi A, Chen D, Wei Y. The role of Th17 cells in inflammatory bowel disease and the research progress. *Front Immunol*. 2023;13:1055914.
212. Lee JY, Hall JA, Kroehling L, et al. Serum Amyloid A Proteins Induce Pathogenic Th17 Cells and Promote Inflammatory Disease. *Cell*. 2020;180(1):79-91.e16.
213. Zhao J, Lu Q, Liu Y, et al. Th17 Cells in Inflammatory Bowel Disease: Cytokines, Plasticity, and Therapies. *J Immunol Res*. 2021;2021:8816041.
214. Wen Y, Wang H, Tian D, Wang G. TH17 cell: a double-edged sword in the development of inflammatory bowel disease. *Therap Adv Gastroenterol*. 2024;17.
215. dos Santos Ramos A, Viana GCS, de Macedo Brigido M, Almeida JF. Neutrophil extracellular traps in inflammatory bowel diseases: Implications in pathogenesis and therapeutic targets. *Pharmacol Res*. 2021;171(105779).
216. Quandt J, Arnovitz S, Haghi L, et al. Wnt-beta-catenin activation epigenetically reprograms Treg cells in inflammatory bowel disease and dysplastic progression. *Nat Immunol*. 2021;22(4):471-484.
217. Blatner NR, Mulcahy MF, Dennis KL, et al. Expression of RORgamma marks a pathogenic regulatory T cell subset in human colon cancer. *Sci Transl Med*. 2012;4(164ra159).
218. Gupta RB, Harpaz N, Itzkowitz S, et al. Histologic Inflammation Is a Risk Factor for Progression to Colorectal Neoplasia in Ulcerative Colitis: A Cohort Study. *Gastroenterology*. 2007;133(4):1099-1105.
219. Porter RJ, Arends MJ, Churchhouse AMD, Din S. Inflammatory Bowel Disease-Associated Colorectal Cancer: Translational Risks from Mechanisms to Medicines. *J Crohns Colitis*. 2021;15(12):2131-2141.
220. Amicarella F, Muraro MG, Hirt C, et al. Dual role of tumour-infiltrating T helper 17 cells in human colorectal cancer. *Gut*. 2017;66(4):692-704.

221. Yang Z, Zhang B, Li D, et al. Mast Cells Mobilize Myeloid-Derived Suppressor Cells and Treg Cells in Tumor Microenvironment via IL-17 Pathway in Murine Hepatocarcinoma Model. *PLoS One*. 2010;5(1):e8922.
222. Yan B, Xiong J, Ye Q, et al. Correlation and prognostic implications of intratumor and tumor draining lymph node Foxp3+ T regulatory cells in colorectal cancer. *BMC Gastroenterol*. 2022;22(1):1-12.
223. Aristin Revilla S, Kranenburg O, Coffey PJ. Colorectal Cancer-Infiltrating Regulatory T Cells: Functional Heterogeneity, Metabolic Adaptation, and Therapeutic Targeting. *Front Immunol*. 2022;13:903564.
224. Wang Q, Feng M, Yu T, Liu X, Zhang P. Intratumoral regulatory T cells are associated with suppression of colorectal carcinoma metastasis after resection through overcoming IL-17 producing T cells. *Cell Immunol*. 2014;287(2):100-105.
225. Knochelmann HM, Dwyer CJ, Bailey SR, et al. When worlds collide: Th17 and Treg cells in cancer and autoimmunity. *Cell Mol Immunol*. 2018;15(5):458-469.
226. Anderson NM, Simon MC. The tumor microenvironment. *Curr Biol*. 2020;30(16):R921-R925.
227. Kim SK, Cho SW. The Evasion Mechanisms of Cancer Immunity and Drug Intervention in the Tumor Microenvironment. *Front Pharmacol*. 2022;13:868695.
228. Lalos A, Tülek A, Tosti N, et al. Prognostic significance of CD8+ T-cells density in stage III colorectal cancer depends on SDF-1 expression. *Sci Rep*. 2021;11(1):775.
229. Tosolini M, Kirilovsky A, Mlecnik B, et al. Clinical impact of different classes of infiltrating T cytotoxic and helper cells (Th1, Th2, Treg, Th17) in patients with colorectal cancer. *Cancer Res*. 2011;71(4):1263-1271.
230. Wherry EJ, Kurachi M. Molecular and cellular insights into T cell exhaustion. *Nat Rev Immunol*. 2015;15(8):486.
231. Deng L, Jiang N, Zeng J, Wang Y, Cui H. The Versatile Roles of Cancer-Associated Fibroblasts in Colorectal Cancer and Therapeutic Implications. *Front Cell Dev Biol*. 2021;9:733270.
232. Li Z, Zhou J, Zhang J, Li S, Wang H, Du J. Cancer-associated fibroblasts promote PD-L1 expression in mice cancer cells via secreting CXCL5. *Int J cancer*. 2019;145(7):1946-1957.
233. Molinari C, Marisi G, Passardi A, Matteucci L, De Maio G, Ulivi P. Heterogeneity in Colorectal Cancer: A Challenge for Personalized Medicine? *Int J Mol Sci*. 2018;19(12).
234. Molodecky NA, Kaplan GG. Environmental Risk Factors for Inflammatory Bowel Disease. *Gastroenterol Hepatol (N Y)*. 2010;6(5):339-346.
235. Sawicki T, Ruskowska M, Danielewicz A, Niedźwiedzka E, Artukowicz T, Przybyłowicz KE. A Review of Colorectal Cancer in Terms of Epidemiology, Risk Factors, Development, Symptoms and Diagnosis. *Cancers (Basel)*. 2021;13(9):2025.
236. Lee HO, Hong Y, Etliglu HE, et al. Lineage-dependent gene expression programs influence the immune landscape of colorectal cancer. *Nat Genet*. 2020;52(6):594-603.
237. Trajkovski G, Ognjenovic L, Karadzov Z, et al. Tertiary Lymphoid Structures in Colorectal Cancers and Their Prognostic Value. *Open Access Maced J Med Sci*. 2018;6(10):1824.
238. Leccese G, Bibi A, Mazza S, et al. Probiotic *Lactobacillus* and *Bifidobacterium* Strains Counteract Adherent-Invasive *Escherichia coli* (AIEC) Virulence and Hamper IL-23/Th17 Axis in Ulcerative Colitis, but Not in Crohn's Disease. *Cells* 2020, Vol 9, Page 1824. 2020;9(8):1824.
239. Wang X, Liu Z, Zhang L, et al. Targeting deubiquitinase USP28 for cancer therapy. *Cell Death Dis*. 2018;9(2):186.
240. Diefenbacher ME, Popov N, Blake SM, et al. The deubiquitinase USP28 controls intestinal homeostasis and promotes colorectal cancer. *J Clin Invest*. 2014;124(8):3407-3418.
241. Wu T, Wang Z, Liu Y, et al. Interleukin 22 protects colorectal cancer cells from chemotherapy by activating the STAT3 pathway and inducing autocrine expression of interleukin 8. *Clin Immunol*. 2014;154(2):116-126.
242. Tokunaga R, Zhang W, Naseem M, et al. CXCL9, CXCL10, CXCL11/CXCR3 axis for immune activation - a target for novel cancer therapy. *Cancer Treat Rev*. 2018;63:40.
243. Mroczo B, Groblewska M, Wereszczynska-Siemiatkowska U, Kedra B, Konopko M, Szmikowski M. The diagnostic value of G-CSF measurement in the sera of colorectal cancer and adenoma patients. *Clin Chim Acta*. 2006;371(1-2):143-147.
244. Camilli C, Hoeh AE, De Rossi G, Moss SE, Greenwood J. LRG1: an emerging player in disease pathogenesis. *J Biomed Sci*. 2022;29(1):6.
245. Nagendran M, Sapida J, Arthur J, et al. 1457 Visium HD enables spatially resolved, single-cell scale resolution mapping of FFPE human breast cancer tissue. *J Immunother Cancer*. 2023;11(Suppl 1):A1620-A1620.

V. Supplemental

Appendix I: USP28 protects development of inflammation in mouse intestine by regulating STAT5 phosphorylation and IL22 production in T lymphocytes

Supplemental figure 1
Supplemental figure 2
Supplemental figure 3
Supplemental figure 4
Supplemental figure 5
Supplemental figure 6

Appendix II: Spatial mapping of epithelial changes and suppressive immune populations in colorectal cancer tumor microenvironment

Supplemental figure 1
Supplemental figure 2
Supplemental figure 3
Supplemental figure 4

Table S1. List of Differentially Expressed Genes (DEGs) per annotated clusters from FindAllMarkers Seurat function.
Table S2. Predicted fraction means per annotated cluster separated by their origin, tumor (T) or normal (N)
Table S3. Predicted fraction means per each manually annotated regions.
Table S4. List of DEGs between tumor and normal tissue for cluster Epithelial_1.
Table S5. List of DEGs between tumor and normal tissue for cluster Epithelial_2
Table S6. List of DEGs between tumor and normal tissue for cluster Epithelial_3
Table S7. List of enriched Gene Ontology Biological Process (GO-BP) terms from DEGs between tumor and normal tissue of Epithelial_1 cluster.
Table S8. List of enriched Gene Ontology Biological Process (GO-BP) terms from DEGs between tumor and normal tissue of Epithelial_2 cluster.
Table S9. List of enriched Gene Ontology Biological Process (GO-BP) terms from DEGs between tumor and normal tissue of Epithelial_3 cluster.
Table S10. List of enriched KEGG terms from DEGs between tumor and normal tissue of Epithelial_1 cluster.
Table S11. List of enriched KEGG terms from DEGs between tumor and normal tissue of Epithelial_2 cluster.
Table S12. List of enriched KEGG terms from DEGs between tumor and normal tissue of Epithelial_3 cluster.
Table S13. List of enriched Reactome terms from DEGs between tumor and normal tissue of Epithelial_1 cluster.
Table S14. List of enriched Reactome terms from DEGs between tumor and normal tissue of Epithelial_2 cluster.
Table S15. List of enriched Reactome terms from DEGs between tumor and normal tissue of Epithelial_3 cluster.
Table S16. List of differentially L-R pairs per type interaction type indicated as (Sender-Receiver) between and within tumor clusters
Table S17. List of DEGs between tumor and normal Macrophage cluster
Table S18. List of enriched Gene Ontology Biological Process (GO-BP) terms from DEGs between tumor and normal tissue of Macrophage cluster.
Table S19. List of DEGs between tumor and normal IC_aggregate cluster
Table S20. List of significantly spatially changed genes with their corresponding model and SPATA2 output variables.
Table S21. List of significantly spatially changed L-R interactions estimated with NICHES and each with the corresponding model and SPATA2 output variables.
Table S22. List of DEGs between the ends of Lineage 1 and Lineage 2 pseudotime trajectories with TradeSeq output
Table S23. List of differentially estimated L-R NICHES between the ends of Lineage 1 and Lineage 2 pseudotime trajectories with TradeSeq output

Appendix III: Deep proteomics characterization of enriched CD4+ T cells in colorectal cancer tumor microenvironment

Figure S1
Figure S2

Table S1. Detection rate percentages of protein groups in cancer and normal samples
Table S2. List of differentially expressed proteins between cancer and normal tissues with their corresponding protein groups, logarithmic fold change (log2FC) and adjusted p-value
Table S3. List of enriched Gene Ontology (GO) terms using differentially expressed proteins as input for PathfindR analysis with the corresponding fold enrichment, metrics, adjusted p-values and involved up-/down-regulated proteins

Table S4. List of enriched KEGG terms using differentially expressed proteins as input for PathfindR analysis with the corresponding fold enrichment, metrics, adjusted p-values and involved up-/down-regulated proteins

Table S5. List of differentially expressed proteins between late and early CRC stages with their corresponding protein groups, logarithmic fold change (log2FC) and adjusted p-value

Table S6. List of enriched Gene Ontology (GO) terms using DEPs and selectively expressed proteins between late and early CRC stages as input for PathfindR analysis with the corresponding fold enrichment, metrics, adjusted p-values and involved up-/down-regulated proteins

Table S7. List of enriched KEGG terms using DEPs and selectively expressed proteins between late and early CRC stages as input for PathfindR analysis with the corresponding fold enrichment, metrics, adjusted p-values and involved up-/down-regulated proteins

Table S8. List of significantly correlated proteins with Treg fractions.

Table S9. List of enriched Gene Ontology (GO) terms using correlated proteins with Treg fractions as input for PathfindR analysis with the corresponding fold enrichment, metrics, adjusted p-values and involved up-/down-regulated proteins

Appendix IV: Plasma protein changes reflect colorectal cancer development and associated inflammation

Supplementary Figure 1. Plasma protein changes and biological processes induced by colorectal cancer.

Supplementary Table 1. List of proteins included in the Olink 384-Oncology Explore panel with their respective Uniprot accession and gene name

Supplementary Table 2. List of proteins included in the Olink 384-Inflammation Explore panel with their respective Uniprot accession and gene name.

Supplementary Table 3. DEPs between patients and age and sex-matched healthy controls. The Fold Change is defined as Patient-Healthy control (P-C).

Supplementary Table 4. KEGG enriched terms for the 202 DEPs between CRC patients and healthy controls. Each term contains an associated description, the size of the gene set, the enrichment score, the normal enrichment score (NES), the p-value; adjusted p-value, q-value, the rank, and the core enrichment with the ENTREZ identifiers of the enriched proteins.

Supplementary Table 5. GO enriched terms for the 202 DEPs between CRC patients and healthy controls.

Supplementary Table 6. DEPs between CRC patients and healthy controls that are identified in the human blood secretome from Human Protein Atlas.

Supplementary Table 7. Proteins significantly correlated with inflammation status with the corresponding correlation coefficient and p-value.

Supplementary Table 8. DEPs between patients with and without inflammation. The FC is defined as patients with inflammation - patients without inflammation (Inf-NonInf).

Supplementary Table 9. KEGG enriched terms for the 26 DEPs between CRC patients with and without inflammation. Each term contains an associated description, the fold enrichment, the occurrence, the support, the lowest/highest p-value in the iterations, as well as the up/down-regulated proteins

Supplementary Table 10. Proteins significantly correlated with cancer stage with the corresponding correlation coefficient and p-value.

Supplementary Table 11. DEPs between early and late-stage patients. The FC is defined as patients with late-stage CRC - patients with early-stage CRC.

Appendix V Mass Spectrometry Proteomics Characterization of Plasma Biomarkers for Colorectal Cancer Associated With Inflammation

Figure S1. Heatmap of DEPs between CRC patients and healthy subjects with z-score by row normalization and distributed by hierarchical clustering.

Table S1 List of proteins only identified in CRC patients and healthy subjects, respectively

Table S2 List of identified proteins by proteomics analysis with Uniprot entries, names and associated Gene Ontology terms

Table S3 List of differentially expressed proteins (DEP) between CRC patients and healthy subjects with the corresponding fold change expressed as (Patient-Control) and adjusted p-value

Table S4 KEGG enriched terms in colorectal cancer patients determined by pathway enrichment analysis via active subnetworks with the DEPs from CRC patients vs healthy subjects

Table S5 List of significantly correlated proteins with cancer-associated inflammation in CRC patients with the corresponding coefficients and p-values

Table S6 List of differentially expressed proteins (DEP) between CRC patients with and without cancer-associated inflammation with the corresponding fold change expressed as (Inf.-Non-Inf.) and adjusted p-value

Table S7 List of significantly correlated proteins with tumor stages in CRC patients with the corresponding coefficients and p-values

Table S8 List of differentially expressed proteins (DEP) between CRC patients with late and early stages with the corresponding fold change expressed as (Late-Early) and adjusted p-value

VI. Co-authorship statements

Place/date: 23/09/2024

MSc. Dominika Miroszewska, University of Gdańsk

(title, name and surname, affiliation)

Co-authorship statement

As a co-author of the publication*: **Animal unit hygienic conditions influence mouse intestinal microbiota and contribute to T-cell-mediated colitis, *Experimental biology and medicine* (Maywood, N.J.), 247(19), 2022, p1752–1763,**

I declare that my own substantial contribution to this publication consists of**:

- performed the experiments
- analyzed data
- wrote parts of the manuscript


.....
(co-author's signature)

* provide title, journal, volume, year, pages

**e.g. development a research idea, creation of research hypothesis, development a research concept, making specific experiments and/or measurements (it's best to indicate which ones), interpretation of results, preparation of manuscript

Place/date: 23/09/2024 Oulu, Finland

Associate Professor, Zhi Chen, University of Oulu

(title, name and surname, affiliation)

Co-authorship statement

As a project manager of the publication*: **Animal unit hygienic conditions influence mouse intestinal microbiota and contribute to T-cell-mediated colitis**, *Experimental biology and medicine* (Maywood, N.J.), 247(19), 2022, p1752–1763,

I declare that my own substantial contribution to this publication consists of**:

- designed the study,
- analyzed data
- wrote the manuscript



.....
(co-author's signature)

* provide title, journal, volume, year, pages

**e.g. development a research idea, creation of research hypothesis, development a research concept, making specific experiments and/or measurements (it's best to indicate which ones), interpretation of results, preparation of manuscript

Place/date: 24/09/2024

Prof. Bin Li, Shanghai Jiao Tong University

.....

(title, name and surname, affiliation)

Co-authorship statement

As a co-author of the publication*: **Animal unit hygienic conditions influence mouse intestinal microbiota and contribute to T-cell-mediated colitis, *Experimental biology and medicine* (Maywood, N.J.), 247(19), 2022, p1752–1763,**

I declare that my own substantial contribution to this publication consists of**:

- provided expertise
- interpretation of results



.....
(co-author's signature)

* provide title, journal, volume, year, pages

**e.g. development a research idea, creation of research hypothesis, development a research concept, making specific experiments and/or measurements (it's best to indicate which ones), interpretation of results, preparation of manuscript

Place/date: 17/09/2024 Oulu, Finland

PhD Mariana Cázares Olivera
University of Oulu, Faculty of Biochemistry and Molecular Medicine,
Disease Networks

(title, name and surname, affiliation)

Co-authorship statement

As a co-author of the publication*: **Animal unit hygienic conditions influence mouse intestinal microbiota and contribute to T-cell-mediated colitis**, *Experimental biology and medicine* (Maywood, N.J.), 247(19), 2022, p1752–1763,

I declare that my own substantial contribution to this publication consists of**:

- performed the experiments
- analyzed data
- wrote parts of the manuscript


.....
(co-author's signature)

* provide title, journal, volume, year, pages

**e.g. development a research idea, creation of research hypothesis, development a research concept, making specific experiments and/or measurements (it's best to indicate which ones), interpretation of results, preparation of manuscript

Place/date: 24/09/2024 Gdańsk, Poland

MD Jacek Kowalski
Department of Pathomorphology
Medical University of Gdańsk
Gdańsk, Poland

(title, name and surname, affiliation)

Co-authorship statement

As a co-author of the publication*: **Animal unit hygienic conditions influence mouse intestinal microbiota and contribute to T-cell-mediated colitis, *Experimental biology and medicine* (Maywood, N.J.), 247(19), 2022, p1752–1763,**

I declare that my own substantial contribution to this publication consists of**:

- provided expertise
- interpretation of results



(co-author's signature)

* provide title, journal, volume, year, pages

**e.g. development a research idea, creation of research hypothesis, development a research concept, making specific experiments and/or measurements (it's best to indicate which ones), interpretation of results, preparation of manuscript

Place/date: 20/09/2024 Oulu, Finland

MSc. Keela Pikkarainen
University of Oulu, Faculty of Biochemistry and Molecular Medicine,
Disease Networks

(title, name and surname, affiliation)

Co-authorship statement

As a co-author of the publication*: **USP28 protects development of inflammation in mouse intestine by regulating STAT5 phosphorylation and IL22 production in T lymphocytes** (2024). *Frontiers in immunology*, 15, 1401949. <https://doi.org/10.3389/fimmu.2024.1401949>

I declare that my own substantial contribution to this publication consists of**:

- Investigation,
- Writing – review & editing



.....
(co-author's signature)

* provide title, journal, volume, year, pages

**e.g. development a research idea, creation of research hypothesis, development a research concept, making specific experiments and/or measurements (it's best to indicate which ones), interpretation of results, preparation of manuscript

Place/date: 23/09/2024 Oulu, Finland

Prof. at the University of Gdańsk, Zhi Chen, University of Gdańsk

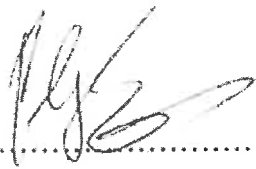
(title, name and surname, affiliation)

Co-authorship statement without contact

As a project manager of the publication*: **USP28 protects development of inflammation in mouse intestine by regulating STAT5 phosphorylation and IL22 production in T lymphocytes (2024). *Frontiers in immunology*, 15, 1401949. <https://doi.org/10.3389/fimmu.2024.1401949>**

I declare that Gwenaëlle Le Menn, who has left the research group, substantial contribution to this publication consists of**:

- Data curation,
- Investigation,
- Visualization,
- Writing – original draft



.....

(co-author's signature)

* provide title, journal, volume, year, pages

**e.g. development a research idea, creation of research hypothesis, development a research concept, making specific experiments and/or measurements (it's best to indicate which ones), interpretation of results, preparation of manuscript

Place/date: 19/09/2024 Oulu, Finland

Professor Thomas Kietzmann
University of Oulu, Faculty of Biochemistry and Molecular Medicine,

Co-authorship statement

As a co-author of the publication*: **USP28 protects development of inflammation in mouse intestine by regulating STAT5 phosphorylation and IL22 production in T lymphocytes** (2024). *Frontiers in immunology*, 15, 1401949. <https://doi.org/10.3389/fimmu.2024.1401949>

I declare that my own substantial contribution to this publication consists of**:

- Supervision,
- Provision of mice and materials
- Writing – review & editing

**Thomas
Kietzmann**
.....
(co-author's signature)

Digitally signed by Thomas
Kietzmann
DN: cn=Thomas Kietzmann,
ou=BMTK,
email=Thomas.Kietzmann@oulu.fi
Date: 2024.09.19.12:45:31 +03'00'

* provide title, journal, volume, year, pages

**e.g. development a research idea, creation of research hypothesis, development a research concept, making specific experiments and/or measurements (it's best to indicate which ones), interpretation of results, preparation of manuscript

Place/date: 17/09/2024

M Sc Dominika Miroszewska
University of Gdańsk

(title, name and surname, affiliation)

Co-authorship statement

As a co-author of the publication*: **USP28 protects development of inflammation in mouse intestine by regulating STAT5 phosphorylation and IL22 production in T lymphocytes** (2024). *Frontiers in immunology*, 15, 1401949. <https://doi.org/10.3389/fimmu.2024.1401949>

I declare that my own substantial contribution to this publication consists of**:

- Investigation,
- Writing – review & editing


(co-author's signature)

* provide title, journal, volume, year, pages

**e.g. development a research idea, creation of research hypothesis, development a research concept, making specific experiments and/or measurements (it's best to indicate which ones), interpretation of results, preparation of manuscript

Place/date: 23/09/2024 Oulu, Finland

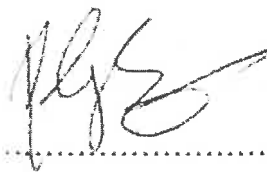
Associate Professor, Zhi Chen, University of Oulu
(title, name and surname, affiliation)

Co-authorship statement

As a co-author of the publication*: **USP28 protects development of inflammation in mouse intestine by regulating STAT5 phosphorylation and IL22 production in T lymphocytes** (2024). *Frontiers in immunology*, 15, 1401949. <https://doi.org/10.3389/fimmu.2024.1401949>

I declare that my own substantial contribution to this publication consists of**:

- Conceptualization,
- Data curation,
- Funding acquisition,
- Investigation,
- Project administration,
- Resources, Supervision,
- Visualization,
- Writing – review & editing.

A handwritten signature in black ink, appearing to be 'Zhi Chen', written over a horizontal dotted line.

(co-author's signature)

* provide title, journal, volume, year, pages

**e.g. development a research idea, creation of research hypothesis, development a research concept, making specific experiments and/or measurements (it's best to indicate which ones), interpretation of results, preparation of manuscript

Place/date: 24/09/2024

MSc. Victor Urbiola-Salvador, University of Gdańsk
(title, name and surname, affiliation)

Co-authorship statement

As a co-author of the publication*: **Spatial mapping of epithelial changes and suppressive immune populations in CRC TME (Unpublished manuscript)**

I declare that my own substantial contribution to this publication consists of**:

- Data analysis
- Visualization
- Writing – Review & editing
- Investigation



.....
(co-author's signature)

* provide title, journal, volume, year, pages

**e.g. development a research idea, creation of research hypothesis, development a research concept, making specific experiments and/or measurements (it's best to indicate which ones), interpretation of results, preparation of manuscript

Place/date: 24/09/2024

Prof. Bin Li, Shanghai Jiao Tong University

.....
(title, name and surname, affiliation)

Co-authorship statement

As a co-author of the publication*: **Spatial mapping of epithelial changes and suppressive immune populations in colorectal cancer tumor microenvironment (Unpublished manuscript)**

I declare that my own substantial contribution to this publication consists of**:

- Supervision
- Writing – review & editing



.....
(co-author's signature)

* provide title, journal, volume, year, pages

**e.g. development a research idea, creation of research hypothesis, development a research concept, making specific experiments and/or measurements (it's best to indicate which ones), interpretation of results, preparation of manuscript

Place/date: 24/09/2024

MSc. Dominika Miroszewska, University of Gdańsk
(title, name and surname, affiliation)

Co-authorship statement

As a co-author of the publication*: **Spatial mapping of epithelial changes and suppressive immune populations in CRC TME (Unpublished manuscript)**

I declare that my own substantial contribution to this publication consists of**:

- Data analysis
- Visualization
- Writing – original draft
- Investigation
- Data curation
- Sample preparation
- Writing – review & editing


.....
(co-author's signature)

* provide title, journal, volume, year, pages

**e.g. development a research idea, creation of research hypothesis, development a research concept, making specific experiments and/or measurements (it's best to indicate which ones), interpretation of results, preparation of manuscript

Place/date: 23/09/2024 Oulu, Finland

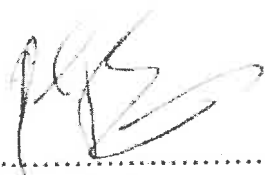
Prof. at the University of Gdańsk, Zhi Chen, University of Gdańsk & University of Oulu
(title, name and surname, affiliation)

Co-authorship statement

As a co-author of the publication*: **Spatial mapping of epithelial changes and suppressive immune populations in CRC TME (Unpublished manuscript)**

I declare that my own substantial contribution to this publication consists of**:

- Conceptualization
- Data curation
- Writing – review & editing
- Supervision
- Funding acquisition
- Project administration



.....
(co-author's signature)

* provide title, journal, volume, year, pages

**e.g. development a research idea, creation of research hypothesis, development a research concept, making specific experiments and/or measurements (it's best to indicate which ones), interpretation of results, preparation of manuscript

Place/date: 17/09/2024 Warszawa, Poland

Dr n med. Agnieszka Jabłońska
The Institute of Biochemistry and Biophysics of the Polish Academy of Sciences
Warszawa, Poland
(title, name and surname, affiliation)

Co-authorship statement

As a co-author of the publication*: **Spatial mapping of epithelial changes and suppressive immune populations in CRC TME (Unpublished manuscript).**

I declare that my own substantial contribution to this publication consists of**:

- sample preparation
- writing—review and editing

.....
(co-author's signature)

* provide title, journal, volume, year, pages

**e.g. development a research idea, creation of research hypothesis, development a research concept, making specific experiments and/or measurements (it's best to indicate which ones), interpretation of results, preparation of manuscript

Place/date: 17/09/2024 Oulu, Finland

PhD Mariana Cázares Olivera
University of Oulu, Faculty of Biochemistry and Molecular Medicine,
Disease Networks

(title, name and surname, affiliation)

Co-authorship statement

As a co-author of the publication*: **Spatial mapping of epithelial changes and suppressive immune populations in CRC TME (Unpublished manuscript)**

I declare that my own substantial contribution to this publication consists of**:

- Sample preparation
- Writing – review & editing


.....
(co-author's signature)

* provide title, journal, volume, year, pages

**e.g. development a research idea, creation of research hypothesis, development a research concept, making specific experiments and/or measurements (it's best to indicate which ones), interpretation of results, preparation of manuscript

Gdańsk, 30/05/24
Place/date.....

MSc. Víctor Urbiola-Salvador, University of Gdańsk
(title, name and surname, affiliation)

Co-authorship statement

As a co-author of the publication*: Deep proteomics characterization of colorectal cancer tumor microenvironment enriched in CD4+ T cells (Unpublished manuscript). I declare that my own substantial contribution to this publication consists of**:

- Software
- Formal analysis
- Investigation
- Data curation
- Visualization
- Writing—original draft preparation



.....
(co-author's signature)

* provide title, journal, volume, year, pages

**e.g. development a research idea, creation of research hypothesis, development a research concept, making specific experiments and/or measurements (it's best to indicate which ones), interpretation of results, preparation of manuscript

30/05/2024

Place/date:.....

M Sc Dominika Miroszewska, University of Gdańsk
(title, name and surname, affiliation)

Co-authorship statement

As a co-author of the publication*: Deep proteomics characterization of colorectal cancer tumor microenvironment enriched in CD4+ T cells (Unpublished manuscript). I declare that my own substantial contribution to this publication consists of**:

- Investigation,
- Validation
- Writing – review & editing
- Visualization
- Data curation
- Software


.....
(co-author's signature)

* provide title, journal, volume, year, pages

**e.g. development a research idea, creation of research hypothesis, development a research concept, making specific experiments and/or measurements (it's best to indicate which ones), interpretation of results, preparation of manuscript

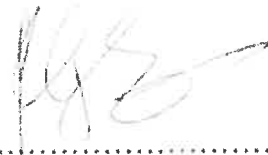
Place/date..... Oulu 2024-1 18

Dr. Zhi Chen, University of Gdańsk and University of Oulu
(title, name and surname, affiliation)

Co-authorship statement

As a co-author of the publication*: Deep proteomics characterization of colorectal cancer tumor microenvironment enriched in CD4+ T cells (Unpublished manuscript). I declare that my own substantial contribution to this publication consists of**:

- Conceptualization
- Data curation
- Writing – Review & Editing
- Project administration
- Supervision
- Funding Acquisition



.....
(co-author's signature)

* provide title, journal, volume, year, pages

**e.g. development a research idea, creation of research hypothesis, development a research concept, making specific experiments and/or measurements (it's best to indicate which ones), interpretation of results, preparation of manuscript

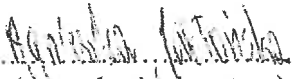
Warsaw, 05.06.2024

Dr n. med. Agnieszka Jabłońska, The Institute of Biochemistry and Biophysics of the Polish Academy of Sciences (title, name and surname, affiliation)

Co-authorship statement

As a co-author of the publication*: Deep proteomics characterization of colorectal cancer tumor microenvironment enriched in CD4+ T cells (Unpublished manuscript). I declare that my own substantial contribution to this publication consists of**:

- Methodology
- Resources
- Investigation
- Writing – Review & Editing


.....
(co-author's signature)

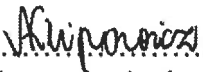
Gdańsk, 5th of June 2024

Dr. Natalia Helena Filipowicz
3P-Medicine Laboratory
Medical University of Gdańsk
(title, name and surname, affiliation)

Co-authorship statement

As a co-author of the publication*: Deep proteomics characterization of colorectal cancer tumor microenvironment enriched in CD4+ T cells (Unpublished manuscript). I declare that my own substantial contribution to this publication consists of**:

- Resources
- Writing – Review & Editing
- Project administration


.....
(co-author's signature)

* provide title, journal, volume, year, pages

**e.g. development a research idea, creation of research hypothesis, development a research concept, making specific experiments and/or measurements (it's best to indicate which ones), interpretation of results, preparation of manuscript

Gdańsk, 30/05/24
Place/date.....

MSc. Dominika Miroszewska, University of Gdańsk
(title, name and surname, affiliation)

Co-authorship statement

As a co-author of the publication*: Plasma protein changes reflect colorectal cancer development and associated inflammation, *Frontiers of Oncology*, 13, 2023, 1158261. I declare that my own substantial contribution to this publication consists of**:

- Writing – Review & Editing


.....
(co-author's signature)

* provide title, journal, volume, year, pages

**e.g. development a research idea, creation of research hypothesis, development a research concept, making specific experiments and/or measurements (it's best to indicate which ones), interpretation of results, preparation of manuscript

Gdańsk, 30/05/24
Place/date.....

MSc. Víctor Urbiola-Salvador, University of Gdańsk
(title, name and surname, affiliation)

Co-authorship statement

As a co-author of the publication*: Plasma protein changes reflect colorectal cancer development and associated inflammation, *Frontiers of Oncology*, 13, 2023, 1158261. I declare that my own substantial contribution to this publication consists of**:

- Methodology
- Formal analysis
- Visualization
- Writing – Review & Editing



.....
(co-author's signature)

* provide title, journal, volume, year, pages

**e.g. development a research idea, creation of research hypothesis, development a research concept, making specific experiments and/or measurements (it's best to indicate which ones), interpretation of results, preparation of manuscript

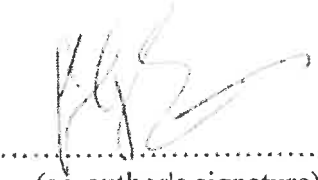
Place/date Oulu, 2024-6-3

Dr. Zhi Chen, University of Gdańsk and University of Oulu
(title, name and surname, affiliation)

Co-authorship statement

As a co-author of the publication*: Plasma protein changes reflect colorectal cancer development and associated inflammation, *Frontiers of Oncology*, 13, 2023, 1158261. I declare that my own substantial contribution to this publication consists of**:

- Conceptualization
- Resources
- Writing – Review & Editing
- Project administration
- Supervision
- Funding Acquisition


.....
(co-author's signature)
Zhi Chen

* provide title, journal, volume, year, pages

**e.g. development a research idea, creation of research hypothesis, development a research concept, making specific experiments and/or measurements (it's best to indicate which ones), interpretation of results, preparation of manuscript

Warsaw, 05.06.2024

Dr n. med. Agnieszka Jabłońska, The Institute of Biochemistry and Biophysics of the Polish Academy of Sciences (title, name and surname, affiliation)

Co-authorship statement

As a co-author of the publication*: Plasma protein changes reflect colorectal cancer development and associated inflammation. *Frontiers in Oncology*, 2023;13:1158261. I declare that my own substantial contribution to this publication consists of**:

- Data curation
- Validation (Luminex, ELISA)
- Writing – Original Draft Preparation
- Writing – Review & Editing
- Project administration

.....
(co-author's signature)

Place/date Gdańsk, 05/06/2024

Dr. Paulina Czaplewska, University of Gdańsk
(title, name and surname, affiliation)

Co-authorship statement

As a co-author of the publication*: Mass spectrometry proteomics characterization of plasma biomarkers for colorectal cancer associated with inflammation. Biomarker Insights, 2024, 11772719241257739. I declare that my own substantial contribution to this publication consists of**:

- Methodology
- Writing – Review & Editing
- Supervision


(co-author's signature)

* provide title, journal, volume, year, pages

**e.g. development a research idea, creation of research hypothesis, development a research concept, making specific experiments and/or measurements (it's best to indicate which ones), interpretation of results, preparation of manuscript

Gdańsk, 30/05/24
Place/date.....

MSc. Dominika Miroszewska, University of Gdańsk
(title, name and surname, affiliation)

Co-authorship statement

As a co-author of the publication*: Mass spectrometry proteomics characterization of plasma biomarkers for colorectal cancer associated with inflammation. Biomarker Insights, 2024, 11772719241257739. I declare that my own substantial contribution to this publication consists of**:

- Investigation
- Writing – Review & Editing


.....
(co-author's signature)

* provide title, journal, volume, year, pages

**e.g. development a research idea, creation of research hypothesis, development a research concept, making specific experiments and/or measurements (it's best to indicate which ones), interpretation of results, preparation of manuscript

Place/date Oulu, 2024-6-3

Dr. Zhi Chen, University of Gdańsk and University of Oulu
(title, name and surname, affiliation)

Co-authorship statement

As a co-author of the publication*: Mass spectrometry proteomics characterization of plasma biomarkers for colorectal cancer associated with inflammation. Biomarker Insights, 2024, 11772719241257739. I declare that my own substantial contribution to this publication consists of**:

- Conceptualization
- Resources
- Data curation
- Writing – Review & Editing
- Project administration
- Supervision
- Funding Acquisition


.....
(co-author's signature)
Zhi Chen

* provide title, journal, volume, year, pages

**e.g. development a research idea, creation of research hypothesis, development a research concept, making specific experiments and/or measurements (it's best to indicate which ones), interpretation of results, preparation of manuscript

Warsaw, 05.06.2024

Dr n. med. Agnieszka Jabłońska, The Institute of Biochemistry and Biophysics of the Polish Academy of Sciences (title, name and surname, affiliation)

Co-authorship statement

As a co-author of the publication*: Mass spectrometry proteomics characterization of plasma biomarkers for colorectal cancer associated with inflammation. Biomarker Insights, 2024. <https://doi.org/10.1177/11772719241257739>. I declare that my own substantial contribution to this publication consists of**:

- Methodology
- Validation
- Investigation
- Writing – Review & Editing

.....
(co-author's signature)

Place/date Gdańsk, 30/05/24

MSc. Víctor Urbiola-Salvador, University of Gdańsk
(title, name and surname, affiliation)

Co-authorship statement

As a co-author of the publication*: Mass spectrometry proteomics characterization of plasma biomarkers for colorectal cancer associated with inflammation. Biomarker Insights, 2024, 11772719241257739. I declare that my own substantial contribution to this publication consists of**:

- Methodology
- Formal analysis
- Visualization
- Data curation
- Writing – Original Draft Preparation
- Writing – Review & Editing



.....
(co-author's signature)

* provide title, journal, volume, year, pages

**e.g. development a research idea, creation of research hypothesis, development a research concept, making specific experiments and/or measurements (it's best to indicate which ones), interpretation of results, preparation of manuscript

Place/date...Oulu,.....²⁰²⁴⁻⁶⁻¹⁸

Dr. Zhi Chen, University of Gdańsk and University of Oulu
(title, name and surname, affiliation)

Co-authorship statement without contact

As a project manager of the publication*: Proteomics approaches to characterize the immune responses in cancer, *Biochimica et Biophysica Acta (BBA) - Molecular Cell Research*, 1869, 2022, 119266. I declare that Talha Qureshi, who has left the university, substantial contribution to this publication consist of**:

- Writing – Original Draft Preparation


.....
(co-author's signature)

* provide title, journal, volume, year, pages

**e.g. development a research idea, creation of research hypothesis, development a research concept, making specific experiments and/or measurements (it's best to indicate which ones), interpretation of results, preparation of manuscript

Warsaw, 05.06.2024

Dr n. med. Agnieszka Jabłońska, The Institute of Biochemistry and Biophysics of the Polish Academy of Sciences (title, name and surname, affiliation)

Co-authorship statement

As a co-author of the publication*: Proteomics approaches to characterize the immune responses in cancer. *Biochimica et Biophysica Acta (BBA) - Molecular Cell Research*, 2022;1869(8):119266.

I declare that my own substantial contribution to this publication consists of**:

- Writing – Original Draft Preparation
- Writing – Review & Editing

.....Agnieszka Jabłońska.....
(co-author's signature)

Gdańsk, 30/05/24
Place/date.....

MSc. Dominika Miroszewska, University of Gdańsk
(title, name and surname, affiliation)

Co-authorship statement

As a co-author of the publication*: Proteomics approaches to characterize the immune responses in cancer, *Biochimica et Biophysica Acta (BBA) - Molecular Cell Research*, 1869, 2022, 119266. I declare that my own substantial contribution to this publication consists of**:

- Writing – Original Draft Preparation
- Writing – Review & Editing


.....
(co-author's signature)

* provide title, journal, volume, year, pages

**e.g. development a research idea, creation of research hypothesis, development a research concept, making specific experiments and/or measurements (it's best to indicate which ones), interpretation of results, preparation of manuscript

Place/date. Oulu, 2024-6-3

Dr. Zhi Chen, University of Gdańsk and University of Oulu
(title, name and surname, affiliation)

Co-authorship statement

As a co-author of the publication*: Proteomics approaches to characterize the immune responses in cancer, *Biochimica et Biophysica Acta (BBA) - Molecular Cell Research*, 1869, 2022, 119266. I declare that my own substantial contribution to this publication consists of**:

- Conceptualization
- Writing – Review & Editing
- Project administration
- Supervision
- Funding Acquisition


.....
(co-author's signature)

Zhi Chen

* provide title, journal, volume, year, pages

**e.g. development a research idea, creation of research hypothesis, development a research concept, making specific experiments and/or measurements (it's best to indicate which ones), interpretation of results, preparation of manuscript

Place/date..... Gdańsk, 30/05/2024

M.Sc. Víctor Urbiola-Salvador, University of Gdańsk
(title, name and surname, affiliation)

Co-authorship statement

As a co-author of the publication*: Proteomics approaches to characterize the immune responses in cancer, *Biochimica et Biophysica Acta (BBA) - Molecular Cell Research*, 1869, 2022, 119266. I declare that my own substantial contribution to this publication consists of**:

- Visualization
- Writing – original draft preparation
- Writing – Review & Editing


.....
(co-author's signature)

* provide title, journal, volume, year, pages

**e.g. development a research idea, creation of research hypothesis, development a research concept, making specific experiments and/or measurements (it's best to indicate which ones), interpretation of results, preparation of manuscript